Université de Bourgogne
UFR Sciences de la Terre et de l'Environnement

UMR 5594 ARTeHIS
Equipe Géoarchéologie

Ecole doctorale E2S

Habilitation à Diriger des Recherches

Cycles biogéochimiques des éléments traces métalliques aux interfaces de l'environnement

par

Fabrice Monna

10 Décembre 2008

Composition du jury

Rapporteurs :
Françoise Elbaz-Poulichet, DR CNRS, Université de Montpellier II
Jean-François Deconinck, Professeur, Université de Bourgogne
Francis Grousset, DR CNRS, Université de Bordeaux I

Examinateurs :
Jean-Louis Colin, Professeur, Université de Paris VII
Janusz Dominik, Professeur, Université de Genève
Claude Mordant, Professeur, Université de Bourgogne
Hervé Richard, DR CNRS, Université de Franche-Comté

Table des matières

Avant propos

Voici venue l'heure du bilan. Bilan de 12 ans de recherches post-thèse consacrées à l'étude des métaux, des métalloïdes et des radio-isotopes dans l'environnement. L'exercice de l'Habilitation à Diriger des Recherches consiste à structurer le travail effectué et à proposer un projet de recherche susceptible d'éclairer des questions qui demeurent en suspens. Au niveau du thème principal d'activité, il est clair que la question des métaux et de leur transfert (ou dynamique) entre compartiments de l'environnement est centrale dans mon travail. Après 16 ans passés à utiliser la géochimie isotopique (en combinaison avec d'autres techniques), je demeure convaincu que cette approche amène de précieux renseignements, difficilement accessibles par d'autres voies. Pour s'en persuader, il suffit de s'attarder sur le nombre croissant de publications présentant des mesures isotopiques, notamment en plomb ; explosion facilitée par l'émergence de techniques analytiques moins coûteuses et tellement plus rapides que le vénérable TIMS… Alors que les années de thèse ont été dédiées à l'étude du message sédimentaire, des eaux de surface et des particules atmosphériques afin d'appréhender les transferts entre ces compartiments sur l'Etang de Thau (Hérault), les années post-thèse ont été plutôt consacrées à l'étude des sols, des tourbières et des bioaccumulateurs que sont les lichens, les aiguilles de pins, ou les poissons, avec des incursions dans les domaines directement liés à l'archéologie. Ceci nécessite des connaissances pointues dans des domaines aussi variés que la pédologie, la diagenèse, l'archéologie, la sédimentologie, la paléobotanique, la paléontologie morphométrique, la biologie, l'écotoxicologie, la médecine vétérinaire, l'océanologie, la géomorphologie, la chimie, la radiochimie, le magnétisme, la modélisation mathématique… Inutile de dire que si je possède quelques bases me permettant de communiquer plus ou moins efficacement avec les spécialistes issus de ces disciplines, je suis loin d'en posséder toutes les subtilités et les connaissances spécifiques. Pourtant, c'est grâce à la pluridisciplinarité et à la diversité des approches que les difficultés peuvent être contournées, surtout lorsqu'il s'agit du milieu naturel où les interactions se révèlent d'une complexité quasi infinie. Dans la suite du présent document, il sera souvent bien difficile pour le lecteur d'identifier ma propre contribution, tant les interactions entre les différents participants aux études présentées sont étroites. Mais cette question est-elle finalement si importante ?

Malgré la diversité des questions traitées et des approches utilisées, quatre axes de recherche ressortent nettement. Le premier est méthodologique. Il est centré sur l'outil géochimique et concerne la détermination de l'origine des métaux dans l'environnement, notamment la dualité signal anthropique *versus* signal naturel, et éventuellement l'identification des sources mises en jeu à l'intérieur d'un groupe générique dit « anthropique ». Le deuxième axe s'articule autour de la modélisation du transfert des micropolluants métalliques dans le milieu naturel. Le troisième axe concerne l'étude de la métallurgie précoce dans une optique archéologique ; un problème abordé ici grâce à des méthodes issues de la géochimie et plus généralement des biogéosciences. Finalement, le besoin de techniques rapides, peu coûteuses et suffisamment fiables m'a conduit à m'investir dans un quatrième axe centré sur les développements analytiques. Le manuscrit est construit autour de ces quatre axes, auxquels viendront s'ajouter mes perspectives de recherche pour les années à venir et un curriculum vitae détaillé qui présente mon implication dans la formation en 3^{e} cycle et la liste exhaustive de mes publications. Dans un souci d'efficacité, plusieurs travaux déjà publiés seront reproduits *in extenso* en annexe. Le lecteur pourra ainsi s'y reporter s'il désire un complément d'information.

Je tiens à remercier mes rapporteurs et mes examinateurs, sans aucun doute très occupés par ailleurs, pour avoir bien voulu prendre le temps de lire ce document et pour leur participation au jury. J'aimerais également exprimer ma gratitude aux nombreux chercheurs avec qui j'ai eu la chance de travailler pour tout ce que j'ai appris à leur contact. Merci à tous mes collègues, personnels administratifs et techniques sans qui l'activité de recherche serait impossible. N'oublions pas non plus les étudiants. Ils sont au centre du système universitaire et ils constituent la relève. Parions qu'ils bouleverseront nos théories et enterreront bon nombre de nos hypothèses !

à mes parents, à Cocotte…

Introduction

Suite à une ***législation de plus en plus contraignante****, les problèmes de pollutions ponctuelles en éléments traces (métaux et métalloïdes)*[1] *se sont pour l'essentiel résorbés au cours des trente dernières années dans les sociétés industrielles occidentales. Cela signifie-t-il que* ***la menace a définitivement disparu?*** *C'est loin d'être sûr…*

Prenons le cas du plomb qui est à plus d'un titre exemplaire puisqu'il s'agit de l'élément dont le cycle naturel a été le plus fortement masqué par l'activité humaine (Patterson, 1983 ; Nriagu, 1988, 1989) ; c'est aussi probablement le plus médiatisé. C'est au début des années 1970, aux États-Unis et au Japon que pour la première fois l'attention des pouvoirs publics se porte sérieusement sur les conséquences néfastes de la contamination en plomb enregistrée au niveau planétaire, notamment grâce aux travaux pionniers de C.C. Patterson (voir Clair C. Patterson Special Issue, *Geochimica et Cosmochimica Acta*, 58, 1994). Les effets de ce métal sur la santé sont multiples : inhibition de la synthèse de l'hémoglobine, altération neuro - comportementales, coliques, voire même paralysie et néphropathie saturnines chez les sujets les plus exposés (Collectif, 1999). Les additifs antidétonants des carburants automobiles sont alors identifiés comme les principaux responsables. En fait, la situation n'est pas nouvelle. Depuis le 2 février 1923, date à laquelle le premier gallon d'essence au plomb a été commercialisé à Dayton (Ohio), les pétroliers ont incorporé des composés du plomb pour élever l'indice d'octane et éviter ainsi les combustions anormales qui provoquent le phénomène de cliquetis particulièrement destructeur pour les moteurs (Joumard *et al.*, 1983). A la fin des années 1970, la France, elle aussi, commence à réduire progressivement la teneur légale en plomb tetraéthyl pour passer finalement d'environ 0,7 g l^{-1} à 0,15 g l^{-1} en 1999. Parallèlement, en 1987, l'introduction des additifs de substitution sur le marché est accompagnée de mesures fiscales incitatives. C'est seulement à partir du 1er janvier 2000 que la vente d'essences

---

[1] En toute rigueur, il est préférable d'utiliser le terme « éléments traces métalliques » ou ETM, plutôt que le terme « métaux lourds » qui historiquement désignait les éléments lourds de masse volumique >5 g.cm^{-3}, susceptibles de précipiter avec le soufre. Il pouvait d'ailleurs s'agir de métaux (Pb, Zn, Cd..) ou de métalloïdes (Se, As...). Les éléments traces ont par définition des concentrations inférieures au pour mille dans la croute et à 0.1 pour mille dans le vivant. Ces recommandations ont été validées par l'Académie des Sciences (rapport n°42, 1998).

plombées est interdite en France, alors que dans de nombreux pays industrialisés cette mesure avait été prise depuis longtemps déjà : début des années 1980 au Japon, 1990 au Canada, 1993 en Suède, 1995 aux E.U. Aujourd'hui, les indicateurs des réseaux de surveillance de la qualité de l'air sont passés au vert (tout au moins dans les pays industrialisés occidentaux) pour ce qui concerne ce métal. L'amélioration est indéniable : le plomb a en partie disparu de l'atmosphère des grandes villes et sa concentration est très inférieure à la limite légale de 2 μg m^{-3} en moyenne annuelle fixée par l'U.E. On estime à plus de 65% la réduction des émissions sur la période 1990 – 1998.

L'exemplarité du plomb tient au fait qu'une unique source émettrice (le plomb ajouté comme antidétonant dans les essences) représentait à elle seule entre 80% et 90% des émissions anthropiques dans les années 1980. Le temps de résidence dans l'atmosphère étant par ailleurs très court, de l'ordre de quelques jours, les progrès peuvent être spectaculaires dès lors que l'on arrive à un consensus au sein des pays les plus industrialisés (cf. Figure 1).

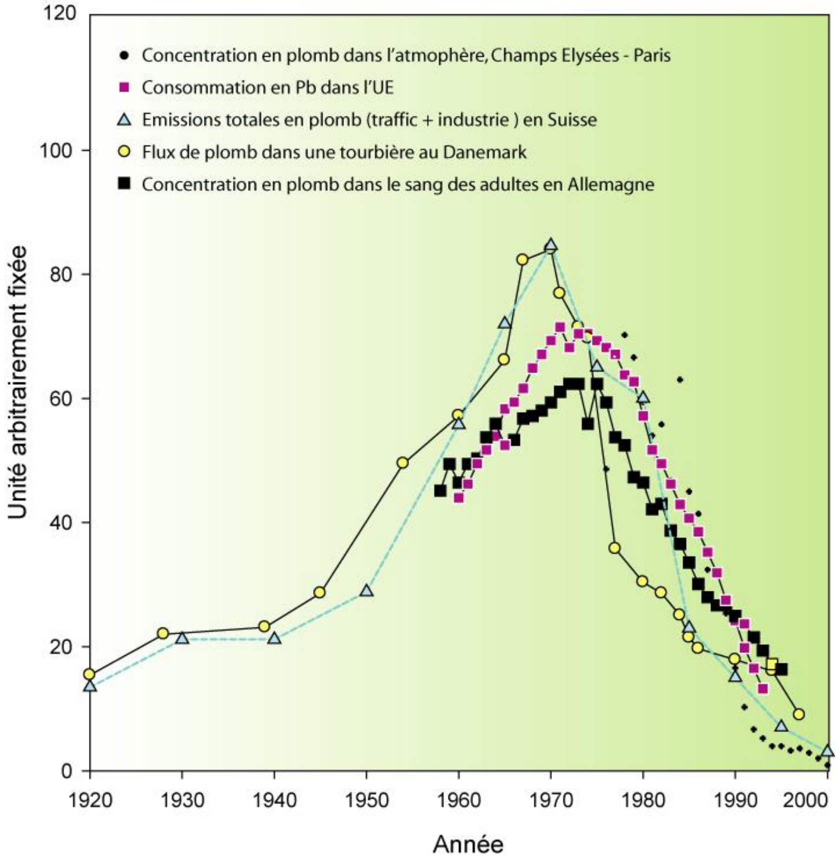

Figure 1 : Evolution des concentrations en plomb dans l'atmosphère, Champs Elysées, Paris (Laboratoire central de la Préfecture de police de Paris, communication personnelle), de la consommation en plomb dans l'U.E. (CONCAWE, 1993), des émissions totales en Pb (trafic + industrie) en Suisse (BUWAL, 1995), des flux de plomb dans une tourbière danoise (Goodsite *et al.* 2001), et de la concentration en plomb dans le sang des adultes en Allemagne (von Storch, *et al.* 2002). L'unité des différentes variables est arbitraire. Toutes ces courbes illustrent l'élimination progressive du Pb dans les essences et les progrès subséquents dans l'environnement.

Comme par ailleurs, les lois environnementales des grands pays industrialisés occidentaux ne se sont pas contentées de réduire les émissions atmosphériques mais ont également fixé des seuils pour les rejets dans les eaux, des règles sur l'épandage des boues ou la mise en décharge, et cela pour le plomb, mais aussi pour de nombreux autres éléments (Hg, Cd, Cu, As, Ni, Zn, Co, Mn), on pourrait être tenté de considérer la question des métaux lourds dans l'environnement comme définitivement réglée, ou tout au moins sous contrôle. Ce serait commettre une très grave erreur. Malgré les bonnes intensions affichées par les pays émergents, on imagine mal que les records de croissance enregistrés durant ces dernières années ne s'accompagnent pas d'impacts environnementaux majeurs, notamment au niveau métallique. Par ailleurs certains pays économiquement en difficulté ne possèdent pas les ressources nécessaires à l'amélioration ou la préservation de la qualité de leur environnement. Toujours pour rester sur le plomb, l'Afrique subsaharienne ne s'est débarrassée des essences plombées que depuis le 1er janvier 2006. L'Afghanistan, l'Algérie, le Bhoutan, le Cambodge, la Corée du Nord, Cuba, l'Irak, le Laos, la Mongolie, l'Ouzbékistan et le Turkménistan n'envisagent toujours pas l'élimination de ces additifs. Le cas du plomb est ici le révélateur d'un problème beaucoup plus profond qui concerne la gestion de l'environnement au sens large, notamment en période de crise économique.

Dans nos sociétés occidentales, même si d'énormes progrès ont été réalisés, on peut considérer que tous les sols ont reçu une contamination métallique diffuse d'origine atmosphérique à laquelle s'ajoutent d'éventuelles contaminations ponctuelles qui dépendent de leur utilisation dans le passé (agriculture intensive, épandage de produits organiques, épandage de sous-produits d'industriels, etc.). Les éléments traces métalliques sont impliqués dans des mécanismes physico-chimiques (i) d'adsorption (sur les phases minérales, sur la matière organique en décomposition…), (ii) de complexation avec des ligands organiques ou inorganiques et (iii) de co-précipitation avec des phases minérales secondaires mal cristallisées (oxyhydroxides de fer, de manganèse,…), ce qui a pour effet d'accroître leur rétention (e.g. Sterckeman *et al.*, 2000, Baize et Tercé, 2002). Outre les phénomènes d'érosion mécanique, des modifications physiques ou chimiques du milieu peuvent entrainer une remobilisation des métaux dans les solutions de sols puis dans les eaux souterraines (Camobreco *et al.*, 1996 ; Denaix *et al.*, 2001 ; Citeau *et al.*, 2003). Certains n'hésitent pas à qualifier cette situation de véritable 'bombe à retardement' (Chang *et al.*, 1997). Dans les sédiments lacustres ou marins, les éléments traces métalliques sont en général mieux stabilisés, mais un dragage, une crue ou un *slump* peuvent très bien entraîner une remobilisation massive. Sans céder au pessimisme, il est donc essentiel d'identifier et de quantifier les transferts, de déterminer les facteurs clés et les mécanismes responsables de la mobilité, et d'évaluer la biodisponibilité des éléments traces métalliques dans l'atmosphère, les sols, les eaux, et les sédiments. Ceci devrait permettre de définir des stratégies durables et raisonnées de gestion des espaces. C'est donc autour de ces thèmes que s'est articulé mon travail de recherche, notamment en privilégiant la notion de temporalité grâce à des échanges entre archéologie/histoire et sciences de l'environnement. Comme le signalent justement Monfrey et Garnier (2007) : « *l'approche historique est cru-*

ciale car elle permet de comprendre comment on est arrivé à la situation actuelle, point de départ des simulations pour le futur ».

AXE 1 : Origine des métaux dans l'environnement

Techniquement, la première étape d'une étude traitant des métaux dans l'environnement consiste le plus souvent à isoler la ***composante anthropique*** *de la* ***contribution naturelle*** *dans l'objet ciblé. Quand cette distinction est réalisée, la fraction anthropique correspond potentiellement à un mélange complexe où plusieurs sources sont impliquées : transports, industrie, activité minière, rejets domestiques, amendements, etc. Pourtant,* ***identifier les sources*** *les plus influentes est indispensable pour élaborer des stratégies spécifiques de réduction des émissions (si bien sûr ces sources sont toujours actives).*

S'il est clair que les cycles naturels d'éléments comme le Pb, le Cd ou le Hg ont été masqués par les émissions anthropiques modernes et contemporaines, il ne faut pas perdre de vue que la composante naturelle (aussi nommé 'background' ou 'fond géochimique') peut être localement élevée au point d'engendrer une sérieuse surestimation de l'impact anthropique (e.g. Baize *et al.* 1999). Discriminer les parts naturelles et anthropiques n'est malheureusement pas une tache triviale ; la seule mesure des concentrations n'étant pas toujours capable de répondre à cette question, notamment lorsque le bruit de fond géochimique est variable ou élevé. Pour cette raison, la simple soustraction d'une valeur, supposée représenter le fond géochimique, est souvent bien peu satisfaisante.

Origine anthropique versus origine naturelle. Plusieurs techniques élaborées ont donc été développées. L'une d'entre elles est basée sur un principe chimique simple. Dans un objet minéral (sol, sédiment), la fraction anthropique devrait essentiellement être adsorbée (notamment sur les argiles) et associée à la matière organique. Dans tous les cas, elle est censée être plus facilement mobilisable que la fraction naturelle, qui est pour l'essentiel intimement liée au réseau cristallin des minéraux. L'idée est donc de cibler plus particulièrement la contribution anthropique, notamment en utilisant un ou plusieurs extractants chimiques, capables d'être sélectifs vis-à-vis des espèces chimiques auxquelles sont supposés être associés les métaux : e.g. simple adsorption, carbonates, oxydes, matière organique, alumino-silicates. De nombreux schémas d'extractions séquentielles ont été développés au cours des 30 dernières années (Tessier *et al.*, 1979 ; McGrath, 1996; Gleyzes *et al.*, 2002; Krishnamurti *et al.*, 2002). J'ai d'ailleurs participé à ce type de recherche durant mon doctorat en proposant un schéma d'extraction basé sur quatre étapes[2] : HAc, HCl, HNO_3, HF. Bien qu'alléchantes dans leur principe, ces techniques souffrent d'un évident manque de contrôle et de sélectivité (McCarty *et al.*, 1998 ; Dold, 2003); défauts que certains jugent rédhibitoires. Aujourd'hui, on tend plutôt à privilégier une extraction unique (Chaignon *et al.*, 2003; Feng *et al.*, 2005), plus facile à maîtriser et dont les résultats sont plus simples à interpréter.

Une autre approche, bien plus reproductible, consiste à mesurer les teneurs en éléments traces sur la totalité du matériel. La discrimination anthropique *vs* naturel s'opère alors grâce à la normalisation par un élément lithophile, par exemple le Ti, le Th, l'Al, le Sc, ou une terre rare qui ne possède pas d'origine anthropique notable (e.g. Grousset *et al.*, 1995 ; Martinez-Cortizas *et al.*, 1997 ; Schettler et Romer, 1998 ; Weiss *et al.*, 2002), voire la quantité de matière minérale (West *et al.*, 1997, Alfonso *et al.*, 2001). Le principe de cette approche repose sur l'hypothèse suivante : dans les conditions naturelles, il devrait exister une relation de proportionnalité entre les teneurs en métaux géogènes (M) et un des éléments lithophiles précités (L). Quand ce rapport M/L est connu, la contribution anthropique peut alors être déduite en utilisant les concentrations de l'élément lithophile retenu comme substitut à la composante métallique naturelle, au facteur M/L près. Certains choisissent d'utiliser les teneurs moyennes de la croûte continentale supérieure pour déterminer le rapport M/L, mais ce choix est critiquable dans la mesure où il s'agit d'estimations grossières qui ne tiennent pas compte des caractéristiques du site étudié ni de la géologie locale (Reinmann et de Carita, 2000, 2005). Il est donc préférable d'obtenir ce coefficient à partir d'échantillons locaux qui ne montrent pas d'influence anthropique notable. Dans le cas des enregistrements sédimentaires ou des sols, il s'agit alors de cibler des niveaux suffisamment profonds pour qu'ils soient exempts de contamination. Dans la séquence tourbeuse représentée Figure 2, la constance du rapport Pb/Sc sous 150 cm de profondeur suggère l'absence de contamination significative[3]. Cette valeur, déterminée localement est alors utilisée pour isoler la contribution anthropique ($Pb_{Anthr.}$) en soustrayant la part naturelle ($Pb_{Nat.}$), estimée à partir de la teneur en Sc, de la concentration totale ($Pb_{Tot.}$).

---

[2] Résultats publiés sous la forme : Monna, F., Clauer N., Toulkeridis, T., Lancelot, J. (2000) Influence of anthropogenic activity on the lead isotope signature of Thau lake sediments (Southern France): origins and temporal evolution. *Applied Geochemistry*. 15, 1291-1305.

[3] Résultats publiés sous la forme : Monna, F., Petit, C., Guillaumet, J.-P., Jouffroy-Bapicot, I., Blanchot, C., Dominik, J., Losno, R., Richard, H., Lévêque, J., Chateau, C. (2004) History and environmental impact of mining activity in Celtic Aeduan territory recorded in a peat-bog (Morvan – France). *Environmental Science and Technology*, 38, 3, 657-673. Cf. ANNEXES.

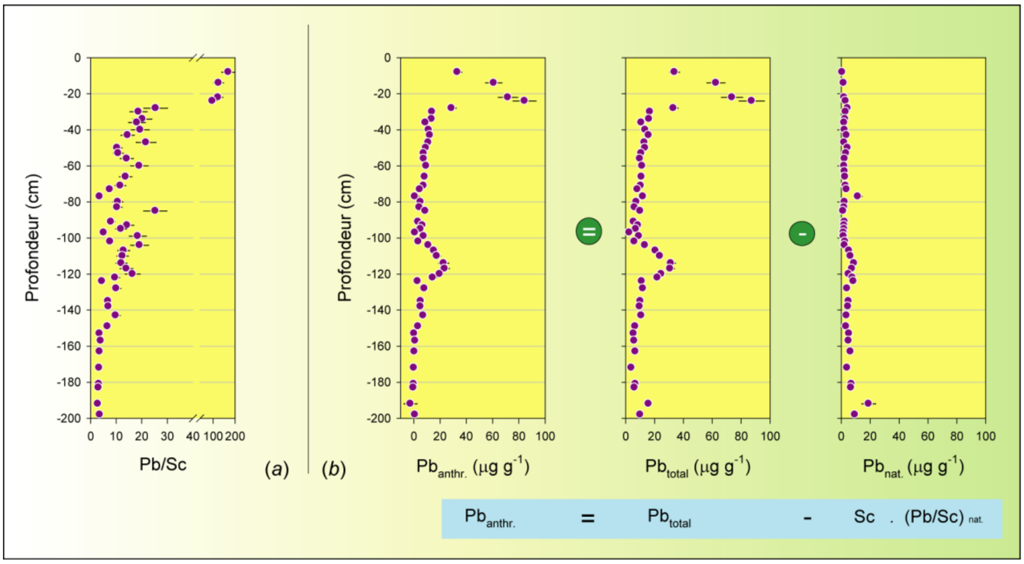

Figure 2 : (a) Rapport Pb/Sc et (b) estimation de la contribution anthropique en plomb dans une carotte de tourbe prélevée dans le Morvan près du site celtique de Bibracte[3].

Les techniques isotopiques, initialement développées pour la radiochronologie et le traçage géologique, vont s'avérer très utiles en sciences de l'environnement. De par leurs sensibilités, elles vont permettre une mise en évidence de l'influence anthropique, tout au moins pour le plomb. Elles peuvent même trahir l'origine du métal sous certaines conditions (voir encadré ci-après pour le principe).

Le composant anthropique : une réalité complexe. A ce point, il est nécessaire de souligner que la réalité cachée derrière la dénomination générique « anthropique » est souvent complexe : un échantillon contaminé, prélevé en milieu naturel, l'est rarement du fait d'une source unique de pollution. Après avoir isolé le signal purement anthropique et sa signature isotopique, on peut tenter une comparaison avec les sources potentielles dont les compositions isotopiques ont été déterminées au préalable. Si une source prédomine largement alors la détermination de l'origine peut être assez simple. C'est le cas de l'exemple ci-dessous mené durant mon stage postdoctoral à l'Université de Genève sous la direction scientifique de Janusz Dominik. Il s'agissait d'identifier l'origine des métaux dans une carotte de sédiments lacustres prélevée au large de Lausanne, dans la Baie de Vidy[4]. Ici, sans les analyses isotopiques, nous serions tentés d'interpréter les variations du plomb (Figure 3a) comme une conséquence directe des émissions automobiles : intensification de l'utilisation des carburants plombés dans les années 1960, croissance drastique jusque dans les années 1970, diminution des teneurs en plomb tétraéthyl dans les essences, introduction des additifs de substitution (1985 en Suisse). Or, ce scénario n'est pas compatible avec l'évolution des valeurs isotopiques du plomb contenu dans le sédiment (Figure 3b). Sur les 30 dernières années, le contaminant présente une signature $^{206}Pb/^{207}Pb$ voisine de 1.14, très différente de celle du plomb contenu

---

[4] Résultats publiés sous la forme : Monna, F., Dominik, J., Loizeau, J.-L. Pardos, M., Arpagaus, P. (1999) Origin and evolution of Pb in sediments of lake Geneva (Switzerland - France). Establishing a stable Pb record. *Environmental Science and Technolology*. 33, 2850-2857. Cf. ANNEXES.

La technique isotopique[5]

Le plomb possède des caractéristiques uniques qui le rendent particulièrement bien adapté à l'étude géochimique (voir Komárek *et al.*, 2008 pour un inventaire des utilisations des isotopes du plomb en environnement). Il est composé de quatre isotopes stables : ^{204}Pb, ^{206}Pb, ^{207}Pb et ^{208}Pb. Le premier de ces isotopes (^{204}Pb) n'est pas radiogénique, c'est-à-dire qu'il n'est pas issu de la désintégration d'un isotope radioactif. Son abondance est donc restée identique depuis la formation de la Terre. Les trois autres isotopes (^{206}Pb, ^{207}Pb et ^{208}Pb) sont produits de façon continue au cours du temps par la désintégration d'isotopes radioactifs : ^{238}U, ^{235}U et ^{232}Th. Pour simplifier, lors de la ségrégation d'une minéralisation, en général sulfurée, le plomb est isolé de ses isotopes pères (U et Th); sa composition isotopique s'en trouve « gelée »; c'est-à-dire qu'elle n'évolue plus à partir de la cristallisation (Faure, 1986 ; Kramers et Tolstikhin, 1997). Inversement, dans des gisements plus jeunes, l'uranium et le thorium ont eu le temps de produire une plus grande quantité de plomb radiogénique avant ségrégation. Pour des raisons purement mathématiques, les compositions isotopiques sont généralement exprimées par rapport à l'isotope stable ^{204}Pb : ^{206}Pb/^{204}Pb, ^{207}Pb/^{204}Pb et ^{208}Pb/^{204}Pb. Cependant, par tradition et pour des raisons analytiques, on utilisera plutôt en environnement les rapports ^{206}Pb/^{207}Pb, ^{208}Pb/^{207}Pb et ^{208}Pb/^{206}Pb. En raison de la différence existant entre les périodes des deux isotopes pères: ^{235}U et ^{238}U (0,70 Ga contre 4,47 Ga), l'essentiel du ^{207}Pb radiogénique a été produit pendant la première moitié de l'histoire terrestre, alors que la production en ^{206}Pb était plus lente. Au contraire, aujourd'hui on peut considérer l'isotope ^{207}Pb comme pratiquement constant, tandis que l'abondance en ^{206}Pb ne cesse de progresser par lente désintégration de ^{238}U restant. Les rapports ^{206}Pb/^{207}Pb permettent donc de distinguer un plomb issu d'une minéralisation ancienne de celui, plus radiogénique, continuellement produit par ses isotopes pères, comme c'est le cas dans les roches et des sols.

En Europe de l'Ouest l'exploitation des gisements de Pb(-Zn) a considérablement diminué durant les 40 dernières années pour cesser totalement dans les années 1990 suite à la pression environnementale, mais aussi en raison des évolutions considérables du marché des métaux. En conséquence, aujourd'hui tout le plomb utilisé par l'industrie de l'U.E. est importé depuis des gisements situés généralement sur d'autres continents. Ces derniers, essentiellement précambriens, sont caractérisés par des signatures isotopiques bien moins radiogéniques que celles du plomb naturellement présent dans les roches et les sols domestiques. Dans l'environnement, on peut donc espérer différencier par leurs compositions isotopiques au moins deux grands composants : le plomb anthropique (importé) et le plomb géogène, local (Hamelin *et al.*, 1989 ; Grousset *et al.*, 1994). En fait, il a même été démontré en Europe de l'Ouest que le plomb anthropique provient de deux sources majeures : le plomb ajouté comme antidétonant dans les essences et celui plus généralement utilisé par l'industrie (Elbaz-Poulichet *et al.*, 1984, 1986; Véron *et al.*, 1999 ; Widory *et al.*, 2004). Les différences des abondances isotopiques effectivement observées dans ces deux groupes dérivent essentiellement de l'origine des importations. Au cours de mon doctorat et en collaboration avec Ian Croudace (Southampton Oceanography Centre) et Andrew Cundy (Brunel University), j'ai eu l'occasion de faire le point sur les différentes sources en France et au Royaume Uni. Ce travail constitue encore aujourd'hui une base de données fréquemment utilisée par la communauté scientifique internationale[6].

dans les essences suisses à la même époque: ^{206}Pb/^{207}Pb = 1.11-1.12 (Chiaradia et Cupelin, 2000). En fait, ces résultats suggèrent qu'il s'agit à plus de 90% d'un plomb émis par la station de traitement des eaux usées de Lausanne, qui a rejeté ses effluents dans la zone d'étude à partir de 1964, et dont la signature typique

---

[5] Partie publiée sous la forme : Monna, F. (2001) Un héritage de plomb. *La Recherche*. 340, 50-54.

[6] Résultats publiés sous la forme : Monna, F., Lancelot, J., Croudace, I., Cundy, A.B., Lewis, T. (1997) Pb isotopic signature of urban air in France and in UK: Implications on Pb pollution sources. *Environmental Science and Technology*, 31, 2277-2286. Cf. ANNEXES.

est comparable à celles observées dans les sédiments les plus récents. En l'absence d'activités industrielles polluantes majeures, l'augmentation des teneurs lors de la mise en place de la station s'explique tout simplement par un effet de proximité des effluents, alors qu'auparavant les apports au lac étaient plus diffus. La diminution des flux observés pendant dans les années 1970 est vraisemblablement due à l'amélioration des conditions de traitement des eaux usées. L'analyse isotopique lève donc l'ambiguïté quant à l'origine de la pollution. Ces interprétations ont plus tard été confirmées par plusieurs études complémentaires, dont deux auxquelles j'ai participé[7,8]. Ces dernières, qui avaient pour but de spatialiser l'information environnementale au sein de la Baie de Vidy, ont clairement mis en évidence un gradient de pollution centré sur zone où les effluents de la station d'épuration sont rejetés dans le Lac Léman.

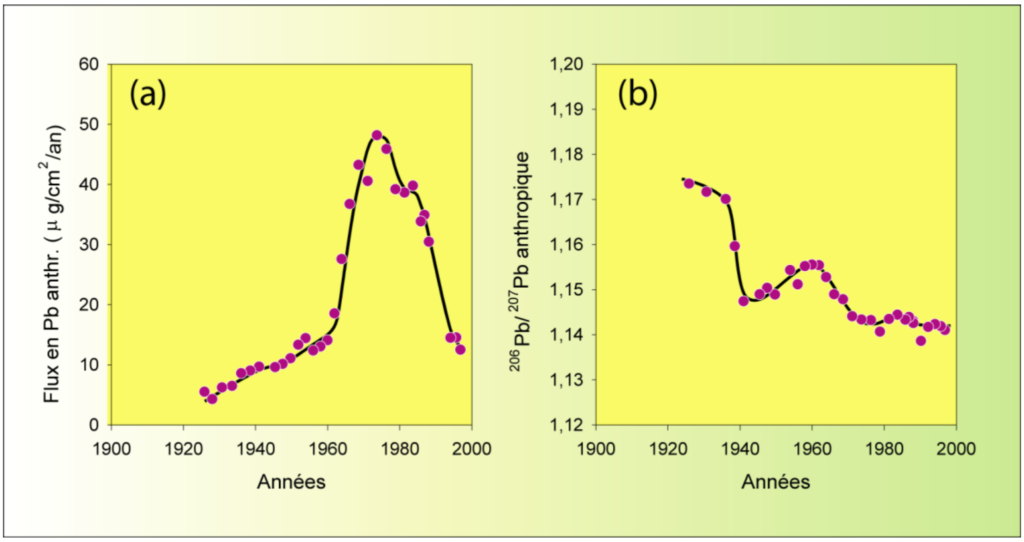

Figure 3 : (a) Evolution temporelle des flux en plomb anthropique dans la carotte BV, prélevée au large de la ville de Lausanne dans la Baie de Vidy. (b) Evolution temporelle du rapport $^{206}Pb/^{207}Pb$ du composant anthropique[4].

Dans cet exemple, il est clair que la connaissance de l'évolution de la signature isotopique du composant anthropique dans le sédiment est essentielle pour identifier l'origine. A la Baie de Vidy, cela ne posait pas de problème particulier dans la mesure où un impact anthropique oblitérait largement le 'fond naturel'. Mais une telle approche peut devenir délicate dans le cas d'une contamination plus discrète. Examinons la situation d'un point de vue théorique. Il est bien connu que l'équation d'un mélange impliquant deux sources, chacune caractérisée par sa propre concentration et sa propre composition isotopique, correspond à une hyperbole dans un diagramme $(^{206}Pb/^{207}Pb)_{\text{mélange}}$ *vs*. $Pb_{\text{mélange}}$, soit à une droite si la représentation $(^{206}Pb/^{207}Pb)_{\text{mélange}}$ *vs*. $1/Pb_{\text{mélange}}$ est préférée. De telles représentations sont très classiques. Elles servent même d'illustrations à la couverture

---

[7] Etude publiée sous la forme : Loizeau, J.-L.; Rozé, S., Peytremann, C., Monna, F., Dominik, J. (2003) Mapping sediment accumulation rate by using volume magnetic susceptibility core correlation in a contaminated bay (Lake Geneva, Switzerland). *Eclogae geologicae Helvetiae*, 96, 73–79.

[8] Etude publiée sous la forme : Loizeau, J.-L., Pardos, M., Monna, F., Peytremann, C., Haller, L., Dominik, J. (2004) The impact of a sewage treatment plant's effluent on sediment quality in a small bay in Lake Geneva (Switzerland–France). Part 2: Temporal evolution of heavy metals. *Lakes & Reservoirs: Research and Management*, 9, 53–63.

du remarquable livre de Günter Faure, véritable bible de la géochimie isotopique (Faure, 1986). Dans le cas d'un enregistrement sédimentaire, si le rapport 1/Pb est utilisé en abscisse, l'intercepte sur l'axe des ordonnées d'une ligne reliant le 'bruit de fond' – censé être constant tant en concentration qu'en origine - à un échantillon contaminé devrait fournir graphiquement la signature isotopique moyenne des polluants mis en jeu (dans cette situation on considère que le polluant est du plomb pur). Cependant, comme nous l'avons vu, le 'bruit de fond' (ou tout au moins la composante naturelle) peut avoir considérablement varié en magnitude aussi bien qu'en origine au cours du temps, de sorte que l'équation de mélange n'est plus valide : le pole 'bruit de fond' est très dispersé dans le diagramme et ne peut fournir de point d'ancrage à la droite permettant la détermination graphique du signal anthropique.

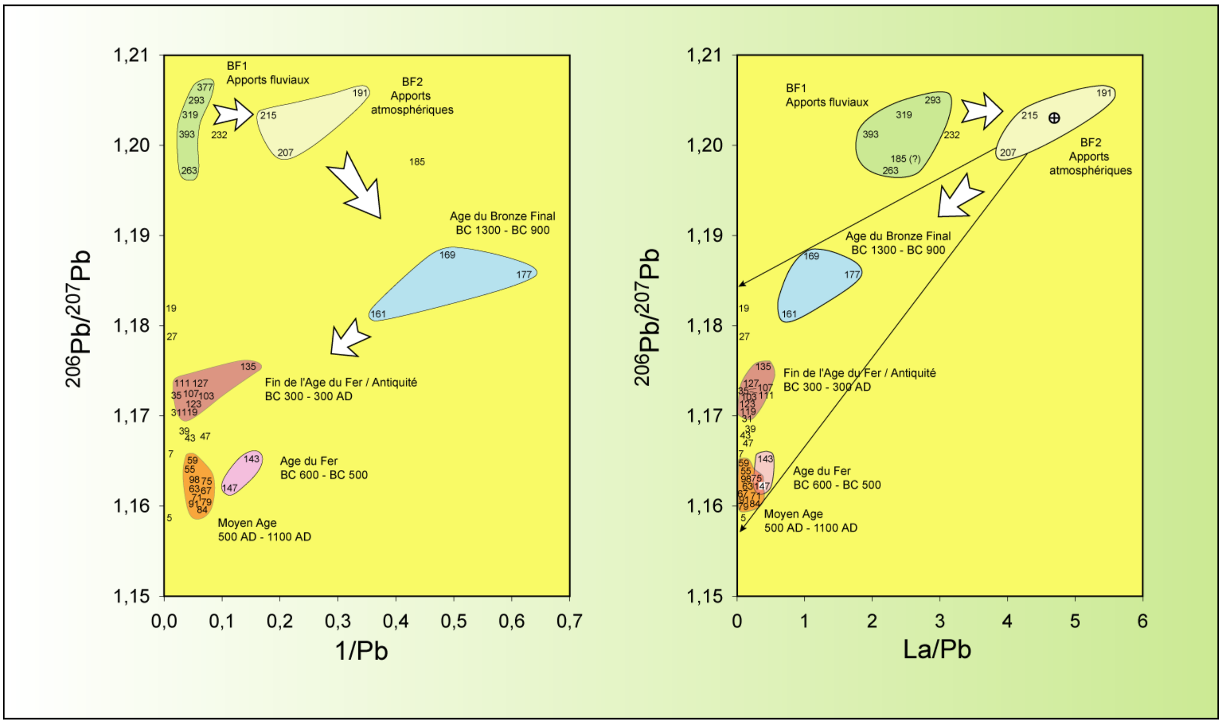

Figure 4 : Rapports $^{206}Pb/^{207}Pb$ vs 1/Pb et (b) Rapports $^{206}Pb/^{207}Pb$ vs La/Pb. Les échantillons proviennent d'une carotte de tourbe prélevées près d'Ogeu par Didier Galop dans un méandre abandonné (Monna *et al.*, en prep.). Les nombres correspondent aux profondeurs auxquelles les échantillons ont été prélevés.

L'utilisation des rapports Sc/Pb ou La/Pb à la place de 1/Pb comme axe des abscisses va permettre d'éliminer ces variations puisque Pb naturel, Sc et La sont supposés varier proportionnellement. Cette représentation originale est donc particulièrement bien adaptée aux situations où la composante naturelle varie suffisamment pour ne pas être négligeable. Dans l'exemple de la séquence tourbeuse présentée dans la Figure 4, le 'bruit de fond' est variable tant en concentration qu'en origine. Sous 230 cm de profondeur les concentrations en Pb sont élevées (BF1). Ce matériel est essentiellement constitué de dépôts alluviaux. A partir de 230 cm, la tourbière devenant ombrogène, les apports alluviaux décroissent et la composante naturelle n'est plus représentée que par les apports atmosphériques (BF2). A partir de l'Age du Bronze, la présence de polluant est identifiée, notamment par la baisse des rapports La/Pb (Figure 4b) et

^{206}Pb/^{207}Pb. Avec la représentation utilisant La/Pb en abscisse, il devient possible d'évaluer la signature isotopique moyenne des polluants mis en jeu au cours de chaque période culturelle : ^{206}Pb/^{207}Pb ~ 1 ,18 à l'Age du Bronze, ~ 1,16 à l'Age du Fer, ~ 1,17 à l'antiquité, ~ 1,16 au Moyen Age…

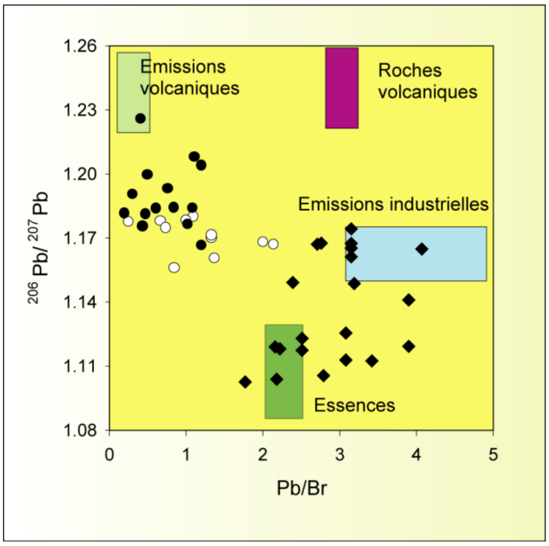

Figure 5 : ^{206}Pb/^{207}Pb en fonction des rapports Pb/Br dans les particules en suspension collectées en milieu urbain ou industriel (◆), les lichens échantillonnés sur l'Etna (○) et à Vulcano (●)[9]. Les sources potentielles (émissions volcaniques, roches, émissions industrielles et essences sont représentées par des rectangles afin de faciliter l'interprétation des résultats obtenus sur les lichens et les particules en suspension.

Quand le nombre de sources mises en jeu est grand, les choses se compliquent ; les compositions isotopiques des différentes sources apparaissant le plus souvent en positions colinéaires dans les diagrammes isotopiques ^{206}Pb/^{207}Pb *vs* ^{208}Pb/^{206}Pb ou ^{206}Pb/^{204}Pb *vs* ^{207}Pb/^{204}Pb. La signature isotopique mesurée dans un échantillon contaminé peut donc résulter, par combinaison linéaire, d'une infinité de mélanges qui impliquent plusieurs sources dans des proportions variables. En conséquence, les isotopes du plomb ne fournissent pas de réponses univoques et il devient nécessaire de rechercher un ou plusieurs autres paramètres discriminants. Examinons un nouvel exemple utilisant cette fois le rapport Pb/Br afin d'étendre les capacités de discrimination. Le brome était, il y a peu, ajouté en grande quantité aux carburants afin de réduire la formation d'oxydes de plomb lors de la combustion. Le rapport Pb/Br des particules ainsi produites à l'époque était bien connu ~ 2,5 –2,7 (Harrison et Sturges, 1983), tandis que le matériel émis par l'activité industrielle montrait des valeurs bien plus élevées. Sa combinaison avec les rapports isotopiques du plomb va permettre de préciser l'origine de la pollution atmosphérique dans une zone relativement complexe : la Sicile. Ce travail a été mené en collaboration avec l'équipe dirigée par Gaetano Dongarra (Université de Palerme)[9,10]. Sur l'île, plusieurs sources potentielles de plomb coexistent (Squeri *et al.*, 1992 ; Di Pietro *et al.*, 1994). Pour simplifier, on trouve de façon naturelle le plomb à l'état de trace dans les roches et les sols, et le plomb issu de l'activité volcanique, qu'elle se matérialise par dégazage passif ou actif, lors des éruptions. Quant au plomb d'origine anthropique, il se divisait en 1998 en deux groupes majeurs : les additifs antidétonants des essences et les émissions industrielles. Des lichens ont donc été prélevés dans les zones proches des édifices volcaniques : l'Etna et l'île de Vulcano. En revanche, en milieu urbain ou industriel, les analyses ont été réa-

---

[9] Résultats publiés sous la forme : Monna, F., Aiuppa A., Varrica D., Dongarrà G. (1999) Pb isotopic compositions in lichens and aerosols from Eastern Sicily: insights on the regional impact of volcanoes on the environment. *Environmental Science and Technolology*. 33, 2517 - 2523. Cf. ANNEXES.

[10] Résultats publiés sous la forme : Monna, F., Varrica, D., Aiuppa, A., Dongarrà, G. (2001) Le point sur l'origine du plomb dans l'atmosphère en Sicile. Apport de la géochimie isotopique et choix du support. *Archives des Sciences de Genève*, 54, 3, 205-222.

lisées sur particules atmosphériques. La combinaison des compositions isotopiques du plomb avec le rapport Pb/Br apparait particulièrement efficace pour déterminer les influences respectives des différentes sources. La position des lichens dans la Figure 5 souligne l'influence des émissions volcaniques, plus particulièrement sur l'île de Vulcano où les émissions anthropiques sont mineures. Dans tous les cas, l'influence du substrat est négligeable comme le suggèrent par ailleurs les rapports Pb/Sc non reportés ici.

AXE 2 : Transferts des métaux dans les environnements superficiels

Depuis plusieurs milliers d'années, l'homme n'a cessé d'exploiter et de redistribuer les métaux dans les environnements superficiels. Si dans certains compartiments comme l'atmosphère, les eaux de surface, ou la biosphère, les ***temps de résidence*** *sont extrêmement courts, il n'en est pas de même dans les sols et les sédiments où l'influence d'un passé lointain peut être encore noté aujourd'hui. Le défi majeur pour le développement de nos sociétés consiste désormais à minimiser autant que possible l'impact de l'homme sur ces milieux.* ***Comprendre et modéliser*** *le transfert et la biodisponibilité des polluants métalliques sur le long terme participent à cet enjeu.*

Il est bien sûr impossible de dresser ici un inventaire exhaustif des travaux menés sur les transferts de métaux aux interfaces de l'environnement tant ces études sont nombreuses et variées. Celles-ci ont permis de dresser un portrait assez précis du cycle biogéochimique des métaux dans les environnements superficiels. Les temps de résidence des métaux émis dans l'atmosphère sont généralement très courts, de l'ordre de quelques jours, et dépendent largement de la taille des particules auxquelles ils sont associés, des modalités d'émission et des conditions météorologiques. Bien que le dépôt ait essentiellement lieu au voisinage de la zone d'émission, une fraction de polluants est susceptible de voyager sur de très longues distances, comme le démontrent les études spectaculaires réalisées dans les zones polaires (Boutron *et al*., 1991 ; Hong *et al*. 1994). Une fois déposés à la surface des sols, les métaux s'associent souvent fortement aux constituants du sol qu'ils soient minéraux ou organiques. Ces derniers constituent en général un compartiment d'accumulation et de stockage, mais une fraction, souvent assez faible, est susceptible de migrer en profondeur pour, *in fine*, intégrer les eaux souterraines. Outre les rejets anthropiques directs, la présence de métal dans les eaux de surface est le plus souvent liée à l'érosion mécanique des sols préalablement pollués et au ruissellement des eaux de pluies. Les métaux sont généralement associés à la matière particulaire, présents sous forme colloïdale, plus rarement sous forme dissoute ; la partition entre ces trois formes dépendant largement du pH. Lorsque la sédimentation des particules intervient en milieu protégé (e.g. lacustre ou marin), le contaminant est stocké sur le long terme. Un transfert vers la biosphère est possible à partir de chaque compartiment : atmosphère, sol, eau, sédiment. Néanmoins, malgré l'abondance et la variété des recherches effectuées, de nombreuses questions persistent (notamment à propos de la biodisponibilité et du comportement des métaux sur le long terme) parce que les interactions dans le milieu naturel sont très complexes. En conséquence, il est souvent difficile de tirer des conclusions générales à partir d'enseignements durement acquis dans un cadre précis, puis de les appliquer en d'autres circonstances.

Au cours de mon doctorat effectué sous la direction scientifique de Joël Lancelot, j'ai examiné plus particulièrement la dynamique des transferts du Pb, du Zn, du Cd, et du Tl dans les eaux de surface et dans les sédiments sur la zone de l'étang de Thau. Le suivi des eaux superficielles a permis d'établir un modèle rudimentaire qui souligne néanmoins l'influence des conditions météorologiques[11]. Il a d'ailleurs été confirmé par la suite (Pettelet *et al.*, 1997). L'étude de quatre séquences sédimentaires prélevées au sein de l'étang a permis de mettre en évidence la contamination métallique provenant de la ville de Sète, mais aussi les apports sédimentaires liés aux crues violentes qui ont lieu épisodiquement dans la région de Montpellier[2,12]. Dans les années post-thèse, mes recherches sur les sédiments et les eaux se sont poursuivies à travers trois programmes. Les deux premiers traitaient de l'origine de la pollution métallique accumulée dans les sédiments du Lac Léman[4] (déjà évoqué précédemment) et d'une baie proche de Rio de Janeiro[13]. Le troisième concernait les facteurs qui contrôlent les dépôts de ^{7}Be et ^{210}Pb lors des précipitations. Cette dernière étude[14] a été réalisée par Stéphane Caillet, étudiant en Master 2 à l'Université de Génève, sous ma direction et celle de Janusz Dominik. Cependant, depuis 1999, j'ai abordé deux nouveaux thèmes: (i) l'évaluation des capacités des organismes bio-accumulateurs (lichens, aiguilles de pins, broméliacées) et des géo-accumulateurs (i.e. façades de bâtiments) à fournir une indication sur la pollution métallique dans l'atmosphère, et (ii) le devenir des métaux dans les sols ; ce dernier thème étant mené en étroite collaboration avec Folkert van Oort (INRA Versailles), spécialiste des relations entre comportement des sols et distribution des métaux.

---

[11] Résultats publiés sous la forme : Monna, F., Ben Othman, D., Luck, J.-M. (1995) Pb isotopes and Pb, Zn and Cd concentrations in the rivers feeding a coastal pond (Thau, southern France): constraints on the origin(s) and flux(es) of metals. *The Science of the Total Environment*. 166, 19-34.

[12] Résultats publiés sous la forme : Monna, F., Lancelot, J., Bernat, M., Mercadier, H. (1997) Taux de sédimentation dans l'étang de Thau (Languedoc) à partir des données géochronologiques, géochimiques et morphostratigraphiques. *Oceanologica Acta*, 20, N4, 627-638.

[13] Résultats publiés sous la forme : Marques, A.N., Monna, F., da Silva Filho, E.V., Fernex, F., Lamego Simões Filho. (2006) Apparent discrepancy in contamination history of a subtropical estuary evaluated through ^{210}Pb profile and chronostratigraphical markers. *Marine Pollution Bulletin*. 52, 532-539.

[14] Résultats publiés sous la forme: Caillet, S., Arpagaus, P., Monna, F., Dominik, J. (2001) Factors controlling ^{7}Be and ^{210}Pb atmospheric deposition as revealed with sampling by individual rain events in the region of Geneva, Switzerland. *Journal of Environmental Radioactivity*. 53, 241-256.

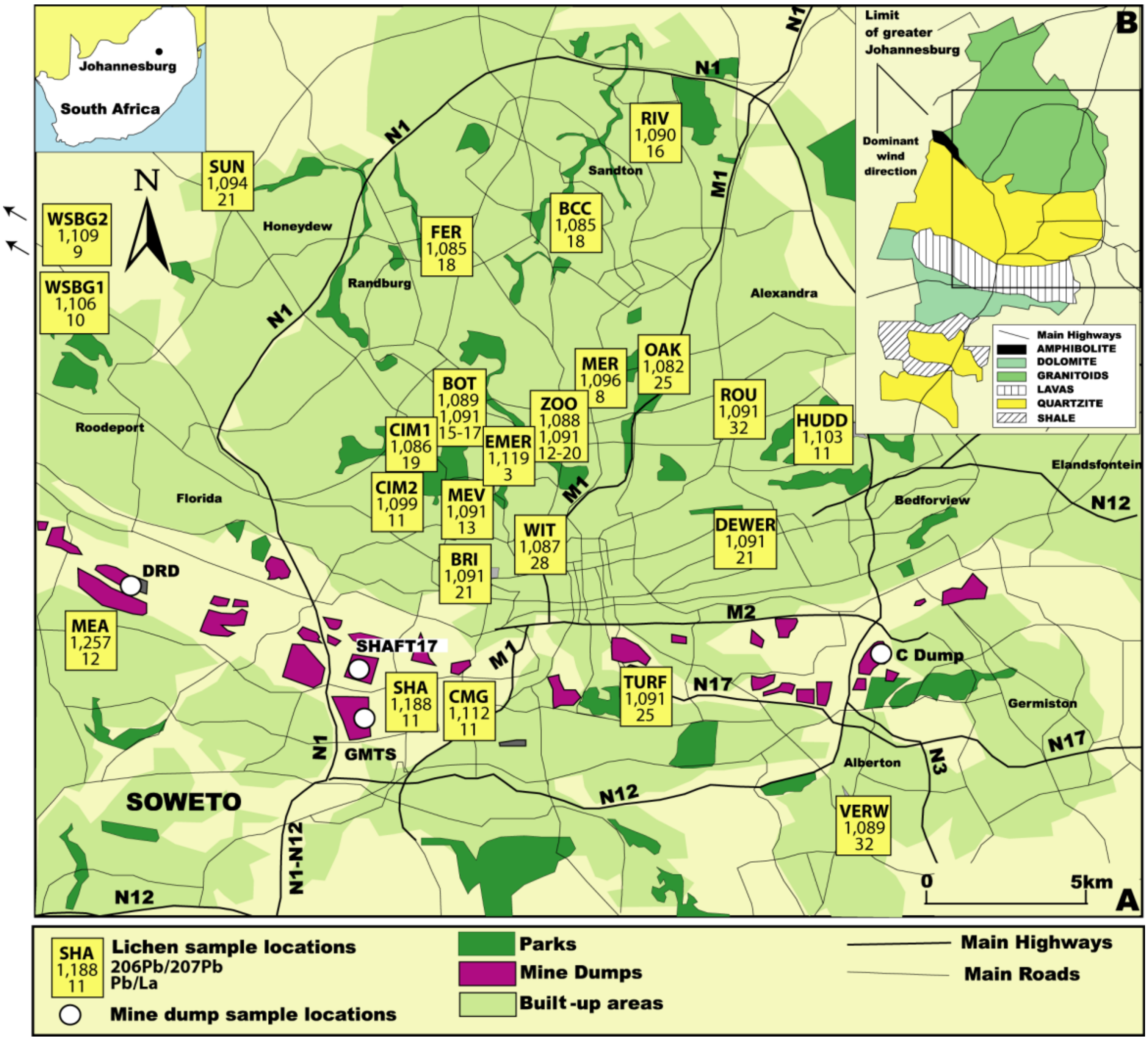

Figure 6 : (a) Carte de Johannesburg et position des lichens échantillonnés. (b) Carte lithologique simplifiée. Les échantillons WSBG1 et WSBG2 ont été prélevés à environ 30 km de Johannesburg. Les valeurs des rapports $^{206}Pb/^{207}Pb$ et Pb/La des différents échantillons sont reportés sur la carte[15].

Bioaccumulateurs et géoaccumulateurs. Les matières en suspension collectées sur des filtres à des pas de temps plus ou moins longs constituent de bons supports pour étudier la qualité de l'air. Néanmoins, les métaux qui leur sont associés montrent en général une grande variabilité tant en concentration qu'en origine (Espinosa *et al*., 2001 ; Flament *et al*., 2002 ; Chen *et al*., 2005). Pour pallier ces problèmes, une alternative consiste à cibler des organismes intégrateurs, tels que les lichens (Garty, 1985 ; Nimis *et al*., 1990 ; Bargagli, 1993 ; Doucet et Carignan, 2001). Ce sont des végétaux à croissance lente. Au cours de leur vie, ils sont censés intégrer les éléments chimiques (sous forme liquide, gazeuse ou particulaire venant de l'atmosphère), mais pas du substrat (arbres ou roches) sur lequel ils vivent (Getty *et al*., 1999; Loppi et Pirintsos, 2003). Leur métabolisme n'est toujours pas parfaitement compris : tandis que la plupart des auteurs imaginent que les lichens tendent à moyenner ou à accumuler le signal atmosphérique sur plusieurs années (Carignan *et al*., 2002), d'autres suggèrent de rapides changements de composition chimique en relation avec la magnitude de la pollution atmosphérique, en d'autres termes la présence de mécanismes d'excrétion (Spiro *et al.*, 2004). Leur âge ne peut être déterminé précisément, pourtant il est clair que ce paramètre doit être corrigé d'une façon ou d'une autre afin de rendre comparables les résultats.

Figure 7 : Marc Poujol échantillonnant un stérile minier près de Johannesburg[15].

Prenons dans un premier temps, l'exemple de Johannesburg. En 2000, parmi toutes les sources potentielles, le plomb issu des émissions automobiles prédominaient largement dans l'atmosphère de la ville (Formenti *et al.*, 1998). Bien que le carburant sans plomb fût alors disponible sur le marché, il ne représentait que 20% des ventes. D'autres sources pouvaient néanmoins être invoquées : les émissions résultant de l'utilisation domestique de charbon, les apports provenant des routes non bitumées en particulier dans les townships, les émissions atmosphériques issues des quelques industries métallurgiques, et bien sûr les stériles miniers qui balafrent la ville suivant un axe Est – Ouest (Figures 6 & 7). Ceci signifie que dans les quartiers pauvres adjacents aux zones minières (historiquement Noirs), les émissions de poussières issues des stériles miniers pouvaient s'ajouter à celles issues du trafic automobile, et étendre ainsi les risques respiratoires des populations vivant aux alentours. A l'initiative de Marc Poujol, alors en poste à l'Economic Geology Research Institute de l'Université de Witwatersrand, un projet regroupant français (Rémi Losno), suisse (Janusz Dominik) et sud africains (Harold Annegarn et Henk Coetzee) a été monté, puis financé par les accords CNRS/NFS, pour évaluer ce risque[15]. Une trentaine de lichens, utilisés comme bioaccumulateurs, des essences, des charbons et des échantillons de stériles miniers (Figure 7) ont été prélevés pour déterminer leurs compositions isotopiques et chimiques. Si les essences et les charbons montrent des signatures isotopiques 'classiques' avec des rapports $^{206}Pb/^{207}Pb$ de l'ordre de 1,067-1,090 et de 1,210 respectivement, les échantillons collectés au sein des stériles miniers présentent des signatures isotopiques tout à fait exceptionnelles : $^{206}Pb/^{207}Pb = 2,182 - 2,882$, du fait des fortes teneurs en uranium qui caractérisent les gisements d'or du Witwatersrand. Les résultats obtenus pour les lichens, exprimés sous forme de rapports $^{206}Pb/^{207}Pb$ et Pb/La sont reportés dans la Figure 6. Il apparait nettement que l'influence des stériles miniers est géographiquement limitée, probablement du fait de la grande taille des particules émises à partir de ces zones. Si l'utilisation domestique de charbons peut être reconnue grâce à leurs signatures isotopiques, cette source reste mineure face aux émissions liées au trafic automobile. Cette étude présente

---

[15] Résultats publiés sous la forme : Monna, F., Poujol, M., Annegarn, H., Losno, R., Coetze, H., Dominik, J. (2006) Origin of atmospheric lead in Johannesburg, South Africa. *Atmospheric Environment.* 40, 6554-6566. Cf. ANNEXES.

l'intérêt d'avoir été réalisée avant l'abandon de l'essence au plomb. Elle fournit donc une base pour de futures comparaisons. Signalons que deux autres projets utilisant les lichens sont en cours. Au Maroc, il s'agit d'évaluer la dispersion des polluants autour de la ville d'Agadir et des mines de l'Anti-Atlas (en collaboration avec Lhoussaine Bouchaou, Université d'Agadir). Au Brésil, nous avons pour objectif (i) de déterminer les capacités respectives du genre *Parmelia crinata* (un lichen) et *Tillandsia usneoides* (une broméliacée) à accumuler la pollution atmosphérique, (ii) d'évaluer la variabilité intra-site des deux espèces et de tester la robustesse et la représentativité des concentrations mesurées et des variables dérivées par normalisation, et (iii) de valider un modèle conceptuel de dispersion atmosphérique autour de la ville de Rio de Janeiro (en collaboration avec Aguinaldo Marquès Jr, Université de Nitéroi).

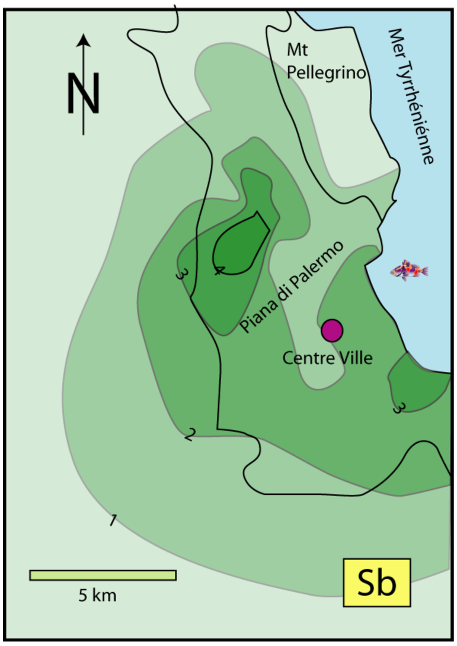

Figure 8 : Carte de distribution des concentrations en Sb ($\mu g\ g^{-1}$) établie à partir de 43 échantillons composites d'aiguilles de pins[16].

Outre les lichens, les parties aériennes de certaines plantes peuvent également collecter les métaux depuis l'atmosphère. Grâce à leur habilité à retenir certains métaux, les aiguilles de pin (*Pinus pinea* L.) sont quelquefois utilisées comme bioaccumulateurs (Bargagli *et al.*, 1991; Bargagli 1993; Dmuchowski et Bytnerowicz 1995). Ces conifères possèdent en outre l'avantage d'être facilement identifiables et abondants. Une étude a été menée en collaboration avec Gaetano Dongarra et des botanistes de l'Université de Palerme à partir d'échantillons composites d'aiguilles de pins dans le but d'estimer la dispersion des polluants autour de la ville de Palerme[16]. Un gradient de concentration est observé depuis le centre ville vers la périphérie pour le Pb, le Br, et le Sb, tous d'origine anthropique (Figure 8). Cependant les résultats isotopiques indiquent clairement qu'une partie importante du plomb mesuré dans les aiguilles de pin provient du sol. Les aiguilles de pins seraient donc moins adaptées que les lichens pour étudier la dispersion des polluants dans l'atmosphère. Notons que ces travaux ont été ensuite complétés par l'étude des particules atmosphériques[17,18].

Les recherches menées à partir d'indicateurs ou d'accumulateurs biologiques sont bien sûr subordonnées à l'occurrence des espèces considérées. En milieu urbain, une approche beaucoup plus naturelle consisterait à utiliser directement

---

[16] Résultats publiés sous la forme: Alaimo, M.G., Dongarra, G., Melati, M.R., Monna, F., Varrica, D. (2000) Recognition of environmental trace metal contamination using pine needles as bioindicators. The urban area of Palermo (Italy). *Environmental Geology*. 39, 8, 914-924.

[17] Résultats publiés sous la forme: Varrica, D., Dongarrà, G., Sabatino, G., Monna, F. (2003) Inorganic geochemistry of roadway dust from the metropolitan area of Palermo, Italy. *Environmental Geology*, 44, 222–230.

[18] Résultats publiés sous la forme: Aiuppa, A., Dongarrà, G., Varrica, D., Monna, F., Sabatino, G. (2001) Livelli di plombo nel particolato atmosferico dei centri urbani della Sicilia. *Aqua Aria*, 1, 99-105.

les façades de bâtiments comme indicateurs de la pollution atmosphérique à laquelle ils ont été soumis depuis leur construction (ou leur éventuel nettoyage). Il est bien connu que l'émission de dioxyde de soufre par l'activité anthropique provoque sur les bâtiments calcaires la cristallisation de gypse ($CaSO_4.2H_2O$) (Rodriguez-Navarro et Sebastian, 1996; Simao, 2006), préférentiellement sur les zones abritées de la pluie (Lefèvre et Ausset, 2002). Ce gypse incorpore les poussières ambiantes, les suies résultant des combustions et d'autres particules anthropiques d'origines variées, ce qui donne à la façade sa teinte sombre correspondant à la 'croûte noire' (Galletti *et al.*, 1997; Ausset, 1999). L'augmentation de la rugosité de surface consécutive à ces cristallisations étend également les capacités de captage mécanique des particules en suspension dans l'atmosphère. En 2006, j'ai initié un programme regroupant des géochimistes (Rémi Losno - Université de Paris XII -, Béatrice Marin - Université de Reims - et Janusz Dominik – Université de Genève), un spécialiste du bâti (Gilles Fronteau – Université de Reims), un géomagnéticien (François Lévêque – Université de La Rochelle) et un étudiant effectuant son stage de Master 1 sous ma direction scientifique (Aurélien Puertas). Le but était de tester les capacités des façades calcaires à retenir l'information environnementale et à fournir des indications sur la magnitude, l'origine et la dispersion des micropolluants métalliques en milieu urbain[19]. Certains paramètres magnétiques, comme la susceptibilité magnétique, peuvent être utiles pour atteindre cet objectif. En effet, les combustions à haute température produisent des sphérules magnétiques de tailles micrométriques qui sont très concentrées en métaux (Hunt *et al.*, 1984; Hoffman *et al.*, 1999). Ce matériel magnétique présente l'avantage d'être rapidement et précisément mesurable, de sorte qu'il est susceptible de fournir à bas coût un indicateur de pollution (Matzka et Maher, 1999 ; Petrovský *et al.*, 2000 ; Sagnotti *et al.*, 2006). Cependant, il n'avait jamais été testé sur le bâti.

La présente étude, menée à partir de plusieurs façades du lycée Carnot, construit fin XIX^{e} siècle à Dijon et aujourd'hui très exposé à la pollution urbaine, fournit des pistes de recherche originales et prometteuses. Il s'avère que les façades calcaires ont conservé des traces de la pollution atmosphérique passée (les émissions liées à l'utilisation de charbon sont par exemple toujours visibles), mais elles peuvent avoir été altérées du fait de l'exposition directe à la pluie ou du micro-ruissellement observé à la surface des pierres de construction. Les particules anthropiques et naturelles sont soumises à des mécanismes de compétition dynamique agissant entre les phénomènes de dépôt/précipitation et lessivage par la pluie. En conséquence, les comparaisons entre façades sont possibles à condition qu'elles soient peu exposées à la pluie battante, qu'elles aient approximativement le même âge, et que le matériau de construction possède un bruit de fond géochimique faible face à la contribution anthropique. Les résultats indiquent que le zinc, le cuivre, le cadmium et le soufre apparaissent comme des polluants diffus, au moins à l'échelle du lycée. En revanche, les teneurs en plomb et en arsenic sont géographiquement contrastées, suivant la proximité des sources émettrices. Signalons qu'aucun gradient vertical n'est observé (Figure 9). Ceci

---

[19] Résultats publiés sous la forme : Monna, F., Puertas, A., Lévêque, F., Losno, R., Fronteau, G., Marin, B., Dominik, J., Petit, C., Forel, B., Chateau, C. (2008) Geochemical records of limestone façades exposed to urban atmospheric contamination as monitoring tools? *Atmospheric Environment*, 42, 999-1011. Cf. ANNEXES.

suggère une intense homogénéisation des particules portant la pollution métallique à l'échelle de la rue, assimilé ici à un canyon urbain. Nous envisageons aujourd'hui de poursuivre les recherches sur ces '*géoaccumulateurs*' que sont les façades de bâtiments. Il s'agirait d'examiner plus particulièrement l'influence du micro-ruissellement sur les capacités de conservation des informations géochimiques et magnétiques. L'ensemble sera regardé à la lumière du degré d'altération du bâti. C'est la raison pour laquelle Christophe Durlet, spécialiste de la diagenèse en milieu carbonaté (Laboratoire Biogéosciences, Université de Bourgogne) complétera l'équipe.

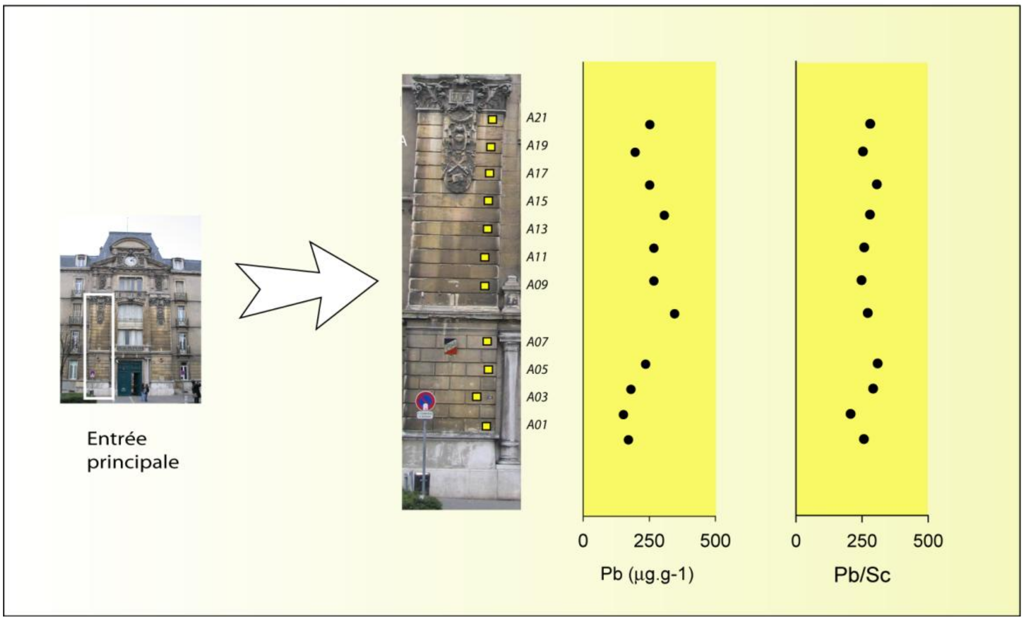

Figure 9 : Localisation des prélèvements sur la façade correspondant à l'entrée principale du lycée Carnot Dijon. Les échantillons ont été obtenus par grattage. Les deux diagrammes de droite représentent l'évolution des teneurs en Pb et des rapports Pb/Sc en fonction de l'altitude.

Immobilité ou mobilité des métaux dans les sols?

Dans les sols, le devenir des métaux est une question de première importance ; leur présence constituant à long terme un risque de pollution des eaux naturelles *via* les solutions de sols, et à court terme un risque de contamination de la végétation (van Oort *et al.*, 2006). En effet, bien que les métaux soient généralement piégés plus ou moins durablement par un grand nombre de constituants (matières organiques, oxydes et hydroxydes de fer et de manganèse, phyllosilicates, phosphates, carbonates…), une fraction non négligeable peut être mobilisée et migrer verticalement sous forme soluble ou sous forme colloïdale (Denaix *et al.*, 2001 ; Citeau *et al.*, 2003), ou bien intégrer la plante par sa rhizosphère pour finalement présenter une menace pour la santé humaine. Dans le milieu naturel, la complexité des interactions est considérable puisque la mobilité des métaux est gouvernée par de nombreux paramètres physicochimiques du sol, tels que le pH, la capacité d'échange cationique, la porosité, la nature des constituants du sol entre autres (Teutsch *et al.*, 2001; Hernandez *et al.*, 2003). A cela, il faut ajouter l'inévitable variabilité liée à l'exploitation humaine, comme par exemple l'interception du dépôt atmosphérique des polluants métalliques par la canopée et l'exportation suite aux récoltes (Jensen et Svensmark, 1989; Blum *et al*., 1997), mais aussi l'influence des pratiques culturales telles que le labour ou l'utilisation de fertilisants qui peuvent modifier largement les caractéristiques du sol (Andersen *et al*., 2002; Fernandez *et al*., 2007).

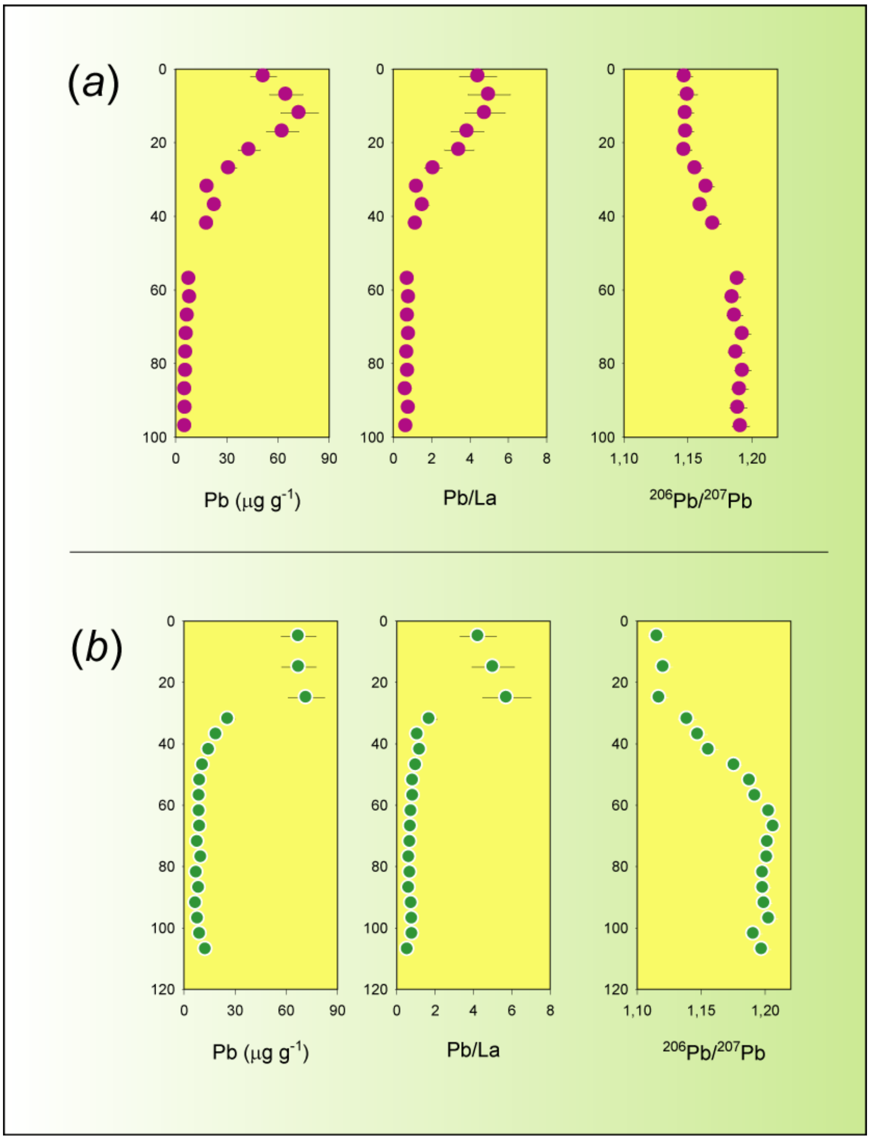

Figure 10 : Evolution des teneurs en Pb, des rapports Pb/La et des rapports ^{206}Pb/^{207}Pb dans le sol sous prairie (a) et dans le sol cultivé (b)[20].

C'est précisément le rôle de l'occupation des sols dans la migration du Pb que Christelle Fernandez a cherché à mettre en évidence dans le cadre de son doctorat (direction Folkert van Oort, INRA Versailles) ; travail auquel j'ai collaboré, notamment sur la partie isotopique. Il s'agissait d'examiner l'influence de l'utilisation des sols sur l'incorporation et la distribution du plomb d'origine anthropique à partir de deux sols voisins, tous deux ayant été soumis aux retombées atmosphériques d'une ancienne fonderie de zinc installée dans le Nord de la

France[20]. Les deux sols sélectionnés pour cette étude ont évolué à partir d'un substrat identique mais n'ont pas connu la même histoire agricole au cours du dernier siècle : l'un a été maintenu pendant près de 100 ans sous prairie pâturée, tandis que l'autre a été annuellement labouré et exploité pour la production de céréales. Il s'avère que l'incorporation verticale la plus importante est observée dans le sol sous prairie (Figure 10). Elle est en grande partie d'origine mécanique et est probablement liée à la forte activité des vers de terre. *A contrario*, le sol cultivé montre une forte accumulation dans l'horizon homogénéisé par le labour, et l'incorporation du plomb en profondeur est bien plus restreinte. Malgré des stocks de plomb anthropique très voisins (~28 et 21 g m^{-2}), il est important de signaler que les compositions isotopiques du plomb indiquent de façon surprenante (mais sans ambiguïté) que ces deux sols n'ont pas intégré le même type de mélange de plomb au cours du temps. De telles différences pourraient être dues aux apports de fertilisants, ou à un phénomène d'exportation lors des récoltes. Ce résultat illustre la difficulté de déterminer des comportements généraux pour les éléments présents à l'état de trace du fait de l'inhérente variabilité spatiale des sols ; d'où la nécessité de collecter un maximum d'informations historiques concernant leur utilisation et les pratiques agricoles liées. Quand bien même, cela pourrait être réalisé, la quantification des processus de transfert, et *a fortiori* de leur modélisation, se heurtent à deux difficultés majeures : (i) le manque de recul temporel puisque les phénomènes de migration dans les sols prennent place sur le très long terme, et (ii) la méconnaissance des flux de polluants au cours du temps. Le plus souvent, la question de la migration des métaux dans les sols est donc abordée de manière très simple, que certains pourraient même qualifier d'un peu trop simpliste, tant les contraintes sont peu réalistes. Par exemple, certains auteurs interprètent les profils observés comme résultant de la migration de composants déposés dans les années 1960-1970 (e.g. Erel, 1998). Si cette période est évidemment reconnue comme celle présentant la plus forte émission de contaminants métalliques dans l'atmosphère, il n'est sans doute pas raisonnable d'occulter l'ensemble des émissions antérieures (cf axe 4, Pyatt *et al.*, 2000). Les taux de migration ainsi calculés ont toutes les chances d'être fortement surestimés. C'est donc en contournant ces deux écueils liés à la temporalité des apports et des processus que des progrès notables pourront être réalisés dans la compréhension et la modélisation des phénomènes de dissipation des métaux dans les sols.

Figure 11 : Le site expérimental dit 'les 42 parcelles' installé au centre INRA de Versailles.

---

[20] Résultats publiés sous la forme: Fernandez, C., Monna, F., Labanowski, J., Loubet, M. van Oort, F. (2008) Anthropogenic lead distribution in soils under arable land and permanent grassland estimated by Pb-isotopic compositions. *Environmental Pollution*. 156, 1083-1091. Cf. ANNEXES.

Dans ce but, nous avons donc dans un premier temps préféré concentrer nos efforts sur le dispositif expérimental de l'INRA de Versailles dit « les 42 parcelles » afin de contraindre très fortement de nombreux paramètres nécessaires à la modélisation (Figure 11). Il s'agit d'un site installé en 1928 pour étudier les effets à long terme des grands groupes de fertilisants sur les propriétés physiques des sols. Chaque année ou presque depuis sa mise en place, chaque parcelle est bêchée et environ un kilogramme de sol superficiel est extrait, broyé, séché, puis stocké pour analyses ultérieures. Une telle collection constitue une mémoire exceptionnelle des bouleversements anthropiques qui ont eu lieu au cours du XX^{e} siècle (Figure 12). Cette série d'échantillon nous a permis, dans le cadre d'un programme mené en étroite collaboration avec, entre autres, Réda Semlali, alors étudiant en thèse à l'INRA de Versailles sous la direction de Folkert van Oort, Jérome Bolte, mathématicien à l'Université de Paris V, et Jean Baptiste Dessogne, étudiant en Master 1 sous ma direction, de proposer un modèle dynamique simple de mobilité du plomb, validé sur la durée, et prédictif[21]. Dans le cas du site de Versailles, les flux au sein de l'horizon de bêchage sont simples à exprimer puisque les parcelles ciblées sont bien isolées les unes des autres et parce qu'elles sont maintenues en sols nus, d'où l'absence d'exportation par la végétation. La dynamique est donc gouvernée par (i) un flux de sortie limité à la migration verticale et supposé proportionnel au stock anthropique présent dans l'horizon de bêchage, et (ii) un flux d'entrée exclusivement lié au dépôt atmosphérique. De là, un modèle simple d'évolution temporelle des concentrations et des compositions isotopiques peut être bâti. En combinant les résultats obtenus à partir de la collection de sols de l'INRA avec la connaissance des flux atmosphériques qui découle de l'étude de tourbières ou de collections de végétaux, des suivis de la qualité de l'air en milieu urbain, ou de la consommation de plomb en Europe (Figure 1 et références citées), il est possible de contraindre le taux de migration depuis l'horizon de bêchage. Il apparaît que ce taux est très faible puisqu'il représente annuellement moins de 0,1% du stock anthropique. En imaginant un arrêt définitif des apports anthropiques, plus de 700 ans seraient nécessaires pour diviser par 2 la quantité de plomb accumulée dans cet horizon.


Figure 12 : La collection de sols de l'INRA de Versailles.

Toujours à partir de la collection de sols issue du dispositif des '42 parcelles', le même type d'approche a été appliqué plus récemment au cas du ^{137}Cs. Ce dernier est un radio-isotope purement artificiel émis dans l'atmosphère dans les années 1950-1960 à la suite des essais

---

[21] Résultats publiés sous la forme : Semlali, R.M., Dessogne, J.-B., Monna, F., Bolte, J., Azimi, S., Navarro, N., Denaix, L., Loubet, M., Chateau, C., van Oort, F. (2004) Modeling lead input and output in soils using lead isotopic geochemistry. *Environmental Science and Technology*, 38, 5, 1513-1531. Cf. ANNEXES.

nucléaires à l'air libre, puis, tout au moins en Europe, par l'accident nucléaire de la centrale de Tchernobyl en 1986. L'objectif de ce travail était double : d'abord (i) déterminer le taux de migration vertical depuis l'horizon homogénéisé par le bêchage, mais aussi (ii) tirer profit des évolutions des paramètres physicochimiques induites par les amendements et les fertilisations (KCl, $NH_4(NO_3)$, superphosphate, fumier de cheval et chaux) répétés pendant 80 ans pour examiner l'influence de facteurs comme le pH, les teneurs en matières organiques ou en cations sur la mobilité du ^{137}Cs. Pour cela j'ai réuni une équipe comprenant radiochimistes, pédologues, géochimistes, un mathématicien et Jérémi Lamri, alors étudiant en Master 1 sous ma direction[22]. Comme pour le Pb, la pertinence d'un simple modèle de boite noire, où le césium est supposé se mouvoir verticalement par des mécanismes de convection a été vérifié. Un taux annuel de perte correspondant à 1,5% du stock présent dans l'horizon de bêchage permet d'obtenir une très bonne concordance entre la simulation et l'évolution des activités observée dans les archives de sols (Figure 13). Pour les parcelles amendées, la recherche des facteurs gouvernant la mobilité est compliquée par le grand nombre de variables physicochimiques affectées subséquemment aux traitements. Néanmoins, puisque les parcelles se sont développées à partir d'un même génoforme (en d'autres termes à partir d'un même substrat), les différents taux de migration calculés peuvent être comparés les uns aux autres.

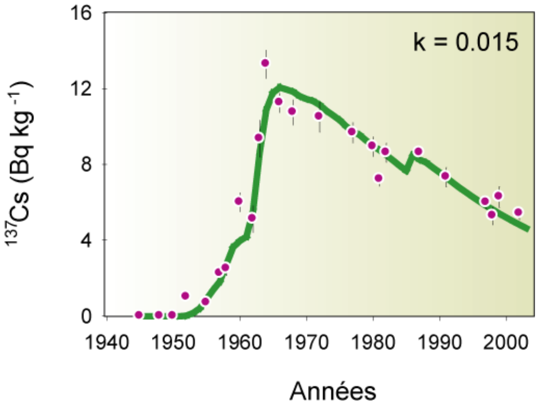

Figure 13 : Activités en ^{137}Cs des sols témoins provenant du dispositif des '42 parcelles' (symboles violets) et activités modélisées en considérant 1,5% de pertes annuelles depuis l'horizon de bêchage (courbe verte). Ces activités ont été corrigées de la désintégration radioactive pour illustrer les caractéristiques au moment du prélèvement sur le terrain[22].

Dans ces deux exemples précédents traitant du Pb et du ^{137}Cs, l'horizon de bêchage est considéré comme une boite noire à partir de laquelle un modèle de migration simple et réaliste est construit. Une telle approche est possible pour les sols du dispositif de Versailles parce que nous possédons une mémoire précise du passé ; situation tout à fait exceptionnelle. Dans la plupart des cas, bien évidemment nous ne disposons pas de suivis sur plusieurs années, voire plusieurs générations. L'estimation des capacités de mobilisation des métaux dans les sols doit donc être réalisée en l'absence de tout recul temporel. C'est en partie la raison pour laquelle des procédés d'extractions séquentielles ont été développés à partir du postulat suivant : les fractions les plus facilement extractibles sont *a priori* les plus mobiles et, logiquement, les plus biodisponibles. Tandis que ces techniques ont été critiquées pour leur manque de sélectivité vis-à-vis des espèces chimiques ciblées, certains auteurs ont privilégié des procédures basées

---

[22] Résultats sous presse sous la forme : Monna, F., van Oort, F., Hubert, P., Dominik, J., Bolte, J., Loizeau, J.-L., Labanowski, J., Lamri, J., Petit, C., Le Roux, G., Chateau, C. Modeling of ^{137}Cs migration in soils using an 80-year soil archive. Role of fertilizers and agricultural amendments. *Journal of Environmental Radioactivity*. 10.1016/j.jenvrad.2008.09.009.

cette fois sur la cinétique d'extraction (Bermond, *et al*. 1998 ; Fangueiro *et al*., 2002). Pour un extractant donné, l'approche cinétique génère deux types de données: (i) la proportion de métaux extraits par rapport aux quantités disponibles dans l'échantillon et (ii) le comportement cinétique de chacun de ces métaux. Cette cinétique d'extraction peut être modélisée par une somme de deux équations différentielles du premier ordre qui permettent la définition de deux 'pools', dits 'labile' et 'moins labile' (Fangueiro *et al*., 2005). Bien que les extractants utilisés ne miment que partiellement les conditions naturelles, ils peuvent en première approximation correspondre aux pools potentiellement mobiles et/ou biodisponibles (Bermond *et al*., 2005), d'autant que Degryse *et al*. (2006) ont montré que la proportion de métal labile est bien corrélée à la quantité de métaux incorporée par les plantes. J'ai récemment participé, notamment sur la partie modélisation mathématique, à une étude basée sur cette approche prometteuse[23]. Cette dernière a été en grande partie conduite par Jérome Labanowski, sous la direction scientifique de Folkert van Oort (INRA Versailles). Il s'agissait de déterminer la cinétique d'extraction du Zn, du Cu, du Cd et du Pb contenus dans un sol contaminé, et cela en utilisant l'EDTA et le citrate. Dans le cas du sol étudié, le 'pool labile' déterminé par des extractions au citrate, est apparu comme un bon indicateur de mobilité par comparaison avec des données obtenues par ailleurs à partir d'études menées en laboratoire ou sur le terrain. L'EDTA extrait de plus grandes quantités de métal que le citrate et fournit plutôt des indications sur les quantités totales de métal extractible sur le long terme.

---

[23] Résultats publiés sous la forme: Labanowski, J. Monna, F., Bermond, A., Cambier, P., Fernandez, C., Lamy, I., van Oort, F. (2008) Kinetic extractions to assess mobilization of Zn, Pb, Cu, and Cd in a metal contaminated soil: EDTA vs citrate. *Environmental Pollution*, 152, 693-701. Cf. ANNEXES.

AXE 3 : Histoire de la métallurgie & liens avec l'archéologie

*Alors que le développement de l'agriculture caractérise le néolithique, la **quête du métal** est un élément constitutif des **sociétés protohistoriques**. La plupart du temps, l'étude de la chaîne opératoire métallurgique est abordée via le **mobilier métallique** puisque les témoins **d'exploitations minières** précoces sont pour l'essentiel masqués ou tout simplement détruits par des travaux ultérieurs qui ont quelquefois perduré jusqu'au XX*^{e} *siècle. C'est pourtant avec cette **information fragmentaire** que l'archéologue doit composer. La géochimie, et plus généralement les approches utilisées en Sciences de la Terre, peuvent fournir des éléments de réponse originaux, ou tout au moins des pistes de travail…*

Il est aujourd'hui assez bien établi que le travail du métal s'est propagé en Europe de l'Est vers l'Ouest, pour simplifier des Balkans vers l'Arc Nord Alpin, et finalement vers la façade atlantique (Chapman et Tylecote, 1983 ; Gale *et al*., 1991). Cependant, au delà de ce schéma général, de nombreuses questions subsistent. Le caractère exceptionnel des découvertes de terrain illustrant la chaîne opératoire métallurgique depuis l'acquisition du minerai jusqu'à sa circulation et son utilisation au cours de la protohistoire (et plus particulièrement au Chalcolithique et à l'Age du Bronze) participe au fait que ces questions sont encore aujourd'hui âprement débattues dans la communauté archéologique. Dans un premier temps, il s'agirait d'identifier les centres de production, même mineurs, ce qui permettrait par extension d'établir des réseaux d'échanges, témoins oubliés d'une certaine organisation sociale ou politique.

Histoire de la métallurgie. Si les témoignages matériels de travaux d'extraction ou de transformation du minerai ont le plus souvent disparu dans les reprises d'exploitation postérieures, les bouleversements environnementaux qui les ont accompagnés, tels que la contamination en métaux lourds (Hong *et al*., 1994 ; Rosman *et al*., 1997) et les modifications du couvert végétal (Richard et Eschenlhor, 1998), peuvent avoir laissé des traces persistantes dans les environnements superficiels. Il existe donc d'autres techniques qui, bien qu'indirectes, peuvent permettre de combler les lacunes de documentations archéologiques et historiques pour obtenir une vue générale de l'évolution de l'activité minière et métallurgique au cours des derniers millénaires sur un site donné. Il s'agit de sélectionner un objet naturel capable de préserver sur le long terme ces informations, puis de les restituer. Les tourbières possèdent de telles qualités car, contrairement aux sols qui accumulent indistinctement les dépôts atmosphériques dans leurs horizons de surface, les tourbières constituent un lent enregistrement dont la chronologie peut être facilement établie sur la base de datations au radiocarbone réalisées à différentes profondeurs (Lee et Tallis, 1973 ; Brännvall *et al.*, 1997, 1999 ; Shotyk *et al.*, 1998 ; Dunlap *et al.*, 1999; Renberg *et al.*, 2000; Martínez-Cortizas *et al.*, 2002). Ces milieux humides très organiques sont favorables à la croissance des sphaignes et d'autres plantes hydrophiles. Au cours de leur développement, micropolluants métalliques, pollens et spores sont piégés. Les conditions physico-chimiques qui règnent dans ces environnements favorisent la bonne conservation du signal géochimique, en particulier celui du plomb. Cet élément possède en effet une très forte affinité avec la matière organique, tandis que pour d'autres éléments plus mobiles par nature, comme le cuivre ou le zinc, la lecture en terme historique devient sauf exception (cf. Mighall, *et al.* 2002) difficile, voire impossible. Notons également que si le plomb est abondant dans toutes sortes de minéralisations, sa seule présence à des niveaux élevés ne permet pas de déterminer la nature du métal extrait dans le passé. Cependant, et même s'il n'était pas directement recherché par les premières sociétés humaines, essentiellement intéressées par le cuivre, l'or, l'argent et l'étain, le plomb a pu être émis dans l'atmosphère durant les phases de traitement dans des quantités suffisamment importantes pour être détectées à l'échelle continentale (Rosman *et al.*, 1997 ; Bindler, 2006), et *a fortiori* aux alentours des zones de production (Mighall *et al.*, 2002, Martinez-Cortizas et al., 2005). C'est donc un excellent traceur pour le problème qui nous occupe. Du fait de sa relative immobilité au sein de la colonne de tourbe (Farmer *et al.*, 1997, Vile *et al.*, 1999), l'évolution de sa teneur en profondeur reflète en grande partie l'ampleur de la contamination atmosphérique au cours du temps, et de là, l'activité humaine liée au métal. Mais une tourbière ne se contente pas de fossiliser les signaux géochimiques. De nombreux indices biologiques sont également enregistrés en son sein. Parmi eux, les grains de pollens et les spores sont probablement les plus utiles à la reconstruction des modifications du couvert végétal par l'homme et/ou le climat[24]. Si des travaux miniers et métallurgiques conséquents ont bien eu lieu sur le site, parions qu'ils ont engendré des prélèvements en bois : attaque au feu du front de taille, étayage des travaux miniers, et transformation du minerai en métal. De telles pratiques sont susceptibles d'introduire des bouleversements dans la végétation aux alentours, et en conséquence, des modifications dans la composition de la pluie pollinique enregistrée dans les tourbières (Galop et Jalut, 1994 ; Richard et Eschenlohr, 1998). Le comptage des grains de pollens le long de séquences de tourbe permet alors de rendre compte de ces variations qui témoignent des phases de déforestation, qu'elles soient associées ou non à des activités agro-pastorales plus classiques.

---

[24] Résultats publiés sous la forme : Jouffroy-Bapicot, I., Pulido, M., Galop, D., Monna, F., Ploquin, A., Baron, S., Petit, C., Lavoie, M., Beaulieu, J.-L., de, Richard, H. (2007) Environmental impact of early palaeometallurgy: pollen and geochemical analysis. *Vegetation History and Archaeobotany*. 251-258.

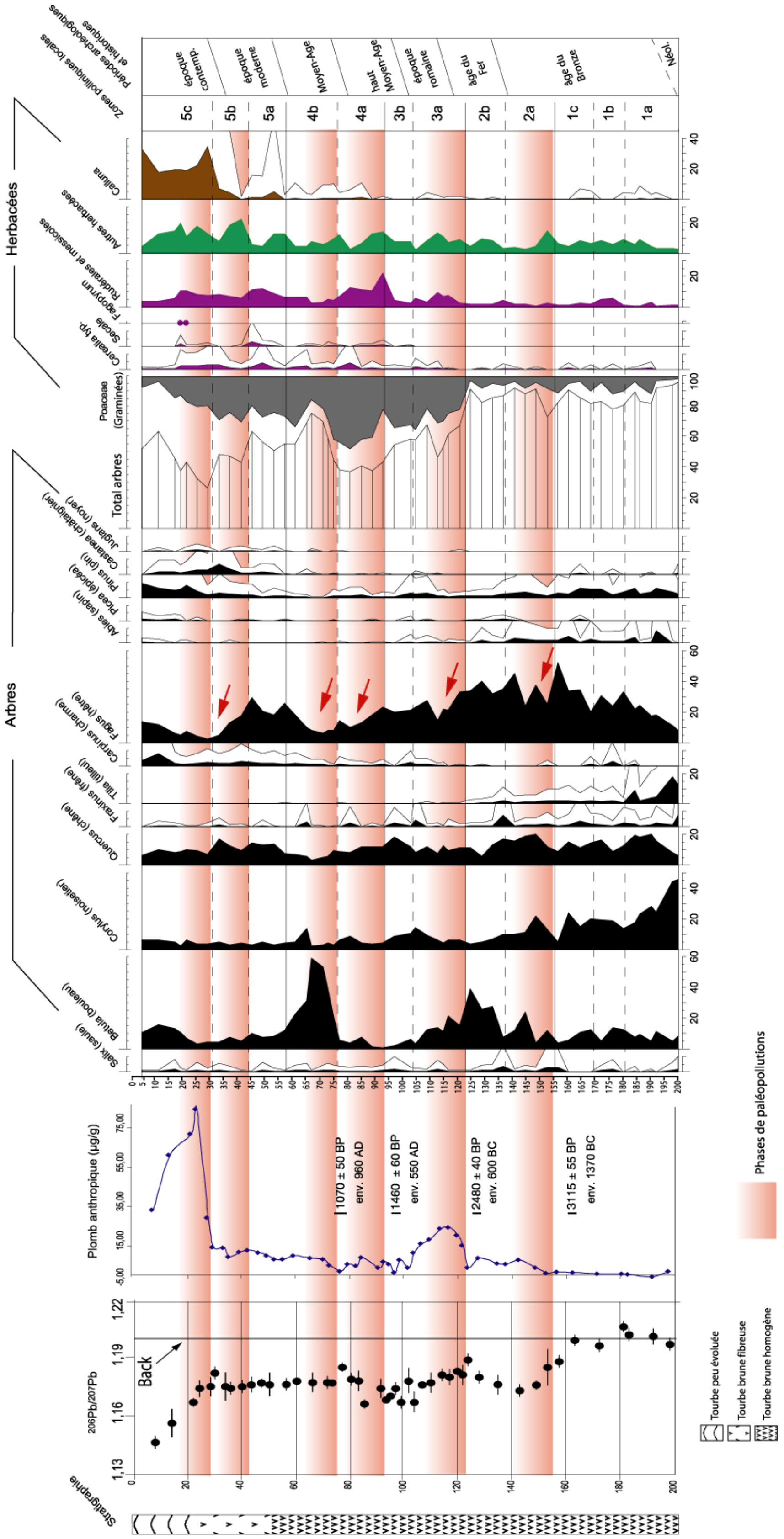

Figure 14 : Evolution des rapports $^{206}Pb/^{207}Pb$, de la composante anthropique du Pb et de la distribution des pollens en fonction de la profondeur - carotte prélevée au Port-des-Lamberts (Nièvre) -3. La chronologie culturelle est reportée dans la partie droite du diagramme afin de faciliter la lecture en termes historiques.

C'est par la combinaison de ces deux approches (géochimie et paléobotanique) que nous avons choisi d'aborder la question de l'activité minière dans deux régions aujourd'hui très faiblement industrialisées mais possédant un fort potentiel minier : le Pays Basque[25,26,27] et le Morvan[3]. Dès 1999, des prospections pédestres menées sur le Mont Beuvray (Morvan) avaient permis de repérer une dizaine de longues tranchées partiellement comblées (Guillaumet *et al.*, 2001). Certains de ces ravins, généralement ouverts dans le sens de la pente, avaient déjà été remarqués sans que leur véritable nature ait été bien cernée. Par leurs formes, elles rappelaient des chantiers d'extraction à ciel ouvert. Dans le cadre de la recherche sur les paléométallurgies celtiques sur le Mont Beuvray (responsable Christophe Petit, financement Centre Archéologique Européen du Mont Beuvray), une première carotte de tourbe a été prélevée au lieu-dit « le Port-des-Lamberts » situé à quelques kilomètres au nord de l'oppidum celtique de Bibracte. La séquence couvrait sans hiatus près de quatre mille ans d'histoire. Son étude a été réalisée en étroite collaboration avec le Laboratoire de Chrono-écologie, Université de Franche-Comté et Isabelle Jouffroy-Bapicot, doctorante paléobotaniste sous la direction scientifique d'Hervé Richard. Une partie de l'étude géochimique a également été réalisée par Cédric Blanchot sous ma direction dans le cadre de son stage de Master 2. A partir de la Figure 14 qui reporte côte à côte analyses paléobotaniques et géochimiques, il est possible de dresser un bref résumé des principaux résultats. Au cours du Bronze Ancien (2300-1650 av. J.-C.), le couvert végétal environnant était dominé par la forêt, principalement composée de noisetiers (Corylus), de chênes (Quercus) et surtout de hêtres (Fagus). Toutefois, la présence de pollens de céréales et de plantes associées aux activités humaines indique une exploitation agricole du milieu. Dès le Bronze Final (vers 1300-1200 av. J.-C.), les teneurs en plomb augmentent et les rapports $^{206}Pb/^{207}Pb$ chutent du fait de l'extraction et du traitement du minerai. Simultanément, la forêt recule, notamment le hêtre (Fagus), sans qu'une ouverture du milieu à des fins agro-pastorales puisse être invoquée. Il s'agit probablement ici d'une réponse à la demande énergétique liée au travail du métal. Le Mont Beuvray aurait donc été un centre minier précoce. La fin de l'Age du Fer (vers 120 av. J.-C.) est également marquée par d'importants signaux de pollution et de déforestation observables jusqu'au début de notre ère (vers 30 av. J.-C.).

A la suite de ce travail, le ravin de la Pâture des Grangerands, situé sur le Mont Beuvray et déjà suspecté d'être une minière protohistorique comblée, a fait l'objet d'une fouille détaillée par Béatrice Cauuet et son équipe[28]. Ouverte perpendiculairement au vallon, la tranchée de fouille a recoupé profondément le versant, révélant un remplissage anthropique, riche en rejets de mobiliers an-

---

[25] Résultats publiés sous la forme : Monna, F., Galop, D., Carozza, L., Tual, M., Beyrie, A., Marembert, F., Chateau, C., Dominik, J., Grousset, F.E. (2004) Environmental impact of early Basque mining and smelting recorded in a high ash minerogenic peat deposit. *The Science of the Total Environment*, 327, 197-214. Cf. ANNEXES.

[26] Résultats publiés sous la forme : Beyrie, A., Galop, D., Monna, F., Mougin, V. (2003) La métallurgie du fer au Pays Basque durant l'Antiquité. Etat des connaissances dans la vallée de Baigorri (Pyrénées-Atlantiques). *Aquitania*, 19, 49-66.

[27] Résultats publiés sous la forme : Carozza, L., Galop, D., Marembert, F., Monna, F. (2005) Quel statut pour les espaces de montagne durant l'âge du Bronze? Regards croisés sur les approches société-environnement dans les Pyrénées occidentale. *Documents d'Archéologie Méridionale*. 28, 7-23.

[28] Résultats publiés sous la forme : Cauuet, B., Tamas, C.G., Guillaumet, J.-P., Petit, C., Monna, F. (2006) Les exploitations minières en pays éduen. (2006). *Les Dossiers de l'Archéologie*. 316. 20-25.

tiques, notamment en rejets métalliques issus des habitats et ateliers de bronziers et de forgerons situés aux abords (Figure 15). La réutilisation de l'excavation en fosse-dépotoir par les habitants de Bibracte confirme l'antériorité de l'ouvrage à la création de la ville. L'élargissement de la fouille a permis de descendre à 4 m sans pour autant atteindre le fond. La fosse taillée en gradins traverse un niveau de rhyolites et la présence de filons de quartz au voisinage ainsi que la topographie particulière de l'ouvrage contribuent à caractériser cette excavation comme une minière protohistorique. Quelques haldes résiduelles retrouvées contre les parements confirment cette hypothèse, de même que les teneurs en cuivre, zinc, plomb et argent mesurées dans les rares cristaux de quartz recueillis alentours. Cependant les données sont encore rares sur la nature des substances exploitées, les techniques d'extraction, les procédés métallurgiques, la chronologie des travaux, les habitats et les nécropoles des populations concernées. Dans l'attente de la suite des recherches, on notera la variété des types de mines dans la région : en roche et en alluvions/colluvions et des gisements, primaires, secondaires, filoniens et chapeaux de fer. Quoi qu'il en soit, ce type de travail de terrain est indispensable dans la mesure où l'approche paléoenvironnementale fournit au mieux des indices indirects d'exploitations minières ou de métallurgie. Ces derniers ne sauraient remplacer la mise au jour d'évidences matérielles.

Figure 15 : Minière en cours de fouille sur le Mont Beuvray. Photo B. Cauuet/CNRS[28].

Fort de ces résultats, trois nouvelles séquences ont plus récemment été prélevées dans la Nièvre : près d'Arleuf, aux environs de Saint-Agnan, et à Prémery, respectivement à environ 15, 60 et 100 km de celle du Port-des-Lamberts. Ce travail a été effectué par Benoît Forel dans le cadre de sa thèse de doctorat co-dirigée par Claude Mordant et moi-même, financée par l'ACR « Bronze » dirigée par Jean François Piningre (conservateur du patrimoine, SRA Besançon) et par un projet de conservation des zones humides de Prémery (direction Isabelle Jouffroy-Bapicot). Signalons également les participations de Rodrigue Guillon et de Cyril

Leuvrey (sous ma direction et celle de Benoît Forel) à ce projet dans le cadre de leur stage de Master 1. Sans déflorer les résultats de la thèse de Benoît Forel, les analyses géochimiques et polliniques confirment le caractère très local des activités minières et métallurgiques puisque les trois séquences fournissent des histoires différentes[29]. S'il s'était agi d'une pollution plus globale, tous les sites auraient alors fourni approximativement le même profil. Notons que la séquence d'Arleuf montre une phase aussi précoce que le Bronze Ancien. Ces résultats nous amènent donc à reconsidérer la position socio-économique du massif du Morvan et plus largement celle de la Bourgogne au cours de la Protohistoire. L'existence d'activités métallurgiques pour cette période, et notamment pour l'Age du Bronze, fait de cette région une zone, non plus dépendante, mais productrice de métal. Au-delà de l'intérêt purement archéologique, l'étude réalisée au Port-des-Lamberts indique que près d'un quart des apports anthropiques en plomb ont intégré la tourbière avant le début de notre ère, et plus de la moitié avant le XVII-XVIII^e^ siècle. Le Morvan, qui est de nos jours une des régions rurales les moins industrialisées du territoire français, fut donc le siège d'importantes activités liées à la métallurgie des Éduens et de leurs prédécesseurs. Cet héritage doit être pris en compte lorsqu'on évalue la qualité de l'environnement actuel afin de ne pas surestimer l'impact de la pollution émise par nos sociétés modernes. La reconstitution des interactions entre les civilisations passées et leur environnement pourrait donc permettre à l'avenir de mieux cerner le comportement sur le long terme de nos contaminations actuelles. Cette thématique est largement développée dans l'équipe « Géoarchéologie » de l'UMR 5594 dirigée par Christophe Petit ; équipe à laquelle j'appartiens.

Signalons que j'avais déjà eu l'occasion d'aborder la question de la paléométallurgie lors de mon stage postdoctoral à l'Université de Brême (responsable Kay Hamer). L'objectif était alors de retrouver les traces d'exploitations minières précoces à partir de la contamination en métaux des sédiments de berge de la Weser[30]. J'interviens aujourd'hui sur de nombreux autres chantiers: dans les Pyrénées Centrales dans le cadre du PCR Montagne Pyrénéenne (responsable Didier Galop, Université de Toulouse), en Roumanie, sur le site de Rosia Montana, siège d'une intense production d'or durant l'Antiquité (responsable Béatrice Cauuet, Université de Toulouse), en Jordanie (responsables Claire Rambeau et Stuart Black, Université de Reading), dans des zones humides aux alentours de La Rochelle (thèse d'Aline Naudin, responsable François Lévêque, Université de La Rochelle) et dans les Vosges où Benoît Forel, toujours dans le cadre de sa thèse de doctorat, a réalisé deux carottages : à Plancher-les-Mines et au Gazon-du-Faing à environ 7 km au sud du Col du Bonhomme.

Typologie et morphométrie. Comme nous l'avons vu, les traces matérielles d'exploitations minières précoces sont souvent ténues et difficiles à re-

---

[29] Résultats publiés sous la forme : Jouffroy-Bapicot I., Forel B., Monna F., Petit C. (sous presse) Paléométallurgie dans le Morvan : l'apport des analyses polliniques et géochimiques ». in *Actes du 131e congrès du CTHS « Tradition et Innovation »* Grenoble 2006.

[30] Résultats publiés sous la forme: Monna, F. Hamer, K, Lévêque, J. Sauer, M. (2000) Pb isotopes as reliable marker of early mining and smelting in the Northern Hartz province (Germany). *Journal of Geochemical Exploration*. (68)3, 201-210.

connaitre, de sorte que, pratiquement, seuls nous parviennent les objets métalliques, stades ultimes de la longue chaîne métallurgique à l'Age du Bronze. Ils sont le plus souvent découverts en contexte de dépôts (regroupements plus ou moins important d'objets enfouis dans le sol) et dans une moindre mesure en contexte funéraire ou d'habitat. Si les raisons de la constitution de dépôts restent un sujet de discussion dans la communauté archéologique, l'étude des objets métalliques qu'ils renferment permet de contraindre l'extension géographique et temporelle des sociétés humaines du passé ainsi que d'estimer les relations qui ont existé entre les différentes cultures. Traditionnellement, les regroupements sont basés sur une approche typo-culturelle du mobilier. Il s'agit de rechercher un ou plusieurs critères discriminants (par exemple la forme générale de l'objet, le décor, certains détails…) intuitivement déterminés à l'œil nu et permettant la définition d'un type générique, caractéristique d'une culture donnée. Cette méthode s'avère très puissante, mais il est clair que le langage, même spécialisé, est inadéquat pour décrire parfaitement les formes sans ambiguïté ou subjectivité. Pour cette raison la description textuelle de la forme est habituellement complétée par une représentation graphique (dessin, photo), en d'autres termes, par la forme elle-même. Pour pallier ces faiblesses, biologistes et géologues ont déjà développé des méthodes de morphométrie et d'analyse statistiques des formes qui pourraient être avantageusement appliquées à l'archéologie des objets métalliques (e.g. Dryden et Mardia, 1998 ; McLeod, 1999).

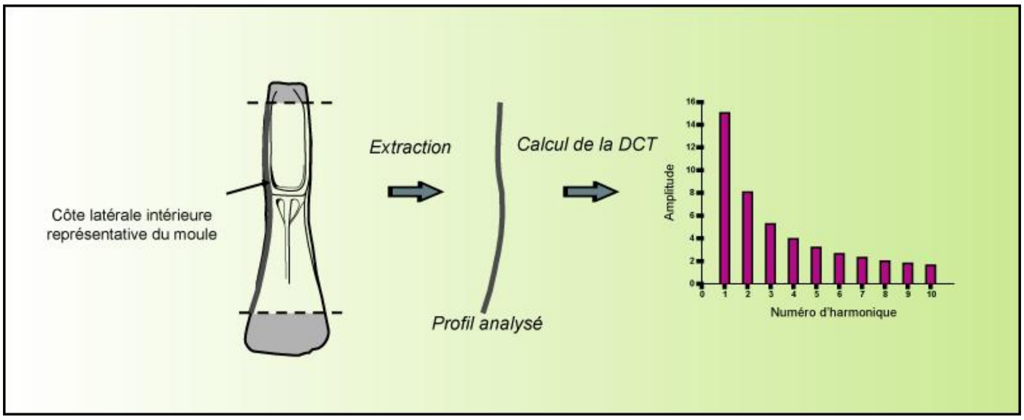

Figure 16 : Extraction de la côte latérale intérieure depuis la documentation archéologique disponible. Décomposition par DCT et représentation sous forme de spectre d'amplitude[31].

La période du Bronze Moyen (1650 – 1350 av. J.-C.) se caractérise par une augmentation très nette du nombre d'objets dans les dépôts. Parmi tous les objets constituant ces ensembles métalliques, les haches à talons, perçues comme une amélioration technique des haches du Bronze Ancien (2300 – 1650 av. J.-C.), sont particulièrement bien représentées. En France, au sein de l'ensemble des haches à talon pouvant être identifiées, deux grands types ont été reconnus par Briard et Verron (1976) : les haches bretonnes et les haches normandes, ainsi nommées par leur zone de plus grande concentration de découverte. Parmi les nombreux critères permettant de les différencier, l'allure du profil latéral semble être particulièrement discriminante (Maréva Gabillot, comm. Pers.). C'est précisément cette hypothèse que Benoît Forel[31] a testé durant sa thèse en utilisant un traitement du profil par DCT (Discrete Cosine Transform), une procédure déjà utilisée par Cyril et Jean-Louis Dommergues et Sylvain Gerber (Laboratoire Biogéosciences, Université de Bourgogne) pour opérer des regroupements au sein d'un lot d'ammonites sur la base de l'allure de leurs côtes (Dommergues *et al.*, 2006, 2007). Cette procédure, particulièrement bien adaptée au traitement de courbes ouvertes décompose le signal, le profil en l'occurrence, en une somme de fonctions trigonométriques, dont chaque harmonique possède sa propre amplitude (Figure 16).

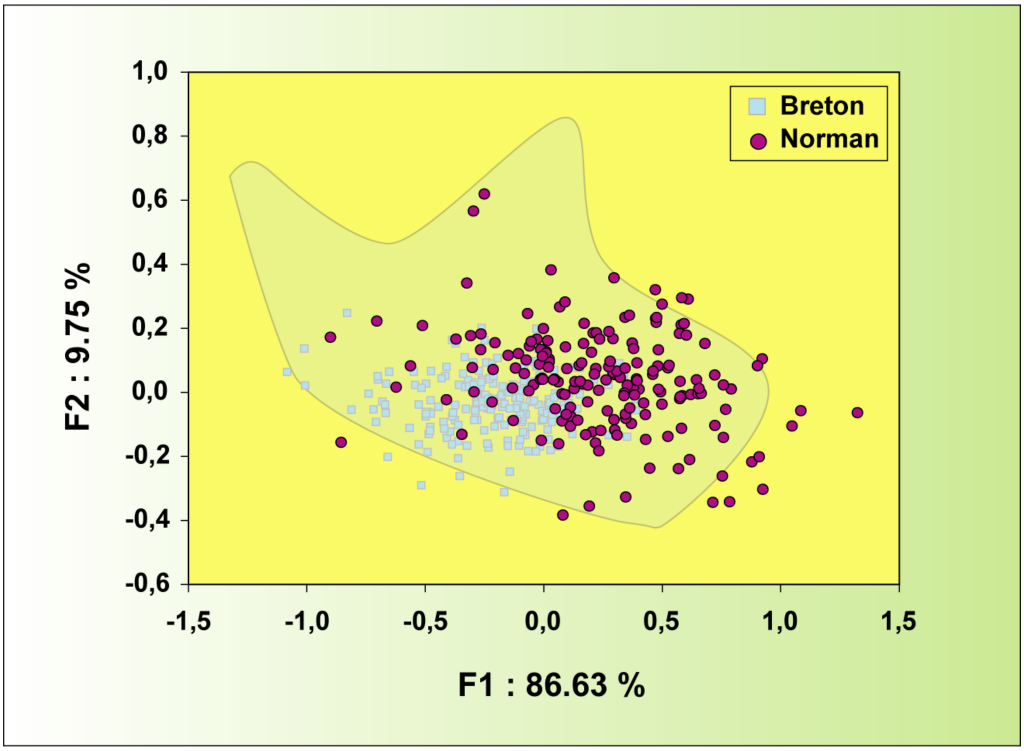

Figure 17 : Analyse en composantes principales des sept premières harmoniques calculées par DCT à partir des haches de type Breton et Normand, puis à partir des haches de Sermizelles (zone verte)[31]. Représentation sur le plan factoriel défini par F1 (87%) et F2 (10%)

Les 400 haches bretonnes et normandes disponibles dans la documentation archéologique ont donc été traitées par DCT, puis par ACP (Figure 17). Les deux populations apparaissent distinctes, ce qui confirme la puissance de l'approche. Les haches provenant des deux dépôts de Sermizelles (Bourgogne), précédemment identifiées comme d'origine bretonne ou normande, présentent une disparité de forme bien trop grande pour être le résultat de ce simple mélange. Une ou plusieurs autres sources mineures doivent donc être invoquées. Il pourrait s'agir d'imitations, pourquoi pas locales, d'autant que l'utilisation des minéralisations du Morvan vient d'être suggérée par l'étude paléoenvironnementale. Le Bronze Moyen voit la montée en puissance des besoins et des diffusions à partir des

---

[31] Résultats soumis sous la forme : Forel, B., Gabillot, M., Monna, F., Forel, S., Dommergues, C.H., Gerber, S., Petit, C. Mordant, C., Château, C. (2008) Morphometry of Middle Bronze Age palstaves by Discrete Consine Transform. *Journal of Archaeological Sciences*. DOI :10.1016/j.jas.2008.10.021.

zones de productions en série. Cette étude est la démonstration qu'au-delà de ce scénario général basé sur la diffusion 'commerciale' d'objets, on assiste également à une transmission des idées et des techniques permettant la fabrication de copies dans des zones éloignées des aires principales de production.

L'approche morphométrique utilisée ici est rapide, reproductible et suffisamment généralisable pour être appliquée à une large variété d'objets de différentes périodes afin de clarifier leur typologie et éventuellement leur origine. Outre la définition d'une forme type, qui correspond au centroïde de l'espace morphométrique, elle permet de quantifier et de visualiser la disparité des formes, habituellement inaccessible à l'œil nu et pourtant aussi chargée de sens que la tendance centrale.

Caractérisation chimique et isotopique du mobilier métallique.

Complémentaire à l'étude typologique, les analyses chimiques et isotopiques permettent d'entrer dans l'intimité des objets en caractérisant le métal qui les constitue. Les premières nous renseignent sur la nature du métal, allié ou non, puis, grâce à l'étude des impuretés ou éléments traces, sur la « recette métallurgique » mise en œuvre (Rychner et Kläntschi, 1995). Les secondes peuvent également permettre une réflexion sur l'origine du métal (e.g. Gale et Stos-Gale 1992 ; Pernicka, 1995 ; Niederschlag *et al.*, 2003), bien que ce point ait donné lieu à un débat fort peu amène au sein de la communauté archéologique dans les années 1980-1990. L'idée de base est simple et semble séduisante à priori : il s'agit de comparer les signatures isotopiques en Pb des objets à celles des minéralisations d'où le métal est potentiellement issu. Si l'objet est en cuivre ou en bronze et qu'il ne contient que très peu de plomb, cette méthode est supposée permettre l'identification de l'origine du cuivre, puisque l'étain éventuellement ajouté n'est pas censé amener de plomb en quantités notables (Gale et Stos-Gale, 2000). Si l'objet correspond à un alliage avec du plomb ajouté intentionnellement ou non, alors c'est ce métal qui gouverne la composition isotopique de l'ensemble et qui donc est tracé. Bien qu'alléchante dans son principe, cette approche souffre de nombreux problèmes au point que certains auteurs appellent à une remise à plat de toute la méthodologie (Pollard et Heron, 1996). Le terme 'déconstruction' est même utilisé par Budd *et al.* (1996). Les reproches adressés à la méthode sont en effet multiples :

- D'abord, la réponse fournie par la technique isotopique n'est pas univoque puisque plusieurs gisements sont susceptibles de présenter la même signature isotopique, d'autant plus que cette signature est souvent variable au sein d'une même minéralisation (Baxter *et al.*, 2000). De ce fait, il n'est pas possible d'attribuer *positivement* un objet à une source. Au mieux, certaines sources peuvent être exclues. Signalons que ce point crucial est loin d'être « une simple question de sémantique » comme le déclarent complaisamment Gale et Stos-Gale (2000).

- Toutes les minéralisations exploitées au cours de la protohistoire n'ont vraisemblablement pas été identifiées et, *a fortiori*, fait l'objet d'analyses isotopiques. Tendre vers l'exhaustivité de l'inventaire minier signifie invariablement élargir les possibilités (e.g. Santos Zalguedi *et al.*, 2004). En conséquence, les conclusions gagnent en ambiguïté. L'apparente puissance de la méthode fait alors place à une confusion croissante.

- Finalement, les compositions isotopiques des artefacts produits à la suite de recyclage d'objets usagés ne trahissent en aucune façon l'origine du métal. Au contraire, elles fournissent une signature isotopique reflétant un mélange plus ou moins complexe. Parions que compte tenu de la diversité des gisements, cette signature finira bien par correspondre à un gîte minéral avec lequel l'objet en question n'a rien à voir…

Ce bref inventaire souligne clairement les faiblesses de l'approche isotopique lorsqu'il s'agit de déterminer l'origine géographique du métal. Mais il serait sans doute hâtif d'abandonner un paramètre qui est pourtant tout à fait caractéristique du métal, d'autant plus que, contrairement à la composition chimique, il n'est pas affecté par les mécanismes de fractionnement intervenant tout au long des multiples étapes composant la chaîne métallurgique. L'outil isotopique ne serait donc pas inadapté à l'archéologie. Seule la question de l'origine ne pourrait être résolue de façon claire par cette méthode, et cela malgré les milliers d'analyses isotopiques de gisements, spécialement entreprises dans le cadre d'une recherche de provenance.

L'idée développée par Benoît Forel au cours de sa thèse de doctorat et lors du stage de Master 2 d'Aline Naudin effectué sous ma direction, consiste à évaluer les potentialités d'une approche résolument différente de celles précédemment évoquées[32]. L'objet n'y est plus considéré comme un individu à part entière pour lequel il faut déterminer l'origine du métal qui le compose, mais comme membre d'un lot (le dépôt par exemple), caractérisé par sa tendance centrale et par son homogénéité ou sa disparité. De ce fait, les problèmes sont maintenant abordés en termes de statistiques des populations et non plus en termes d'individus. Les individus 'aberrants', ou tout au moins ne se conformant pas à la tendance générale, perdent de leur poids puisqu'il s'agit maintenant d'observer les 'zones' isotopiques ou chimiques où se trouvent les plus grandes densités d'individus. Les comparaisons effectuées entre lots (i.e. les dépôts), choisis selon des critères géographiques ou chronologiques, devraient donc permettre la mise en évidence de différences dans les pratiques métallurgiques ou dans l'origine du métal (sans bien sûr en préciser l'origine géographique exacte). L'étude approfondie de la disparité au sein des lots, qu'elle soit d'ordre chimique ou isotopique, pourrait également permettre d'évaluer l'intensité du recyclage, sachant que plus le métal est recyclé par mélange, plus l'ensemble des individus converge vers la tendance centrale. Cette approche souffre néanmoins d'un handicap sévère: elle nécessite

---

[32] Résultats publiés sous la forme : Gabillot, M., Forel, B., Monna, F., Naudin, A., Losno, R., Piningre, J.-F., Mordant, C., Dominik, J., Bruguier, O. (sous presse) Influences atlantiques dans les productions métalliques en Bourgogne et Franche-Comté au Bronze moyen. *Actes du colloque en hommage à C. Millote*, Besançon.

un grand nombre d'analyses pour être pleinement applicable. Compte tenu de la large gamme de variation des compositions isotopiques, l'utilisation de l'ICP-MS quadripolaire, tant décriée pour son manque de précision par quelques archéomètres toujours en quête d'origine, a été privilégiée ici. La mesure du seul isotope du plomb dont l'abondance absolue n'a pas évolué depuis la formation de la Terre : le ^{204}Pb, a été également abandonnée. Pourtant il présente un fort potentiel de discrimination. Ces choix vont à l'encontre des travaux publiés récemment par certains membres de la communauté archéométrique qui privilégient des appareils de pointe comme le MC-ICP-MS pour sa précision considérable. N'oublions pas, cependant, que la méthode isotopique est intrinsèquement limitée pour les raisons énumérées ci-dessus, et qu'un gain de précision analytique ne sera jamais capable de pallier les problèmes dus à la variabilité des signatures isotopiques au sein des minéralisations et les ambiguïtés qui en découlent. Dans notre cas, l'inévitable perte de précision devrait être très largement compensée par la quantité d'individus mesurés, pour un coût identique. La Figure 18 reporte, dans un diagramme ^{208}Pb/ ^{206}Pb *vs* ^{206}Pb/^{207}Pb, les analyses isotopiques en plomb des objets contenus dans le dépôt de Larnaud qui date du Bronze Final. La représentation graphique utilise la méthode KDE (Kernel Density Estimate) particulièrement bien adaptée à cette approche (Baxter, 2003). Il s'avère que bien que la gamme de variation isotopique soit considérable, la plupart des individus se situe dans une zone où les rapports ^{206}Pb/^{207}Pb et ^{208}Pb/^{206}Pb sont compris entre 1,16 et 1,17 et entre 2,10 et 2,11 respectivement. Ces valeurs devront ensuite être comparées à celles caractérisant d'autres dépôts comme ceux de Sermizelles.

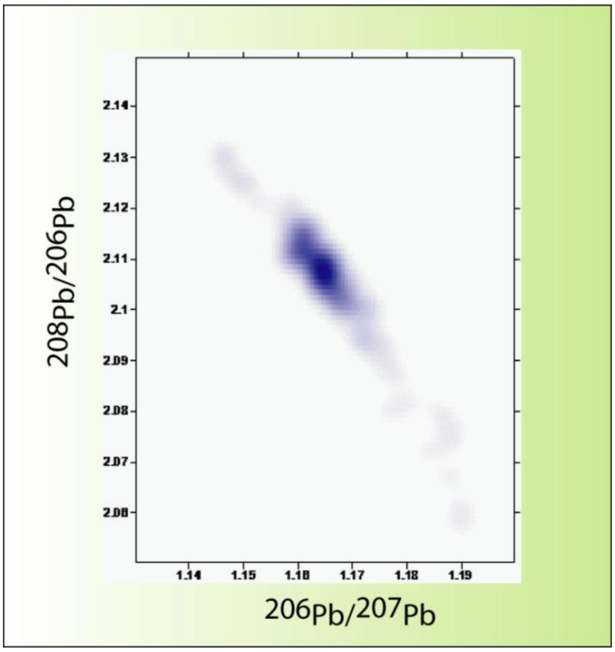

Figure 18 : Compositions isotopiques des objets constituant les dépôts de Larnaud (Age du Bronze Final) [32]

Autres travaux. Outre les questions directement liées à la métallurgie, je suis également intervenu dans une étude visant à évaluer l'impact de l'agriculture Maya sur la dégradation des sols ; impact qui peut être lu aujourd'hui dans l'enregistrement sédimentaire.[33]

---

[33] Résultats publiés sous la forme: Carozza, J.-M., Galop, D., Métailié, J.-P., Vannière, B., Bossuet, G., Monna, F., Lopez-Saez, J.A., Arnauld, M.-C., Breuil, V., Forne, M., Lemonnier, E. (2007) Land-use and soil degradation in the southern Maya lowlands, from Pre-Classic to Post-Classic times: The case of La Joyanca (Petén, Guatemala). *Geodinamica Acta*, 20,4, 195-207.

AXE 4 : Développements analytiques

Mesurer plus justement, plus précisément, plus rapidement, plus facilement, et à moindre coût, voici le but avoué de tout analyste. Si la quête de la ***sensibilité*** *et de la* ***précision*** *est louable pour un chimiste car elle ouvre la voie à de nouvelles possibilités, le chercheur en Sciences Naturelles doit veiller à* ***adapter*** *le choix des techniques utilisées au problème posé, et ceci ne passe pas forcement par un gain en termes de précision…*

En Sciences Naturelles, nous faisons face à des problèmes d'une grande complexité où les interactions sont multiples. Il s'agit de faire ressortir un 'pattern' ou un mécanisme particulier en éliminant, ou tout au moins en réduisant, le bruit lié à la variabilité naturelle. Ceci peut s'obtenir par différentes approches : en augmentant l'échantillonnage, en sélectionnant un objet naturel intégrateur (cf. le cas des lichens précédemment exposé), en recherchant une précision accrue ou en multipliant les paramètres mesurés. Cependant, il ne faut pas perdre de vue que cette réduction de la variabilité naturelle passe nécessairement par des efforts tant en moyens qu'en temps. Ces moyens étant limités, des choix doivent être faits. Quand bien même les ressources seraient considérables, il n'est pas raisonnable de les appliquer à la résolution d'un problème qui ne le justifie pas, soit parce ce que son importance est mineure, soit parce qu'il est finalement assez simple à résoudre, ou bien parce qu'une compréhension partielle mais suffisante peut être atteinte plus simplement et de façon moins coûteuse. En cela, l'étroitesse des moyens alloués aux universités françaises possède au moins le mérite de favoriser l'adéquation problème posé / échantillonnage / techniques mises en œuvre, en suscitant un questionnement *a priori*, susceptible d'évoluer au fur et à mesure de l'acquisition des résultats.

Alors que la quête de la précision est essentielle dans l'absolu parce qu'elle ouvre de nouveaux horizons, l'application de ces techniques de pointes à certains problèmes, très bruités par nature, perd tout son sens. Dans de telles situations, un échantillonnage plus conséquent, couplé à des techniques moins précises mais moins coûteuses serait alors beaucoup plus approprié. Il s'agit donc d'obtenir une combinaison judicieuse entre débit analytique, précision et budget.

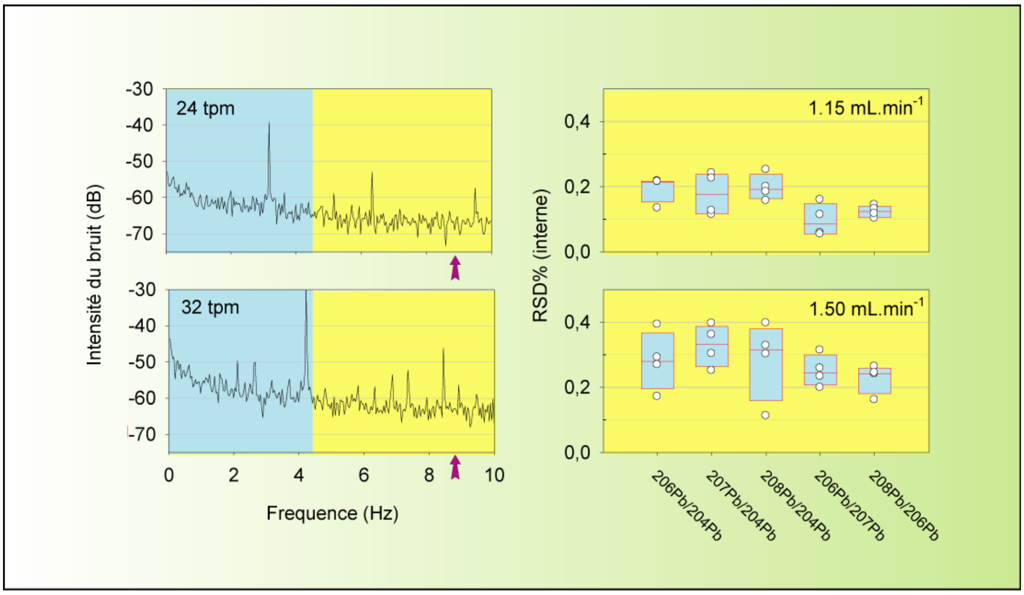

Figure 19 : Spectre de Fourier représentant le bruit entre 0 to 10 Hz et les erreurs associées exprimées en RSD% (relative standard déviation) interne sur les différents rapports isotopiques. Deux vitesses de rotation de la pompe péristatique sont testées : 24 tours min^{-1} et 32 tours min^{-1} qui produisent un débit de 1.15 et 1.50 ml min^{-1}, respectivement. A gauche, les flèches représentent la fréquence d'échantillonnage des isotopes du plomb (un sweep), et la zone bleutée, le domaine de fréquence dans lequel l'influence du bruit est réduite. Quatre mesures ont été réalisées pour chaque vitesse de pompage[36].

La mesure isotopique du plomb. En raison de sa très grande précision, le TIMS (Thermal Ionization – Mass Spectrometer) est longtemps resté l'outil de référence pour la mesure isotopique des éléments lourds, en particulier en géologie. Il souffre néanmoins de nombreux inconvénients : lourde préparation des échantillons, faible débit analytique et coût très élevé. C'est pourquoi, au cours de ma thèse de doctorat[34] et de mes deux stages post-doctoraux, je me suis intéressé au cas de la mesure des isotopes du plomb par ICP-MS quadripolaire (Inductively Coupled Plasma – Mass Spectrometry), utilisé dans le cadre de recherches environnementales. Dans l'environnement, les compositions isotopiques du plomb varient largement : environ de 1,08 à 1,22 pour le rapport ^{206}Pb/^{207}Pb. Bien qu'une telle gamme, couvrant un peu plus de 10^{-1}, puisse paraitre finalement assez restreinte aux yeux du néophyte, elle doit être mise en perspective avec la précision analytique. Celle du TIMS est susceptible de descendre bien en dessous de 10^{-4} pour ce rapport, tandis que l'ICP-MS quadripolaire permet d'atteindre 10^{-3}. En effet, en adaptant le temps de comptage de chacun des isotopes afin de compenser leurs différences d'abondance[35] et en choisissant judicieusement la fréquence d'échantillonnage afin de réduire l'influence des bruits non aléatoires tels que ceux provoqués par les galets de la pompe péristaltique[36] (Figure 19), il est possible d'atteindre des erreurs qui correspondent

---

[34] Résultats publiés sous la forme : Fillon, N., Clauer, N., Samuel, J., Verdoux, P., Monna, F., Lancelot, J. (1996) Dosage isotopique du Sr dans les eaux et du Pb dans les sédiments et les cendres d'un incinérateur urbain à l'aide d'un ICP-MS. *Comptes rendus de l'Académie des Sciences*, 322, II a, 1029-1039.

[35] Résultats publiés sous la forme : Monna, F., Loizeau, J.-L., Thomas, B.A., Guéguen, C., Favarger, P.-Y. (1998) Pb and Sr isotope measurements by inductively coupled plasma - mass spectrometer: efficient time management for precise improvement. *Spectrochimica Acta, part B*. 59/09, 1317-1333.

[36] Résultats publiés sous la forme : Monna, F., Loizeau, J.-L., Thomas, B., Guéguen, C., Favarger, P.-Y., Losno, R., Dominik, J. (2000) Noise identification and sampling frequency determination for precise isotopic measurements by quadrupole-based Inductively Coupled Plasma Mass Spectrometry. *Analusis*. 28, 750- 757. Cf. ANNEXES.

presque exclusivement à la statistique de comptage (Figure 20). Cependant, il ne faut pas perdre de vue que l'abandon quasi systématique du seul isotope invariant du plomb, le ^{204}Pb, lors des mesures ICP-MS se traduit par une perte irrémédiable d'information, comme cela avait déjà été évoqué dans la partie traitant des analyses isotopiques du mobilier archéologique. Avec des RSD internes (RSD = *relative standard deviation*) de l'ordre de 0,1 - 0,2% pour les rapports ^{206}Pb/^{207}Pb et ^{208}Pb/^{206}Pb, l'ICP-MS quadripolaire devient néanmoins un outil tout à fait adapté à l'approche environnementale. Cette technique offre un important débit analytique : de l'ordre de 80 à 100 échantillons par jour. La fastidieuse séparation chimique du plomb sur résine échangeuse d'ions ne reste indispensable que pour les échantillons très faiblement concentrés. Dans ce cas, elle est réalisée dans le but d'atteindre un flux d'ion suffisant sans être obligé d'introduire dans le spectromètre des solutions fortement concentrées en sels dissouts qui pourraient entraîner à terme des pertes de sensibilité.

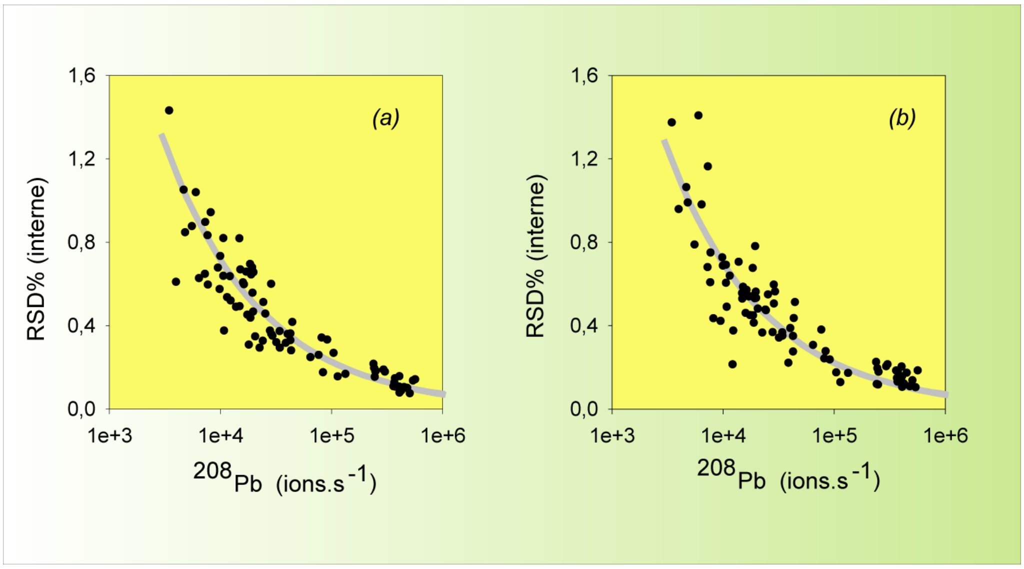

Figure 20 : Ecart type (en %) des 10 répliques représentant une mesure isotopique typique en fonction de la concentration en Pb de la solution, exprimée en flux de ^{208}Pb atteignant le détecteur. (a) pour le rapport ^{206}Pb/^{207}Pb; (b) pour le rapport ^{208}Pb/^{206}Pb. La courbe grise représente l'écart type théorique calculé sur la seule base de la statistique de comptage par la loi de Poisson[36].

En plus de la mesure des compositions isotopiques en plomb, j'ai initié durant ma thèse un projet qui visait à évaluer les potentialités de la scintillation liquide PERALS pour déterminer les taux de sédimentation dans les sédiments récents[37]. Plus tard, durant mon stage postdoctoral à l'Université de Genève, j'ai également participé à une étude méthodologique concernant la séparation des métaux à l'aide de la résine CHELEX 100[38].

---

[37] Résultats publiés sous la forme: Monna, F., Mathieu, D., Marques Jr., A.N., Lancelot, J., Bernat, M. (1996) A comparison of P.E.R.A.L.S. with alpha and beta spectrometry to determine the sedimentation rate. Example of the Thau basin (Southern France). *Analytica Chimica Acta*, 330, 107-115.

[38] Résultats publiés sous la forme: Guéguen, C., Belin, C., Thomas, B.A., Monna, F., Favarger, P.-Y., Dominik, J. (1999) Influence of UV-irradiation on Chelex-100 preconcentration of trace metals in freshwater. *Analytica Chimica Acta*, 386, 155-159.

Projet de recherche

Mon projet de recherche s'articule autour de deux volets complémentaires qui s'inscrivent dans la continuité des thématiques exposées ci-dessus. Ils traitent de (i) la ***mobilité*** *et de la* ***spéciation des métaux*** *dans les sols et de (ii)* ***l'impact des sites miniers*** *abandonnés sur les écosystèmes aquatiques et terrestres actuels. Ces projets privilégient l'aspect* ***dynamique****, la* ***modélisation*** *des cycles, la* ***biodisponibilité*** *des métaux et leurs conséquences sur le vivant. Ils nécessitent une vision pluridisciplinaire de l'environnement, et sont centrés sur le traçage géochimique utilisé soit comme marqueur des mécanismes de transfert, soit comme marqueur d'origine.*

Premier volet : Généralisation des modèles de mobilité des métaux dans les sols

Au cours du temps, les sols accumulent indistinctement les métaux déposés par voie atmosphérique dans les horizons de surface. De là, on assiste à une lente migration en profondeur dont on peut, au mieux, observer l'état *actuel* par la mesure de la distribution des éléments traces métalliques au sein d'un profil de sol. Compte tenu de l'absence de connaissance au sujet de l'évolution de ces distributions dans le passé et du manque de données concernant les flux atmosphériques, il n'est généralement pas possible de modéliser les mécanismes de migration des micropolluants métalliques, contrairement à ce qui a pu être réalisé pour le ^{137}Cs, historiquement bien mieux contraint (e.g. Bossew et Kirchner, 2004 ; Hrachowitz *et al*., 2005). Sur le territoire français, il existe pourtant d'importants sites miniers et métallurgiques anciens dont la chronologie est bien connue. Les contaminations générées par ces activités constituent autant d'analogues archéologiques ou historiques susceptibles d'illustrer le comportement des métaux dans les sols à une échelle temporelle (milliers d'années) qui est importante dans l'analyse du risque environnemental sur le long terme. Les enseignements apportés par une telle dimension temporelle d'étude dépassent largement ce que l'on peut raisonnablement obtenir dans le cadre d'expériences ponctuelles menées en laboratoire, sur des colonnes de sol par exemple.

L’objectif de mon projet de recherche est donc d’établir un modèle fidèle et prédictif du transfert des métaux dans les sols naturels. Pour cela il sera nécessaire de confronter mes expériences acquises à la fois sur les tourbières et sur les sols.

Dans un premier temps, il s’agira d’identifier dans les tourbières à proximité de ces sites miniers les traces laissées par les activités métallurgiques passées, en d’autres termes, de déterminer précisément l’histoire, la magnitude des flux anthropiques des éléments qui n’ont pas subit de migration post-dépôt (c'est-à-dire au moins Pb, Cd, Bi), et l’évolution temporelle de la signature isotopique en plomb du contaminant. Une fois cette étape réalisée, il s’agira d’identifier, de sélectionner et de caractériser des sols voisins de ces tourbières qui n’ont pas été soumis notablement à des phénomènes d’érosion ou de sédimentation, puis d’établir la distribution en éléments traces et majeurs à des échelles pertinentes : celles des horizons, des constituants et des micro-organisations (Thiry et van Oort, 1999 ; van Oort *et al.*, 2002). Cette approche est basée sur la conduite en parallèle d'études détaillées permettant d’appréhender (i) la nature et l’organisation des constituants des sols, et (ii) les teneurs totales en éléments métalliques dans les horizons des sols et dans les fractions de constituants. Ces dernières seront séparées sur la base de leur taille, de leur densité ou des propriétés magnétiques (fractionnements granulo-densimétriques et/ou magnétiques, Lamy *et al.*, 1999 ; Latrille *et al.*, 1998).

Au regard des résultats obtenus à partir des tourbières et des sols, il sera possible :

- d’identifier les constituants et les organisations

- de déterminer la localisation des éléments traces métalliques dans les différentes fractions du sol.

- d’évaluer la stabilité des associations entre éléments traces et les constituants minéraux et/ou organiques

afin de

- bâtir un modèle basé sur des transferts entre horizons régit par des mécanismes de convection, cette fois ci sur l’ensemble de la colonne de sol, et non plus sur le seul horizon de bêchage (cf Axe 2 du présent document).

Par ailleurs, avec Folkert van Oort de l'INRA de Versailles, un projet innovant a été déposé pour confirmer et généraliser l'existence d'une voie originale d'atténuation naturelle des risques liée à l’immobilisation durable des métaux au sein de complexes organométalliques de petites tailles, stade ultime de la décomposition de débris végétaux en présence de métaux (Labanowski *et al.*, 2007). L'application de telles études dans un cadre de sols archéologiques, avec une connaissance précise de l'historique des pollutions, permettra de vérifier la séquestration mutuelle carbone-métaux sur le long terme, d'établir la chronologie dans le cas du plomb, et de démonter le caractère récalcitrant du carbone dans les complexes organométalliques.

Deuxième volet : Impact des sites miniers abandonnés sur les écosystèmes aquatiques et terrestres actuels.

Il est bien connu que l'extraction minière, les procédés de concentration du minerai et sa transformation en métal contribuent à la libération des métaux naturellement présents dans les roches en les rendant plus facilement biodisponibles (Alloway, 1995). A cela, il faut ajouter la lente diffusion depuis tous les déchets enrichis en métaux lourds (haldes, stériles, scories) ou depuis les sols alentours contaminés durablement par les retombées atmosphériques issues des activités métallurgiques passées. Il s'agit de *prendre en compte le poids du passé industriel sur nos écosystèmes aquatiques et terrestres actuels*.

Cette connaissance, qui constitue le cœur de ce projet, s'articulera suivant trois axes :

1. Quantifier la biodisponibilité des métaux transférés (Pb, Cd, As, Tl, + oligo-éléments Cu, Zn…) depuis les sites miniers abandonnés vers les compartiments aquatiques et terrestres.

2. Déterminer l'influence de l'âge des travaux, de leur nature, et du substrat géologique sur les capacités de mobilisation des polluants à moyen et long terme.

3. Modéliser l'impact des sites miniers sur les écosystèmes aquatiques et terrestres, notamment dans le temps et dans l'espace.

Un premier pas a déjà été réalisé dans le Parc national des Cévennes (PNC) qui compte de nombreux sites miniers parsemés de déchets métallurgiques. Ces derniers résultent d'exploitations couvrant une large période, allant de l'Antiquité à l'époque moderne (Baron *et al.,* 2005, 2006). A l'initiative de Paul Revelli, alors vétérinaire pour le PNC, j'ai coordonné en 2007 une étude préliminaire intitulée « Contamination de l'écosystème aquatique par l'héritage métallurgique – Parc national des Cévennes». Cette étude a été menée par une équipe pluridisciplinaire, impliquant notamment Paul Revelli (vétérinaire), Paul Alibert (morphométricien, Université de Bourgogne), Alain Ploquin et Sandrine Baron (géochimistes, CRPG), Olivier Bruguier (Université de Montpellier II), Céline Thomas et Céline Biville, deux étudiantes en Master 1 et Master 2 qui ont réalisé leur stage sous ma direction scientifique ou celle de Paul Alibert. Cette étude, financée par le PNC a consisté à mesurer les teneurs en éléments traces (Pb, Cd, Tl, Cu, Zn, U, Ba, Rb) dans les foies et les chairs de 120 truites *Salmo trutta fario* Linnaeus. Six sites plus ou moins proximaux d'édifices miniers ou de haldes associées ont été sélectionnés. Les résultats démontrent l'impact des sites miniers en déshérence (Pb, Cd, Tl), notamment des plus récents (c'est-à-dire post-XVIII^{e} siècle), et au-delà l'influence de la géologie (U, Ba, Rb). Les concentrations atteignent 100 µg g^{-1} pour le Pb et 40 µg g^{-1} pour le Cd, foies secs ; de tels niveaux ne sont jamais reportés dans la littérature consultée (Figure 21). Les compositions isotopiques du plomb confirment sans ambiguïté l'origine minière. Dans ce contexte, un marqueur biologique potentiellement sensible à des concentrations élevées en métaux lourds a été mesuré: l'instabilité de développement morphologique des truites, déterminée par le biais de l'estimation des niveaux d'asymétrie fluctuante. La fonction de stabilité de développement des organismes est connue pour être directement affectée par les stress d'origine génétique ou environnementale subis durant le développement (Møller et Swaddle, 1997; Alibert et Auffray, 2003, Stige *et al.*, 2006). Des relations nettes sont apparues entre concentrations en métaux lourds dans les foies et l'asymétrie fluctuante de 8 caractères morphologiques parmi les 9 mesurés. Le stress environnemental est tel, qu'il semble affecter ici la stabilité de développement des truites étudiées.

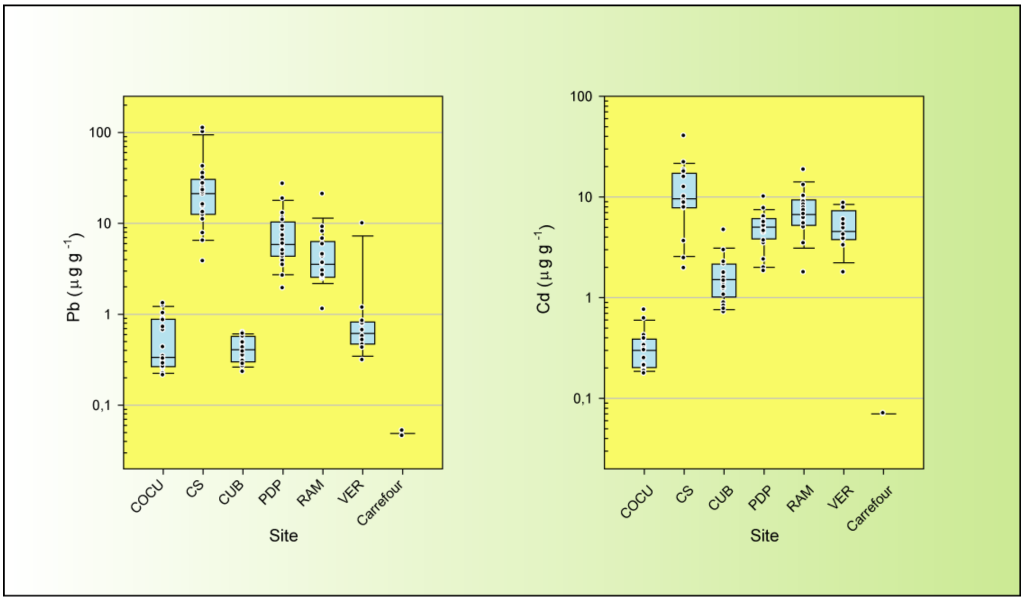

Figure 21 : Concentrations en Pb et Cd (exprimées en µg g^{-1}, foie sec) dans les foies des 120 truites prélevées dans le PNC pour l'étude préliminaire. Les boites grisées représentent les quartiles Q1 et Q3. Ils contiennent la médiane Q2. Les boites sont prolongées par les étendues non atypiques. Secteurs VER : Vérié, milieu granitique non minier ; RAM : Ramponenche, importante mine et laverie, Pb Zn, Ba, XIX^{e}-XX^{e} ; PDP : Pont de la Planche, mine et fonderie de Vialas, Pb, XVIII^{e}-XIX^{e}; CUB : Cubières, mine de Neyrac avec réseau GR, Pb, et reprise moderne ; CS ; Combe Sourde, mine et laverie du Bleymard, Pb/Zn, XIX^{e}-XX^{e} ; COCU : Cocurès, bassin versant minéralisé avec exploitations anciennes M.A., Pb, et exploitation U au XXe des Bondons, CARREF pour des truites provenant de la grande distribution (hypermarché Carrefour).

L'extension à la sphère terrestre est désormais indispensable. En outre, une ouverture géographique vers le Parc Naturel régional du Morvan, situé à la bordure nord-est du Massif Central apparait opportune. Comme le PNC, il s'agit d'une zone à dominante hercynienne, peu soumise à l'activité anthropique moderne, mais qui présente de nombreuses minéralisations et sites miniers aujourd'hui abandonnés. L'activité dans le Morvan a débuté à l'Age du Bronze, soit plus précocement que sur le PNC. Les travaux y sont plus discrets, de natures variées, mais plus abondants, entraînant une pollution sans doute plus diffuse mais sensible. L'extension au Parc Naturel régional du Morvan et la comparaison avec le PNC devrait donc faciliter l'établissement d'un schéma général de comportement des micropolluants, qui pourrait servir d'analogue à des contaminations plus récentes. En outre, ces zones protégées de moyenne montagne sont supposées *a priori* peu polluées et, de ce fait, souffrent face aux zones urbaines ou industrielles, **d'un important déficit d'études environnementales traitant spécifiquement de la contamination métallique**.

La biodisponibilité dans l'écosystème aquatique sera évaluée comme dans l'étude préliminaire *via Salmo trutta fario* Linnaeus. Il s'agit d'un poisson ubiquiste, abondant, relativement sédentaire, et qui est fréquemment utilisé comme biomoniteur (e.g. Linde, 1996 ; Olsvik *et al*., 2001). Il nous renseigne essentiellement sur les transferts liés au lessivage des sites miniers et des sols contaminés environnants. Concernant l'écosystème terrestre, le campagnol (*Microtus Sp.*) possède les mêmes qualités (O'Brian *et al*., 1993). Le transfert métallique s'effectue par contact et ingestion (Metcheva *et al*., 2001). Sa position à la base de la chaine trophique permet de s'affranchir des biais induits par les processus d'accumulation / élimination à chaque étage de prédation. Il nous renseigne sur la biodisponibilité des contaminations accumulées dans les sols soit par dépôt atmosphérique, soit par stockage direct de déchets métallurgiques. L'obtention de cartes de biodisponibilité autour des édifices miniers nous permettra d'établir des stratégies de gestion de ces espaces sur le moyen et long terme.

Bibliographie

Alfonso, S., Grousset, F., Massé, L., Tastet, J.-P. (2001) A European lead isotope signal recorded from 6000 to 300 years BP in coastal marshes (SW France). *Atmospheric Environment*, 35, 3595-3605.

Alibert, P., Auffray, J.-C. (2003). Genomic coadaptation, outbreeding depression and developmental instability. in Polak M. (ed) Developmental instability: Causes and Consequences. New York: Oxford University Press, pp. 116-134

Alloway, B. J. (1995), in B. J Alloway (ed.). Heavy Metals in Soils, Blackie Acad. & Professional, London, pp. 38-57.

Andersen, M.K., Raulund-Rasmussen, K., Hansen, H.C.B., Strobel, W. (2002) Distribution and fractionation of heavy metals in pairs of arable and afforested soils in Denmark. *European Journal of Soil Science* 53, 491-502.

Ausset, P., Del Monte, M., Lefèvre, R.A. (1999) Embryonic sulphated black crusts on carbonate rocks in atmospheric simulation chamber and in the field: role of carbonaceous fly-ash. *Atmospheric Environment*, 33, 1525-1534.

Baize, D., Deslais, W., Gaiffe, M. (1999) Anomalies naturelles en cadmium dans les sols de France. *Étude et Gestion des Sols*, 2, 85-104.

Baize, D., Tercé, M. (2002) Les Éléments traces métalliques dans les sols - Approches fonctionnelles et spatiales. INRA Éditions, Paris. 570 p.

Bargagli, R., Barghigiani, C., Siegel, B.Z., Siegel, S.M. (1991) Trace metals anomalies in surface soils and vegetation on two active island volcanoes: Stromboli and Vulcano (Italy). *Science of The Total Environment*, 102, 209-222.

Bargali, R. (1993) Plant leaves and lichens as biomonitors of natural or anthropogenic emissions of mercury. pp. 461-484. In : Plant as biomonitors. Indicators for heavy Metals in the Terrestrial Environment. Ed. Markert B. Weinhein.

Baron, S., Lavoie, M., Ploquin, A., Carignan, J., Pulido, M., de Beaulieu, J. L. (2005). Record of Metal Workshops in Peat Deposits: History and Environmental Impact on the Mont-Lozère Massif (France). *Environmental Science and Technology*, 39, 5131-5140.

Baron, S., Carignan, J., Laurent, S., Ploquin, A. (2006) Medieval lead making on Mont-Lozère Massif (Cévennes-France): tracing ore sources by using Pb isotopes. *Applied Geochemistry*, 21, 241-252.

Baxter, M.J., Beardah, C.C., Westwood, S. (2000) Sample size and related issues in the analysis of lead isotope data. *Journal of Archaeological Science*. 27, 973-980.

Baxter, M. J. (2003). Statistics in Archaeology. Arnold: London.

Bermond, A., Yousfi, I., Ghestem, J-P. (1998) Kinetic approach to the chemical speciation of trace metals in soils. *Analyst*, 123, 785-789.

Bermond, A., Varrault, G., Sappin-Didier, V., Mench, M. (2005) A kinetic approach to predict soil trace metal bioavailability: preliminary results. *Plant and Soil*, 275, 21-29.

Bindler, R. (2006) Mired in the past — looking to the future: Geochemistry of peat and the analysis of past environmental changes. *Global and Planetary Change*, 53, 209–221

Blum, W.E.H., Brandstetter, A., Wenzel, W.W. (1997) Trace element distribution in soil as affected by land use. In: Biogeochemistry of trace metals. Advances In Environmental Science, Adriano, D.C., Chen, Z.S., Yang, S.S., Iskandar, I-K., (Eds), Science Reviews, Northwood, England, pp. 61-73.

Bossew, P., Kirchner, G. (2004) Modelling the vertical distribution of radionuclides in soils. Part 1: the convection – dispersion equation revisited. *Journal of Environmental Radioactivity*, 73, 127-150.

Boutron, C. F., Gorlach, U., Candelone, J. P., Bolshov, M. A. and Delmas, R. J. (1991) Decrease in anthropogenic lead, cadmium and zinc in Greenland snows since the late 1960s. *Nature*, 353, 153-156.

Brännvall, M.-L., Bindler, R., Emteryd, O., Nilsson, M., Renberg, I. (1997) Stable isotope and concentration records of atmospheric lead pollution in peat and lake sediments in Sweden. *Water Air and Soil Pollution*, 100, 243-252.

Brännvall, M.-L., Bindler, R., Renberg, I., Emteryd, O., Bartnicki, J., Billström, K. (1999) The medieval metal industry was the cradle of modern large-scale atmospheric lead pollution in Northern Europe. *Environment Science and Technology*, 33, 4391-4395.

Briard, J., Verron, G. (1976) Typologie des objets de l'âge du Bronze en France, III : Haches (1), IV : Haches (2), herminettes. *Société Préhistorique Française*, Commission du Bronze. Paris.

Budd, P., Haggerty, R., Pollard, A.M., Scaife, B., Thomas, R.G. (1996) Rethinking the quest for provenance. *Antiquity*. 70, 168-174.

BUWAL. VomMenschen verursashte Luftshaldstoffe-Emissionen in der Schwiez von 1900 bis 2010; Bundesamt für Umwelt, Wald und Landschaft: Bern, Switzerland, 1995.

Camobreco, V.J., Richards, B.K., Steenhuis, T.S., Peverly, J.H., McBride, M.B. (1996) Movement of heavy metals through undisturbed and homogenized soil columns. *Soil Science*, 161, 740-750.

Carignan, J., Simonetti, A., Gariépy, C. (2002) Dispersal of atmospheric lead in northeastern North America as recorded by epiphytic lichens. *Atmospheric Environment*, 36, 3759–3766.

Chang, A.C., Hyun, H.N., Page, A.L. (1997) Cadmium uptake for Swiss chard grown on composted sewage sludge treated field plots: Plateau or time bomb? *Journal of Environmental Quality*, 26, 11-19.

Chapman J.-C., Tylecote R.-F. (1983) Early copper in the Balkan, *Proceedings of the Prehistoric Society*, 49, 373-379.

Chen, J.M., Tan, M.G., Li, Y., Zhang, Y., Lu, W., Tong, Y., Zhang, G., Li, Y. (2005) A lead isotope record of Shanghai atmospheric lead emissions in total suspended particles during the phasing out of leaded gasoline. *Atmospheric Environment*, 39, 1245-1253.

Chiaradia, M., Cupelin, F. (2000) Behaviour of airborne lead and temporal variations of its source effects in Geneva (Switzerland): comparison of anthropogenic versus natural processes. *Atmospheric Environment*, 34, 959-971.

Citeau, L., Lamy., I., van Oort, F., Elsass, F. (2003) Colloidal facilitated transfer of metals in soils under different land use. *Colloids and Surfaces*, 217, 11-19.

Collectif (1999) Plomb dans l'environnement : Quels risques pour la santé ? INSERM Eds. 461 pp.

C.O.N.C.A.W.E. (1993) review - thirtith anniversary 1963-1993, 2(2) 26p

Degryse, F, Smolders, E., Merckx, R. (2006) Labile Cd complexes increase Cd availability to plants. *Environmental Science and Technology*, 40, 830-836.

Denaix, L., Semlali, R.M., Douay. F. (2001) Dissolved and colloidal transport of Cd, Pb, and Zn in a silt loam soil affected by atmospheric industrial deposition. *Environmental Pollution*, 113, 29-38.

Di Pietro, A., Grillo, O.C., Minolfi, P., Munoa, F., Pizzimenti, G., Scoglio, M.E. (1994) Particolato sospeso e metalli pesanti nell'aria del centro urbano di Messina. *Acqua Aria*, 8, 727-734.

Doe, B.R. (1970) Lead isotopes, Springer, Berlin

Dommergues, J.L., Dommergues, C.H., Meister, C. (2006) Exploration of the Oxynoticeratidae ornemental morphospace using the discrete cosine transform (DCT) to analyze rib patterns. *Paleobiology*, 32, 628 – 651.

Dommergues, C.H., Dommergues, J.L., Verrecchia, E.P. (2007) The Discrete Cosine Transform, a Fourier-related method for morphometric analysis of open contours. *Mathematical Geology*, 33, 749-763.

Dold, B. (2003) Speciation of the most soluble phases in a sequential extraction procedure adapted for geochemical studies of copper sulfide mine waste. *Journal of Geochemical Exploration*, 80, 55-68.

Doucet, F.J., Carignan, J. (2001) Atmospheric Pb isotopic composition and trace metal concentration as revealed by epiphytic lichens: an investigation related to two altitudinal sections in Eastern France. *Atmospheric Environment*, 35, 3681-3690.

Dmuchowski, W., Bytnerowicz, A. (1995) Monitoring environmental pollution in Poland by chemical analysis of scots pine (Pinus sylvestris L.) needles. *Environmental Pollution*, 87, 87-104.

Dryden, I.L., Mardia, K.V. (1998) Statistical shape analysis. John Wiley & Sons Ltd, First Edition.

Dunlap, C. E., Steinnes, E., Flegal, A. R. (1999) A synthesis of lead isotopes in two millenia of European air. *Earth Planetary Science Letters*, 167, 81-88.

Elbaz-Poulichet, F., Holliger, P., Huang, W. W., Martin, J. M. (1984) Lead cycling in estuaries, illustrated by the Gironde estuary, France. *Nature*, 308, 409-414.

Elbaz-Poulichet, F., Holliger, P., Martin, J. M., Petit, D. (1986) Stable lead isotopes ratios in major french rivers and estuaries. *The Science of the Total Environment*, 54, 61-76.

Erel, Y. (1998) Mechanisms and velocities of anthropogenic Pb migration in Mediterranean soils. *Environmental Research*, 78, 112-117.

Espinosa, A.J., Rodriguez, M.T., Barragan de la Rosa, F.J., Sanchez, J.C. (2001) Size distribution of metals in urban aerosols in Sevilla (Spain). *Atmospheric Environment*, 35, 2595-2601.

Fangueiro, D., Bermond, A., Santos, E., Carapuça, H., Duarte, A. (2002) Heavy metal mobility assessment in sediments based on a kinetic approach of the EDTA extraction: search for optimal experimental conditions. *Analytica Chimica Acta* 459, 245-256.

Fangueiro, D., Bermond, A., Santos, E., Carapuça, H., Duarte, A. (2005) Kinetic approach to heavy metal mobilization assessment in sediments: choose of kinetic equations and models to achieve maximum information. *Talanta* 66, 844-857.

Farmer, J. G., Mackenzie, A. B., Sugden, C. L., Edgar, P. J., Eades, L. J. (1997) A comparison of the historical lead pollution records in peat and freshwater lake sediments from Central Scotland. *Water Air and Soil Pollution*, 100, 253-270.

Faure G. (1986) Principles of isotope geology, 2nd edition, John Wiley and Sons, 589 pp.

Fernandez, C., Labanowski, J., Cambier, P., Jongmans, A.G., van Oort, F. (2007) Fate of airborne metal pollution in soils as related to agricultural management. 1. Zn and Pb distributions in soil profiles. *European Journal of Soil Science*, 58, 547-559.

Flament, P., Bertho, M.-L., Deboudt, K., Véron, A., Puskaric, E. (2002) European isotopic signatures for lead in atmospheric aerosols: a source apportionment based upon ^{206}Pb/^{207}Pb ratios. *Science of The Total Environment*, 296, 35-57.

Formenti, P., Annegarn, H.J., Picket, S.J. (1998) Time resolved aerosol monitoring in the urban centre of Soweto. *Nuclear Instrumentation & Methods in Physics Research*, 948–954.

Gale N.H, Stos-Gale Z.A., Livov P., Dimitov M., Todorov T. (1991) Recent studies of neolithic copper ores and artefacts in Bulgaria. In : Découverte du métal. Eluère, Mohen dir., Paris, (ed.). Picard, coll. " Millénaires ", pp. 49-75.

Gale, N.H., Stos-Gale, Z.A. (1992) Lead isotope studies in the Aegean. *Proceedings of the British Academy*, 77, 63-108.

Gale, N.H., Stos-Gale, S., (2000) Lead isotope analyses applied to provenance studies. In Modern analytical methods in art and archaeology. Eds Ciliberto, E et Spoto, G. Wiley Science.

Galletti, G., Bochini, P., Cam, D., Chiavari, G., Mazzeo, R. (1997) Chemical characterization of the black crust present on the stone central portal of St. Denis abbey. *Fresenius Journal of Analytical Chemistry*, 357, 1211-1214.

Galop, D., Jalut, G. (1994) Differential human impact and vegetation history in two adjacent Pyrenean valleys in the Ariège basin, southern France, from 3000 BP to the present. *Vegetation History and Archeobotany*, 3, 225-244.

Garty, J. (1985). The Amount of Heavy Metals in Some Lichens of the Negev Desert. *Environmental Pollution*, 10, 287-300.

Getty, S.R., Gutzler, D.S., Asmeron, Y., Shearer, C.K., Free, S.J. (1999) Chemical signals of epyphytic lichens in southwestern North America ; natural versus man-made sources for airborne particulates. *Atmospheric Environment*, 33, 5095-5104.

Gleyzes, C., Tellier, S., Astruc, A. (2002) Fractionation studies of trace elements in contaminated soils and sediments: a review of sequential extraction procedures. *Trends in Analytical Chemistry*, 21, 451-467.

Goodsite, M.E., Heinemeier, J., Rom, W., Lange, T., Ooi, S., Appleyby, P.G., Shotyk, W., van der Knaap, W.O., Lohse, C., Hansen, T.S. (2002) High resolution AMS ^{14}C dating of post bomb peat archives of atmospheric pollutants. *Radiocarbon*, 43, 495-515.

Grousset, F.E., Quétel, C.R., Thomas, B., Buat-Ménard, P., Donard, O.F.X. and Buchet, A. (1994) Transient Pb isotopic signatures in the western European atmosphere. *Environmental Science and Technology*, 28, 1605-1608.

Grousset, F.E., Quétel, C.R., Thomas, B., Donard, O.F.X., Lambert, C.E., Guillard, F., Monaco, A. (1995) Anthropogenic vs. lithogenic origins of trace elements (As, Cd, Pb, Rb, Sc, Sn, Zn) in water column particles: northwestern Mediterranean Sea. *Marine Chemistry*, 48, 291-310.

Guillaumet J.-P., Niaux R., Moreau R. (2001) Traces d'exploitation de minerai en Morvan. *Académie du Morvan*, 51, 36-40.

Hamelin, B., Grousset, F., Sholkovitz, E.R. (1990) Pb isotopes in superficial pelagic sediments from the North Atlantic. *Geochimica Cosmochimica Acta*, 54, 37-47.

Harrison, R.M., Sturges, W.T. (1983) The measurement and interpretation of Br/Pb ratios in airborne particles. *Atmospheric Environment*, 17, 311-328.

Hernandez, L., Probst, A., Probst, J.-L., Ulrich, E. (2003) Heavy metal distribution in some French forest soils: evidence for atmospheric contamination. *The Science of the Total Environment*, 312, 195-219.

Hong, S., Candelone, J.-P., Patterson, C.C., Boutron, C.F. (1994) Greenland ice evidence of hemispheric lead pollution two millenia ago by greek and roman civilizations. *Science*, 265, 1841-1843.

Hrachowitz, M., Maringer, F.-J., Steineder, C., Gerzabek, M.H. (2005) Soil redistribution model for undisturbed and cultivated sites based on Chernobyl-derived Cesium-137 fallout. *Journal of Environmental Quality*, 34, 1302-1310.

Jensen, N. P., Svensmark, B. (1989) Distribution and concentration of Pb and Cd in two adjacent Luvisols under grassland and forest in Denmark. *Zeitschrift für Pflanzenernährung und Bodenkunde,* 152, 121-124.

Joumard, R., Chiron, M., Delsey, J. and Lambert, J. (1983) Le dossier du plomb additif des carburants automobiles. IRT. Novembre 1983. ISSN 0339-8676

Komárek, M., Ettler, V., Chrastný, V., Mihaljevič, M. (2008) Lead isotopes in environmental sciences: A review. *Environment International*, 34, 562-577.

Krishnamurti, G.S., Smith, L.H., Naidu, R. (2002) Method for assessing plant-available cadmium in soils. *Australian Journal of Soil Research*, 38, 823-836.

Kramers, J.D., Tolstikhin, I.N. (1997) Two terrestrial lead isotope paradoxes, forward transport modelling, core formation and the history of the continental crust. *Chemical Geology*, 139, 75-110.

Labanowski, J., Sebastia, J., Foy, E., Jongmans, T., Lamy, I., van Oort, F. (2007) Fate of metal-associated POM in a soil under arable land use contaminated by metallurgical fallout in northern France. *Environmental Pollution*, 149, 59-69.

Lamy I., Latrille C., Ducaroir J. (1999) Apport des fractionnements physiques dans l'étude de la dynamique des éléments trace dans les sols. in: La spéciation des métaux dans les sols, Les cahiers du club CRIN – Club CRIN "Environnement" et Ministère de l'Environnement, Edition ECRIN, Paris, France, pp. 56-72.

Latrille C., Elsass F., van Oort F., Denaix L. (2001) Physical speciation of trace metals in Fe-Mn concretions from a rendzic lithosol soil developed on Sinemurian limestones (France). *Geoderma*, 100, 127-146.

Lee J. A., and Tallis, J. H. (1973) Regional and historical aspects of lead pollution in Britain. *Nature*, 245, 216-218.

Lefèvre, R.A., Ausset, P. (2002) Atmospheric pollution and building materials: stone and glass. Natural Stone, Weathering Phenomena, Conservation Strategies and Case studies. Geological Society, London, Special Publications. 205, 329-345.

Linde, A. R., Arribas, P., Sanchez-Galan, S., García-Vásquez, E. (1996) Eel (Anguilla anguilla) and brown trout (Salmo trutta) target species to assess the biological impact of trace metal pollution in freshwater ecosystems. *Arch. Environ. Con. Tox.*, 31, 297-302.

Loppi, S., Pirintsos, S.A. (2003) Epiphytic lichens as sentinels for heavy metal pollution at forest ecosystems (central Italy). *Environmental Pollution*, 121, 327–332.

Martínez-Cortizas, A., Pontevedra-Pombal, X., Nóvoa-Muñoz, J.C., García-Rodeja, E. (1997) Four thousand years of atmospheric Pb, Cd and Zn deposition recorded by the ombrotrophic paet bog of Penido Vello (Northwestern Spain). *Water Air and Soil Pollution*, 100, 387-403.

Martínez-Cortizas, A., Garcia-Rodeja, E., Pontevedra Pombal, X., Nóvoa-Muñoz, J.C., Weiss, D., Cherbukin, A. (2002) Atmospheric Pb deposition in Spain during the last 4600 years recorded by two ombrotrophic peat bogs and implications for the use of peat as archive. *The Science of The Total Environment*, 292, 33-44.

Martínez Cortizas, A., Mighall, T., Pontevedra Pombal, X., Nóvoa, Muñoz, J.C., Peiteado Varela, E., Piñeiro Rebolo, R. (2005) Linking changes in atmospheric dust deposition, vegetation change and human activities in northwest Spain during the last 5300 years. *Holocene*, 15, 698–706.

Matzka, J., Maher, B. A. (1999) Magnetic biomonitoring of roadside tree leaves: Identification of spatial and temporal variations in vehicle derived particles. *Atmospheric Environment*, 33, 4565– 4569.

McCarty, D.K., Moore, J.N., Marcus, W.A. (1998) Mineralogy and trace element association in an acid mine drainage iron oxide precipitate; comparison of selective extractions. *Applied Geochemistry*, 13, 165– 176.

McGrath, D. (1996) Application of single and sequential extraction procedures to polluted and unpolluted soils. *The Science of the Total Environment*, 178, 37-44.

MacLeod, N. (1999) Generalizing and Extending the Eigenshape Method of Shape Space Visualization and Analysis. *Paleobiology*, 25, 107-138.

Mighall, T. M., Abrahams, P. W., Grattan, J. P., Hayes, D., Timberlake, S., Forsyth, S. (2002) Geochemical evidence for atmospheric pollution derived from prehistoric copper mining at Copa Hill, Cwmystwyth, mid-Wales, UK. *The Total Environment*, 292, 69-80.

Metcheva, R., Teodorava, S., Topashka-Ancheva, M. (2001). A comparative analysis of the heavy metals and toxic elements loading indicated by small mammals in diferent bulgarian regions. *Acta Zoologica Bulgarica*. 53, 61-80.

Møller, A. P., Swaddle, J. P. 1997. Asymmetry, Developmental Stability and Evolution. Oxford: Oxford University Press.

Monfray, P., Granier, A. Prospective SIC 2007, atelier 4 « Impact du changement global » Synthèse du 18 Janvier 2007.

Niederschhlag, E., Pernicka , E., Seifert, T., Bartelheim, M.(2003) The determination of lead isotope ratios by multiple collector ICP-MS: a case study of Early Bronze age artefacts and their possible relation with ore deposits of the Erzgebirge. *Archaeometry*, 45, 61-100.

Nimis, P.L., Castello, M., Perotti, M. (1990) Lichens as bioindicators of heavy metal pollution: a case study at La Spezia (N. Italy). *Lichenologist*, 22, 265 - 284.

Nriagu, J. O. (1988) Quantitative assessment of worldwide contamination of air, water and soils by trace metals. *Nature*, 333, 134-139.

Nriagu, J. O. (1989) A global assessment of natural sources of atmospheric trace metals. *Nature*, 338, 47-49.

O'Brien, D.J., Kaneene, J.B., Poppenga, R.H. (1993). The use of mammals as sentinels for human exposure to toxic contaminants in the environment. *Environmental Health Perspectives*. 99, 351-368.

Olsvik, P. A., Hindar, K., Zachariassen, K. E., Andersen, R. A. (2001) Brown trout (Salmo trutta) metallothioneins for metal exposure in two Norwegian rivers. *Biomarkers*, 6, 274-288.

Patterson, C.C. (1983) Criticism of "flow of metals into the atmosphere". *Geochimica et Cosmochimica Acta*, 47, 1163-1168.

Pernicka, E. (1995) Crisis or Catharsis in lead isotope analysis? *Journal of Mediterranean Archaeology*, 8, 59-64.

Petelet, E., Ben Othman, D., Luck, J.M. (1997) Etude des charges dissoute et particulaire dans une rivière méditerranéenne (Vène, Hérault, France): apport des éléments majeurs, traces et des isotopes du plomb et du strontium sur l'origine et la circulation des eaux et des charges transportées. *C.R. Acad. Sci.*, 324 IIa, 753-761.

Petrovský, E., Kapička, A., Jordanova, N., Knap, M., Hoffmann, V. (2000) Low-field magnetic susceptibility: a proxy method of estimating increased pollution of different environmental systems. *Environmental Geology*, 39, 312-318.

Pollard, A.M., Heron, C. (1996) Archaeological Chemistry. The Royal Society of Chemistry Eds. 375 pp.

Pyatt, F.B., Gilmore, G., Grattan, J.P., Hunt, C.O., McLaren, S. (2000) An imperial legacy? An exploration of the environmental impact of ancient metal mining and smelting in southern Jordan. *Journal of Archaeological Science*, 27, 771-778.

Reinmann, C., de Carita, P. (2000) Intrinsic flaws of element enrichment factors (EFs) in environmental geochemistry. *Environmental Science and Technology*, 34, 5084-5091.

Reinmann, C., de Carita, P. (2005) Distinguishing between natural and anthropogenic sources for elements in the environment: regional geochemical surveys versus enrichment factors. *The Science of the Total Environment*, 337, 91-107.

Renberg, I., Brännvall, M.-J., Bindler, R., Emteryd, O. (2000) Atmospheric lead pollution history during four millenia (2000 BC to 2000 AD) in Sweden. *Ambio*, 29, 150-156.

Richard, H., Eschenlhor, L. (1998) Essai de corrélation entre les données polliniques et les données archéologiques: le cas des forêts de Lajoux dans les Franches-Montagnes (Lajoux-Suisse). *Revue d'archéométrie*, 22, 29-37.

Rodriguez-Navarro, C., Sebastian, E. (1996) Role of particulate matter from vehicle exhaust on porous building stones (limestone) sulfation. *The Science of the Total Environment*, 187, 79-91.

Rosman, K. J. R., Chisoholm, W., Hong, S., Candelone, J.-P., Boutron, C. F. (1997) Lead from Carthaginian and roman Spanish mines isotopically identified in Greenland ice dated from 600 B.C. to 300 A.D. *Environmental Science and Technology*, 31, 3413-3416.

Rychner, V., Klaentschi, N. (1995) Arsenic, nickel et antimoine. Lausanne, 1995, t. 1, 112 p. *Cahier d'archéologie romande*, 63.

Sagnotti, L., Macri, P., Egli, R., Mondino., M. (2006) Magnetic properties of atmospheric particulate matter from automatic air sampler stations in Latium (Italy): Toward a definition of magnetic fingerprints for natural and anthropogenic PM_{10} sources. *Journal of Geophysical Research*, 111, B12S22.

Schettler, G., Romer, R. L. (1998) Anthropogenic influences on Pb/Al and lead isotopic signature in annually layered Holocene Maar lake sediments. *Applied Geochemistry*, 13, 6, 787-797.

Shotyk, W., Weiss, D., Appleby, P.G., Cheburkin, A.K., Frei, R., Gloor, M., Kramers, J.D., Reese, S., Van der Knaap, W.O. 1998. History of atmospheric lead deposition since 12,370 14C yr BP from a peat bog, Jura Mountains, Switzerland. *Science*, 291, 1635-1640.

Simão, J., Ruiz-Agudo, E., Rodriguez-Navarro, C. (2006) Effects of particulate matter from gasoline and diesel vehicle exhaust emissions on silicate stones sulfation. *Atmospheric Environment*, 40, 6905-6917.

Spiro, S., Weiss, D.J., Purvis, O.W., Mikhailova, I., Williamson, B.J., Coles, B.J., Udachin, V. (2004) Lead isotopes in lichens transplants around a Cu smelter in Russia determined by MC-ICP-MS reveal transient records of multiple sources. *Environmental Science and Technology* 38, 6522–6528.

Squeri, L.O.C., Grillo, A., di Pietro, F., Munao, P., Lagana, Scoglio, M.E. (1992) Livelli di piombo presenti nell'aria del centro urbano di Messina. *Inquinamento*, 34, 118-123.

Sterckeman, T., Douay , F., Proix, N., Fourrier, H. (2000) Vertical distribution of Cd, Pb and Zn in soils near smelters in the North of France. *Environmental Pollution*, 107, 377-389.

Stige, L. C., David, B., Alibert, P. (2006) On hidden heterogeneity in directional asymmetry - can systematic bias be avoided? *Journal of Evolutionary Biology*, 19, 492-499.

Tessier, A., Campbell, P.G.C., Bisson, M. (1979) Sequential extraction procedure for the speciation of particulate trace metals. *Analytical Chemistry*, 51, 844-851.

Teutsch, N., Erel, Y., Halicz, L., Banin, A. (2001) Distribution of natural and anthropogenic lead in Mediterranean soils. *Geochimica et Cosmochimica Acta*, 65, 2853-2864.

Thiry M., van Oort F. (1999) De l'échantillonnage à la spéciation : pertinence des analyses minéralogiques par diffraction des Rayons-X dans les sites et sols pollués par des métaux. In: La spéciation des métaux dans les sols, Les cahiers du club CRIN – Club CRIN "Environnement" et Ministère de l'Env., Edition ECRIN, Paris, France, pp. 96-107, 108-156.

van Oort, F., Gaultier, J.P., Hardy, R., Bourennane, H. (2002) Distributions spatiales de métaux et stratégies d'échantillonnage dans les sols du périmètre agricole d'une friche industrielle. In : Les Eléments métalliques dans les sols - Approches fonctionnelles et spatiales. (D. Baize, M. Tercé, coords), 281-297, INRA-Ed., Versailles.

van Oort, F., Jongmans, A.G., Citeau, L., Lamy, I., Chevallier, P. (2006) Microscale Zn and Pb distribution patterns in subsurface soil horizons: an indication for metal transport dynamics. *European Journal of Soil Science*, 57, 154-166.

van Storch H., Hagner C., Costa-Cabral M., Feser F., Pacyna J.M., Pacyna E., Kolb, S. (2002) Curbing the omnipresence of lead in the European environment since the 1970's - a successful example of efficient environmental policy. *EOS*, 83, 393-399.

Vile, M.A., Wieder, R.K., Novàk, M. (1999) Mobility of lead in Sphagnum-derived peat. *Biogeochemistry*, 45, 35-52.

Weiss, D., Shotyk, W., Boyle, E.A., Kramers, J.D., Appleby, P.G., Cheburkin, A.K. (2002) Comparative study of the temporal evolution of atmospheric lead deposition in Scotland and eastern Canada using blanket peat bogs. *The Science of the Total Environment*, 292, 7-18.

West, S., Charman, D. J., Grattan, J. P. and Cherburkin, A. K. (1997) Heavy metals on Holocene peats from South West England: detecting mining impacts and atmospheric pollution. *Water Air and Soil Pollution*, 100, 343-353.

Widory, D., Roy, S., Le Moullec, Y., Goupil, G., Cocherie, A., Guerrot, C. (2004) The origin of atmospheric particles in Paris: a view through carbon and lead isotopes. *Atmospheric Environment*, 38, 953–961.

Zalduegui, J.F.S., De Madinabeitia, S.G., Ibarguchi, J.I.G., Palero, E. (2004) A lead isotope database: The Los Pedroches-Alcudia area (Spain); Implications for archaeometallurgical connections across southwestern and southeastern Iberia. *Archaeometry*, 46, 625-634.

Curriculum vitae

Fabrice Monna

Né le 13 Avril 1968
Adresse professionnelle : UMR CNRS – Culture - Université de Bourgogne 5594 ARTéHIS, Equipe Géoarchéologie, Centre des Sciences de la Terre, Université de Bourgogne, 6, bd Gabriel, F-21 000 Dijon.
Tel : +33 (0)3 80 39 63 60, Fax : +33 (0) 3 80 39 62 87,
Email : Fabrice.Monna@u-bourgogne.fr

SITUATION ACTUELLE

Maître de Conférences (35ème section CNU) à l'Université de Bourgogne.
- Rattaché à l'UFR Sciences de la Terre et de l'Environnement
- Rattaché à l'UMR 5594 ARTéHIS

Domaine de recherche : Cycles biogéochimiques des éléments traces métalliques aux interfaces de l'environnement.

PARCOURS PROFESSIONNEL

- 1992 : DEA T.G.G.H. (Tectonique, Géophysique, Géochimie, Hydrologie). Université de Montpellier II, Laboratoire de Géochimie Isotopique.
- De 1992 à 1996 : Moniteur CIES.
- De 1992 à 1996 : Thèse de Doctorat, Université de Montpellier II, Laboratoire de Géochimie Isotopique.
- Sujet de recherche : «*Utilisation des isotopes du Pb dans les études environnementales. Application à l'évolution temporelle et à l'origine des apports en Pb dans l'étang de Thau (Hérault-France)*» sous la direction scientifique du Pr. J. Lancelot. Mention très honorable et félicitations du jury.
- 1996 : Attaché Temporaire d'Enseignement et de Recherche (ATER), Université de Montpellier II
- 1996 : Stage post doctoral à l'Université de Brême (Allemagne). Laboratoire de Géochimie et d'Hydrogéologie. Mission : Mesure des rapports isotopiques du Pb à l'aide d'une ICP-MS Finningan-Mat type SOLA. Responsables : Pr H.D. Schultz and Dr K. Hamer
- De 1997 à 1999 : Stage post doctoral à l'institut FA Forel (Suisse)- Université de Genève. Missions : Rôle des colloïdes dans le transfert des polluants en milieu lacustre. Mesure des rapports isotopiques du Pb à l'aide

d'une ICP-MS Thermo Jarrell Ash type POEMS et HP 4500. Application aux sédiments du lac Léman en vue de déterminer l'origine et l'évolution temporelle de la contamination. Responsable : Pr J. Dominik.
- De 1999 à 2003 : Maître de Conférences à l'UMR A111, Microbiologie des sols, équipe GéoSol, Université de Bourgogne.
- Depuis 2003 : Maître de Conférences à l'UMR 5594, ARTéHIS, équipe Géoarchéologie, Université de Bourgogne.

BOURSES ET PRIMES

- De 1992 à 1995 : Allocation de recherche MNERT (+ allocation de monitorat)
- Depuis 2005 : Titulaire de la Prime d'Encadrement Doctoral et de Recherche
- Depuis 2005 : Titulaire d'une prime pédagogique en tant que responsable de la licence 2eme année Sciences de la Terre et de l'Environnement.

EXPERIENCES D'ENSEIGNEMENT

Université de Bourgogne (depuis 1999)

Licence 1. TD/TP Géologie générale (1999-2002), CM/TD/TP Géodynamique externe (1999-2008)
Licence 2. CM/TD Statistiques (2000-2008), TD/TP Tectonique (1999), CM/TD Géochimie (2003-2008), CM/TD/TP Géodynamique externe (1999-2008).
Licence 3. CM/TD Thermodynamique (1999), CM/TD Statistiques (2000-2008)
Master 1. M1 Sciences de la Terre, de l'Environnement, de la Vigne, Géoarchéologie : CM/TD Transferts continentaux (1999-2001), CM/TD Fonctionnement des écosystèmes (2000-2008), CM/TD/TP Statistiques (2000-2008) ; M1 Biologie des populations : CM/TD Hydrogéologie, Hydrologie de Surface (1999-2002) ;
Master 2. M2 GEE : Géochimie Isotopique (1999-2006), Transfert des polluants (1999-2005) ; M2 Géoarchéologie : Statistiques (2001-2008), Géochimie appliquée à l'archéologie, PAO (2002-2006).
Préparation CAPES/AGREGATION. CM/TD Géochronologie (2001-2008), leçons en géochimie isotopique et hydrologie.

Université de Franche-Comté (depuis 2005)

Master 2 Santé Environnement : CM Géochimie Isotopique (4-6h/an)

Université de Chambéry (depuis 2007)
Master 2 : Géochimie isotopique appliquée à l'étude des paléoenvironnements (4h).

Université de Fribourg (2006)

Master 2 : Cours bloc (14h) Géochimie isotopique appliquée à l'étude des paléo-environnements.

Université de Genève (1997-1999)

Master 2 DESNE : Géochimie isotopique (6h/an)

Université de Montpellier II, moniteur et ½ ATER (1992-1996)

Licence 1 et 2 (spécialités Biologie et Sciences de la Terre) : TD Techniques informatiques.
Master 2 spécialité Géochimie et Géophysique : Géochimie isotopique.

Autres

Intervenant au titre de la formation continue CNRS à destination des chercheurs de l'UMR 5594 (2006) : Techniques statistiques appliquées à l'archéologie (35h).

RESPONSABILITES ADMINISTRATIVES (HORS RECHERCHE)

Actuelles

Depuis 2005 : Coresponsable (avec J. Thierry), puis responsable de la Licence 2eme année option Sciences de la Terre et de l'Environnement (à partir de 2006), Université de Bourgogne. Porteur du projet de renouvellement (2007).
Depuis 2006 : Membre élu du Conseil d'UFR Sciences de la Terre et de l'Environnement, Université de Bourgogne.
Depuis 2002 : Membre de commission de spécialistes Université de Reims (section Sciences de la Terre), titulaire (section 35).

Passées

2002-2006 : Membre nommé du comité scientifique de la SEIVA, Structure d'Echange et d'Information sur Valduc (site CEA, Côte d'Or).
1999-2001 : Responsable du Secteur Analytique du Centre des Sciences de la Terre, Université de Bourgogne.

Animation de la recherche

PARTICIPATION ET ANIMATION DE PROGRAMMES DE RECHERCHE ET DE CONTRATS (DEPUIS 1999)

- Responsable du volet géochimie du Programme Commun de Recherche (PCR) « Paléoenvironnement et dynamique de l'anthropisation en montagne Basque » (1999 – 2002), financement : Ministère de la Culture. Responsable du programme : Didier Galop.
- Co-responsable (avec Rémi Losno, LISA, Paris) des accords CNRS/NRF (2002): « Pb isotopes and heavy metal content for deciphering the origin of contamination in the Johannesburg atmosphere (South Africa), using lichens as bio-indicators, and airborne particles." N° 13281.
- Responsable du volet géochimie de l'Action Collective de Recherche « Age du Bronze » (2003-2005), financement : Ministère de la Culture. Responsable du programme : Jean-François Piningre.
- Responsable du volet géochimie du programme : « Archéologie et géoarchéologie à Rosia Montana, Roumanie ». (2004-2007) Responsable Béatrice Cauuet.
- Co-responsable (avec Christophe Petit.) du projet de recherche « Paléoenvironnement du Mont Beuvray » (2002 – 2005). Financement du Centre Archéologique Européen du Mont-Beuvray.
- Responsable du volet géochimie de l'Action Collective de Recherche "Rythmes et causalités des dynamiques de l'anthropisation en milieu montagnard : l'exemple de la construction des territoires pyrénéens de la fin du Mésolithique à l'aube de notre ère ". (2003 – 2007), financement : CNRS. Responsables du programme : Didier Galop, Laurent Carozza, Nicolas Valdeyron.
- Co-responsable (avec Claude Mordant) du projet: « Productions métalliques et pollutions anciennes en Bourgogne et en France Orientale. » (2005-2007) Financement Région Bourgogne.
- Responsable du projet (2005-2007): « Contamination métallique de l'écosystème aquatique par l'héritage métallurgique. Parc des Cévennes, France. ». Financement Parc des Cévennes.
- Responsable du projet (2007-2008): « Complément à l'étude écotoxicologique d'éventuelles contaminations par le Plomb liée à la métallurgie ancienne sur le Mont Lozère. ». Financement Parc des Cévennes.

EXPERTISES ET JURYS

Examinateur des jurys de thèse suivants :

- Stéphanie Alfonso (2000) Etude de Paléoenvironnements Littoraux. Etablissement d'une échelle chronostratigraphique à partir des retombées atmosphériques de métaux. Direction F. Grousset. Université de Bordeaux.
- Sébastien Ariès (2001) Mise en évidence de contaminations métalliques historiques à partir de l'étude d'enregistrements sédimentaires de lacs de haute montagne. Direction M. Polvé. Université de Toulouse.
- Frédéric Planchon (2001) Les métaux lourds et leur isotope dans les neiges et glaces de l'Antarctique : traceurs de la pollution globale et des paramètres climatiques des derniers cycles glaciaires. Direction C. Boutron. Université de Grenoble.
- Sandrine Baron (2005) Traçabilité et évolution d'une pollution métallurgique médiévale de plomb argentifère sur le Mont-Lozère. Direction F. Elbaz-Poulichet, A. Ploquin, J. Carignan. Université de Montpellier II.
- Christelle Fernandez (2006) Devenir du Zn, Pb et Cd issus de retombées atmosphériques dans les sols, à différentes échelles d'étude. -Influence de l'usage des sols sur la distribution et la mobilité des métaux- Direction P. Cambier, F. van Oort. INA-PG, Paris.

Expertises :

- 1997-1999 : Membre du comité éditorial de « The Science of the Total Environment », Elsevier Science publication
- Membre du comité scientifique du 2nd European Meeting on Environmental Chemistry 12-15 Dec. 2001, Dijon, France
- Membre du comité scientifique de la Réunion des Sciences de la Terre, avril 2006, Dijon, France
- Expertises fréquentes (6-8 fois/an) pour les revues : Environmental Science and Technology, Environmental Pollution, Atmospheric Environment, Environmental Chemistry, Geochimica et Cosmochimica Acta, The Science of the Total Environment, Australian Journal of Chemistry, Journal of Environmental Radioactivity, Environment International, Earth Planetary Sciences Letters, Estuarine Coastal and Shelf Science, Water Air and Soil Pollution, Comptes rendus de l'Académie des Sciences, Ecotoxicology and Environmental Safety, Applied Geochemistry, Quaternary International, Environmental Monitoring and Assessment.
- Expert extérieur en 2006 pour le Natural Environment Research Council (NERC), UK.
- Expert pour programmes ECLIPSE et IPEV.

FORMATION PAR LA RECHERCHE : ENCADREMENT DE 3^e CYCLE

Doctorat :

Forel Benoît. « *Approvisionnement et consommation métalliques en France Orientale protohistorique : approches paléo-environnementales et caractérisations chimiques du mobilier métallique.* » Co-dir. Claude Mordant (50%)
Début de thèse : novembre 2004, soutenance prévue le 10 décembre 2008
Projet : Action Collective de Recherche « Age du Bronze », financement : Ministère de la Culture.
Financement : Bourse Docteur Ingénieur (CNRS, Région Bourgogne)
Publications co-signées :

Gabillot, M., Forel, B. , Monna, F., Naudin, A. , Losno, R., Piningre, J.-F., Mordant, C., Dominik, J., Bruguier, O. (sous presse) Influences atlantiques dans les productions métalliques en Bourgogne et Franche-Comté au Bronze moyen. *Actes du colloque en hommage à C. Millote*, Besançon.

Jouffroy-Bapicot I., Forel B., Monna F., Petit C. Paléométallurgie dans le Morvan : l'apport des analyses polliniques et géochimiques. *in Actes du 131e congrès du CTHS « Tradition et Innovation »* Grenoble 2006. (à paraître).

Forel, B., Gabillot, M., Monna, F., Forel, S., Dommergues, C.H., Gerber, S., Petit, C. Mordant, C., Château, C. (2008) Morphometry of Middle Bronze Age palstaves by Dis-crete Consine Transform. *Journal of Archaeological Sciences*. DOI :10.1016/j.jas.2008.10.021.

Master 2 :

Caillet Stéphane (1999) « *Apports atmosphériques en Pb-210 et Be-7 dans la région du lac Léman.* » Co-dir. Janusz Dominik (50%). Diplôme en Sciences Naturelles de l'Environnement.
Projet : intégration au programme FNRS
Publication co-signée:

Caillet, S., Arpagaus, P., Monna, F., Dominik, J. (2001) Factors controlling ^{7}Be and ^{210}Pb atmospheric deposition as revealed with sampling by individual rain events in the region of Geneva, Switzerland. *Journal of Environmental Radioactivity*. 53, 241-256.

Situation professionnelle : Enseignement

Tual Magali (2001) « *Histoire des activités métallurgiques en montagne Basque. Une démarche intégrée.* » DEA GEE, Co-dir. Didier Galop (50%).
Projet : intégration au Programme Commun de Recherche « Paléoenvironnement et dynamique de l'anthropisation en montagne Basque » financé par le Ministère de la Culture.
Publications co-signées:

Galop, D., Tual, M., Monna, F., Dominik, J., Beyrie, A. (2001) Cinq millénaires de métallurgie en Montagne Basque. Les apports d'une démarche intégrée alliant palynologie et géochimie isotopique du plomb. *Sud Ouest Européen*, 11, p 3-15.

Monna, F., Galop, D., Carozza, L., Tual, M., Beyrie, A., Marembert, F., Chateau, C., Dominik, J., Grousset, F.E. (2004) Environmental impact of early Basque mining and smelting recorded in a high ash minerogenic peat deposit. *Science of the Total Environment*, 327, 197-214.

Situation professionnelle : Ingénieur en bureau d'étude, Paris (environnement).

Blanchot Cédric (2001) « *Histoire des pollutions en plomb reconstituée à partir de la tourbière géo-ombrotrophique du Port des Lamberts, Nièvre, France.* » DEA GEE. Co-dir. Christophe Petit (50%).
Projet : intégration au projet «Paléoenvironnement du Mont Beuvray » (Financement : Centre Archéologique Européen du Mont Beuvray).
Publication co-signée:

Monna, F., Petit, C., Guillaumet, J.-P., Jouffroy-Bapicot, I., Blanchot, C., Dominik, J., Losno, R., Richard, H., Lévêque, J., Chateau, C. (2004) History and environmental impact of mining activity in Celtic Aeduan territory recorded in a peat-bog (Morvan – France). *Environmental Science and Technology*, 38, 3, 657-673.

Situation professionnelle : Ingénieur qualité, Dijon (environnement).

Boisson Jérome (2003) « *Inventaire des ressources et des exploitations minières métalliques dans le Morvan.* » DESS Géoarchéologie, Co-dir. Christophe Petit (50%).
Projet : intégration au projet «Paléoenvironnement du Mont Beuvray » (Financement : Centre Archéologique Européen du Mont Beuvray).
Situation professionnelle : ?

Forel Benoît (2004) « *Histoire des paléo-pollutions dans la tourbière de Plancher-les-Mines (Haute-Saône, Franche-Comté) – Approche géochimique.* » DESS Géoarchéologie, Université de Bourgogne. Co-dir. Christophe Petit (50%).
Projet : Action Collective de Recherche « Age du Bronze », financement : Ministère de la Culture.
Situation professionnelle : Thèse, titulaire d'une Bourse Docteur Ingénieur, en cours, Université de Bourgogne.

Naudin Aline (2006) « Etude des compositions chimiques et isotopiques du mobilier métallique de Sermizelles, Yonne (Age du Bronze). » DEA CEPS.
Projet : Action Collective de Recherche « Age du Bronze », financement : Ministère de la Culture.
Publication co-signée:

Gabillot, M., Forel, B. , Monna, F., Naudin, A. , Losno, R., Piningre, J.-F., Mordant, C., Dominik, J., Bruguier, O. (sous presse) Influences atlantiques dans les productions métalliques en Bourgogne et Franche-Comté au Bronze moyen. *Actes du colloque en hommage à C. Millote*, Besançon.

Cursus post-Master 2 : Thèse, titulaire d'une Bourse Région, en cours, Université de La Rochelle.

Biville Céline (2007) « *Etude écotoxicologique d'éventuelles contaminations par le plomb liée à la métallurgie ancienne sur le Mont Lozère*. » Master 2 CEPS. Co. Dir. Paul Alibert (50%).
Projet : « Contamination métallique de l'écosystème aquatique par l'héritage métallurgique. Parc des Cévennes, France. ». Financement Parc des Cévennes.
Cursus post-Master 2 : Ingénieur Environnement, GeoteK, Quétigny.

Thomas Céline (2008) « *Contamination des organes et de la chair de poissons (Salmo trutta Fario).* » Master 2 ERE en cours.
Projet : « Contamination métallique de l'écosystème aquatique par l'héritage métallurgique. Parc des Cévennes, France. ». Financement Parc des Cévennes.

Autres encadrements

Depuis 1999, j'ai encadré 8 stages de recherche d'étudiants en Maîtrise / Master 1. Certains d'entre eux ont été associés à des publications :

Semlali, R.M., Dessogne, J.-B., Monna, F., Bolte, J., Azimi, S., Navarro, N., Denaix, L., Loubet, M., Chateau, C., van Oort, F. (2004) Modeling lead input and output in soils using lead isotopic geochemistry. *Environmental Science and Technology*, 38, 5, 1513-1531.

Monna, F., Puertas, A., Lévêque, F., Losno, R., Fronteau, G., Marin, B., Dominik, J., Petit, C., Forel, B., Chateau, C. (2008) Geochemical records of limestone façades exposed to urban atmospheric contamination as monitoring tools? *Atmospheric Environment*, 42, 999-1011.

Monna, F., van Oort, F., Hubert, P., Dominik, J., Bolte, J., Loizeau, J.-L., Labanowski, J., Lamri, J., Petit, C., Le Roux, G., Chateau, C. Modeling of ^{137}Cs migration in soils using an 80-year soil archive. Role of fertilizers and agricultural amendments. *Journal of Environmental Radioactivity*. DOI.10.1016/ j.jenvrad.2008.09.009.

FORMATION PAR LA RECHERCHE : ENSEIGNEMENT EN 3EME CYCLE

Enseignement 3^{e} cycle

Université de Bourgogne : Master 2. M2 GEE : Géochimie Isotopique (1999-2006), puis CEPS (2007); M2 Géo-archéologie : Statistiques (2001-2008), Géochimie appliquée à l'archéologie), PAO (2002-2006).

Université de Franche-Comté : Master 2 Santé Environnement, Géochimie Isotopique (4-6h/an).

Université de Chambéry (2007), Master 2 : Géochimie isotopique appliquée à l'étude des paléo-environnements (4h).

Université de Fribourg (2006), Master 2 : Cours bloc (14h) Géochimie isotopique appliquée à l'étude des paléo-environnements.

Université de Genève (1997-1999), Master 2 DESNE : Géochimie isotopique (6h/an)

Liste des travaux

PUBLICATIONS

Articles publiés dans des revues référencées JCR

Les travaux repérés par le symbole "*" sont directement issus de ma thèse de doctorat. Le facteur d'impact (IF) des revues est indiqué entre crochets à la suite de la référence (source JCR 2006, sauf Analusis et Oceanologica Acta qui ont changé de nom, source JCR 2001).
Les références encadrées sont reproduites in extenso en annexe (en suivant l'ordre chronologique).

[1]* Monna, F., Ben Othman, D., Luck, J.-M. (1995) Pb isotopes and Pb, Zn and Cd concentrations in the rivers feeding a coastal pond (Thau, southern France): constraints on the origin(s) and flux(es) of metals. *The Science of the Total Environment*. 166, 19-34. [IF=2,36]

[2]* Fillon, N., Clauer, N., Samuel, J., Verdoux, P., Monna, F., Lancelot, J. (1996) Dosage isotopique du Sr dans les eaux et du Pb dans les sédiments et les cendres d'un incinérateur urbain à l'aide d'un ICP-MS. *Comptes rendus de l'Académie des Sciences*, 322, II a, 1029-1039. [IF=0,97]

[3]* Monna, F., Mathieu, D., Marques Jr., A.N., Lancelot, J., Bernat, M. (1996) A comparison of P.E.R.A.L.S. with alpha and beta spectrometry to determine the sedimentation rate. Example of the Thau basin (Southern France). *Analytica Chimica Acta*, 330, 107-115. [IF=2,89]

[4]* Monna, F., Lancelot, J., Bernat, M., Mercadier, H. (1997) Taux de sédimentation dans l'étang de Thau (Languedoc) à partir des données géochronologiques, géochimiques et morphostratigraphiques. *Oceanologica Acta*, 20, N4, 627-638. [IF=0,72]

[5]* Monna, F., Lancelot, J., Croudace, I., Cundy, A.B., Lewis, T. (1997) Pb isotopic signature of urban air in France and in UK: Implications on Pb pollution sources. *Environmental Science and Technology*, 31, 2277-2286. [IF=4,04]

[6] Monna, F., Loizeau, J.-L., Thomas, B.A., Guéguen, C., Favarger, P.-Y. (1998) Pb and Sr isotope measurements by inductively coupled plasma - mass spectrometer: efficient time management for precise improvement. *Spectrochimica Acta, part B.* 59/09, 1317-1333. [IF=3,09]

[7] Guéguen, C., Belin, C., Thomas, B.A., Monna, F., Favarger, P.-Y., Dominik, J. (1999) Influence of UV-irradiation on Chelex-100 preconcentration of trace metals in freshwater. *Analytica. Chimica Acta*, 386, 155-159. [IF=2,89]

[8] Monna, F., Aiuppa A., Varrica D., Dongarrà G. (1999) Pb isotopic compositions in lichens and aerosols from Eastern Sicily: insights on the regional impact of volcanoes on the environment. *Environmental Science and Technolology*. 33, 2517 - 2523. [IF=4,04]

[9] Monna, F., Dominik, J., Loizeau, J.-L. Pardos, M., Arpagaus, P. (1999) Origin and evolution of Pb in sediments of lake Geneva (Switzerland - France). Establishing a stable Pb record. *Environmental Science and Technolology*. 33, 2850-2857. [IF=4,04]

[10] Alaimo, M.G., Dongarra, G., Melati, M.R., Monna, F., Varrica, D. (2000) Recognition of environmental trace metal contamination using pine needles as bio-indicators. The urban area of Palermo (Italy). *Environmental Geology*. 39, 8, 914-924. [IF=0,61]

[11]* Monna, F., Clauer N., Toulkeridis, T., Lancelot, J. (2000) Influence of anthropogenic activity on the lead isotope signature of Thau lake sediments (Southern France): origins and temporal evolution. *Applied Geochemistry*. 15, 1291-1305. [IF=1,87]

[12] Monna, F. Hamer, K, Lévêque, J. Sauer, M. (2000) Pb isotopes as reliable marker of early mining and smelting in the Northern Hartz province (Germany). *Journal of Geochemical Exploration*. (68)3, 201-210. [IF=0,92]

[13] Monna, F., Loizeau, J.-L., Thomas, B., Guéguen, C., Favarger, P.-Y., Losno, R., Dominik, J. (2000) Noise identification and sampling frequency determination for precise isotopic measurements by quadrupole-based Inductively Coupled Plasma Mass Spectrometry. *Analusis*. 28, 750- 757. [IF=0,65]

[14] Monna, F., Varrica, D., Aiuppa, A., Dongarrà, G. (2001) Le point sur l'origine du plomb dans l'atmosphère en Sicile. Apport de la géochimie isotopique et choix du support. *Archives des Sciences de Genève*, 54, 3, 205-222. [IF=0,21]

[15] Caillet, S., Arpagaus, P., Monna, F., Dominik, J. (2001) Factors controlling ^{7}Be and ^{210}Pb atmospheric deposition as revealed with sampling by individual rain events in the region of Geneva, Switzerland. *Journal of Environmental Radioactivity*. 53, 241-256. [IF=1,07]

[16] Loizeau, J.-L.; Rozé, S., Peytremann, C., Monna, F., Dominik, J. (2003) Mapping sediment accumulation rate by using volume magnetic susceptibility core correlation in a contaminated bay (Lake Geneva, Switzerland). *Eclogae Geologicae Helvetiae*, 96, 73–79. [IF=1,23]

[17] Varrica, D., Dongarrà, G., Sabatino, G., Monna, F. (2003) Inorganic geochemistry of roadway dust from the metropolitan area of Palermo, Italy. *Environmental Geology*, 44, 222–230. [IF=0,61]

[18] Semlali, R.M., Dessogne, J.-B., Monna, F., Bolte, J., Azimi, S., Navarro, N., Denaix, L., Loubet, M., Chateau, C., van Oort, F. (2004) Modeling lead input and output in soils using lead isotopic geochemistry. *Environmental Science and Technology*, 38, 5, 1513-1531. [IF=4,04]

[19] Monna, F., Galop, D., Carozza, L., Tual, M., Beyrie, A., Marembert, F., Chateau, C., Dominik, J., Grousset, F.E. (2004) Environmental impact of early Basque mining and smelting recorded in a high ash minerogenic peat deposit. *The Science of the Total Environment*, 327, 197-214. [IF=2,36]

[20] Monna, F., Petit, C., Guillaumet, J.-P., Jouffroy-Bapicot, I., Blanchot, C., Dominik, J., Losno, R., Richard, H., Lévêque, J., Chateau, C. (2004) History and environmental impact of mining activity in Celtic Aeduan territory recorded in a peat-bog (Morvan – France). *Environmental Science and Technology*, 38, 3, 657-673. [IF=4,04]. (Etude sélectionnée comme un 'fait marquant' pluridisciplinaire par le département Science de l'Homme et de la Société du CNRS).

[21] Marques, A.N., Monna, F., da Silva Filho, E.V., Fernex, F., Lamego Simões Filho. (2006) Apparent discrepancy in contamination history of a subtropical estuary evaluated through 210Pb profile and chronostratigraphical markers. *Marine Pollution Bulletin*. 52, 532-539. [IF=2,01]

[22] Monna, F., Poujol, M., Annegarn, H., Losno, R., Coetze, H., Dominik, J. (2006) Origin of atmospheric lead in Johannesburg, South Africa. *Atmospheric Environment*. 40, 6554-6566. [IF=2,63]

[23] Jouffroy-Bapicot, I., Pulido, M., Galop, D., Monna, F., Ploquin, A., Baron, S., Petit, C., Lavoie, M., Beaulieu, J.-L., de, Richard, H. (2007) Environmental impact of early palaeometallurgy: pollen and geochemical analysis. *Vegetation History and Archaeobotany*. 251-258. [IF=0,65]

[24] Carozza, J.-M., Galop, D., Métailié, J.-P., Vannière, B., Bossuet, G., Monna, F., Lopez-Saez, J.A., Arnauld, M.-C., Breuil, V., Forne, M., Lemonnier, E. (2007) Land-use and soil degradation in the southern Maya lowlands, from Pre-Classic to Post-Classic times: The case of La Joyanca (Petén, Guatemala). *Geodinamica Acta*, 20,4, 195-207. [IF=0,73]

[25] Labanowski, J. Monna, F., Bermond, A., Cambier, P., Fernandez, C., Lamy, I., van Oort, F. (2008) Kinetic extractions to assess mobilization of Zn, Pb, Cu, and Cd in a metal contaminated soil: EDTA vs citrate. *Environmental Pollution*, 152, 693-701. [IF=2,77]

[26] Monna, F., Puertas, A., Lévêque, F., Losno, R., Fronteau, G., Marin, B., Dominik, J., Petit, C., Forel, B., Chateau, C. (2008) Geochemical records of limestone façades exposed to urban atmospheric contamination as monitoring tools? *Atmospheric Environment*, 42, 999-1011. [IF=2,63]

[27] Fernandez, C., Monna, F., Labanowski, J., Loubet, M. van Oort, F. (2008) Anthropogenic lead distribution in soils under arable land and permanent grassland estimated by Pb-isotopic compositions. *Environmental Pollution*. 156, 1083-1091.[IF=2,77]

[28] Monna, F., van Oort, F., Hubert, P., Dominik, J., Bolte, J., Loizeau, J.-L., Labanowski, J., Lamri, J., Petit, C., Le Roux, G., Chateau, C. (2008) Modeling of ^{137}Cs migration in soils using an 80-year soil archive. Role of fertilizers and agricultural amendments. Sous presse à *Journal of Environmental Radioactivity*. DOI: 10.1016/ j.jenvrad.2008.09.009. [IF=1,07]

[29] Forel, B., Gabillot, M., Monna, F., Forel, S., Dommergues, C.H., Gerber, S., Petit, C. Mordant, C., Château, C. Morphometry of Middle Bronze Age palstaves by Discrete Cosine Transform. Sous presse à *Journal of Archaeological Sciences*. DOI :10.1016/j.jas.2008.10.021. [IF=1,44]

Articles publiés dans des revues non référencées JCR

[30] Guillaumet, J.P., Monna, F., Paris, P., Petit, C. (2000) "Etude paléoenvironnentale des tourbières autour du Mont Beuvray : premiers résultats", in Bibracte, Centre archéologique européen, p.305-308.

[31] Galop, D., Tual, M., Monna, F., Dominik, J., Beyrie, A. (2001) Cinq millénaires de métallurgie en Montagne Basque. Les apports d'une démarche intégrée alliant palynologie et géochimie isotopique du plomb. *Sud Ouest Européen*, 11, 3-15.

[32] Aiuppa, A., Dongarrà, G., Varrica, D., Monna, F., Sabatino, G. (2001) Livelli di plombo nel particolato atmosferico dei centri urbani della Sicilia. *Aqua Aria*, 1, 99-105.

[33] Beyrie, A., Galop, D., Monna, F., Mougin, V. (2003) La métallurgie du fer au Pays Basque durant l'Antiquité. Etat des connaissances dans la vallée de Baigorri (Pyrénées-Atlantiques). *Aquitania*, 19, 49-66.

[34] Loizeau, J.-L., Pardos, M., Monna, F., Peytremann, C., Haller, L., Dominik, J. (2004) The impact of a sewage treatment plant's effluent on sediment quality in a small bay in Lake Geneva (Switzerland–France). Part 2: Temporal evolution of heavy metals. *Lakes & Reservoirs: Research and Management*, 9, 53–63.

[35] Monna, F., Petit, C., Guillaumet, J.-P., Jouffroy-Bapicot, I., Richard, H., Tamas, C.G., Cauuet, B., Dominik, J., Losno, R. (2005) Du plomb chez les gaulois du Morvan. *UB Sciences*, 1, 100-104.

[36] Carozza, L., Galop, D., Marembert, F., Monna, F. (2005) Quel statut pour les espaces de montagne durant l'âge du Bronze? Regards croisés sur les approches société-environnement dans les Pyrénées occidentale. *Documents d'Archéologie Méridionale*. 28, 7-23.

Actes de colloques expertisés

[37] Galop, D., Monna, F., Beyrie, A., Carozza, L., Mougin, V., Parent, G., Marembert, F. (2002) Métallurgie et histoire de l'environnement en Pays Basque nord (Vallée de Baigorri, Pyrénées Atlantiques, France) : résultats préliminaires d'une approche interdisciplinaire. *Archeologia Postmedievale*, 6, 155-169.

[38] Gabillot, M., Forel, B., Monna, F., Naudin, A., Losno, R., Piningre, J.-F., Mordant, C., Dominik, J., Bruguier, O. (sous presse) Influences atlantiques dans les productions métalliques en Bourgogne et Franche-Comté au Bronze moyen. *Actes du colloque en hommage à C. Millote*, Besançon.

[39] Jouffroy-Bapicot I., Forel B., Monna F., Petit C. (sous presse) Paléométallurgie dans le Morvan : l'apport des analyses polliniques et géochimiques ». in *Actes du 131e congrès du CTHS « Tradition et Innovation »* Grenoble 2006.

Chapitres d'ouvrages expertisés

[40] Lévêque, J., Phillippe, S., Baize, D., Monna, F., Haack, U. (2002) Utilisation des isotopes stables du plomb pour la détermination des sources de pollutions et l'étude de son transfert dans les sols contaminés. In « *Les éléments traces mé-*

talliques dans les sols. Approches fonctionnelles et spatiales » INRA Ed. D. Baize & M. Tercé, coord. 375-391.

Diffusion grand public

[41] Monna, F. (2001) Un héritage de plomb. *La Recherche*. 340, 50-54.
[42] Monna, F. (2001) Una herencia de plomo. *Mundo Cientifico*. 21, 48-52.
[43] Forel, B., Jouffroy-Bapicot, I., Monna, F., Petit, C., Guillaumet, J.-P., Gabillot, M., Mordant, C., Piningre, J.-F. (2006) Les Éduens, producteurs de métal et pollueurs. *Les Dossiers de l'Archéologie*. 316. 28-29.
[44] Cauuet, B., Tamas, C.G., Guillaumet, J.-P., Petit, C., Monna, F. (2006) Les exploitations minières en pays éduen. *Les Dossiers de l'Archéologie*. 316. 20-25.
[45] Jouffroy-Bapicot, I., Petit, C., Monna, F., Richard, H. (2007) Evolution de la végétation du massif du Morvan : résultats des premières analyses polliniques et mise ne évidence de l'impact des activités paléométallurgiques. *Bourgogne Nature*. HS 3, 97-104.

Mémoires

Monna, F. (1992) Identification des apports de surface en métaux lourds à l'étang de Thau : Les isotopes du Plomb et les concentrations en Cadmium, Thallium, Plomb et Zinc. Mémoire de DEA Tectonique, Géophysique, Géochimie, Hydrologie, option Géochimie-Géochronologie. Université de Montpellier II.
Monna, F. (1996) Utilisation des isotopes du Pb dans les études environnementales. Application à l'évolution temporelle et à l'origine des apports en Pb dans l'étang de Thau (Hérault-France). Thèse de doctorat de l'Université de Montpellier II.

Autre diffusion

Monna, F. (2001) Emission « Le monde change », Radio France International.

PARTICIPATIONS À DES COLLOQUES

[1] Monna, F., Ben Othman, D., Luck, J.-M. (1993) Identification of anthropogenic pollution with isotopic lead composition and lead, zinc and cadmium concentrations in the streams feeding the Thau Pond (Southern France, Herault). E.U.G. VII, Strasbourg 4-8 Avril 1993.
[2] Monna, F., Lancelot, J., Bernat M. (1994) Evolution temporelle et spatiale des apports anthropiques dans les sédiments de l'étang de Thau (Hérault), 15e réunion des Sciences de la Terre - Nancy 26-28 Avril 1994.
[3] Lancelot, J., Monna, F., Mercadier, H. (1995) Lead isotope, major and trace element analysis tracing pollution and natural contributions in the recent sediments of the Thau basin (Southern France). E.U.G. VIII, Strasbourg 9-13 Avril 1995.

[4] Monna, F., Mathieu, D., Marques Jr., A.N., Bernat M. (1995) P.E.R.A.L.S.: A precise, reproductive, rapid and easy technique to measure the sedimentation rate? Example of the Thau basin (Southern France). E.U.G. VIII, Strasbourg 9-13 Avril 1995.

[5] Marques Jr., A.N., Monna, F., Fernex, F., Perrin, P., Silva Filho, E.V. (1995) Isótopos de Pb na Lagoa de Maricá, R.J. (Brasil) : implicações na sua história sedimentar recente. V Congresso Brasileiro de Geoquímica e III Congresso de Geoquímica dos Países de Língua Portuguesa, Unisersidade Federal Fluminense, R.J. Brasil

[6] Monna, F., Techer, I., Clavel, O., Lancelot, J., Williamson, D., Lévêque, F. (1996) Correlation of Pb isotope and magnetic parameters in recent sediment of ETANG DE THAU. AGS, La Haye, Netherland, Mai 1996.

[7] Monna, F., Lancelot, J. (1996) Signatures isotopiques en Pb des aérosols urbains français: implications sur l'origine du Pb. 16e réunion des Sciences de la Terre - Orléans 9-12 Avril 1996.

[8] Monna, F., Lancelot, J., Croudace, I.W., Cundy, A.B., Lewis, J.T. (1997) Pb isotopes as indicators of Pb pollution origin in urban airborne particulate matter from France and the U.K. 4th International scientific symposium Transport and Air pollution. Avignon.

[9] Monna, F., Clauer, N., Toulkeridis, T., Lancelot, J. (1997) Identification of the mineral sites hosting anthropogenic Pb in lacustrian sediments. E.U.G. IX, Strasbourg 23-27 Mars 1997.

[10] Guéguen, C., Belin, C., Thomas, B.A., Monna, F., Favarger, P.-Y. and Dominik. J. (1998) Influence of UV-irradiation on Chelex-100 preconcentration of trace metals in freshwater. Deauville Conf. 6th SAS Valencia, 22-24 juin 1998.

[11] Favarger, P.-Y., Thomas, B., Guéguen, C., Monna, F. (1998) Evaluation of simultaneous ICPMS/-OES sediment analysis based on reference samples. Deauville Conf. 6th SAS Valencia, 22-24 juin 1998.

[12] Monna, F.; Loizeau, J.-L., Thomas, B.A., Guéguen, C., Favarger, P.-Y. (1998) Efficient time management for precision improvement of Pb and Sr isotope measurements by Inductively Coupled Plasma - Mass Spectrometer. Deauville Conf. 6th SAS Valencia, 22-24 juin 1998.

[13] Monna, F., Dominik, J., Loizeau, J.-L. Piccard, J., Arpagaus, P. (1998) High resolution lead-isotope record in Lake Geneva sediments (Switzerland - France). 8th Goldchmidt Conf. Toulouse, 30 aout - 3 septembre 1998.

[14] Aiuppa, A., Dongarra, G., Monna, F., Varrica, D. (1998) Lead isotope composition in urban airborne particles of Silicy. 78° Congresso Societa' di Mineralogia, Petrografia e Geochimica. Monopoli 1-3 ottobre 1998.

[15] Dongarrà, G., Monna, F., Varrica, D., Aiuppa, A. (1998) Metalli in traccia ed Isotopi del plombo nel particolato atmosferico. Indagine ambientale in aree vulcaniche e nei maggiori centri urbani della Sicilia. II Christmas workshop sulla qualita' della vita. Agriria, 16-17 Dicembre 1998.

[16] Aiuppa, A., Dongarra, G., Monna, F., Varrica, D. (1999) Lead isotope composition in lichens from urban, rural and volcanic sites in eastern Sicily. 5th ICOPTE '99, Vienna, 11-15 July 1999.

[17] Monna, F., Thomas, B., Martin, M., Loizeau, J.L., Guéguen, C., Favarger P.-Y. (1999). Isotopic measurements by quadrupole based ICP-MS - Limitations & improvements -. Winter'99. 10-15 janvier 1999. Pau France.

[18] Monna, F., Dominik, J., Dongarrà, G., Hamer, K., Aiuppa, A., Martin, M., Varrica, D., Sauer, M., Thomas, B., Loizeau, J.L., Buffle, J., Arpagaus, P., Pardos, M., Robin, D. (1999) Isotopic measurements by quadrupole based ICP-MS - A few examples of Pb isotopic geochemistry in the environment - Winter'99. 10-15 janvier 1999. Pau France.

[19] Favarger, P.-Y., Guéguen, C., Thomas, B.A., Monna, F. (1999) Hydride forming elements in fresh water sediment by ICP-OES: limits and quality control of a simplified analytical procedure. Winter'99. 10-15 janvier 1999. Pau France.

[20] Caillet, S., Dominik, J., Monna, F., Arpagaus, P. (1999) Be-7 and Pb-210 bulk atmospheric deposition in the region of lake Geneva and its relation to the rainfall. EUG 10, 28th march - 1st april, Strasbourg, France.

[21] Hamer, K, Monna, F., Sauer, M. (1999) Pb isotopes as reliable marker of early mining and smelting in the Northern Hartz province (Germany). EUG 10, 28th march - 1st april, Strasbourg, France.

[22] Dominik, J., Pardos, M., Loizeau, J.L., Monna, F., Wildi, W. (2000) Sewage treatment plants discharging to lakes may produce highly contaminated, shallow water dumping sites: a case from Lake Geneva. International Conference on Heavy Metals in the Environment, 6-10 August 2000, Ann Arbor, Michigan, USA.

[23] Semlali, R.M., Monna, F., Bolte, J., Lévêque, J. (2001) Mobility of Pb in topsoils assessed via temporal changes in concentrations and isotopic compositions. European Union of Geosciences XI, Strasbourg - France.

[24] Galop, D., Tual, M., Monna, F., Dominik, J. (2001) Histoire des activités paléométallurgiques en montagne basque. Les apports d'une démarche croisée alliant palynologie et géochimie isotopique du plomb. XVIe Symposium de l'Association des Palynologues de Langue Française, 2001.

[25] Blanchot, C., Guillaumet, J.-P., Monna, F., Petit, C., Leveque, J., Dominik, J. (2001) Historical reconstruction of metallic pollution using a geo-ombrogenic peat bog in Eduens Gallic territory (Bibracte, France). 2nd European Meeting on Environmental Chemistry 12-15 December 2001, Dijon, France.

[26] Monna, F., Tual, M., Galop, D., Dominik, J., Beyrie, A., Marembert, F. (2001) A reconstruction of the history of early environmental stress in the Basque country from the geochemical and pollinic signals recorded in a peat bog. 2nd European Meeting on Environmental Chemistry 12-15 December 2001, Dijon, France.

[27] Coetzee, H., Poujol, M., Monna, F., Losno, R., Annegarn, H. & Rademeyer, M. (2003) Fingerprinting environmental lead concentrations using isotope ratios in South Africa. Public Health Association of South Africa conference, Mars 2003, Cape Town, South Africa.

[28] Monna, F., Petit, C., Guillaumet, J.-P., Jouffroy, I., Blanchot, C., Dominik, J., Losno, R., Richard, H., Lévêque, J. (2003) A history of mining activity in Celtic Aeduan territory, an its environmental impact (Morvan - France). Joint Assembly: American Geophysical Union - European Union of Geosciences - European Geophysical Society, Nice 2003.

[29] Semlali, R.M., Dessogne, J.B., Monna, F., Bolte, J., Azimi, S., Denaix, L., Loubet, M., van Oort, F. (2003) Modeling metal inputs and outputs in soils by using lead isotopic geochemistry. Joint Assembly: American Geophysical Union - European Union of Geosciences - European Geophysical Society, Nice 2003.

[30] Jouffroy-Bapicot, I., Pulido, M., Galop, D., Baron, S., Richard, H., Ploquin, A., Lavoie, M., Monna, F., Petit, C., Beaulieu, J.-L. de. (2004) Environmental impact of early palaeometallurgy: pollen and geochemical analysis. XIth International Palynological Congress, Granada, 2004.

[31] Tamas, G., Cauuet, B., Guillaumet, J.-P., Monna, F., Petit, C. (2004) Archeomineral research in the Morvan massif (north east Massif Central) – First results. European Association of Archeologists, Lyon, 2004.

[32] Forel, B., Bosch, D., Bruguier, O., Cauuet, B., Guillaumet, J.-P., Guillon, R., Jouffroy-Bapicot, I., Monna, F., Petit, C., Richard, H., Tamas, C. (2005) Plus de trois milles ans de métallurgie sur le site Eduen de Bibracte (Morvan - France) : conséquences historiques et environnementales. GMPCA (Groupe de Méthodes Pluridisciplinaires Contribuant à l'Archéologie) 2005, Saclay avril 2005.

[33] Forel, B., Monna, F., Petit, C., Jouffroy-Bapicot, I., Guillaumet, J.-P., Mordant, C., Bruguier, O., Piningre, J.-F. (2006) Perceptions environnementales des activités minières et métallurgiques locales -Exemple du Morvan à l’âge du Bronze (2300 – 800 av. J.-C.). Réunion des Sciences de la Terre. Dijon, Avril 2006.

[34] Monna, F., Poujol, M., Losno, R., Dominik, J., Coetzee, H. (2006) Origin of atmospheric lead in Johannesburg - South Africa –. Réunion des Sciences de la Terre. Dijon, Avril 2006.

[35] Forel, B., Monna, F., Petit, C., Piningre, J.-F., Guillaumet, J.-P., Mordant, C., Guillon, R., Jouffroy-Bapicot, I., Bruguier, O. (2007) A palaeo-environmental approach brings to light evidence of early mining and metallurgical activities: the example of the Morvan massif (Burgundy, France). 2nd International Conference of Archaeometallurgy in Europe. Juin 2007, Aquileia.

[36] Ploquin A., Baron S., Monna F. et al. – (2008) Le plomb ancien du Mont Lozère (48, France) Des minéralisations aux ateliers, impacts environnementaux. Réunion des Sciences de la Terre. Nancy, Avril 2008.

[37] Thomas, C., Monna, F., Alibert, P., Revelli P., Biville C., Bruguier O., Baron S., Ploquin A. (2008) Impact des sites miniers abandonnés sur les écosystèmes aquatiques et terrestres : De la veille sanitaire des rapaces du Parc national des Cévennes à la géochimie environnementale. GEEFSM 2008, Barcelonnette Mai 2008.

[38] Naudin A., Lévêque F., Monna F., Galop D., Camus A., Mathé V. (2008). Potential correlations between magnetic and environmental variations records in peat bogs. 11th Castle Meeting. Paleo, Rock and Environmental Magnetism. Bojnice Castle, Slovak Republic. 22-28 june 2008.

[39] Lévêque, F., Monna, F., Puertas, A., Losno, R., Fronteau, R., Marin, B., Janusz, D., Petit, C., Forel, B., Château, C. (2008) Limestone façades exposed to urban atmospheric contamination: magnetic susceptibility and geochemical monitoring. 11th Castle Meeting. Paleo, Rock and Environmental Magnetism. Bojnice Castle, Slovak Republic. 22-28 june 2008.

[40] Pellenard, P., Deconinck, J.-F., Fortwengler, D., Marchand, D., Monna, F. (2008) Middle-Upper Jurassic volcanic ash layers (bentonites) as potential interbasinal high-resolution stratigraphic and radiometric markers. International Geological Congress, 33rd IGC, Oslo, Aout 2008.

Séminaires (invité)

Monna, F. (1996) Using Pb isotopes in environmental studies. Université de Brême, Allemagne.

Monna, F. (2000) Les isotopes du plomb en environnement. Université de Lille, Wimereux, France.

Monna, F. (2001) An archaeological use of lead isotopes. Johannesburg, Afrique du Sud.

Monna, F. (2005) Environmental impacts of early mining and smelting recorded in peat bog archives. University of St John's, Terre Neuve, Canada.

Monna, F. (2008) Un héritage de plomb. Université de Genève, Suisse.

Conférences (invité)

Monna, F. (2003) Le cycle géochimique du Plomb. Journée technique : les métaux dans l'environnement, colloque organisé par l'APESA (avec actes), Pau.

Monna, F. (2008) Workshop on Lead Isotopes and Archaeometallurgy: A Progress Report, 19-20 June 2008, Université de Fribourg, Suisse.

Annexes

Monna, F., Lancelot, J., Croudace, I., Cundy, A.B., Lewis, T. (1997) Pb isotopic signature of urban air in France and in UK: Implications on Pb pollution sources. *Environmental Science and Technology*, 31, 2277-2286.

Monna, F., Dominik, J., Loizeau, J.-L. Pardos, M., Arpagaus, P. (1999) Origin and evolution of Pb in sediments of Lake Geneva (Switzerland - France). Establishing a stable Pb record. *Environmental Science and Technolology*. 33, 2850-2857.

Monna, F., Aiuppa A., Varrica D., Dongarrà G. (1999) Pb isotopic compositions in lichens and aerosols from Eastern Sicily: insights on the regional impact of volcanoes on the environment. *Environmental Science and Technolology*. 33, 2517 - 2523.

Monna, F., Loizeau, J.-L., Thomas, B., Guéguen, C., Favarger, P.-Y., Losno, R., Dominik, J. (2000) Noise identification and sampling frequency determination for precise isotopic measurements by quadrupole-based Inductively Coupled Plasma Mass Spectrometry. *Analusis*. 28, 750- 757.

Monna, F., Galop, D., Carozza, L., Tual, M., Beyrie, A., Marembert, F., Chateau, C., Dominik, J., Grousset, F.E. (2004) Environmental impact of early Basque mining and smelting recorded in a high ash minerogenic peat deposit. *The Science of the Total Environment*, 327, 197-214.

Semlali, R.M., Dessogne, J.-B., Monna, F., Bolte, J., Azimi, S., Navarro, N., Denaix, L., Loubet, M., Chateau, C., van Oort, F. (2004) Modeling lead input and output in soils using lead isotopic geochemistry. *Environmental Science and Technology*, 38, 5, 1513-1531.

Monna, F., Petit, C., Guillaumet, J.-P., Jouffroy-Bapicot, I., Blanchot, C., Dominik, J., Losno, R., Richard, H., Lévêque, J., Chateau, C. (2004) History and environmental impact of mining activity in Celtic Aeduan territory recorded in a peat-bog (Morvan – France). *Environmental Science and Technology*, 38, 3, 657-673.

Monna, F., Poujol, M., Annegarn, H., Losno, R., Coetze, H., Dominik, J. (2006) Origin of atmospheric lead in Johannesburg, South Africa. *Atmospheric Environment*. 40, 6554-6566.

Labanowski, J. Monna, F., Bermond, A., Cambier, P., Fernandez, C., Lamy, I., van Oort, F. (2008) Kinetic extractions to assess mobilization of Zn, Pb, Cu, and Cd in a metal contaminated soil: EDTA vs citrate. *Environmental Pollution*, 152, 693-701.

Monna, F., Puertas, A., Lévêque, F., Losno, R., Fronteau, G., Marin, B., Dominik, J., Petit, C., Forel, B., Chateau, C. (2008) Geochemical records of limestone façades exposed to urban atmospheric contamination as monitoring tools? *Atmospheric Environment*, 42, 999-1011.

Fernandez, C., Monna, F., Labanowski, J., Loubet, M. van Oort, F. (2008) Anthropogenic lead distribution in soils under arable land and permanent grassland estimated by Pb-isotopic compositions. *Environmental Pollution*. 156, 1083-1091

Environ. Sci. Technol. **1997**, *31,* 2277−2286

Pb Isotopic Composition of Airborne Particulate Material from France and the Southern United Kingdom: Implications for Pb Pollution Sources in Urban Areas

FABRICE MONNA,*,†,‡ JOEL LANCELOT,†
IAN W. CROUDACE,§
ANDREW B. CUNDY,‖ AND
JAMES T. LEWIS§

Laboratoire de Géochimie Isotopique, URA-CNRS 1763, Université de Montpellier II, Place E. Bataillon, Case courrier 066, 34095 Montpellier Cedex 05, France, Department of Geology, Southampton Oceanography Centre, Southampton, SO14 3ZH, U.K., and Department of Geography & Earth Sciences, Brunel University, Borough Road, London TW7 5DU, U.K.

Pb isotopic studies of airborne particulate matter, incinerator ash, and gasoline have been carried out to determine sources of Pb pollution in urban areas from France and the southern United Kingdom. ^{206}Pb/^{207}Pb ratios in gasoline range from 1.061 to 1.094 (average values are 1.084 for France and 1.067 for the U.K.) while for industrially-derived Pb, ^{206}Pb/^{207}Pb ratios vary from 1.143 to 1.155. Natural Pb is more radiogenic and literature values for pre-industrial sediments give ^{206}Pb/^{207}Pb ratios of 1.19−1.20 in France and 1.17−1.19 in the U.K. The measured Pb isotopic signature of airborne particulate matter reflects the relative importance of each of these sources, and samples taken from urban areas close to traffic in France and the U.K. show ^{206}Pb/^{207}Pb ratios that vary widely from 1.085 to 1.158. While alkyl-lead additives in gasoline are typically still the dominant source of Pb in urban particulate matter, the relative importance of gasoline-derived Pb has decreased, and as a result other sources (industrial and natural) can be identified using isotopic studies. This is a consequence of recent EU environmental legislation that significantly limits concentrations of Pb in gasoline and the increased market penetration of unleaded gasoline. In addition, at a given location, the Pb isotopic composition of particulate matter can vary considerably due to temporal variations in sources (i.e., variations in traffic density) and with wind direction.

Introduction

Investigative studies of lead isotope compositions are well-established in geochemistry and geochronology and are increasingly used in environmental science (see the Clair C. Patterson Special Issue, *Geochim. Cosmochim. Acta* **1994**, *58*). While Pb concentration measurements may provide useful information about potential enrichments of this element, the sources of this Pb will often be ambiguous. To resolve this uncertainty, Pb isotope ratios are studied. Pb has four stable isotopes: ^{204}Pb, ^{206}Pb, ^{207}Pb, and ^{208}Pb. The last three are radiogenic isotopes and are produced by the radioactive decay of ^{238}U, ^{235}U, and ^{232}Th respectively (^{204}Pb is non-radiogenic). Each lead ore deposit has its own characteristic Pb isotopic composition, depending on its age (strictly the time that the lead separated from its source rocks) and on its conditions of genesis (*1*). The isotopic composition of Pb in environmental materials is thus dependent on the ore bodies from which it was derived. In the environment, Pb isotopic ratios reflect the mixing of local/natural Pb with anthropogenic inputs, and mixing processes can be quantified if each source of lead has a distinctive isotopic composition. This principle has been used in a variety of media to determine anthropogenic Pb sources, for example, in freshwater (*2*−*5*), in sediments (*6*−*11*), and in aerosols (*12*−*19*). In France and the U.K., and in western Europe as a whole, the Pb currently used in anthropogenic processes is derived from foreign sources (ore bodies) that commonly have distinctly different isotopic compositions from the local/natural Pb present in rocks and soils. The isotopic signature of this anthropogenic lead is subject to economic factors (commodity, prices) and consequently may change with time according to the origin of the Pb ores used. It is thus essential to make frequent isotopic measurements to maintain a reliable database of anthropogenic Pb for a particular cultural region. Where investigations of environmental fluxes of Pb over a long period are made (i.e., in sedimentary or ice cores), it is clear that a good knowledge of the isotopic character of anthropogenic Pb is required if reliable historical pollution reconstructions are to be carried out. Studies of Pb in the United States are well established and varied, and the subject has a long history (*8, 20*−*23*). However, the European perspective is not so well established, and fewer data are available.

In this study, recently acquired isotopic data for pollution sources in France and the U.K. are presented, with measurements of airborne particulate matter collected from urban areas. The data provide a better understanding of local variability in Pb sources and show the relative importance of natural and anthropogenic Pb sources in urban air at a number of differing sites. The changing contributions of gasoline-derived Pb to the overall anthropogenic input of lead, due to changes in the use of unleaded petrol over the last 20 years, is also discussed.

Methodology

Sampling. Airborne particulate matter was sampled in 12 French cities and two cities in the U.K. Where possible, sampling was carried out using a PPA60 (France) or TEOM (U.K.) instrument (Amiens, Caen, Le Havre, Lille, Paris, Montpellier, Strasbourg, Toulouse, and London). These devices have a multidirectional head that removes airborne particulate matter above 10 μm and aspirates the ambient air at a fixed-flow rate of 25 L mn^{-1} (PPA60) or 13 L mn^{-1} (TEOM). Samples were collected over 24 h on cellulose−nitrate membrane filters (porosity, 0.8; total diameter, 47 mm; exposed diameter, 33 mm). For other cities, where this equipment was not available, particulate matter was sampled using FILTROMAT equipment over a 24-h period at a fixed-flow rate of 100 L h^{-1} (Bar-le-Duc, Clermont Ferrand, Nantes, and Nice) or using precleaned 0.2-μm PTFE membrane filters attached to a diaphragm pump (Southampton sites). Samples from Southampton were collected over periods ranging from 7 to 10 days and so represent a time-integrated measurement. In addition, five ash samples were removed from electrostatic filters from a French urban incinerator, and 16 leaded gasoline samples were collected in both countries into precleaned glass vials directly from the pump.

---

* Corresponding author e-mail: monna@sc2a.unige.ch.

† Université de Montpellier II.

‡ Present address: Institut FA Forel, 10 Route de Suisse, CH 1290 Versoix, Switzerland.

§ Southampton Oceanography of Centre.

‖ Brunel University.

S0013-936X(96)00870-X CCC: $14.00

Chemical and Isotopic Analysis. (A) TIMS Analysis. Analyses of French and United Kingdom (London) samples were performed using TIMS at Montpellier. Sample preparation was carried out under Class 100 laminar air flow clean benches in a clean room. Almost all the particulate matter was removed from the filters by ultrasonic agitation in 5 mL of deionized water with the help of a PTFE spatula. Filters were agitated for 2 min only to avoid partial decomposition of the filter, which may introduce a significant blank contribution. Acid digestion of the matrix was avoided for the same reason. The 100% removal of particulate material from the filter is not essential (as the above method of removal is unlikely to be particle size selective), and so the Pb isotopic composition of the material extracted is likely to be representative of the entire sample (Pb isotopic composition is independent of the amount of Pb extracted). After the removal of the filter, the water mixture containing the collected particulate matter was evaporated to dryness, and the residue was digested in 2 mL of high-purity aqua regia at 90 °C for 24 h. For the incinerator ashes, a few milligrams was digested in a PTFE beaker with a mixture of distilled HF, HNO_3, and HCl heated at 90 °C for 1 week. For gasoline, 5 μL was slowly evaporated at 20 °C, and the residue was digested following the same procedure. The solutions were then evaporated, and 200 μL of 0.5 N HBr was added.

Pb separation was achieved using Bio-Rad AG1-X4 anion exchange resin following the conventional technique (*5, 24*): loading of the sample in 0.5 N HBr, washing twice with 1 mL of 0.5 N HBr, and a final elution of Pb with 0.5 mL of 6 N HCl. This operation was repeated to purify the sample and to ensure a stable thermal emission during measurements. Pb was loaded on a single Re filament using the silica gel/phosphoric acid method (*25*). Measurements of Pb isotopic ratios were carried out by thermal ionization mass spectrometry (TIMS) on a VG SECTOR mass spectrometer equipped with five Faraday cups using simultaneous multicollection in static mode. Regular measurements of the Pb standard, NIST 981, allowed the correction of the data for mass fractionation (1.35 ± 0.05 ‰ per amu). Analytical precision was found to be better than 1‰ for $^{206}Pb/^{204}Pb$, $^{207}Pb/^{204}Pb$, and $^{208}Pb/^{204}Pb$ ratios and better than 0.2‰ for $^{206}Pb/^{207}Pb$ and $^{208}Pb/^{206}Pb$ ratios. Blank measurements, determined using a ^{207}Pb spike, show that Pb added during the analytical procedure by the operator is less than 0.25% of the Pb concentration in the samples and thus does not require correction. Duplicates of three aerosol samples (Le Havre, Lille, and Paris) show good reproducibility and confirm the significance of the analytical data.

(B) ICP−MS Measurements. Isotopic analyses of Southampton airborne particulate samples and of U.K. gasoline were performed at Southampton using a VG PlasmaQuad 2+ ICP−MS. This instrument has a very high sensitivity and produces a count rate of approximately 5.10^5 cps/ppb for Pb. Pb was preconcentrated in a similar manner to that described above, and the details are given in ref 11. MilliQ+ water and PRIMAR acids (Fisher) were used during all chemical manipulations. NIST 981 was used to monitor accuracy and to correct for mass fractionation, and procedural blanks were run to determine possible contamination from reagents and general handling. The only notable interference in ICP−MS measurements is the ^{204}Hg isobaric overlap on ^{204}Pb that is readily corrected for by monitoring ^{200}Hg. Analytical precision was generally better than 1% for $^{206}Pb/^{204}Pb$, $^{207}Pb/^{204}Pb$, and $^{208}Pb/^{204}Pb$ ratios and better than 8‰ for $^{206}Pb/^{207}Pb$ and $^{208}Pb/^{206}Pb$ ratios.

Results

Geochemists prefer conventionally to use Pb isotopic ratios incorporating ^{204}Pb due to the mathematical simplification of using a non-radiogenic isotope. However, environmental scientists tend to use $^{206}Pb/^{204}Pb$ vs $^{206}Pb/^{207}Pb$ or $^{206}Pb/^{207}Pb$ vs $^{208}Pb/^{206}Pb$ because of their better analytical precision. Here we use $^{206}Pb/^{207}Pb$ vs $^{208}Pb/^{206}Pb$ for comparability with recent studies obtained using ICP−MS and also present conventional $^{206}Pb/^{204}Pb$ vs $^{208}Pb/^{204}Pb$ diagrams.

The environmental materials analyzed in the present study have distinct lead isotopic signatures (Tables 1 and 2). Gasolines possess the least radiogenic isotopic signatures, and Pb isotopic ratios show little regional variation. In France, $^{206}Pb/^{207}Pb$ ratios range from 1.069 to 1.094 (average: 1.084 ± 0.009 at 1σ) whereas in the U.K. slightly lower values are found: $^{206}Pb/^{207}Pb$ ratios ranging between 1.059 and 1.079 (average: 1.067 ± 0.007). Ashes from the French urban incinerator gave much higher (more radiogenic) $^{206}Pb/^{207}Pb$ ratios ranging from 1.143 to 1.154 (average: 1.149 ± 0.005), similar to values for liquid urban wastes from Southern France (*5*) (average $^{206}Pb/^{207}Pb = 1.157 \pm 0.007$, 1$\sigma$). The greatest variations in isotopic composition occurred in urban airborne particulate matter (sampled in nine French cities and two U.K. cities during the period November 1994−January 1996) that had $^{206}Pb/^{207}Pb$ ratios between 1.085 and 1.158. Both regional and temporal variations in the Pb isotopic composition of urban airborne particulate matter were obvious. At a national scale, $^{206}Pb/^{207}Pb$ ratios varied between 1.100 at Nantes and 1.145 at Toulouse, while locally two different sites in the same city, examined during the same day, show very distinct isotopic signatures: 1.104 (Toulouse station 6) and 1.145 (Toulouse station 12) (Table 1). In addition, substantial temporal variations were observed at west London (Teddington), where the Pb isotopic composition of airborne particles was monitored daily over two periods of approximately 1 week each in November 1995 and in January 1996. Here, the $^{206}Pb/^{207}Pb$ ratios varied between 1.114 and 1.127 during the November 1995 sampling period and between 1.124 and 1.158 during the January 1996 sampling period (Table 2). For each period, the more radiogenic values are observed during the weekend or when the wind is from a SE direction (authors preliminary unpublished data). If the integrated sampling time is longer, as at Southampton (3−7 days), these variations are less clear. The regional and temporal variability in Pb isotopic composition reflects local variations in the relative importance of gasoline, industrial, and natural Pb sources and is discussed in the following sections.

Discussion

Isotopic Characterization of Pb Sources. (A) Pb from Gasoline. Despite direct pump sampling of several different gasoline suppliers (Esso, Total, Agip, etc.), the range of measured $^{206}Pb/^{207}Pb$ ratios is rather small for each country and so represents a relatively homogeneous source. The values are the lowest ever reported for French and U.K. gasoline: the average $^{206}Pb/^{207}Pb$ ratio for French samples is 1.084 ± 0.009 (1σ), while the average for U.K. samples is 1.067 ± 0.007. In France and the U.K., the Octel Co. (Associated Octel in the U.K.) is the main producer of tetraethyl and tetramethyl lead (TEL−TML) added to fuels as an anti-knock compound. This company supplies nearly 80% of the Pb alkyls used in the refineries of both countries. Production of TEL−TMLs from U.S. companies has totally ceased due to national legislative requirements. Most of the Pb currently used in TEL−TML production is derived from the Precambrian Pb−Zn ore deposits of Australia and Canada, with minor contributions from Morocco and other sources [Octel Co., France (1995) and Associated Octel, U.K., personal communication, (1996)]. Pb from Australian and Canadian ores are characterized by low radiogenic signatures; the 1600−1700 Ma Broken Hill (New South Wales) and Mount Isa (Queensland) Pb ores show $^{206}Pb/^{207}Pb$ ratios in the range 1.03−1.04 (*1*). The Mesozoic Pb−Zn province from Morocco shows a much more radiogenic $^{206}Pb/^{207}Pb$ ratio of approximately 1.16−1.17. A mixing of 80% Australian Pb with

TABLE 1. Pb Isotopic Composition of Airborne Particulate Matter, Gasoline, and Incinerator Ashes in France

location/(station)	organization	date	characteristics	^{206}Pb/^{204}Pb	^{207}Pb/^{204}Pb	^{208}Pb/^{204}Pb	^{206}Pb/^{207}Pb	^{208}Pb/^{206}Pb
Airborne Particulate Matter								
Amiens	ASQAP	Sep 1, 1995	urban	17.276 ± 0.006	15.552 ± 0.006	37.10 ± 0.02	1.1108 ± 0.0001	2.1476 ± 0.0003
Bar-le-duc	AIRLOR	Sep 1, 1995		17.543 ± 0.005	15.553 ± 0.005	37.38 ± 0.01	1.1279 ± 0.0001	2.1309 ± 0.0003
Caen	ESPAC	Sep 7, 1995		17.329 ± 0.011	15.535 ± 0.010	37.15 ± 0.03	1.1155 ± 0.0001	2.1440 ± 0.0003
		Sep 8, 1995		17.350 ± 0.008	15.548 ± 0.008	37.19 ± 0.02	1.1158 ± 0.0001	2.1438 ± 0.0003
Clermont-Ferrand	AMPAC	Sep 1, 1995		17.448 ± 0.011	15.553 ± 0.011	37.28 ± 0.03	1.1219 ± 0.0001	2.1366 ± 0.0003
Le Havre	AIR NORMAND	Aug 14, 1995		17.236 ± 0.004	15.536 ± 0.005	37.09 ± 0.01	1.1094 ± 0.0001	2.1517 ± 0.0003
duplicate				17.248 ± 0.005	15.552 ± 0.005	37.09 ± 0.02	1.1091 ± 0.0001	2.1508 ± 0.0003
Lille	AREMA LRT	Sep 1, 1995		17.288 ± 0.009	15.544 ± 0.009	37.16 ± 0.02	1.1123 ± 0.0001	2.1492 ± 0.0003
duplicate				17.285 ± 0.005	15.540 ± 0.006	37.11 ± 0.02	1.1124 ± 0.0001	2.1469 ± 0.0003
Paris	Préfecture de Police	Sep 13, 1995		17.425 ± 0.005	15.542 ± 0.005	37.26 ± 0.02	1.1212 ± 0.0002	2.1386 ± 0.0004
duplicate				17.448 ± 0.011	15.553 ± 0.011	37.28 ± 0.03	1.1219 ± 0.0001	2.1366 ± 0.0003
Montpellier								
station 1	AMPADI	Jan 27, 1995		17.453 ± 0.007	15.567 ± 0.007	37.28 ± 0.02	1.1211 ± 0.0001	2.1361 ± 0.0003
station 4		Jan 29, 1995		17.382 ± 0.004	15.577 ± 0.005	37.23 ± 0.01	1.1159 ± 0.0001	2.1421 ± 0.0003
station 1		Jan 29, 1995		17.401 ± 0.007	15.564 ± 0.007	37.24 ± 0.02	1.1181 ± 0.0001	2.1402 ± 0.0003
station 1		Sep 7, 1995		17.202 ± 0.005	15.543 ± 0.005	37.05 ± 0.02	1.1068 ± 0.0001	2.1539 ± 0.0003
Nantes	LOIRESTU'AIR	Sep 7, 1995		17.084 ± 0.005	15.519 ± 0.005	36.91 ± 0.01	1.1008 ± 0.0001	2.1603 ± 0.0003
Nice	QUALIT'AIR06	Sep 21, 1995		17.445 ± 0.005	15.547 ± 0.005	37.27 ± 0.02	1.1221 ± 0.0001	2.1363 ± 0.0003
Strasbourg	ASPA	Sep 1, 1995		17.566 ± 0.018	15.490 ± 0.016	37.31 ± 0.04	1.1342 ± 0.0002	2.1236 ± 0.0004
		Sep 4, 1995		17.611 ± 0.006	15.558 ± 0.006	37.42 ± 0.02	1.1319 ± 0.0001	2.1250 ± 0.0003
Toulouse								
station 6	ORAMIP	Sep 7, 1995		17.139 ± 0.013	15.522 ± 0.013	36.96 ± 0.03	1.1042 ± 0.0001	2.1563 ± 0.0004
station 12		Sep 7, 1995	urban/smelter	17.892 ± 0.004	15.622 ± 0.004	37.90 ± 0.01	1.1453 ± 0.0001	2.1184 ± 0.0004
Gasolines								
ELF	Leaded gasoline	Oct 1995	pump	16.564 ± 0.005	15.490 ± 0.005	36.41 ± 0.02	1.0693 ± 0.0001	2.1980 ± 0.0004
Leclerc Supermarket				16.759 ± 0.004	15.510 ± 0.005	36.59 ± 0.02	1.0806 ± 0.0001	2.1832 ± 0.0004
Monoprix Supermarket				17.014 ± 0.003	15.549 ± 0.004	36.95 ± 0.01	1.0942 ± 0.0001	2.1719 ± 0.0004
total		Nov 1995		16.996 ± 0.007	15.534 ± 0.007	36.89 ± 0.02	1.0942 ± 0.0001	2.1705 ± 0.0003
Esso		Dec 1995		16.679 ± 0.005	15.511 ± 0.005	36.53 ± 0.01	1.0753 ± 0.0001	2.1904 ± 0.0003
AGIP				16.897 ± 0.006	15.534 ± 0.006	36.80 ± 0.02	1.0878 ± 0.0001	2.1777 ± 0.0003
BP				16.641 ± 0.007	15.499 ± 0.008	36.47 ± 0.02	1.0736 ± 0.0001	2.1914 ± 0.0004
Shell				16.837 ± 0.006	15.510 ± 0.006	36.70 ± 0.02	1.0856 ± 0.0001	2.1796 ± 0.0003
Carrefour Supermarket				17.068 ± 0.004	15.597 ± 0.005	37.09 ± 0.02	1.0943 ± 0.0001	2.1728 ± 0.0004
Industrial Pb								
urban incinerator	CIVOM Sete	Sep 30, 1993	ashes	17.894 ± 0.004	15.661 ± 0.005	38.00 ± 0.01	1.1427 ± 0.0001	2.1236 ± 0.0003
		Oct 29, 1993		18.057 ± 0.007	15.698 ± 0.007	38.25 ± 0.02	1.1501 ± 0.0002	2.1183 ± 0.0007
		Dec 03, 1993		17.987 ± 0.003	15.634 ± 0.004	38.03 ± 0.01	1.1504 ± 0.0001	2.1143 ± 0.0003
		Jan 06, 1994		18.009 ± 0.003	15.595 ± 0.010	37.95 ± 0.01	1.1547 ± 0.0001	2.1070 ± 0.0002

TABLE 2. Pb Isotopic Composition of Airborne Particulate Matter and Gasoline in the U.K.

location	date	characteristics	^{206}Pb/^{204}Pb	^{207}Pb/^{204}Pb	^{208}Pb/^{204}Pb	^{206}Pb/^{207}Pb	^{208}Pb/^{206}Pb
			Airborne Particulate Matter				
Portswood (Southampton)	Nov 10, 1994	city suburb	17.05 ± 0.05		36.92 ± 0.05	1.105 ± 0.002	2.165 ± 0.003
	Jan 8, 1995		17.05 ± 0.05		36.92 ± 0.05	1.102 ± 0.002	2.165 ± 0.003
	Nov 28, 1994		17.20 ± 0.05		37.08 ± 0.05	1.111 ± 0.002	2.155 ± 0.003
Southampton	Oct 21, 1994	city center	16.91 ± 0.05		36.76 ± 0.05	1.089 ± 0.003	2.175 ± 0.003
	Oct 20, 1994		16.92 ± 0.05		36.79 ± 0.05	1.096 ± 0.003	2.174 ± 0.003
	Oct 28, 1994		17.02 ± 0.05		36.89 ± 0.05	1.098 ± 0.003	2.167 ± 0.003
	Nov 18, 1994		16.92 ± 0.05		36.74 ± 0.05	1.098 ± 0.003	2.172 ± 0.003
	Nov 5, 1994		17.09 ± 0.05		36.99 ± 0.05	1.098 ± 0.003	2.165 ± 0.003
	Nov 25, 1994		17.02 ± 0.05		36.86 ± 0.05	1.101 ± 0.003	2.166 ± 0.003
	Dec 10, 1994		17.10 ± 0.05		36.96 ± 0.05	1.101 ± 0.003	2.161 ± 0.003
	Dec 17, 1994		17.00 ± 0.05		36.86 ± 0.05	1.101 ± 0.003	2.168 ± 0.003
	Dec 3, 1994		17.05 ± 0.05		36.82 ± 0.05	1.102 ± 0.003	2.160 ± 0.003
	Dec 27, 1994		16.97 ± 0.05		36.80 ± 0.05	1.103 ± 0.003	2.169 ± 0.003
	Dec 23, 1994		17.01 ± 0.05		36.83 ± 0.05	1.104 ± 0.003	2.165 ± 0.003
	Dec 30, 1994		17.10 ± 0.05		36.89 ± 0.05	1.106 ± 0.003	2.157 ± 0.003
London (Teddington)	Sat Nov 4, 1995	urban	17.564 ± 0.004	15.602 ± 0.005	37.66 ± 0.01	1.1257 ± 0.0001	2.1440 ± 0.0003
	Sun Nov 5, 1995		17.573 ± 0.003	15.588 ± 0.003	37.64 ± 0.01	1.1273 ± 0.0001	2.1418 ± 0.0003
	Mon Nov 6, 1995		17.341 ± 0.003	15.563 ± 0.003	37.31 ± 0.01	1.1143 ± 0.0001	2.1513 ± 0.0003
	Wed Nov 8, 1995		17.347 ± 0.003	15.546 ± 0.004	37.21 ± 0.01	1.1159 ± 0.0001	2.1449 ± 0.0003
	Thu Nov 9, 1995		17.351 ± 0.007	15.537 ± 0.007	37.15 ± 0.02	1.1168 ± 0.0001	2.1409 ± 0.0003
	Fri Nov 10, 1995		17.379 ± 0.007	15.568 ± 0.007	37.27 ± 0.02	1.1163 ± 0.0001	2.1444 ± 0.0003
	Thu Jan 18, 1996		17.513 ± 0.006	15.575 ± 0.006	37.39 ± 0.02	1.1244 ± 0.0001	2.1347 ± 0.0003
	Fri Jan 19, 1996		17.522 ± 0.010	15.588 ± 0.010	37.43 ± 0.03	1.1241 ± 0.0002	2.1360 ± 0.0004
	Sat Jan 20, 1996		17.790 ± 0.003	15.602 ± 0.003	37.69 ± 0.01	1.1403 ± 0.0001	2.1187 ± 0.0003
	Sun Jan 21, 1996		18.074 ± 0.007	15.606 ± 0.007	37.95 ± 0.02	1.1582 ± 0.0001	2.0993 ± 0.0003
	Mon Jan 22, 1996		18.032 ± 0.007	15.602 ± 0.007	37.86 ± 0.02	1.1557 ± 0.0001	2.0997 ± 0.0003
			Gasolines				
Texaco (Southampton)	Nov−Dec 1994	leaded 4* gasoline	16.61 ± 0.05		36.49 ± 0.05	1.059 ± 0.003	2.197 ± 0.003
Tesco Supermarket (S'ton)			16.52 ± 0.05		36.44 ± 0.05	1.061 ± 0.003	2.196 ± 0.003
BP (Southampton)			16.50 ± 0.05		36.39 ± 0.05	1.062 ± 0.003	2.197 ± 0.003
total (Southampton)			16.59 ± 0.05		36.43 ± 0.05	1.066 ± 0.003	2.195 ± 0.003
Esso (Southampton)			16.54 ± 0.05		36.39 ± 0.05	1.068 ± 0.003	2.191 ± 0.003
ELF (Southampton)			16.70 ± 0.05		36.59 ± 0.05	1.076 ± 0.003	1.189 ± 0.003
Shell (Southampton)			16.72 ± 0.05		36.65 ± 0.05	1.079 ± 0.003	2.186 ± 0.003

20% of Moroccan Pb gives a ratio of 1.06. This calculated value is comparable with the mean of $^{206}Pb/^{207}Pb$ ratio measured today in French gasoline (1.084 ± 0.009; 1σ). In the U.K. in the late 1980s, Associated Octel used a mixture of Australian and Canadian ores in the approximate proportion 70:30 giving a $^{206}Pb/^{207}Pb$ ratio of 1.076 (*26*) similar to the mean currently measured. The virtual monopoly for alkyllead additives held by the Octel Co., in both France and the U.K., implies a signature that is relatively homogeneous regardless of gasoline supplier. However, it should be noted that U.K. additives may not be exactly identical to those recipes used in France since the Octel Co. operates independently in both countries and may therefore purchase Pb from different sources.

(B) Pb from Industrial Emissions. It is difficult to precisely define the isotopic signature of an overall industrial Pb source because of the multiplicity of existing emissions. In addition, the Pb used by U.K. and French industry is dominantly imported since all indigenous Pb−Zn mineral deposits have been worked out in both countries. In the case of gasoline, it is possible to characterize a general Pb isotopic signature due to the effective market monopoly of the Octel Co., but it is obviously not possible to follow the same approach for industrial emissions. While it is likely that industrial emissions have a widely varying Pb isotopic composition (as shown by several workers), Mukai et al. (*16*) and Hamester et al. (*19*) have shown that the Pb isotopic composition of fly ashes from refuse incinerators can be used as a useful indicator of industrial Pb sources. All Pb-containing products are burned and mixed, and the lead isotope ratios are averaged to provide a representative "industrial Pb" signature. Data for the urban incinerator at Sète give $^{206}Pb/^{207}Pb$ ratios varying from 1.143 to 1.155 (Table 1). The range may be due to slight variation in the nature of burned products. Identical ratios have been recently found for the same kind of samples from Germany ∼1.142−1.159 (*19*) and in Japan 1.15 (*16*). These values are comparable to those previously found in liquid urban waste (∼1.147−1.160) in southern France (*5*) and are much more radiogenic than those from gasoline. The application of the Student's *t*-test indicates that the differences between Pb from gasoline and industrial Pb are significant at greater than the 99.9% level. The imports thus are likely to include younger Pb ores (which are more radiogenic) than those from Australia. It is interesting to note that this range also corresponds to the world average of the main Pb ore deposits.

(C) Natural Pb Derived from Rocks and Soils. In France, $^{206}Pb/^{207}Pb$ ratios ranging from 1.193 to 1.200 were measured in pre-industrial sediments sampled in the Thau basin (southern France) and dated at more than 200 yr BP (*27*). Almost the same values were observed (1.197−1.210) in the pre-industrial sediments of the Seine, Loire, Gironde, and Rhône Rivers (*3*). This ratio is likely to be typical throughout France because most of the natural Pb is derived from Variscan continental crust (granite and metamorphic rocks) and from Mezosoic and Cenozoic sediments. This Pb has a $^{206}Pb/^{207}Pb$ ratio ranging from 1.18 to 1.20 (*28*). A remote contribution due to dust transport from North Africa and the Sahara may also occur, although the isotopic composition of these aerosols does not differ significantly from the local/natural Pb. Aerosols from Senegal and a sample from the Matmata loess (southern Tunisia) exhibit $^{206}Pb/^{207}Pb$ ratios of 1.193 and 1.198, respectively (*18, 29*). Due to the lack of isotopic variation between these natural Pb sources, they will simply be considered as French natural lead.

In the U.K., the situation is very similar, however, with slightly less radiogenic ratios as shown by the studies of Hamilton and Clifton (*7*), Croudace and Cundy (*11*), and Sugden et al. (*15*). Pre-industrial sediments from Swansea Bay, Southampton Water, and central Scotland analyzed in these studies gave $^{206}Pb/^{207}Pb$ ratios between 1.17 and 1.19.

Origin of Pb in Airborne Particulate Matter from Urban Areas. In many previous studies, the Pb isotopic composition of urban particulate material, sampled in zones exposed to heavy vehicle traffic, has been considered to be dominated by automotive exhaust emissions. However, since the Pb isotopic composition of airborne particles in both countries shows a wide range of $^{206}Pb/^{207}Pb$ ratios (1.085−1.158), they cannot be due entirely to automotive emissions because measured gasolines range from 1.059 to 1.094. Plotted on $^{206}Pb/^{207}Pb$ vs $^{208}Pb/^{206}Pb$ and $^{206}Pb/^{204}Pb$ vs $^{208}Pb/^{204}Pb$ diagrams, the points fall between the gasoline and the industrial domains (Figure 1). It is clear that the Pb from gasoline is an indisputable source since the Pb isotopic compositions of the urban aerosols cannot be explained by simple binary mixing between natural Pb and industrial Pb alone. In addition, the contribution of natural Pb cannot be excluded because the observed signatures can be reconstructed by three end member as well as two end member mixing. For these reasons, it is impossible to calculate the contribution of each component precisely. To do this, an examination of local influences such as the proximity of industries, traffic density, wind direction, and long-term monitoring of Pb isotopes would be required. Such calculations, though possible, are of limited use because they require generalizations to describe the behavior of the Pb at a given site based on only a few samples. Estimations of the gasoline component that avoid the problem of a ternary mixing solution can be made by initially considering binary mixing of gasoline and industrial Pb using the following conventional mixing equation:

$$X_1 = \frac{(^{206}\mathrm{Pb}/^{204}\mathrm{Pb})_{\mathrm{SAMP}} - (^{206}\mathrm{Pb}/^{204}\mathrm{Pb})_{\mathrm{IND}}}{(^{206}\mathrm{Pb}/^{204}\mathrm{Pb})_{\mathrm{G}} - (^{206}\mathrm{Pb}/^{204}\mathrm{Pb})_{\mathrm{IND}}} \tag{1}$$

where X_1 is the percentage contribution of gasoline; $(^{206}Pb/^{204}Pb)_G$, $(^{206}Pb/^{204}Pb)_{IND}$, and $(^{206}Pb/^{204}Pb)_{SAMP}$ are the isotopic signatures of the gasoline and industrial end-members and of the airborne particulate sample, respectively. This equation uses the $^{206}Pb/^{204}Pb$ ratio, but similar equations can be developed for the other isotope ratios.

Furthermore, binary mixing between gasoline and the more radiogenic natural Pb component gives the following equation:

$$X_2 = \frac{(^{206}\mathrm{Pb}/^{204}\mathrm{Pb})_{\mathrm{SAMP}} - (^{206}\mathrm{Pb}/^{204}\mathrm{Pb})_{\mathrm{NAT}}}{(^{206}\mathrm{Pb}/^{204}\mathrm{Pb})_{\mathrm{G}} - (^{206}\mathrm{Pb}/^{204}\mathrm{Pb})_{\mathrm{NAT}}} \tag{2}$$

where X_2 represents the contribution of gasoline in this mixing model and $(^{206}Pb/^{204}Pb)_{NAT}$ is the isotopic composition of pre-industrial sediments. The average isotopic compositions of each end member used for the mixing models are shown in Table 3. Although the isotopic composition of the industrial end member has not yet been empirically defined for the southern U.K., a French signature is assumed to be reasonable.

Some differences occur between the $^{206}Pb/^{207}Pb-^{208}Pb/^{206}Pb$ and $^{206}Pb/^{204}Pb-^{208}Pb/^{204}Pb$ graphs (Figure 1): particularly for gasoline values near the lower part of the $^{206}Pb/^{207}Pb-^{208}Pb/^{206}Pb$ couple and for U.K. particulate material. This is explained by the fact that samples having different $^{206}Pb/^{204}Pb$ and $^{207}Pb/^{204}Pb$ ratios can have a similar $^{206}Pb/^{207}Pb$ ratio, which is also true for all other ratios that do not include the ^{204}Pb isotope. To reduce this effect, X_1 and X_2 are calculated by averaging the results obtained with each ratio. The range between X_1 and X_2 is a measure of the uncertainty on the estimate of the percentage contribution of gasoline-derived Pb when considering mixing between gasoline, industrial, and natural Pb.

As described below, the isotopic composition of gasoline-derived Pb has shown significant changes over the last 30 years. The models used here assume that resuspension of

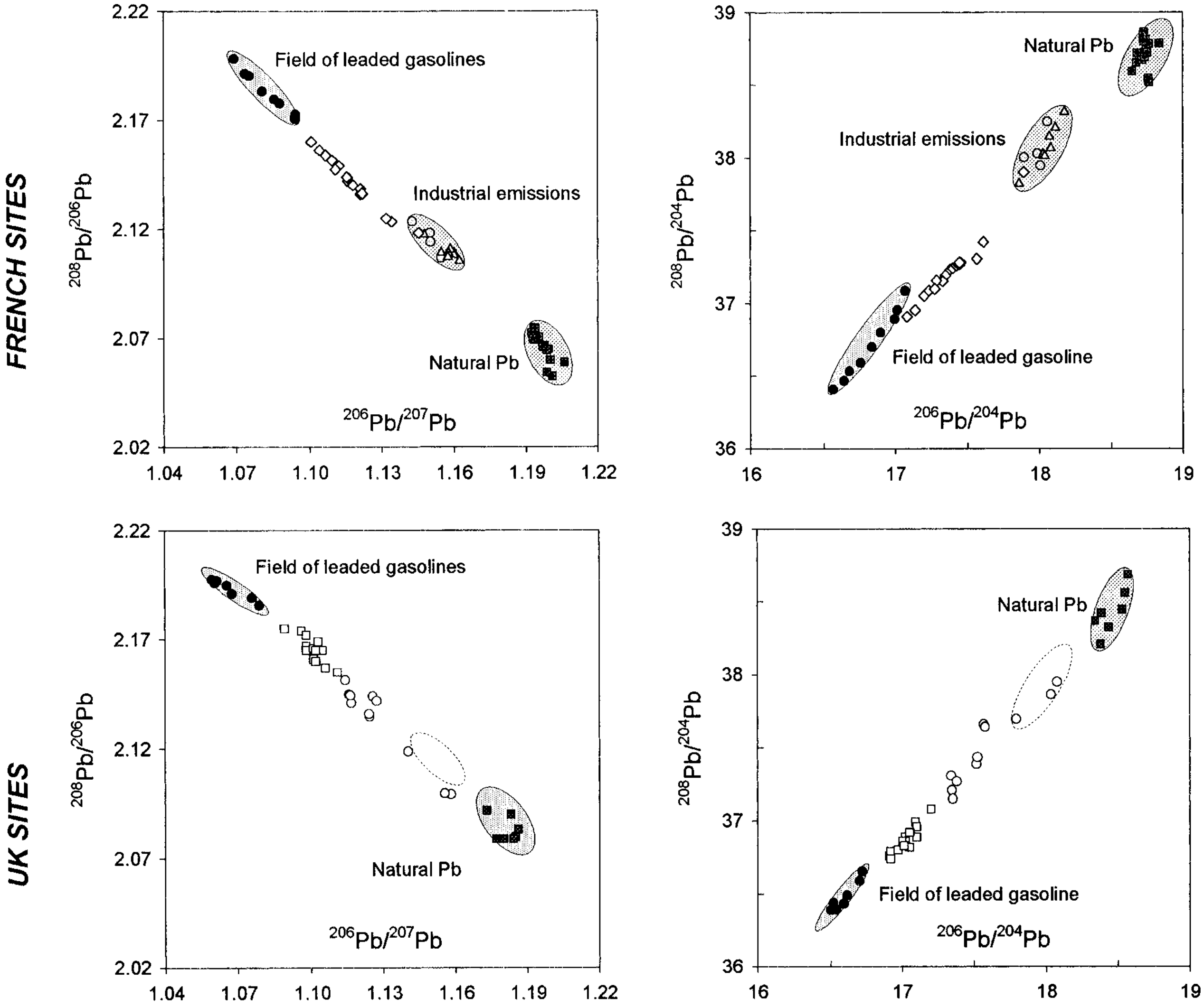

FIGURE 1. ^{208}Pb/^{206}Pb vs ^{206}Pb/^{207}Pb and ^{208}Pb/^{204}Pb vs ^{206}Pb/^{204}Pb in environmental samples from France and the U.K. (●) leaded gasoline, (gray circles) ashes from urban incinerator, (△) liquid urban waste (*5*), (■) pre-industrial sediment (*3*, *5*, *7*, *26*), (◇) airborne particulate matter from French urban areas, (○) airborne particulate matter from London, (□) airborne particulate matter from Southampton.

TABLE 3. Average Isotopic Composition of Gasoline-Derived, Industrial, and Local/Natural Pb in France and the U.K.[a]

	n	^{206}Pb/^{204}Pb	^{208}Pb/^{204}Pb	^{206}Pb/^{207}Pb	^{208}Pb/^{206}Pb
		End Members in France			
gasoline	9	16.83	36.71	1.084	2.182
industrial emissions	13	18.03	38.07	1.155	2.112
pre-/early industrial sediments	16	18.73	38.72	1.197	2.066
		End Members in U.K.			
gasoline	7	16.60	36.48	1.067	2.193
industrial emissions	*b*	18.03	38.07	1.155	2.112
pre-/early industrial sediments	7	18.45	38.41	1.184	2.082

[a] *n*, number of samples. [b] Isotopic composition of the 'industrial' end member in the U.K. is assumed to be the same as in France.

"old" gasoline-derived Pb into the urban atmosphere has an insignificant impact on the gasoline end member. Several studies have shown that contaminants introduced into urban areas (i.e., ^{137}Cs) have relatively low residence time in urban dusts, with half-lives usually less than 1 year (*30*, *31*). That part of the Pb emitted in the 1960s and 1970s that has not been removed from urban areas by rainfall is likely to be present in a form not readily amenable to resuspension (e.g., in soils). Consequently, in the vicinity of dense automotive traffic, the contribution of old gasoline-derived Pb is likely to be relatively small.

Origin of Pb in French Airborne Particulate Matter. It is apparent that if the isotopic signature of airborne particulate matter is similar to that of gasoline, the uncertainty (range between X_1 and X_2) is slight, i.e., for Nantes (Figure 2). By contrast, if the isotopic signature approaches industrial values, as found for station 12 of Toulouse, the contribution from gasoline is poorly constrained. In spite of this sometimes poor discrimination, samples can be divided into three groups. For Nantes, Toulouse station 6, Montpellier, and Le Havre, measurements show that 70–80% of Pb is derived from gasoline combustion, decreasing to 40–70% for Clermont-Ferrand, Paris, Amiens, Strasbourg, Lille, Caen, and Bar-le-Duc. Finally, a gasoline Pb contribution ranging from 10 to 40% is calculated for airborne particulate matter collected from Toulouse station 12. Figure 3 shows the change in

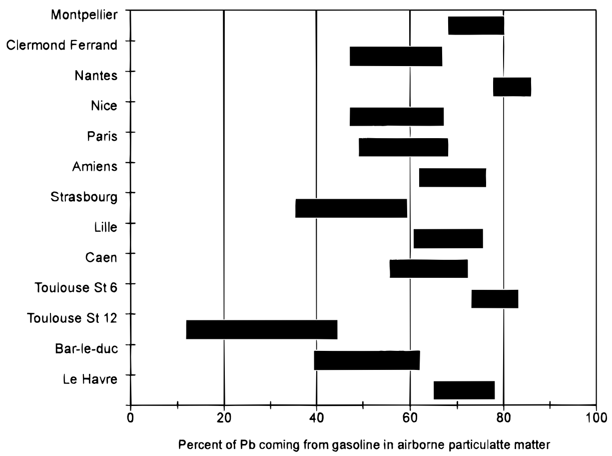

FIGURE 2. Calculated percentage contribution of gasoline-derived Pb to total airborne particulate Pb in urban areas from France.

airborne Pb concentration over time at the various French sites used in this study, since 1984. At most sites examined, the airborne Pb concentration has greatly decreased due to EU (European Union) legislation that has imposed reductions on the amount of Pb added to gasoline (0.15 g/L at present, compared with 0.65 g/L in the period 1965−1975, Associated Octel, personal communication) and on permitted Pb emissions and also the increasing use of unleaded gasoline. Pb concentrations shown in Figure 3 are generally much lower than the upper limit fixed by the EU of 2 μg/m^3 Pb as an annual average. Only Toulouse station 12 has not seen a general Pb decrease. This station, located in the center of the city, is close to a lead smelter used for battery recycling. This factory is a significant Pb polluter with an average emission rate of 0.2 kg day^{-1} (1993 value). The influence of an industrial input is evident at station 12, and only ~10% of the total Pb at this site is derived from gasoline combustion based on calculations using eq 1; the natural component is relatively insignificant. The other sampling site at Toulouse (station 6), located 4 km from station 12, is exposed to very dense vehicle traffic and shows a relatively high airborne Pb concentration when compared to the other French cities. Here, the ^{206}Pb/^{207}Pb ratio (1.104) indicates that, on the day sampled, the contribution from industrial activities was negligible, highlighting the dominantly local impact of the smelter. At Strasbourg, a rather radiogenic signature has also been found. This cannot be explained by a more radiogenic contribution from German gasolines because these have approximately the same Pb isotopic composition as French gasoline (*19*). Moreover, it is notable that in recent years more than 90% of German gasoline used is unleaded as compared with 50% and 40% for the U.K. and France, respectively (Associated Octel, personal communication). A more likely explanation is that sampling of material at Strasbourg was carried out in a zone that is now traffic-free, which explains why the Pb content and the gasoline contribution are so low.

Origin of Pb in U.K. Airborne Particulate Matter. (A) Teddington, West London. Airborne particulate samples collected from the Teddington area of west London show a large range in Pb isotopic ratios (Figure 4). This short-term variability is likely to be a result of varying wind direction and traffic densities. The major road in this area is to the west of the sampling site, and the least radiogenic values are found when the wind is from the west. Under SE winds, which cross areas of low traffic density, the most radiogenic data are found. The data confirm that Pb isotopic composition is also a function of traffic density since more radiogenic values are measured at the weekends. During weekend periods, traffic density is substantially lower than on weekdays when considerable congestion occurs due to commuter traffic. Even during days with higher traffic density, the contribution of Pb derived from gasoline does not exceed ~ 60% (Figure 4).

(B) Southampton. Samples in Southampton were collected using a low-volume air sampler over several days, and therefore the data represent generalized values and cannot be used to evaluate short-term effects. Air particles were

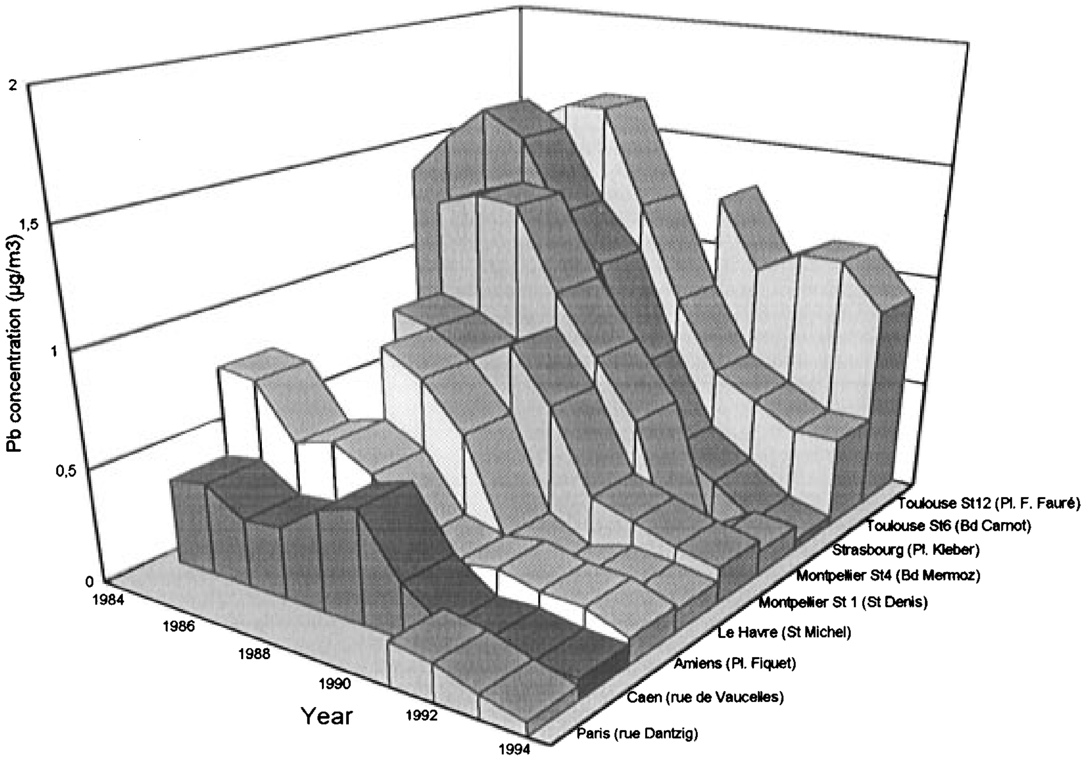

FIGURE 3. Temporal change in Pb concentration in urban air at various French sites (data from ORAMIP, ASPA, AMPADI, AIRNORMAND, ASQAP, ADEME, and LCPP, personal communication, 1995).

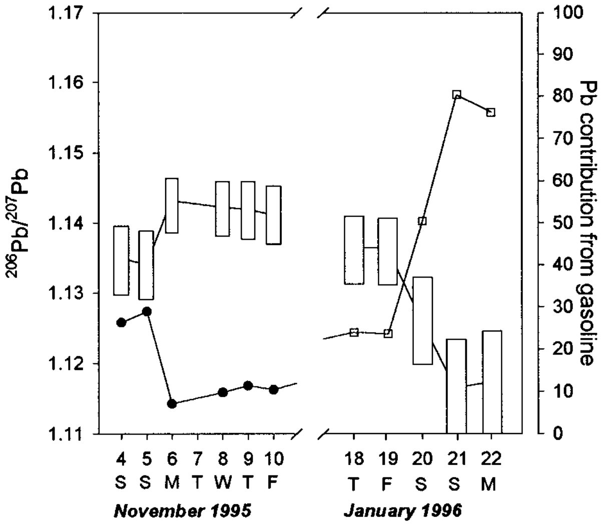

FIGURE 4. Evolution of $^{206}Pb/^{207}Pb$ ratios in airborne particulate matter collected at London (Teddington) in November 1995 (●) and January 1996 (□). The boxes represent the calculated contribution of Pb from gasoline (from eqs 1 and 2).

collected from a busy city center site and also from a suburb of the city (Portswood) that is also exposed to appreciable traffic. The former sampling site was by the main road while the latter was a garden site. The results show that gasoline-derived Pb makes a major contribution to particulate Pb in both areas: 61−84% of Pb is derived from gasoline combustion at the city center site and 56−74% at the Portswood suburban site.

These results confirm that gasoline is the main source of Pb in most French and in southern U.K. urban areas. However, following environmental legislation restricting concentrations of Pb in gasoline and the increased market penetration of unleaded gasoline, other sources of Pb can now be identified using isotopic studies and are likely to become increasingly evident.

Evolution of Pb Isotopic Signatures in Environmental Materials. The results from this study can be used to extend the existing database that describes the changing isotopic composition of anthropogenic Pb with time (Figure 5). This type of information is indispensable in historical reconstruction of Pb pollution sources in sediment and ice-core records or other environments (*32−35*). Table 4 summarizes the published data since 1965. In France, Chow et al. (*22*) measured a $^{206}Pb/^{207}Pb$ ratio of 1.162−1.163 in gasoline directly whereas many other workers have obtained data indirectly through the sampling of aerosols. These later workers considered that their results were more or less representative of automotive emissions. In 1975, grass sampled in the vicinity of a Parisian highway gave a ratio of 1.128 while in 1981 filtered aerosols taken in a car park near Paris were measured at 1.101 (*2, 3*). During the same period, Flament (*36*) found a similar ratio of 1.093 for aerosols collected along a highway in northern France. Monna et al. (*5*) reported slightly higher values of 1.109−1.111 for airborne particulate matter sampled in 1987, a few meters from heavy traffic in Montpellier. Finally, in 1988 Grousset et al. (*29*) collected aerosols from Lyon that had $^{206}Pb/^{207}Pb$ ratios of 1.096. In the U.K., the available data are more limited. Hamilton and Clifton (*7*) reported $^{206}Pb/^{207}Pb$ ratios of 1.126 and 1.105 in 1968 and 1971, respectively, measured in airborne particles from London and 1.134 in airborne particulate matter from Cardiff in 1968. More recently, Sugden et al. (*15*) found $^{206}Pb/^{207}Pb$ ratios ranging from 1.056 to 1.093 in Edinburgh over the period 1989−1991. The trends in the U.K. and France show a significant decrease in the $^{206}Pb/^{207}Pb$ ratio during

TABLE 4. Previously Published Pb Isotopic Compositions of Environmental Samples from France and the U.K.

	ref	method	year	sampling	$^{206}Pb/^{204}Pb$	$^{207}Pb/^{204}Pb$	$^{208}Pb/^{204}Pb$	$^{206}Pb/^{207}Pb$	$^{208}Pb/^{206}Pb$
					France				
Paris	22	TIMS	1966	gasoline	18.25			1.162	2.113
Paris	22	TIMS	1966	gasoline	18.24			1.163	2.113
Paris	2	TIMS	1975	grass sample				1.128	
Paris	2, 3	TIMS	Dec 1981	aerosols car park	17.25 ± 0.05	15.56 ± 0.05	37.49 ± 0.13	1.101 ± 0.001	
Gravelines	3	TIMS	1984	aerosol/highway	16.99	15.54	36.87	1.093	2.170
Montpellier	5	TIMS	Sep 1987	urban air/filter	17.385 ± 0.044	15.663 ± 0.039	37.471 ± 0.101	1.1093 ± 0.0004	
Montpellier	5	TIMS	Sep 1987	urban air/filter	17.270 ± 0.003	15.556 ± 0.004	37.172 ± 0.011	1.1102 ± 0.0001	
Montpellier	5	TIMS	Sep 1987	urban air/filter	17.332 ± 0.029	15.603 ± 0.027	37.306 ± 0.064	1.1108 ± 0.0003	
Lyon	29	ICP−MS	1988	car parking	16.749 ± 0.111	15.280 ± 0.086	35.274 ± 0.331	1.096 ± 0.003	2.102
					U.K.				
Cardiff	7	TIMS	1968	air particles	17.66			1.134	2.155
London	7	TIMS	1968	air particles	17.45			1.126	2.141
London	7	TIMS	1971	air particles	17.32			1.105	
Edinburgh	15	ICP−MS	1989−1991	urban air/filter				1.056−1.093	

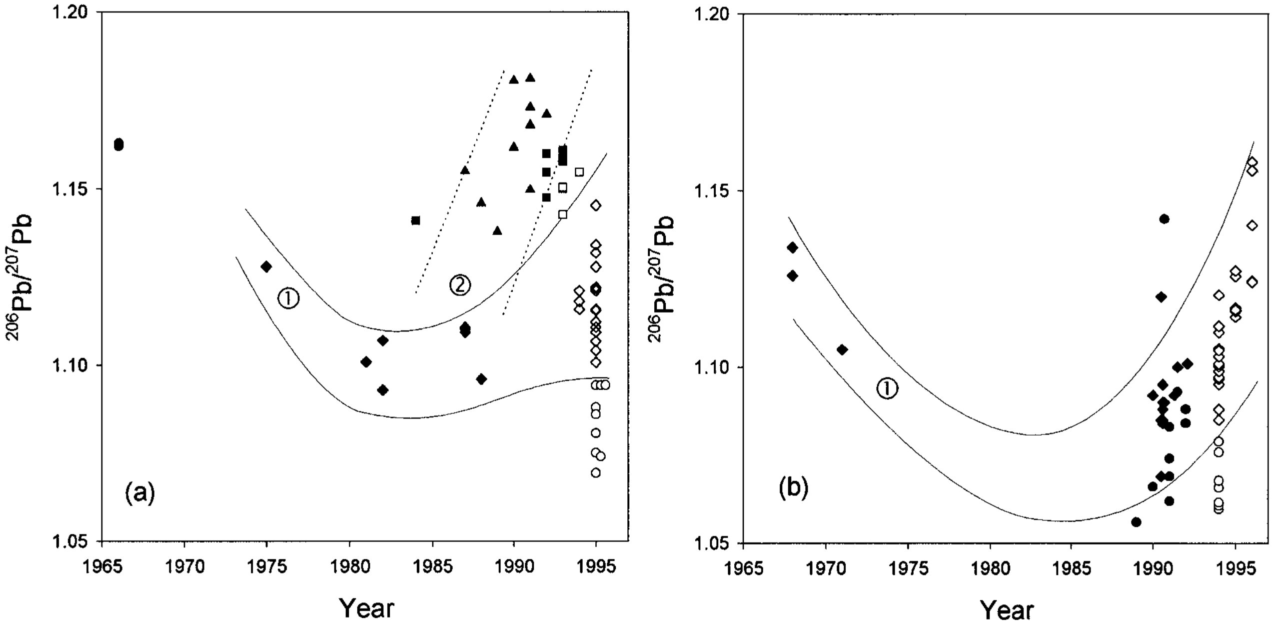

FIGURE 5. Change in ^{206}Pb/^{207}Pb ratio since 1965 for potential sources of Pb and airborne particulate matter in France (a) and the U.K. (b). Closed symbols, data from literature (see Table 4 for references); open symbols, this study: (○) gasoline, (□) industrial emissions. Field 1 represents the isotopic evolution of samples collected in urban areas (◇), and field 2 represents the isotopic evolution of aerosols collected in French mountains (△) (*18*).

1965–1980, which could be interpreted as a growing use of Australian lead. However, as mentioned above for both countries, modern urban aerosols have an isotopic signature that is always more radiogenic than those of gasoline, and so it is uncertain that the Pb isotopic ratios obtained in the past for aerosols perfectly reflect those in gasoline. Consequently, all results obtained using indirect sampling can only be considered as the upper limit of the gasoline component since other contributions cannot be excluded.

Concerning industrial Pb, there are few direct measurements available. In 1984, Petit measured ^{206}Pb/^{207}Pb ratios close to 1.141 in the atmosphere at various industrial sites of northern France (*3*), and ^{206}Pb/^{207}Pb ratios between 1.147 and 1.161 have been measured in liquid urban waste (*5*). This kind of sampling allows a general assessment of the isotopic composition of industrially derived Pb, although values obtained may be slightly low due to mixing with gasoline-derived Pb. However, such values are in agreement with the range found from ashes from urban incinerators: 1.143–1.155. Although the database is preliminary, the isotopic signature seems to have remained rather constant over the last decade, but there are insufficient data available prior to the 1980s.

Grousset et al. (*18*) have shown a decrease of Pb content and a corresponding increase in ^{206}Pb/^{207}Pb ratios in French mountain aerosols since 1985 (see Figure 5), which was attributed to the decreasing input of Pb from automobile emissions. In urban areas, the same phenomenon is often noted, but to a lesser extent due to proximity to the sources of Pb pollution. In the urban environment, Pb derived from other sources (industrial and natural) has increased in relative terms and can no longer be neglected when assigning a characteristic anthropogenic Pb signature. Hence, even where Pb isotopes can be successfully applied in environmental studies, great care must be taken to define the isotopic character of all individual sources of Pb with representative sampling programs. Additionally, it is desirable that such isotopic monitoring is carried out frequently to provide a better database showing variations with time so that evolutionary changes in the Pb pollution record can be understood.

Acknowledgments

We wish to express special thanks to M. Ducate and B. Vuillot, AMPADI, R. Stroebel, ADEME; M. Geraud, QUALITAIR 06; J. P. de la Massa, ORAMIP; A. Target, ASPA; J. P. Goguet, ESPAC; M. Luittre, ASQAP; J. F. Laquerriere, AIR NORMAND; O. Soudier, AIRLOR; J. Attia, LCPP; S. Pellier, AMPAC; L. Levaudel, AIRMARAIX; and S. Gottard, AREMA for their help during sampling and also N. Clauer and F. Grousset for their precious experience and their helpful comments. The Southampton group thank Prof. Bob Nesbitt for the use of the Fisons Elemental PQ2+ ICP–MS and Dr. Nakhwa of Associated Octel for his generous assistance with supplying data. John Coates of the London Borough of Richmond upon Thames is thanked for providing air filters and traffic flow and weather data.

Literature Cited

(1) Doe, B. R.; Stacey, J. S. *Econ. Geol.* **1974**, *69*, 757.
(2) Elbaz-Poulichet, F.; Holliger, P.; Huang, W.; Martin, J.-M. *Nature* **1984**, *308*, 409.
(3) Elbaz-Poulichet, F.; Holliger, P.; Martin J-M.; Petit, D. *Sci. Total Environ.* **1986**, *54*, 61.
(4) Erel, Y.; Patterson, C. *Geochim. Cosmochim. Acta* **1994**, *58*, 3289.
(5) Monna, F.; Ben Othman, D.; Luck, J.-M. *Sci. Total Environ.* **1995**, *166*, 19.
(6) Petit, D. *Earth Planet. Sci. Lett.* **1974**, *23*, 199.
(7) Hamilton, E. I.; Clifton, R. J. *Estuarine Coastal Mar. Sci.* **1979**, *8*, 271.
(8) Shirahata, H.; Elias, R. W.; Patterson, C. C. *Geochim. Cosmochim. Acta* **1980**, *44*, 149.
(9) Petit, D.; Mennessier, J. P.; Lamberts, L. *Atmos. Environ.* **1984**, *18* (6), 1189.
(10) Hirao, J.; Mabuchi, H.; Fukuda, E.; Tanaka, H.; Imamura, T.; Todoroki, H.; Kimura K.; Matsumoto, E. *Geochem. J.* **1986**, *20*, 1.
(11) Croudace, I. W.; Cundy, A. B. *Environ. Sci. Technol.* **1995**, *29* (5), 1288.
(12) Maring, H.; Settle, D. M.; Buat-Ménard, P.; Dulac, F.; Patterson, C. C. *Nature* **1987**, *300*, 154.
(13) Hamelin, B.; Grousset, F. E.; Biscaye, P. E.; Zindler, A.; Prospero, J. M. *J. Geophys. Res.* **1989**, *94* (C11), 16243.
(14) Hopper, J. F.; Ross, H. B.; Sturges, W. T.; Barrie, L. A. *Tellus* **1991**, *43B*, 45.
(15) Sugden, C. L.; Farmer, J. G.; Mackenzie, A. B. *Environ. Geochem. Health* **1993**, *15*, 50.

(16) Mukai, H.; Furuta, N.; Fujii, T.; Ambe, Y.; Sakamoto, K.; Hashimoto, Y. *Environ. Sci. Technol.* **1993**, *27* (7), 1347.
(17) Mukai, H.; Tanaka, A.; Fudjii, T.; Nakao, M. *J. Geophys. Res.* **1994**, *99* (D2), 3717.
(18) Grousset, F. E.; Quétel, C. R.; Thomas, B.; Buat-Ménard, P.; Donard O. F. X.; Buchet, A. *Environ. Sci. Technol.* **1994**, *28*, 1605.
(19) Hamester, M.; Stechmann, H.; Steiger, M.; Dannecker, M. *Sci. Total Environ.* **1994**, *146/147*, 321.
(20) Rabinowitz, M. B.; Wetherill, G. W. *Environ. Sci. Technol.* **1972**, *6* (8), 705.
(21) Chow, T. J.; Earl, J. L. *Nature* **1973**, *176*, 510.
(22) Chow, T. J.; Snyder, C.; Earl, J. L. In *Isotope ratios as pollutant source and behaviour indicators*; IAEA: Vienna, 1975; p 95.
(23) Sturges, W. T.; Barrie, L. A. *Nature* **1987**, *329*, 144.
(24) Strelow, F. W. E. *Anal. Chem.* **1978**, *50* (9), 1359.
(25) Cameron, A. E.; Smith D. H.; Walker, R. L. *Anal. Chem.* **1969**, *41* (3), 525.
(26) Delves, H. T. *Chem. Brit.* **1988**, *24*, 1009.
(27) Lancelot, J.; Monna, F.; Mercadier, H. Presented at the EUG VIII conference, Strasbourg, France, 1995.
(28) Michard-Vitrac, A.; Albarede, F.; Allegre, C. J. *Nature* **1981**, *291*, 460.
(29) Grousset, F. E.; Quetel, C. R.; Thomas, B.; Donard, B. F. X.; Lambert, C. E.; Guillard, F.; Monaco, A. *Mar. Chem.* **1995**, *48*, 291.
(30) Dominik, J.; Burrus, D.; Vernet, J.-P. *Earth Planet. Sci. Lett.* **1987**, *84*, 165.
(31) Allott, R. W.; Kelly, M.; Hewitt, C. N. *Environ. Sci. Technol.* **1992**, *26*, 2142.
(32) Rosman, K. J. R.; Chisholm, W.; Boutron, C. F.; Candelone, J. P.; Hong, S. *Geochim. Cosmochim. Acta* **1994**, *58* (15), 3265.
(33) Rosman, K. J. R.; Chisholm, W.; Boutron, C. F.; Candelone, J. P.; Görlach, U. *Nature* **1993**, *362*, 333.
(34) Farmer, J. G.; Eades, L. J.; MacKenzie, A. B.; Kirika, A.; Bailey-Watts, T. E. *Environ. Sci. Technol.* **1996**, *30*, 3080.
(35) Bacon, J. R.; Jones, K. C.; McGrath, S. P.; Jonhston, A. E. *Environ. Sci. Technol.* **1996**, *30*, 2511.
(36) Flament, P. Ph.D. Dissertation, University of Lille, France, 1985.

Received for review October 9, 1996. Revised manuscript received February 19, 1997. Accepted February 25, 1997.[⊗]

ES960870+

[⊗] Abstract published in *Advance ACS Abstracts*, May 1, 1997.

Environ. Sci. Technol. **1999**, *33,* 2850−2857

Origin and Evolution of Pb in Sediments of Lake Geneva (Switzerland−France). Establishing a Stable Pb Record

FABRICE MONNA,*,† JANUSZ DOMINIK,†,‡
JEAN-LUC. LOIZEAU,†,‡
MICHEL PARDOS,† AND
PHILIPPE ARPAGAUS†

Institut FA FOREL, 10 route de Suisse, CH-1290 Versoix, Switzerland, and Centre d'Etudes en Sciences Naturelles de l'Environnment, 10 route de Suisse, CH-1290 Versoix, Switzerland

Pb isotopes and Pb concentrations were measured in two sediment cores sampled in Lake Geneva (i) at the center of the basin (central plain) and (ii) in an area which receives the effluents of the wastewater treatment plant of Lausanne as well as runoff inputs. The presence of an anthropogenic contribution is observed over all the sampled period (∼150 years), even at the center of the lake. At both sites, the maximum contamination of Pb occurred in the late 1970s, and has declined to present. The site close to Lausanne received much more Pb than the one at the center of the lake. Surprisingly, the Pb isotopes show that gasoline-derived Pb has had a minor influence, at least over the last 20 years. Instead, deposition of Pb from industrial (and domestic) activities predominates. This study demonstrates that one of the major limitations of the isotopic method is the poor (or partial) knowledge of how the isotopic compositions of potential sources have evolved through the past. A simple method of sample dissolution, based on HNO_3 leaching assisted by microwave, is also presented. We believe that this sample preparation can be extensively used because it provides a reliable estimate of Pb having an anthropogenic origin.

Introduction

Pb added into gasoline as antiknock compounds was considered for a long time to be the major source of Pb contamination, with a maximum worldwide contamination occurring in the mid-1970s (*1*). In Switzerland, unleaded gasoline was introduced in 1985, and nowadays less than 20% of gasoline still contains leaded additives. The National Air Pollutant Observation Network (NABEL) reported that, between 1988 and 1993, the Pb dry deposition decreased by more than 50% at five of six stations over Switzerland (*2*). As a consequence, other sources such as industrial (or domestic) activities may become relatively more important in the total anthropogenic Pb budget (*3*). In addition, the presence of a point-source, such as a wastewater treatment plant, an industrial area, or runoff may locally dominate the pollutant inputs.

Stable Pb isotope geochemistry in environmental studies can be used for tracing the origin of Pb. This method is based on the differences in isotopic abundance existing between different groups of materials (e.g. local rocks, gasoline additives, industrial emissions, etc.). The determination of Pb isotopes in the sedimentary column allowed the reconstructing of the history of Pb inputs (i.e. annual/decade scale or more) in lakes (*4*−*10*) or marine/estuarine environments (*11*−*16*). However, Pb in sediments is generally derived from multiple sources. Contributions, as well as their isotopic signatures, likely evolved through time, since the location of input has frequently changed relative to the economic condition (*17*). Such an isotopic database is unfortunately either poor or nonexistent, depending on the country. In addition, the study of a single binary mixing (e.g. natural, anthropogenic) is relatively easy, whereas it becomes much more ambiguous for multicomponent mixing, where several anthropogenic end-members are involved.

The aim of this study was to investigate the origin and the history of Pb inputs at an in-shore site potentially influenced by industrial/domestic wastewater effluents and by urban runoff, where gasoline-derived Pb should dominate. For comparison a reference site was chosen in the center of the lake, far from direct human inputs. The results were compared to the few studies previously carried out in Switzerland: ice from a high alpine site (*18, 19*), lake Zug sediments close to Zurich (*10*). and peat bog in Jura Mountains (*20, 21*).

Setting

Lake Geneva is the largest freshwater body in Europe, with a volume of 89 km^3 (Figure 1). The Rhone River is its major tributary and drains 70% of the lake watershed, including industrial and urban sites, agricultural lands, glaciated areas, pasture, and forests. The biggest city on the lake shore is Lausanne, which releases treated domestic and industrial wastewater into the Bay of Vidy (200 000 equiv inhabitants). The wastewater treatment plant started in 1964 with biological treatment, followed in 1971 by the implementation of a phase for the phosphate elimination using $FeCl_3$. A pipe also drains the runoff into the bay. A core (BV) has been sampled at about 700 m from the plant effluent, at a depth of 51 m. For comparison, another core (PC) has been recovered from the central plain and deepest part of the lake (307 m).

Methodology

Sampling and Subsampling. The cores were recovered using poly(vinyl chloride) liners (50 cm in length), from the submersible F. A. Forel (*22*). Volume magnetic susceptibility (VMS) was determined on the BV core using a Bartington MS2. The subsampling of the PC core (44 cm long) was carried out at an interval of 0.5 cm for the first 20 cm, and 1 cm for the remaining section, whereas a 1 cm interval was used all along the BV core (41 cm long). Samples were gently air-dried at 60 °C for 2 days; the water content and porosity were calculated following the method of Sugai et al. (*23*). The depth scale was expressed in term of mass depth (g cm^{-2}).

Analysis. Dating was based on ^{210}Pb and ^{137}Cs methods, measured by α- and γ-ray spectrometry, respectively (*22*). Excess Pb ($^{210}Pb_{xs}$) was obtained by subtracting the supported activity, determined via measurement of the ^{214}Pb isotope by γ-ray spectrometry. Loss on ignition (LOI), a surrogate for organic matter content, was measured after 4 h at 550 °C.

It has already been demonstrated that anthropogenic component can be partly separated from the total Pb by a dilute acid leaching (*5, 13, 24*). Graney et al. (1995) have also

---

[†] Institut FA FOREL.

[‡] Centre d'Etudes en Science Naturelles de l'Environment.

[*] Corresponding author. fax: 0041 22 755 1382; e-mail: monna@sc2a.unige.ch.

10.1021/es9902468 CCC: $18.00

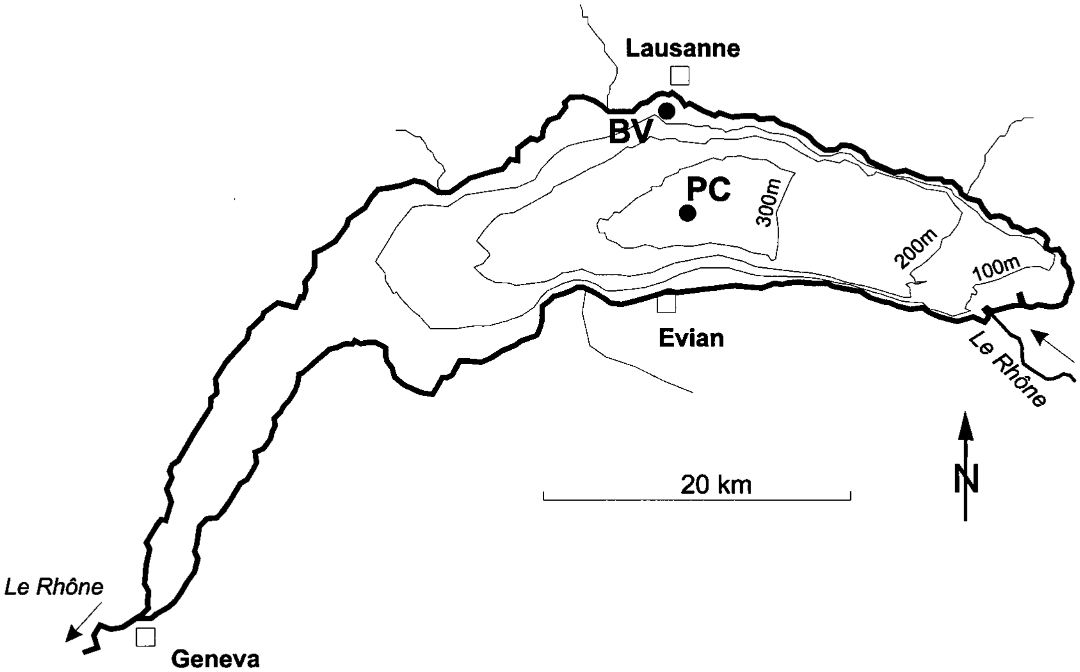

FIGURE 1. Map of lake Geneva with location of cores. Central Part of the lake (PC): 46°28′38″ N, 6°38′35″ E, depth = 307 m. Bay of Vidy (BV): 46°30′42″ N, 6°35′06″ E, depth = 51 m.

reported that the strength and the nature of acid (HCl or HNO_3) have only little effect on the concentration and isotopic ratios of leached Pb and that the leached fraction of a contaminated sediment are isotopically distinct from those removed from the silicate minerals after HF digestion (*9*). This does not mean that only anthropogenic Pb is removed by dilute acid, nor that the residue is totally free from some anthropogenic Pb persisting after leaching, but simply that dilute acid can be used to extract preferentially anthropogenic Pb from a contaminated sediment. Such a procedure was carried out here using nitric acid for evident reasons of convenience for further ICP-MS measurements. The procedure consisted of (i) a partial dissolution of about 500 mg of sediment with 10 mL of suprapure 2 N HNO_3 and (ii) the total dissolution of the residue of 14 selected samples with suprapure and concentrated $HF/HNO_3/HCl$ mixture (3 mL of each). The partial dissolution was carried out in closed, pressurized Teflon bombs, in a microwave assistance oven (ETHOS, Milestone) with the following settings: 5 min at 400 W, 2 min at 100 W, 10 min at 600 W, and finally 10 min at 700 W (magnetic stirring; pressure max, 20 bar). After centrifugation the residues were washed again with 10 mL of suprapure 2 N HNO_3 and centrifuged. Total dissolution was carried out using the settings above for the microwave. Chemical preparation was performed in a class 100−1000 clean room. Pb concentrations were then measured by a quadrupole-based ICP-MS (POEMS1, TJA) using Rh/Re internal calibration. Reproducibility of Pb concentrations was better than 10% on the basis of numerous replicates. Blanks were systematically measured for each set of eight unknown samples and were always found to be negligible compared to Pb in samples.

Isotopic ratios were measured using the same quadrupole-based ICP-MS. Separation of Pb, mass bias correction via NBS 981 measurements, and typical settings are reported elsewhere (*25*, *26*).

Results

Pb Isotopes. Leachates of Lake Geneva sediments are plotted on two diagrams of $^{208}Pb/^{204}Pb$ vs $^{206}Pb/^{204}Pb$ and $^{208}Pb/^{206}Pb$ vs $^{206}Pb/^{207}Pb$ (Figure 2). The measured changes in isotope ratios are much greater than the uncertainties in the measurements and are significant in all cases. For both cores, the linear trends indicate an influence of one or more less radiogenic (anthropogenic) sources contaminating the naturally occurring Pb. In Figure 2a, the PC samples seem generally shifted to less thorogenic values (lower $^{208}Pb/^{204}Pb$ ratios), but this tendency does not appear in Figure 2b.

Bay of Vidy. The uppermost 22 cm (0−10.9 g cm^{-2}) are almost black, characterized by relatively constant porosity (except the uppermost 3 cm), high organic matter content, and high values of VMS (Figure 3a, Table 1). Below 22 cm, the sediments turn gray with numerous laminae in which the organic matter content and VMS remain steady at lower values. The ^{137}Cs profile exhibits two distinct peaks reaching 200 and 130 mBq g^{-1} at mass depths of 6 and 10.5 g cm^{-2}, respectively. The $^{210}Pb_{tot}$ activities increase from bottom to top, from about 59 to 170 mBq g^{-1}, following the same evolution as the porosity profile. The ^{214}Pb activities slightly decrease toward the top from 55 to 44 mBq g^{-1}.

Leached Pb. Relatively low Pb contents (~30 μg g^{-1}) are observed at the core bottom. They increase, slowly at first up to 10.9 g cm^{-2} (~ 90 μg g^{-1}) and then rapidly to reach a maximum at 8.4 g cm^{-2} (~ 300 μg g^{-1}). Finally, the Pb contents decline up to the surface (~120 μg g^{-1}). The BV core is characterized by a decrease of the $^{206}Pb/^{207}Pb$ ratios proceeding in four steps: (i) a decrease from ~1.195 at the bottom to ~1.170 at 16.3 g cm^{-2}, (ii) a stabilization up to 10.9 g cm^{-2}, (iii) another decline at about 1.150 up to 9 g cm^{-2}, and (iv) another stabilization up to the surface.

Residual Pb. It is always low comparatively to the total Pb content, but can vary between 5.1 and 17.8 μg g^{-1}; the highest value being recorded in the strongest contaminated layer. Its isotopic signature follows the same trend as the leachate fraction, but it is systematically more radiogenic.

Central Plain. The porosity profile indicates a regular compaction with depth, except that shifts are observed at ~1 and 4.3 g cm^{-2} (Figure 3b, Table 2). The organic matter content regularly decreases in the first 7 g cm^{-2} and then stabilizes around 4%. Two peaks of ^{137}Cs reaching 550 and 230 mBq g^{-1} are observed at 1.5 and 3.5 g cm^{-2}, respectively; whereas $^{210}Pb_{tot}$ activities increase from 50 mBq g^{-1} at the bottom, up to nearly 300 mBq g^{-1} at the surface. However, ^{137}Cs, $^{210}Pb_{total}$, and LOI profiles are perturbed in the low

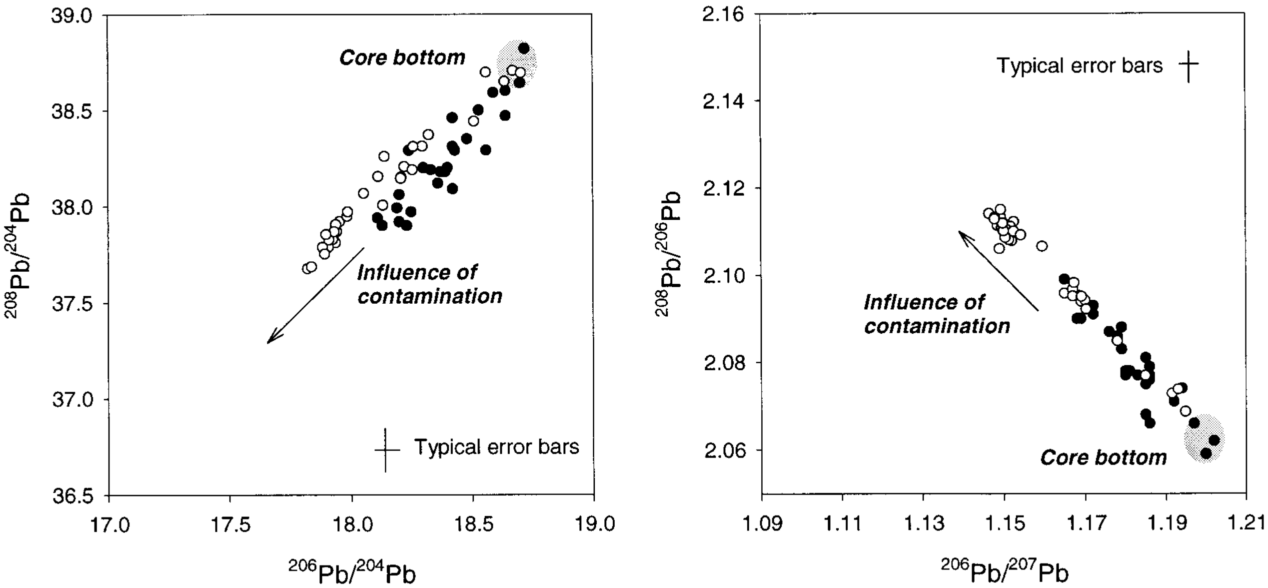

FIGURE 2. Pb isotopic compositions of leachates in the sediments coming from (○) BV core and (●) PC core.

porosity layers. Outside these horizons, the ^{214}Pb activities are fairly constant at about 45 mBq g^{-1}.

Leached Pb. In contrast to the BV site, the Pb content remains low and shows a two-step trend: (i) an increase from bottom to 2 g cm^{-2} (maximum 63 μg g^{-1}, about 5 times lower than at BV) and (ii) a decrease to the surface. The ^{206}Pb/^{207}Pb ratios decline more or less regularly from ~1.20 at the bottom, to a turning point at a mass depth of 2.3 g cm^{-2} (1.165), and then an increase to the surface (1.186).

Residual Pb. The Pb remaining in the residue is nearly constant along the core (Pb $= 4 \pm 1$ μg g^{-1}). These values are similar to the lowest observed in the same fraction at BV. The ^{206}Pb/^{207}Pb ratios are fairly stable, varying in a narrow range: 1.198−1.205. Only the sample at 2.3 g cm^{-2} is slightly different, with a ^{206}Pb/^{207}Pb ratio of 1.180. It also presents the highest Pb content, 7.4 μg g^{-1}.

Discussion

Core Dating. The atypical low porosity and ^{210}Pb, ^{137}Cs, and organic matter values in few horizons of the PC core can be explained by rapid deposition of sediments, probably related to sporadic events such as turbidity currents or floods. This may considerably complicate the establishment of a reliable chronology. However, the two ^{137}Cs peaks allow an absolute dating of both 1963/64 and 1986 horizons, which correspond respectively to worldwide maximum deposition of Cs from nuclear weapon tests in the atmosphere and the Chernobyl accident. ^{210}Pb chronology was obtained using the CRS model (constant rate supply), which assumes that the variations of the ^{210}Pb deposition are negligible over the last 100 years (*27*). This model is generally well-adapted to a context of variable sedimentation rate (*28*). ^{137}Cs and ^{210}Pb data provide a compatible (and likely reliable) chronology in the PC core.

At the BV site, the ^{137}Cs peaks of 1986 and 1963/64 are clearly identified, but the ^{137}Cs Chernobyl inventory appears abnormally high as compared to data from the PC core and other sites in Lake Geneva (*29*). An explanation could be a slump, occurring shortly after 1986, which brought ^{137}Cs-rich material, initially deposited elsewhere around the coring area. Moreover, the high Chernobyl ^{137}Cs inventory may also result from the focusing of the runoff from the Lausanne agglomeration collected in the waterwater treatment plant and rejected into the lake close to the sampling site. The CRS model becomes invalid, because the hypothesis of the constant ^{210}Pb$_{xs}$ supply no longer applies. Reported in a semilog diagram, the ^{210}Pb$_{xs}$ activity evolves linearly between 0 and 1.8 g cm^{-2}, and deeper than 5.2 g cm^{-2}. The CF:CS model (constant flux:constant rate) (*30, 31*) applied to these two sections gives sedimentation rates of 0.10 ± 0.01 g cm^{-2} a^{-1} ($r^2 = 0.99$) and 0.16 ± 0.02 g cm^{-2} a^{-1}. In this way, the ^{210}Pb$_{xs}$ and ^{137}Cs data provide a coherent time scale. In addition, the increase of VMS, which coincides with the introduction of $FeCl_2$ in the water treatment process in 1971 (*32*), gives an absolute indicator fitting well with the above dating.

Isotopic Signatures of the Potential Sources. The Pb added to Swiss gasoline today comes predominantly from Precambrian ore deposits of Australia and Canada (*18*). A mean ^{206}Pb/^{207}Pb ratio of 1.117 was measured in gasoline at Bern in 1995 (*33*), while ^{206}Pb/^{207}Pb variations between 1.101 and 1.124 were observed during 1996/97 in gasoline at Geneva (avg, 1.116) (*34*). To our knowledge, only one early measurement was done in Bern in the early 1970s (^{206}Pb/^{207}Pb $\approx$ 1.145) (*35*).

The emissions from waste incinerators contain lead with a representative average of man-made material (*3, 18, 36*). ^{206}Pb/^{207}Pb ratios of ~1.15 were measured in 1995 in the exhausts of an incinerator at Bern (*18*). To evaluate the local influence of the sewage treatment plant of Lausanne on the BV site, particles from its effluent were also measured (^{206}Pb/^{207}Pb, 1.146−1.149, $n = 3$). All these values are more radiogenic than modern gasoline-derived Pb, and they are quite similar to those reported for industrial sources in other countries (*3, 36, 37*).

Another source is the geogenic Pb. Theoretically, the analysis of residues should reflect the natural/local Pb source, because the anthropogenic (acid soluble) Pb should have been removed by preliminary HNO_3 leaching. Unfortunately, even if the isotopic compositions of the residues are systematically more radiogenic than in the associated leachates (that indicates a greater proportion of geogenic Pb), they depict large variations. This is particularly clear in the BV core, where the residual ^{206}Pb/^{207}Pb ratios vary between 1.157 and 1.197, while the Pb content concomitantly varies between 17.8 and 5.1 μg per gram of untreated bulk sediment. This strongly suggests that some residues may be still contaminated by a less radiogenic anthropogenic Pb, despite a second washing step. Nonetheless, the geogenic input can be assessed with the most radiogenic residues of the PC

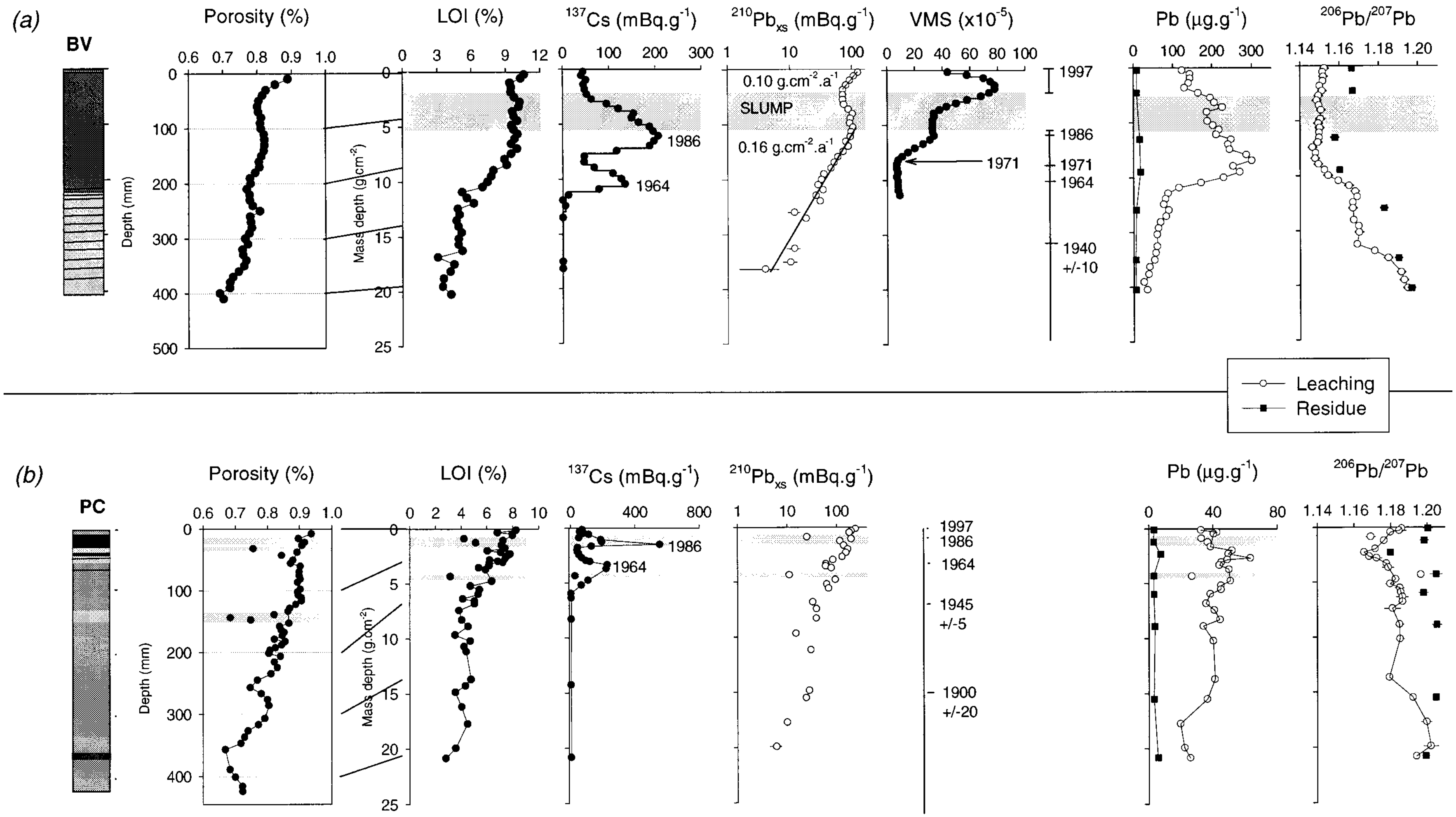

FIGURE 3. Profiles of porosity, LOI, ^{137}Cs, ^{210}Pb, SMV, Pb contents, and ^{206}Pb/^{207}Pb ratios in BV (a) and PC (b) cores.

TABLE 1. Core for Bay of Vidy (BV)

sample name/depth (cm)	mass depth[a]	^{214}Pb*	^{210}Pb$_{tot}$*	^{137}Cs*	Pb	^{206}Pb/^{204}Pb**	^{208}Pb/^{204}Pb	^{206}Pb/^{207}Pb	^{208}Pb/^{206}Pb
BV: 0-1	0.2		170 ± 5	44 ± 2	124	17.95 ± 0.04	37.92 ± 0.09	1.153 ± 0.002	2.112 ± 0.004
BV: 1-2	0.6	44 ± 6	152 ± 5	41 ± 1	144	17.98 ± 0.03	37.95 ± 0.07	1.152 ± 0.001	2.110 ± 0.003
BV: 1-2 R					8.2	18.32 ± 0.02	38.55 ± 0.08	1.167 ± 0.001	2.097 ± 0.003
BV: 2-3	1.0		137 ± 4	50 ± 3	144			1.152 ± 0.002	2.108 ± 0.004
BV: 3-4	1.4		125 ± 5	45 ± 2	141	17.99 ± 0.03	37.97 ± 0.03	1.152 ± 0.001	2.111 ± 0.002
BV: 4-5	1.8		116 ± 3	48 ± 2	130	17.93 ± 0.05	37.84 ± 0.03	1.150 ± 0.001	2.111 ± 0.003
BV: 5-6	2.3		116 ± 4	52 ± 2	165	17.94 ± 0.04	37.81 ± 0.08	1.151 ± 0.002	2.108 ± 0.005
BV: 5-6 R					8.1	18.34 ± 0.02	38.49 ± 0.08	1.167 ± 0.001	2.099 ± 0.003
BV: 6-7	2.7		116 ± 4	62 ± 2	196			1.150 ± 0.002	2.111 ± 0.004
BV: 7-8	3.2	49 ± 7	123 ± 3	96 ± 2	206	17.93 ± 0.05	37.86 ± 0.09	1.149 ± 0.002	2.111 ± 0.005
BV: 8-9	3.6		137 ± 4	120 ± 3	226	17.94 ± 0.04	37.87 ± 0.09	1.150 ± 0.001	2.111 ± 0.004
BV: 9-10	4.0		150 ± 4	153 ± 5	187	17.92 ± 0.05	37.83 ± 0.10	1.151 ± 0.002	2.110 ± 0.003
BV: 10-11	4.4		143 ± 3	150 ± 4					
BV: 11-12	4.8		141 ± 5	165 ± 5	189	18.05 ± 0.04	38.07 ± 0.10	1.151 ± 0.002	2.109 ± 0.003
BV: 12-13	5.2		152 ± 5	187 ± 3	202	17.94 ± 0.03	37.90 ± 0.06	1.149 ± 0.002	2.113 ± 0.003
BV: 13-14	5.7	50 ± 7	146 ± 4	196 ± 4	218	17.91 ± 0.03	37.79 ± 0.10	1.150 ± 0.002	2.110 ± 0.004
BV: 14-15	6.1	-	143 ± 4	207 ± 4	211	17.91 ± 0.04	37.82 ± 0.09	1.150 ± 0.001	2.112 ± 0.003
BV: 15-16	6.5	45 ± 6	128 ± 4	197 ± 4	248	17.93 ± 0.03	37.87 ± 0.05	1.150 ± 0.002	2.112 ± 0.003
BV: 15-16 R					15.5	18.21 ± 0.04	38.31 ± 0.10	1.158 ± 0.002	2.104 ± 0.004
BV: 16-17	7.0		135 ± 3	234 ± 5	241			1.149 ± 0.002	2.106 ± 0.005
BV: 17-18	7.4		121 ± 4	117 ± 2	244	17.82 ± 0.05	37.68 ± 0.10	1.147 ± 0.002	2.114 ± 0.004
BV: 18-19	7.9		108 ± 3	47 ± 2	286	17.88 ± 0.03	37.79 ± 0.07	1.148 ± 0.002	2.113 ± 0.003
BV: 19-20	8.4	51 ± 7	100 ± 3	47 ± 1	301	17.84 ± 0.06	37.69 ± 0.06	1.148 ± 0.002	2.113 ± 0.005
BV: 20-21	9.0		97 ± 4	68 ± 2	252	17.90 ± 0.03	37.85 ± 0.10	1.149 ± 0.002	2.115 ± 0.004
BV: 21-22	9.5		84 ± 2	109 ± 3	270	17.89 ± 0.05	37.75 ± 0.08	1.153 ± 0.001	2.110 ± 0.003
BV: 21-22 R					17.8	18.30 ± 0.03	38.47 ± 0.08	1.160 ± 0.001	2.105 ± 0.002
BV: 22-23	10.0		80 ± 2	127 ± 4	230	18.14 ± 0.04	38.26 ± 0.07	1.154 ± 0.002	2.109 ± 0.002
BV: 23-24	10.5		77 ± 2	135 ± 4	172	18.11 ± 0.03	38.15 ± 0.05	1.160 ± 0.001	2.107 ± 0.004
BV: 24-25	10.9	52 ± 7	83 ± 3	78 ± 2	115	18.13 ± 0.06	38.00 ± 0.14	1.165 ± 0.002	2.096 ± 0.004
BV: 25-26	11.4		75 ± 3	12 ± 1	87	18.21 ± 0.03	38.15 ± 0.07	1.168 ± 0.002	2.095 ± 0.002
BV: 26-27	11.9	-	79 ± 4		81	18.30 ± 0.04	38.31 ± 0.07	1.169 ± 0.001	2.094 ± 0.002
BV: 27-28	12.4			6 ± 3	77	18.22 ± 0.03	38.21 ± 0.09	1.167 ± 0.002	2.097 ± 0.005
BV: 28-29	13.0	55 ± 8	67 ± 3		90	18.21 ± 0.04	38.15 ± 0.08	1.167 ± 0.002	2.095 ± 0.002
BV: 28-29 R					6.7	18.68 ± 0.05	38.86 ± 0.10	1.183 ± 0.002	2.080 ± 0.004
BV: 29-30	13.5		73 ± 3		83				
BV: 30-31	14.0				69	18.26 ± 0.05	38.31 ± 0.09	1.167 ± 0.001	2.098 ± 0.002
BV: 31-32	14.6				63	18.32 ± 0.04	38.37 ± 0.07	1.170 ± 0.001	2.094 ± 0.003
BV: 32-33	15.2				60	18.25 ± 0.05	38.19 ± 0.10	1.170 ± 0.002	2.092 ± 0.003
BV: 34-35	16.3		67 ± 3		60			1.169 ± 0.001	2.095 ± 0.004
BV: 35-36	16.9				56	18.56 ± 0.03	38.70 ± 0.07	1.178 ± 0.001	2.085 ± 0.003
BV: 36-37	17.5		66 ± 3		53	18.51 ± 0.04	38.44 ± 0.07	1.185 ± 0.002	2.077 ± 0.002
BV: 36-37 R					5.1	18.78 ± 0.04	38.93 ± 0.08	1.190 ± 0.002	2.072 ± 0.003
BV: 37-38	18.2	56 ± 8	59 ± 3		40				
BV: 38-39	18.8				38	18.67 ± 0.06	38.70 ± 0.09	1.192 ± 0.002	2.073 ± 0.004
BV: 39-40	19.5				26	18.64 ± 0.04	38.65 ± 0.08	1.193 ± 0.002	2.074 ± 0.004
BV: 40-41	20.2				34	18.70 ± 0.03	38.69 ± 0.08	1.195 ± 0.002	2.069 ± 0.002
BV: 40-41 R					5.4	18.98 ± 0.06	39.23 ± 0.10	1.197 ± 0.002	2.067 ± 0.004

[a] Mass depth expressed in g cm^{-2}, radiochemical data (^{137}Cs and ^{210}Pb and ^{214}Pb) in mBq g^{-1}, Pb Contents in μg g^{-1} (error ~ 10%) Pb isotopic compositions are of leachates, except for Residues (R). Errors: *66% at confidence level and **95% confidence level.

core: ^{206}Pb/^{207}Pb $\sim 1.203 \pm 0.002$, assumed free of human contribution, because of their very low Pb contents (3.1−3.8 μg g^{-1}). This signature is in good agreement with the literature values characterizing the background Pb in central and western Europe (*10*, *20*, *21*, *38*, *39*).

The leachate fraction should mostly contain Pb desorbed from oxyhydroxide surfaces but also integrate Pb primarly hosted by carbonates, organic matter, or simply adsorbed to the particle surface (*40*, *41*).

Even in the deepest horizons, the leachates are slightly less radiogenic than their associated residues, suggesting a contribution of a low radiogenic anthropogenic source. That is in agreement with what was previously observed in an ombrothrophic bog in the Jura (*20, 21*) and in the Thau basin (*41*).

The isotopic signature of the anthropogenic Pb added to the sediment can be obtained by subtracting the natural (background) leachable component from the total leached Pb. The mathematical formulation is the same that was reported elsewhere (*9*):

$$^{206}\text{Pb}/^{207}\text{Pb anthropogenic Pb component} = [(^{206}\text{Pb}/^{207}\text{Pb TL})(\text{ppm Pb TL}) - (^{206}\text{Pb}/^{207}\text{Pb BC})(\text{ppm Pb BC})]/(\text{ppm Pb TL} - \text{ppm Pb BC}) \quad (1)$$

where TL = total leach and BC = background leachable component.

The amount of leachable natural Pb was assumed to be about 23 ± 3 μg g^{-1}. This value was obtained by averaging the concentrations in leaches of the three deepest and the least polluted horizons of the PC core.

Although 95% of anthropogenic Pb are removed by leaching, up to 5% may remain in the residue which results in a considerable change in Pb isotopic compositions. However, the procedure of leaching proposed here appears highly convenient for rapid and reliable assessment of the anthropogenic component. In addition, it presents the advantage of being fairly reproducible (better than 10%) and

TABLE 2. Core for Central Part of the Lake (PC)

sample name/depth (cm)	mass depth[a]	^{214}Pb*	^{210}Pb$_{tot}$*	^{137}Cs*	Pb	^{206}Pb/^{204}Pb**	^{208}Pb/^{204}Pb	^{206}Pb/^{207}Pb	^{208}Pb/^{206}Pb
PC:0-1	0.1		283 ± 13	72 ± 3	32.6	18.59 ± 0.04	38.59 ± 0.09	1.186 ± 0.001	2.076 ± 0.002
PC:0-1 R					3.2			1.200 ± 0.003	2.059 ± 0.005
PC:1-2	0.3		242 ± 8	57 ± 5	42.6	18.42 ± 0.06	38.09 ± 0.10	1.185 ± 0.004	2.068 ± 0.008
PC:2-2.5	0.5		226 ± 6	82 ± 3	40.5	18.23 ± 0.05	37.90 ± 0.14	1.180 ± 0.001	2.077 ± 0.006
PC:2.5-3	0.6			114 ± 2					
PC:3-3.5	0.9	28 ± 4		52 ± 5	32.8	18.19 ± 0.03	37.99 ± 0.14	1.169 ± 0.003	2.090 ± 0.008
PC:3.5-4	1.0		241 ± 6	188 ± 5					
PC:4-4.5	1.2		162 ± 7	194 ± 14	36.7	18.42 ± 0.03	38.46 ± 0.08	1.176 ± 0.001	2.087 ± 0.004
PC:4-4.5 R					3.1			1.198 ± 0.002	2.062 ± 0.003
PC:4.5-5	1.5			553 ± 5					
PC:5-5.5	1.6		184 ± 6	130 ± 2	38.6				
PC:5.5-6	1.8			44 ± 2					
PC:6-7	2.0		212 ± 6	40 ± 5	51.9	18.20 ± 0.02	38.06 ± 0.12	1.172 ± 0.002	2.091 ± 0.005
PC:7-7.5	2.1	52 ± 6		42 ± 2					
PC:7.5-8.5	2.3		198 ± 5	50 ± 3	49.5	18.24 ± 0.03	38.29 ± 0.07	1.165 ± 0.001	2.099 ± 0.002
PC:7.5-8.5 R					7.4			1.180 ± 0.002	2.078± 0.003
PC:8.5-9	2.4			52 ± 3					
PC:9-10	2.7		174 ± 5	69 ± 3	63.3	18.13 ± 0.07	37.90 ± 0.16	1.168 ± 0.001	2.090 ± 0.004
PC:10-10.5	2.8				49.0	18.11 ± 0.06	37.94 ± 0.17	1.172 ± 0.003	2.093 ± 0.009
PC:10.5-11	3.0		129 ± 4	95 ± 3					
PC:11-11.5	3.0			120 ± 3	45.2				
PC:12-12.5	3.3		106 ± 4	228 ± 10	44.0	18.33 ± 0.05	38.19 ± 0.15	1.178 ± 0.002	2.086 ± 0.006
PC:12.5-13	3.5		105 ± 3						
PC:13-13.5	3.7	62 ± 8	123 ± 3	222 ± 9	49.8	18.20 ± 0.07	37.92 ± 0.07	1.179 ± 0.003	2.083 ± 0.006
PC:14-14.5	4.3		56 ± 2	27 ± 1	26.9	18.70 ± 0.02	38.64 ± 0.07	1.197 ± 0.001	2.066 ± 0.002
PC:14-14.5 R					3.0			1.205 ± 0.003	2.051 ± 0.006
PC:15-15.5	4.7		139 ± 4	109 ± 2	50.8	18.25 ± 0.06	37.97 ± 0.11	1.183 ± 0.002	2.077 ± 0.007
PC:16-16.5	5.2		108 ± 3	67 ± 2	45.0	18.36 ± 0.07	38.12 ± 0.08	1.180 ± 0.002	2.078 ± 0.008
PC:17-17.5	5.5		114 ± 4		45.0	18.39 ± 0.07	38.18 ± 0.13	1.185 ± 0.002	2.077 ± 0.005
PC:18-18.5	6.0			3 ± 0.8	38.4	18.53 ± 0.02	38.50 ± 0.09	1.186 ± 0.001	2.077 ± 0.003
PC:18-18.5 R					3.2			1.198 ± 0.003	2.065 ± 0.006
PC:19-19.5	6.4	41 ± 5		4 ± 2		18.40 ± 0.04	38.20 ± 0.09	1.186 ± 0.003	2.066 ± 0.006
PC:20-20.5	6.8		78 ± 3		35.7	18.43 ± 0.06	38.29 ± 0.16	1.186 ± 0.002	2.079 ± 0.006
PC:21-22	7.4		84 ± 3		40.9	18.37 ± 0.05	38.18 ± 0.15	1.181 ± 0.004	2.078 ± 0.006
PC:23-24	8.3	45 ± 5	84 ± 3	5 ± 1	44.3				
PC:24-25	8.9				34.0	18.48 ± 0.04	38.35 ± 0.11	1.185 ± 0.002	2.075 ± 0.008
PC:24-25 R					3.8			1.205 ± 0.003	2.052 ± 0.005
PC:25-26	9.6		60 ± 2						
PC:26-27	10.2				40.2	18.42 ± 0.05	38.31 ± 0.12	1.185 ± 0.002	2.081 ± 0.004
PC:28-29	11.2		75 ± 3						
PC:29-30	13.7				41.2	18.30 ± 0.05	38.20 ± 0.05	1.179 ± 0.002	2.088 ± 0.005
PC:30-31	14.3	50 ± 6		1.5 ± 0.3					
PC:31-32	14.8		73 ± 2						
PC:32-33	15.5		69 ± 2		36.5	18.64 ± 0.04	38.60 ± 0.09	1.192 ± 0.001	2.071 ± 0.002
PC:32-33 R					3.2			1.205 ± 0.001	2.052 ± 0.003
PC:35-36	17.7		55 ± 2		19.6	18.56 ± 0.04	38.29 ± 0.07	1.200 ± 0.003	2.059 ± 0.004
PC:38-39	19.9		51 ± 2		22.1	18.64 ± 0.03	38.47 ± 0.10	1.202 ± 0.004	2.062 ± 0.003
PC:39-40	20.8	40 ± 5		4 ± 0.7	25.7	18.72 ± 0.03	38.82 ± 0.06	1.194 ± 0.001	2.074 ± 0.003

[a] Mass depth expressed in g cm^{-2}, radiochemical data (^{137}Cs, ^{210}Pb, and ^{214}Pb) in mBq g^{-1}. Pb contents in μg g^{-1} (error ~10%). Pb isotopic compositions of leachates, except for residues (R) Errors: *at 66% confidence level and **at 95% confidence level.

to be in a medium (HNO_3) that allows the direct measurement of concentrations by ICP-MS.

Fluxes and Origin of Pb. The anthropogenic flux of Pb, *F(t)*, can be assessed as follows:

$$F(t) = (\text{ppm Pb TL} - \text{ppm Pb BC})R(t) \qquad (2)$$

where $R(t)$ is the sedimentation rate. For both sites, a peak of contamination occurred in the late 1970s (Figure 4). Afterward, the anthropogenic inputs declined likely under the implementation of environmental policies. However, at the Bay of Vidy, the Pb fluxes were at least 1 order of magnitude higher than at the center of the lake. A sharp increase is recorded when the water treatment plant of Lausanne started in 1964, because of the proximity of the sampling site to the input source. The amount of Pb (and other metals, Pardos, Personal Communication) buried at that bay is considerable and may constitute a potential hazard for biota in the bay.

The isotopic compositions of the anthropogenic component generally follow the same evolution at both sites. Obviously, as already noticed by Graney et al. (*9*), the anthropogenic Pb signature is less well resolved in the PC core than in BV, because of the higher contribution of the lithogenic end-member. The discrimination of both industrial and gasoline components in both cores is however complicated by the lack of details concerning the evolution of the isotopic compositions of the anthropogenic sources through the past. As previously mentioned, the ^{206}Pb/^{207}Pb signatures of the gasoline component have varied widely, at least between 1.145 in the early 1970s (*35*) and 1.10−1.12 at the present (*34*). In addition only recent data are available for the industrial sources. Nonetheless, by analogy with the neighboring countries, where the primary sources, of Pb have changed only little over the last 15−20 years (*3, 42*), we can reasonably assume that the Swiss leaded gasoline and industrial-derived Pb have remained steady since the early

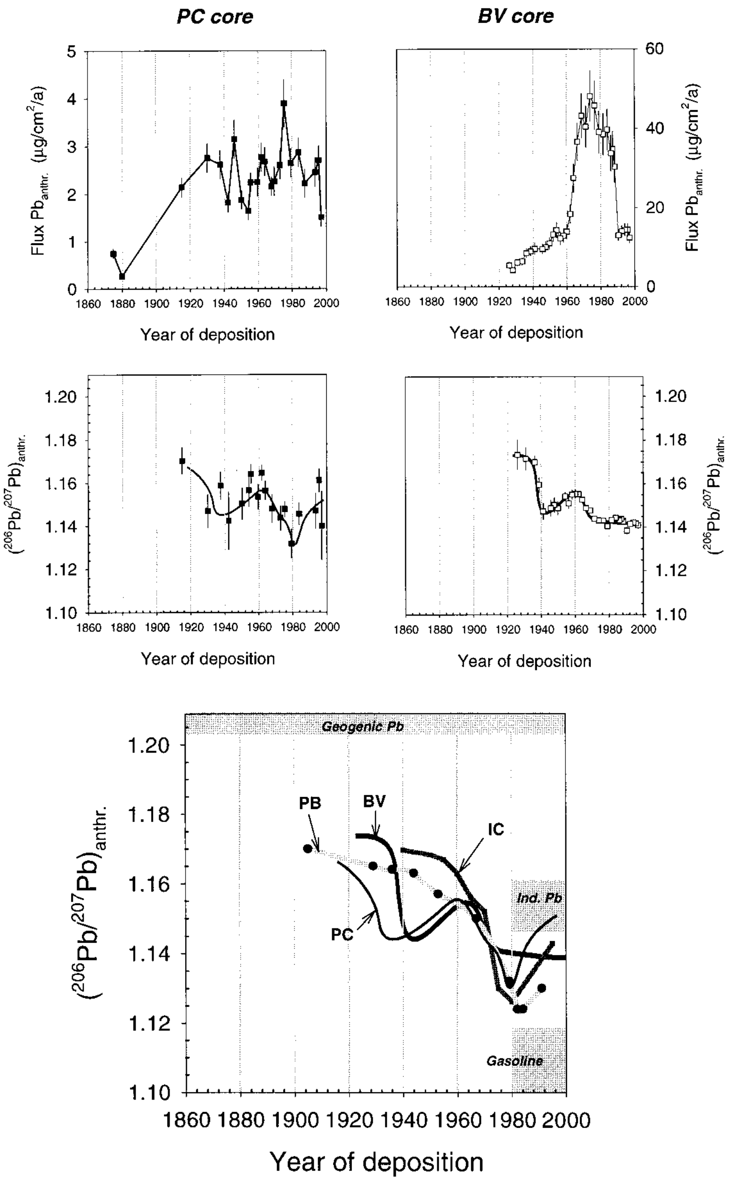

FIGURE 4. Fluxes of Pb, expressed in μg cm^{-2} a^{-1}, and $^{206}Pb/^{207}Pb$ ratios of the anthropogenic sources through the last century, at (■) PC site and (□) BV site. For comparative purpose, Pb isotopes recorded in an ice core at an high alpine site (IC) (*19*) and in a peat bog in the Jura Mountains (PB) (*20, 21*) are also reported.

1980s with $^{206}Pb/^{207}Pb$ ratios at 1.11 ± 0.01 and 1.15 ± 0.01, respectively. With such an assumption, it becomes possible to roughly assess the origin of Pb, at least over the last 20 years. At the Bay of Vidy, the Pb isotopes demonstrated a large predominance of industrial/domestic–derived Pb, with maybe a small contribution from leaded gasoline which did not exceed 10%. As a consequence, most of the Pb originated from wastewater inputs. The storm runoff, which mainly removes car-derived aerosols from roads and streets, has never played an important role. The center of the lake received industrial/domestic Pb as well, except in the early 1980s, where the relative contribution from gasoline seemed to be a little bit more important.

In the 1920s, the isotopic composition of the anthropogenic end-member was more radiogenic ($^{206}Pb/^{207}Pb \sim 1.17$). This corresponded to a mix of industrial emissions and coal burning. It should be remembered that, at those times, industrial Pb mainly came from the major European Pb ore deposits characterized by $^{206}Pb/^{207}Pb$ ratios of about 1.16–1.18 (*43, 44*). A drop in $^{206}Pb/^{207}Pb$ ratios occurred later in the 1930s through the 1940s. Such a change has already been noted approximately at the same period in the UK and was explained as an increased use of imported ores and coal with lower isotope ratios, or possibly as the reduced use of relatively radiogenic coal (*17, 45*). Historical knowledge well supports such an explanation. Indeed in Switzerland, coal imports averaged 230 000 t/a during 1850–1870; that values increased to 2.7 Mt/a from 1900 to 1920, and from 1930, with the introduction of heating oil, came the gradual replacement of coal (*46*).

All these data can be compared to a few isotopic studies previously undertaken in Switzerland. Similar isotopic trends were observed in an ice core sampled in a high alpine site (*19*) and a peat bog in the Jura Mountains (*20, 21*), with however more pronounced variations (Figure 4). In the early 1980s, the relative contribution of gasoline-derived Pb was more important in ices and peat bog than at the PC site. Actually, this discrepancy can be easily explained by the fact that ice integrates only the atmospheric deposition (mainly coming from automotive and industrial exhausts), while lake sediments record both atmospheric and fluvial inputs (including domestic and industrial effluents as well). One can imagine that the Rhône river, which drains numerous industrial effluents, was one of the major sources of pollution in Lake Geneva, at least in the zones far from the direct human contributions such as Bay of Vidy. That could explain also why a major influence of leaded gasoline was observed in Lake Zug (close to Zurich) (*10*) and not in Lake Geneva.

This study also proves that the Pb isotopic method, combined with dilute acid leaching, is efficient for identifying the anthropogenic component in relatively contaminated sediments. However its power of discrimination is limited by the establishment of a reliable and complete database describing the isotopic evolution of the main anthropogenic sources through the past. This lack of data was recognized by several authors (*3, 17, 39*), and efforts should be undertaken to rectify this situation.

Acknowledgments

We wish to express special thanks to J. Piccard and his crew, S. Girardclos, and A. Hoffman for their help during sampling. M. Martin and the Forel's ICP-MS team, B. Thomas, P.-Y. Favarger, and C. Guéguen, are greatly thanked for their technical assistance. R. L. Thomas, M. Kanth and two anonymous reviewers are thanked for their reviewing. This work was in part supported by the Swiss National Research Fund no. 21-43508-95, and the Fondation pour l'étude et la protection du patrimoine lacustre.

Literature Cited

(1) Nriagu, J. O. *Nature*, **1989**, *338*, 47.
(2) Luftbelastung 1993 (Messresultate des Nationalen Beobachtungsnetzes für Luftfremdstoffe NABEL); Schrifenreihe Umwelt No. 230; Bundesamt für Umwelt, Wald und Landschaft BUWAL.; Bern, 1994; pp 68−72.
(3) Monna, F.; Lancelot, J. R.; Croudace, I. W.; Cundy, A.; Lewis, J. T. *Environ. Sci. Technol.* **1997**, *31* (8), 2777.
(4) Petit, D. *Earth Planet Sci. Lett.* **1974**, *23*, 199.
(5) Shirahata, H.; Elias, R. W.; Patterson, C. C.; Koide, M. *Geochim. Cosmochim. Acta* **1980**, *44*, 149.
(6) Petit, D.; Mennessier, J. P.; Lamberts, L. *Atmosph. Environ.* **1984**, *6*, 1189.
(7) Keinonen, M. *Sci. Tot. Environ.* **1992**, *113*, 251.
(8) Ritson, P. I.; Esser, B. K.; Niemeyer, S.; Flegal, R. *Geochim. Cosmochim. Acta* **1994**, *58* (15), 3297.
(9) Graney, J. R.; Halliday, A. N.; Keeler, G. J.; Nriagu, J. O.; Robbins, J. A.; Norton, S. A. *Geochim. Cosmochim. Acta* **1995**, *59* (9), 1715.
(10) Moor, H. C.; Schaller, T.; Sturm, M. *Environ. Sci. Technol.* **1996**, *30* (10), 2928.
(11) Hamilton, E. I.; Clifton, R. J. *Estuarine Coastal Mar. Sci.* **1979**, *8*, 271.
(12) Hirao, Y.; Mabuchi, H.; Fukuda, E.; Tanaka, H.; Imamura, T.; Todoroki, H.; Kimura, K.; Matsumoto, E. *Geochem. J.* **1986**, *20*, 1.
(13) Hamelin, B.; Grousset, F.; Sholkovitz, E. R. *Geochim. Cosmochim. Acta* **1990**, 54, 37.
(14) Ohlander, B.; Ingri, J.; Ponter, C. *Applied Geochem.* **1993**, *Suppl. Issue No. 2*, 67.
(15) Croudace, I. W.; Cundy, A. B. *Environ. Sci. Technol.* **1995**, *29*, 1288.
(16) Kersten, M.; Grabe-Schönberg, C.-D.; Thomsen, S.; Anagnostou, C.; Sioulas, A. *Environ. Sci. Technol.* **1997**, *31* (5), 1295.
(17) Bacon, J. R.; Jones, K. C.; McGrath, S. P.; Johnson, A. E. *Environ. Sci. Technol.* **1996**, *30* (8), 2511.
(18) Döring, T.; Schwikowski, M.; Gäggeler, H. W. *Fresenius J. Anal. Chem.* **1997**, *359*, 382.
(19) Döring, T.; Gäggeler, W.; Schotterer, U.; Schwitkowski, M. **1998**. Identification and quantification of the main sources of lead in the historical european atmosphere by lead isotope ratio measurements with ICP-MS. Annual report. PSI.
(20) Shotyk, W.; Cheburkin, A. K.; Appleby, P. G.; Fankhauser, A.; Kramers, J. D. *Earth Planet. Sci. Lett.* **1996**, 145, E1.
(21) Shotyk, W.; Weiss, D.; Appleby, P. G.; Cheburkin, A. K.; Frei, R.; Gloor, M.; Kramers, J. D.; Reese, S.; Van der Knaap, W. O. *Science* **1998**, *281*, 1635.
(22) Dominik, J.; Loizeau, J.-L.; Span, D. *Climate Dyn.* **1992**, *6*, 145.
(23) Sugai, S. F.; Alperin, M. J.; Reeburgh, W. S. *Mar. Chem.* **1994**, *116*, 351.
(24) Ng, A.; Patterson, C. C. *Geochim. Cosmochim. Acta* **1982**, *46*, 2307.
(25) Monna, F.; Ben Othman, D.; Luck, J.-M. *Sci. Tot. Environ.* **1995**, *166*, 19.
(26) Monna, F.; Loizeau, J.-L.; Thomas, B.; Guéguen, C.; Favarger, P.-Y. *Spectrochim. Acta B* **1998**, *53*, 1317.
(27) Appleby, PG.; Oldfield, F. *Catena* **1978**, *5*, 1.
(28) Dominik, J.; Mangini, A.; Müller, G. *Sedimentol.* **1981**, *28*, 653.
(29) Dominik, J. In *Unmweltradioktivität und Strahlendosen in der Schweiz*. Bundesamt für Gesundheitswesen; 1993; pp B3.11.1-B3.11.17.
(30) Goldberg, ED. In *Radioactive dating*; IAEA: Vienna, 1963; p 121.
(31) Krishnaswamy, S.; Lal, D.; Martin, J.-M.; Merbeck, M. *Earth Planet. Sci. Lett.* **1971**, *11*, 407.
(32) Pardos, M.; Benninghoff, C.; Monna, F.; Wildi, W. Submitted to *Environ. Poll.*
(33) Altofer, T. Diploma Thesis, Universität Bern, 1996.
(34) Chiaradia, M.; Cupelin, F. Submitted to *Atmosph. Environ*.
(35) Chow, T. J.; Earl, J. L. *Science* **1973**, *176*, 510.
(36) Mukai, H.; Furuta, N.; Fujii, T.; Ambe, Y.; Sakamoto, K.; Hashimoto, Y. *Environ. Sci. Technol.* **1993**, *27* (7), 1347.
(37) Hamester, M.; Stechmann, H.; Steiger, M.; Dannecker, M. *Sci. Tot. Environ.* **1994**, *146/147*,
(38) Kersten, M.; Försten, U.; Krause, P.; Kriews, M.; Dannecker, W. In *Impact of heavy metals on the environment*; Vernet, J.-P., Ed.; Elsevier: Amsterdam, 1992; pp 311−325.
(39) Grousset, F. E.; Quétel, C. R.; Thomas, B.; Buat-Ménard, P.; Donard, O. X.; Buchet, A. *Environ. Sci. Technol.* **1994**, *28*, 1605.
(40) Erel, Y.; Patterson, C. C.; Scott, M. J.; Morgan, J. M. *Chem. Geol.* **1990**, *85*, 383.
(41) Monna, F.; Clauer, N.; Toulkeridis, T.; and Lancelot, J. Submitted to *Appl. Geochem*.
(42) Elbaz-Poulichet, F.; Hollinger, P.; Martin, J. M.; Petit D. *Sci. Tot. Environ.* **1986**, *54*, 61.
(43) Le Guen, M.; Orgeval, J.-J. Lancelot, J. *Miner. Depos.* **1991**, *26*, 180.
(44) Lévêque, J.; Haak, U. *Monogr. Ser. Miner. Depos.* **1993**, *30*, 197.
(45) Sugden, C. L.; Farmer, J. G.; MacKenzie, A. B. *Environ. Geochem. Health* **1993**, *15*, 59.
(46) Müller, K. Die Beilerseesedimente 1878−1978. Ph.D. Thesis, Ins. Inorganic Chemistry, University Berne, 1982.

Received for review March 3, 1999. Revised manuscript received May 24, 1999. Accepted June 3, 1999.

ES9902468

Environ. Sci. Technol. **1999**, *33,* 2517−2523

Pb Isotope Composition in Lichens and Aerosols from Eastern Sicily: Insights into the Regional Impact of Volcanoes on the Environment

FABRICE MONNA,*,†
ALESSANDRO AIUPPA,‡
DANIELA VARRICA,‡ AND
GAETANO DONGARRA‡,§

Institut FA Forel, 10 route de Suisse, CH-1290, Switzerland, Dipartimento C.F.T.A., Via Archirafi 36, 90123 Palermo, Italy, and Istituto Geochimica dei Fluidi del CNR, Via U. La Malfa 153, 90135 Palermo, Italy

A total of 25 lichen thalli of *Parmelia conspersa* (Ehrh), collected at Vulcano island and at Mt. Etna, during a one-year biogeochemical survey, were analyzed for Pb, Br, Al, Sc, $^{206}Pb/^{207}Pb$, and $^{208}Pb/^{206}Pb$ ratios. Lead isotope ratios were also measured on aerosols samples from urban areas and industrial sites of Sicily. The observed $^{206}Pb/^{207}Pb$ range for urban and industrial aerosols (1.103−1.174) closely matches the anthropogenic signature (1.080−1.165). Lichens ($^{206}Pb/^{207}Pb = 1.156-1.226$), instead, are closer to the compositional field of ^{206}Pb rich geogenic sources. This natural input is more evident at Vulcano island than at Mt. Etna, where the anthropogenic activities are considerably more effective. On the basis of lead isotope data, Pb/Br ratios and calculated lead enrichment factors, a "natural" lead pollution from volcanoes is suggested. Volcanic lead contribution ranges from 10 to 30% at Mt. Etna to 10−80% at Vulcano island.

Introduction

Dongarrà and Varrica (*1*) and Varrica et al. (*2*) recently reported data on trace metal contents in lichen samples collected around Mt. Etna and on the island of Vulcano, two of the most active volcanic areas in Italy. The aim of their studies was to evaluate the effect of volcanic activity on the environmental dispersion of trace metals. One of their underlying working hypotheses was the following: if the amount of lead introduced into the atmosphere by volcanoes may be considered as a small fraction of the global lead budget, it may become considerably more important in the surroundings of volcanic areas, where lead and other trace metals are constantly released by volcanic plumes and high-temperature fumarole gases. The above authors demonstrated that even passive volcanic degassing tends to increase the background levels of some metals in air. This means that, in towns and cities near volcanic areas, natural emissions are added to those due to anthropogenic activities and may enhance the risk level for populations living nearby. In particular, they observed high enrichment factors for Pb, Br, and Sb which could not be attributed exclusively or prevalently to automotive fuel combustion but were partly the result of volcanic exhalations.

From a different point of view, the intense lead release due to human activities during the last two centuries has led scientists to investigate possible perturbations induced by anthropogenic emissions on atmospheric geochemical cycling. Industrial lead has been introduced in the atmosphere from several sources (mainly fossil fuel combustion and smelting), so that such an industrial lead flux has largely altered natural concentrations in oceans (*3*, *4*), lakes (*5*), and recent snow layers in Antarctica and Greenland (*6*, *7*). On a global scale, anthropogenic lead has been estimated at 95% of the total budget (*8, 9*). Currently, the restricted use of lead additives in gasoline and the introduction of catalytic converters requiring unleaded gasoline have led to a worldwide decrease in Pb emissions (*10*).

The purpose of the present work was to investigate and possibly to apportion volcanic and anthropogenic additions to air and soils of Eastern Sicily by means of the Pb isotope compositions in lichens.

Lead isotopes have been widely used within the environmental sciences as tracers of pollution sources (see the Clair C. Patterson Special Issue, *Geochim. Cosmochim. Acta* **1994**, *58*). Lead introduced in the environment by human activities has the isotope composition of the ore body from which it was extracted. Each lead ore deposit is characterized by its own isotope composition which depends on initial Pb isotope compositions, U/Pb−Th/Pb ratios, and age (actually, the time elapsed since the lead separated from its source rock) (*11*). At least in Western Europe, soil-derived Pb has an isotope signature which is distinct from that of industrial lead(s), so that, once the isotope compositions of the various potential sources are known, mixing processes may be quantified. Another clue can be given by the Pb/Br ratios. As a matter of fact Harrison and Sturges (*12*) have shown that the Pb/Br ratio can be used as a marker of anthropogenic emissions. The rationale of this fingerprint is based on the fact that leaded gasoline contains brominated compounds added to reduce the formation of lead oxides inside the automotive engines. According to gasoline composition, the Pb/Br mass ratio in fresh automotive produced leaded particles should be around 2.5 (*12*). While many data have been published on lead content and isotope compositions of airborne particles collected in urban and rural sites (*13, 14*), only a few papers deal with stable lead isotope ratios in lichens (*15, 16*). Lichens have been widely used in environmental science as they act as bioaccumulators of pollutants (*1, 17*−*21*). Lichens are an extraordinary symbiotic association of fungi and algae with peculiar physiology and morphology (thallous structure; absence of cuticle and stomata) which forces them to absorb and accumulate chemical elements in gaseous, liquid, or particulate form from the atmosphere. Owing to the absence of excretion mechanisms in lichens, the xenobiotic substances cannot be expelled and accumulate over the years. Therefore, data from lichens may provide integrated measurements over a long period of time (10−20 years) and thus furnish important insights on lead contributions to the atmosphere from varying sources over past decades.

Study Area

Volcanism in eastern Sicily results from collision between the African plate and the European continental block (*22*). Mt. Etna and Vulcano are two of the most active volcanoes in the area (Figure 1).

---

* Corresponding author phone: +41 22 950 92 12; fax: +41 22 755 13 82; e-mail: monna@sc2a.unige.ch.
† Institut FA Forel.
‡ Dipartimento C.F.T.A.
§ Istituto Geochimica dei Fluidi del CNR.

10.1021/es9812251 CCC: $18.00

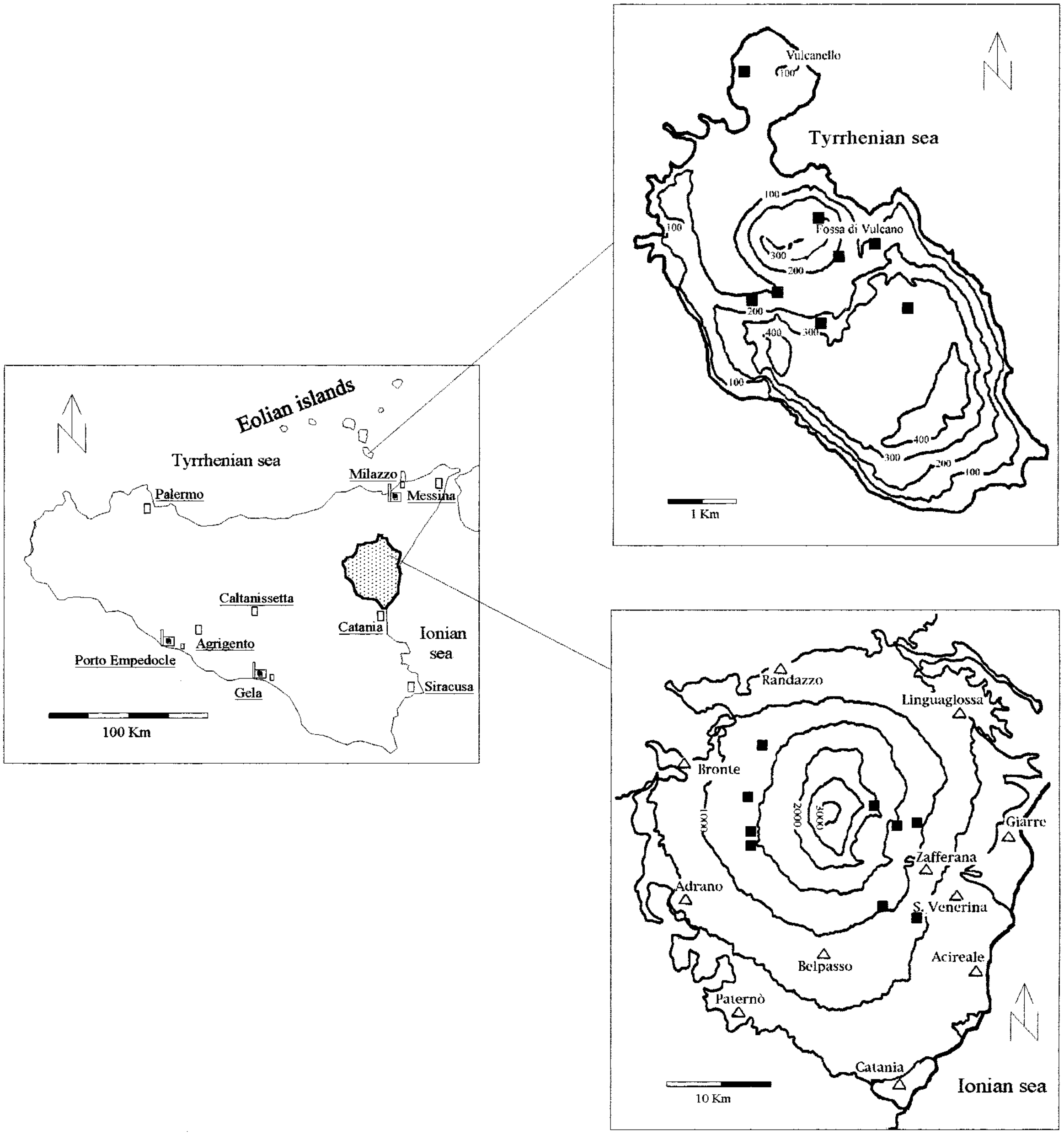

FIGURE 1. Map of Sicily and sampling location.

Mt. Etna formed 500 000−700 000 years ago and is in a persistent effusive-degassing state of activity. The volcano has a complex structure (a basic "old" shield volcano overlaid by a "recent" strato-volcano) which formed during successive phases of accretion (*23*). Volcanic products range in composition from alkali basalts to hawaiites. After the last eruption (1991−1993), the volcano is now in a state of continuous degassing from central craters.

The island of Vulcano belongs to the Aeolian volcanic arc. Volcanic activity started around 120 000 years ago (*24*), but recent eruptions (younger than 15 000 years) started from the pyroclastic and lava cone of La Fossa, where present-day hydrothermal activity is concentrated. The island is entirely made up of volcanic rocks.

The climate in eastern Sicily is ascribed to the typical "Mediterranen Regime", characterized by a dry hot summer season (with minimum precipitation during July−August) and a rainy cold season (October−February). In the Mt. Etna area, the prevailing westerly winds drive the volcanic plume over the eastern slope of the edifice, where it is funneled into a fan-shaped volcanogenic-gravitational depression called Valle del Bove. At Vulcano Island, winds blow mainly from the northern sectors.

Sampling and Analytical Techniques

A total of 25 thalli of *Parmelia conspersa* (Ehrh), a foliose species of lichen, collected on Vulcano and Mt. Etna during a one-year biogeochemical survey, were analyzed for their $^{206}Pb/^{207}Pb$ and $^{208}Pb/^{206}Pb$ isotope ratios and Pb, Br, Al, and Sc contents. Samples were all collected from a rocky substrate (cf. Figure 1). No lichen samples were found on Mt. Etna at an altitude higher than 1800 m above sea level or on the Vulcano crater. Each sample was dried at 40 °C, carefully separated from substrate particles with a toothbrush and toothpicks under a low-magnification stereomicroscope, and then finely powdered. For further insight into the source of lead, aerosol samples from five Sicilian cities (Messina, Palermo, Catania, Siracusa, and Caltanissetta) and three industrial areas (Gela, Milazzo, and Porto Empedocle) were collected using a Tecora Bravo H2 sampler (Figure 1), working at a fixed flow-rate of 25 L/mn over 24 h. Sartorius cellulose-nitrate membrane filters (porosity 0.8 μm; diameter 47 mm)

TABLE 1. Pb Isotopic Compositions and Pb, Br, and Sc Contents in Lichens Sampled at Mt. Etna and Vulcano Island[a]

sample	^{206}Pb/^{207}Pb	^{208}Pb/^{206}Pb	Br (μg·g^{-1})	Sc (μg·g^{-1})	Pb (μg·g^{-1})	Pb/Br	EF$_{Pb}$
			Etna Lichens				
71 EP	1.175 ± 0.002	2.088 ± 0.002	23	1.4	17	0.74	23
72 EP	1.178 ± 0.003	2.074 ± 0.006	22	2.7	22	1.00	16
74 EP	1.178 ± 0.002	2.085 ± 0.006	21	1.9	14	0.67	14
76 EP	1.171 ± 0.004	2.090 ± 0.008	24	2	32	1.33	31
81 EP	1.168 ± 0.002	2.095 ± 0.006	22	1	44	2.00	85
81 EP dupl	1.168 ± 0.002	2.094 ± 0.004					
87 EP	1.167 ± 0.003	2.093 ± 0.003	22	1.4	47	2.14	65
90 EP	1.170 ± 0.002	2.093 ± 0.005	36	2.1	48	1.33	44
96 EP	1.178 ± 0.002	2.084 ± 0.005	20	1.9	5	0.25	5
97 EP	1.180 ± 0.002	2.080 ± 0.005	21	1.4	23	1.10	32
99 EP	1.161 ± 0.002	2.104 ± 0.001	19	1.8	26	1.37	28
100 EP	1.156 ± 0.005	2.105 ± 0.006	26	1.2	22	0.85	35
			Vulcano Lichens				
5 VUP	1.182 ± 0.004	2.073 ± 0.003	25	1.9	5	0.20	3
10 VUP	1.204 ± 0.003	2.045 ± 0.004	25	1.5	30	1.2	21
13 VUP	1.226 ± 0.002	2.034 ± 0.002	27	1.4	11	0.41	8
16 VUP	1.181 ± 0.002	2.078 ± 0.001	55	1.3	26	0.47	21
17 VUP	1.193 ± 0.004	2.067 ± 0.007	38	3	29	0.76	10
22 VUP	1.167 ± 0.002	2.094 ± 0.004	15	1.1	18	1.2	17
23 VUP	1.208 ± 0.002	2.060 ± 0.005	36	1.2	40	1.1	34
25 VUP	1.177 ± 0.001	2.085 ± 0.001	41	2.2	42	1.0	20
25 VUP dupl.	1.176 ± 0.001	2.081 ± 0.004					
38 VUP	1.184 ± 0.003	2.077 ± 0.005	31	2.7	26	0.84	10
40 VUP	1.191 ± 0.001	2.071 ± 0.001	80	4.3	24	0.30	6
40 VUP dupl.	1.190 ± 0.001	2.067 ± 0.003					
43 VUP	1.176 ± 0.001	2.085 ± 0.004	55	4	24	0.44	6
46 VUP	1.200 ± 0.002	2.064 ± 0.005	38	3	19	0.5	7
48 VUP	1.184 ± 0.001	2.078 ± 0.002	37	2	40	1.1	21
50 VUP	1.184 ± 0.004	2.078 ± 0.003	23	3.2	14	0.61	5

[a] Enrichment factor of Pb (EF$_{Pb}$) is computed as described in the text. The errors of Pb/Pb ratios correspond at 95% confidence level. Duplicate is abbreviated as dupl.

were used. Some airborne particulate samples, collected in a similar way as previously described, were provided by local municipal agencies.

Sc and Br were analyzed by INAA, Pb and Al by inductively coupled plasma mass spectrometer (ICP-MS) after microwave digestion with $HNO_3 + HF + HClO_4$ added to the filter. Indium was used as internal standard during ICP-MS analyses.

For isotopic analysis, approximately 200 mg of lichens were totally dissolved with 2 mL each of concentrated HNO_3 and HCl of suprapure grade. The digestion was achieved under microwave assistance (MLS ETHOS) in pressured Teflon bombs. A blank was systematically measured for each set of eight unknown samples and was always found negligible by comparison to the total amount of Pb in lichens. Extraction of particulate material from the filters and Pb purification on AG1 × 4 resin were achieved following the procedure described elsewhere (*25*). The Pb isotopic ratios were measured by quadrupole-based ICP-MS (POEMS1-TJA and HP 4500). More details about settings, analytical time management, and correction of mass bias via NBS 981 can be found in Monna et al. (*26*). Few duplicates showed that the ^{206}Pb/^{207}Pb and ^{208}Pb/^{206}Pb ratio measurements are quite reproducible, considering the analytical precision (0.1%−0.2% at 95% confidence level). Although the ratios including the ^{204}Pb isotope were measured when possible, they are not presented here because a complete discussion of these ratios in addition to the ^{206}Pb/^{207}Pb and ^{208}Pb/^{206}Pb ratios may appear redundant.

Enrichment factors for Pb, relative to local volcanic rocks, were computed according to the following formula: $EF_{Pb} = (Pb/Sc)_{lich}/(Pb/Sc)_{subst}$. On the basis of several rock chemistry determinations (Dongarrà, unpublished data), a $(Pb/Sc)_{subst}$ ratio of 0.56 was used for the Etna and 0.98 for Vulcano. Metal concentrations and lead isotopic compositions in lichens are reported in Table 1. Lead isotope ratios in urban aerosols and gasoline samples are reported in Table 2.

Results and Discussion

Isotopic Signatures of Pb Sources. Lead in a natural environment usually derives from distinct sources: organolead used as antiknock additives in gasoline, industrial activities, and natural inputs. At the studied sites, two main natural sources can be expected: soil dust derived particles and volcanic emissions. Lead isotopic compositions of volcanics from Mt. Etna (^{206}Pb/^{207}Pb: 1.240−1.280; av: 1.260; ^{208}Pb/^{206}Pb: 1.981−2.009; av: 1.990) and sublimates from the Fossa Crater of Vulcano island (^{206}Pb/^{207}Pb: 1.230−1.235; av: 1.234; ^{208}Pb/^{206}Pb: 2.011, 2.045; av: 2.030) have been determined by Carter and Civetta (*27*) and Ferrara et al. (*28*), respectively. A few measurements carried out during our survey on fresh scoriae and on plume particles collected at Bocca Nuova crater, Mt. Etna (^{206}Pb/^{207}Pb: 1.211−1.260; ^{208}Pb/^{206}Pb: 1.999−2.048), fall close to the range previously defined by Carter and Civetta (Table 2). A further natural contribution, as often has been invoked, may come from desert-derived dust, as Saharan winds often spread over Sicily. However, given the low Pb content in desert aerosols (less than 20 μg/g, (*9*)), Saharan lead is probably of minor importance. Seawater was not considered as its contribution to the total lead content in lichens is rather low.

It has been shown that lead isotope ratios in gasoline in Western Europe have frequently shifted during the past decades in response to changing lead ores used as additives (*29*). In France, a decrease of the ^{206}Pb/^{207}Pb ratios from 1.162 in 1966 (*30*) to much lower values of 1.069−1.094 (av: 1.084) in 1995 has been explained by the increasing use of a major component of Pb coming from Australian and Canadian lead ores, all characterized by low radiogenic signatures (*25, 31*). However, the situation can be quite different from one country to another, depending on the main suppliers and on the location of their importation. Regarding Italy, the only data to our knowledge are those reported by Facchetti et al.

TABLE 2. Pb Isotopic Compositions and Pb/Br Ratios of Airborne Particulate Matter and Gasoline in Eastern Sicily[a]

sampling location	name	characteristics	^{206}Pb/^{207}Pb	^{208}Pb/^{206}Pb	Pb/Br
Palermo	G.51	town	1.119 ± 0.001	2.144 ± 0.004	2.2
Palermo	G.66	town	1.118 ± 0.001	2.143 ± 0.005	2.2
Palermo	G.137	town	1.106 ± 0.001	2.149 ± 0.004	2.8
Palermo	G.37	town	1.123 ± 0.002	2.142 ± 0.004	2.5
Palermo	G.39	town	1.117 ± 0.002	2.148 ± 0.005	2.5
Siracusa	SR2	town	1.167 ± 0.001	2.102 ± 0.003	2.7
Siracusa	SR3	town	1.168 ± 0.003	2.098 ± 0.004	2.8
Messina	Mess 27	town	1.103 ± 0.002	2.152 ± 0.004	1.8
Messina	Mess C7	town	1.104 ± 0.002	2.153 ± 0.005	2.2
Milazzo	Mess 122	town/industrial	1.119 ± 0.002	2.136 ± 0.004	3.9
Milazzo	Mess 117	industrial	1.141 ± 0.003	2.116 ± 0.006	3.9
Caltanissetta	SC	town	1.107 ± 0.002	2.150 ± 0.003	
Caltanissetta	CL	town	1.113 ± 0.002	2.145 ± 0.005	3.1
Caltanissetta	CL2	town	1.126 ± 0.001	2.134 ± 0.004	3.2
Gela	GELA 1	town/industrial	1.113 ± 0.001	2.147 ± 0.004	3.4
Gela	GELA 2	industrial	1.165 ± 0.002	2.098 ± 0.003	4.1
Porto Empedocle	PE1	industrial area	1.149 ± 0.003	2.110 ± 0.008	2.4
Porto Empedocle	PE2	industrial area	1.149 ± 0.003	2.109 ± 0.009	3.2
Catania	CAT F	town	1.165 ± 0.003	2.108 ± 0.005	3.2
Catania	CAT C	town	1.161 ± 0.001	2.110 ± 0.004	3.1
Catania	CAT D	town	1.174 ± 0.002	2.090 ± 0.006	3.2
Catania	CAT XI	town	1.168 ± 0.003	2.095 ± 0.004	3.2
AGIP		gasoline	1.066 ± 0.004	2.205 ± 0.009	
SHELL		gasoline	1.137 ± 0.006	2.112 ± 0.008	
IP		gasoline	1.084 ± 0.004	2.166 ± 0.006	
ASH1		Bocca Nuova Mt. Etna	1.211 ± 0.004	2.043 ± 0.005	
ASH2		Bocca Nuova Mt. Etna	1.260 ± 0.004	1.999 ± 0.010	

[a] The errors of Pb/Pb ratios correspond at 95% confidence level.

(*32*) giving a mean value of 1.18 in Turin (North Italy) for 1974−1975 and by Colombo et al. (*33*) with a mean value of 1.16, for the same town, in 1985. This radiogenic isotopic signature reflected the use of young U.S. and Western European (Greece, Yugoslavia) lead ores.

To establish the lead isotope compositions in gasoline used at the present time in Sicily, samples were collected directly from petrol stations of the most important suppliers (AGIP, IP, and ESSO). The ^{206}Pb/^{207}Pb ratios (Table 2) vary rather widely from 1.067 to 1.137 (av: 1.085), proving that the different supplier companies have added Pb having a variable primary origin but always including a significant proportion of unradiogenic Pb.

The isotopic composition of lead emitted by industries is more difficult to assess given the high variability of the possible origins due to the presence of a Pb market much more open than that of gasoline additives. Excluding Gela 1 and Mess 122 samples, likely contaminated by leaded gasoline because of the surrounding car traffic, the observed range of ^{206}Pb/^{207}Pb ratios (1.141−1.165) for samples collected near Sicilian industrial sites (Gela, Milazzo, and Porto Empedocle) is similar to that reported for German and French industrial emissions (1.142−1.159) (*25*−*34*). Such a range is considerably more radiogenic than gasoline-derived lead. In our study we will therefore assume the range 1.141−1.165 as characterizing the industrial lead isotopic composition.

Lead Isotope Composition in Urban Airborne Particulate Material. Lead isotope ratios measured on aerosols samples from five Sicilian urban areas (Palermo, Catania, Messina, Siracusa, and Caltanissetta) and from three industrial sites (Gela, Milazzo, and Porto Empedocle) are plotted in Figure 2. We must keep in mind that aerosol samples only reflect a punctual situation, and it is therefore hazardous to draw general conclusions from these data. Temporal variation in atmospheric ^{206}Pb/^{207}Pb ratios in urban site can be high, depending on the day of the week and on the wind direction (*25*).

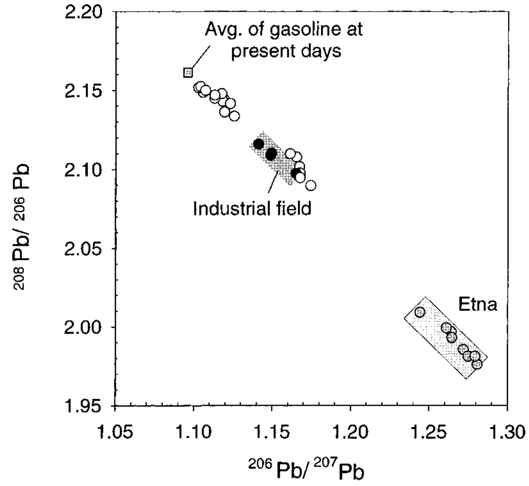

FIGURE 2. ^{208}Pb/^{206}Pb vs ^{206}Pb/^{207}Pb in aerosols collected in urban environment (○), and industrial areas (●). The compositional fields of the natural and anthropogenic lead sources are also plotted for comparative purposes.

The observed ^{206}Pb/^{207}Pb ratios range between the gasoline-derived lead signature and natural input values. Samples from Messina, Caltanisseta, and Palermo urban areas show the less radiogenic isotope signatures (^{206}Pb/^{207}Pb = 1.103−1.126), and they are the most affected by automotive lead. In Figure 3 are plotted the ^{206}Pb/^{207}Pb isotopic ratios against the Pb/Br ratios observed in airborne particles as well as the compositional fields of anthropogenic (gasoline and industrial) and natural sources (*35, 36*). The measured Pb/Br ratios in urban particulate material from Messina (1.8−2.2) and Palermo (2.2−2.8) are very close-to-this ratio, confirming the importance of automobile combustion in the dispersion of lead and bromine in the urban atmosphere.

Urban aerosols from southeastern Sicily (Catania and Siracusa), on the contrary, are considerably more radiogenic (^{206}Pb/^{207}Pb = 1.161−1.174) and present higher Pb/Br ratios (2.8−3.2), suggesting a more significative contribution of industrial lead, while the contribution of soil dust is rather

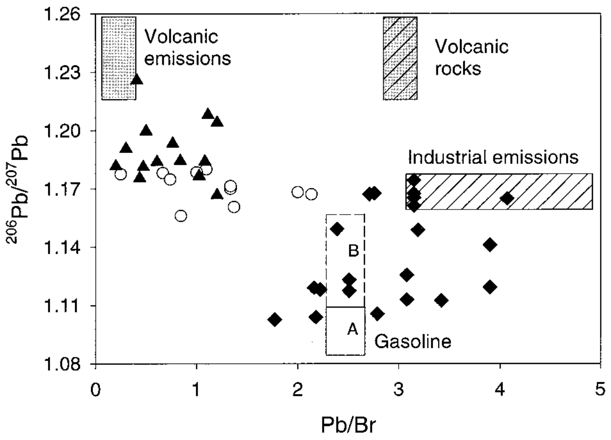

FIGURE 3. $^{206}Pb/^{206}Pb$ vs Pb/Br in aerosol (◆) and lichen samples from Mt. Etna (○) and Vulcano island (▲). Potential lead sources are also shown.

limited on the basis of the very low content of Sc and Al, considered as totally natural occurring elements.

Airborne particulate matter collected on filters indicates therefore that automobile exhausts and industrial emissions are the prominent source of atmospheric lead in the studied urban sites. This means that, over short term, no risk seems to be associated with lead emissions from volcanic activity, at least in urban areas far from the volcanoes.

Lead Isotopic Composition in Lichens. Figure 4 (parts a and b) displays the lead isotopic ratios in lichens sampled at Mt. Etna and Vulcano island, respectively. Both isotopic patterns fit straight lines, defined by extreme end-members corresponding to gasoline and the natural sources. The geogenic input is much more evident at Vulcano island ($^{206}Pb/^{207}Pb = 1.176-1.226$) than at Mt. Etna ($^{206}Pb/^{207}Pb = 1.156-1.180$), where the surrounding anthropogenic activities are considerably more effective. The same observations can be drawn from Figure 3, where lichens are clearly shifted toward the compositional field of a low Pb/Br natural (volcanic) source. As a consequence, a mixture of anthropogenic Pb (gasoline + industrial) with one (or more) geogenic source has to be invoked. Two possible geogenic sources may be suggested: soil(substrate)-derived dust and volcanic emissions. Unlikely, their relative contribution cannot be apportioned on the basis of the sole isotopic data, because of their similar isotopic signatures. However, substratum-derived lead (Pb_{subst}) in each lichen sample can be estimated by

$$Pb_{subst} = (Pb/Sc)_{subst} \times (Sc)_{lich}$$

where $(Pb/Sc)_{subst}$ and $(Sc)_{lich}$ are the average ratio in local volcanics and the total Sc concentration in lichens, respectively. Both Sc and Al may be used due to their very low solubility and because they have no apparent biological function in lichens. Soil-derived lead, as estimated by the above equation, always results in a minor fraction of the total lead content. Such a minor contribution is consistent with the high values (up to 85) of lead enrichment factors (Table 1).

As a matter of fact, although volcanic aerosols (i.e. solid and liquid particles emitted by volcanic plumes and fumaroles) have a lead isotope composition similar to the local substrate, they are characterized by higher Pb/Sc ratios (and high Pb EFs). During magma degassing, volatile elements (as Pb) are preferentially partitioned into the rising gas phase with respect to lithophile elements (as Sc or Al). Therefore, according to the estimated lead fluxes from Mt. Etna and Vulcano island (*37*), a "natural" pollution from volcanoes may be suggested.

TABLE 3. Proposition of Pb Coming from Substratum, Volcanic Emissions, and Anthropogenic Sources in the Lichens of Mt. Etna and Vulcano Island[a]

	substratum %	volcanic emissions %	anthropogenic %
		Etna Lichens	
71 EP	4 ± 1	24 ± 11	72 ± 11
72EP	6 ± 2	25 ± 10	69 ± 10
74 EP	7 ± 2	24 ± 10	69 ± 10
76 EP	3 ± 1	22 ± 11	74 ± 11
81 EP	1 ± 1	22 ± 12	77 ± 12
87 EP	2 ± 1	21 ± 12	78 ± 12
90 EP	2 ± 1	22 ± 11	75 ± 11
96 EP	20 ± 6	11 ± 10	70 ± 10
97 EP	3 ± 1	29 ± 10	68 ± 10
99 EP	4 ± 1	14 ± 14	83 ± 15
100EP	3 ± 1	12 ± 12	85 ± 12
		Vulcano Lichens	
5 VUP	37 ± 11	9 ± 9	54 ± 9
10 VUP	5 ± 1	63 ± 6	32 ± 6
13 VUP	12 ± 4	78 ± 2	10 ± 2
16 VUP	5 ± 1	39 ± 11	56 ± 11
17 VUP	10 ± 3	46 ± 9	44 ± 9
22 VUP	6 ± 2	23 ± 14	71 ± 14
23 VUP	3 ± 1	69 ± 6	28 ± 6
25 VUP	5 ± 2	34 ± 12	61 ± 12
38 VUP	10 ± 3	37 ± 11	53 ± 11
40 VUP	17 ± 5	36 ± 9	46 ± 9
43 VUP	16 ± 5	22 ± 12	62 ± 12
46 VUP	15 ± 5	48 ± 7	37 ± 7
48 VUP	5 ± 1	42 ± 11	53 ± 11
50 VUP	22 ± 7	25 ± 11	53 ± 11

[a] See text for details about calculation.

The contribution from volcanic emissions may be estimated by using the following set of equations

$$Pb_{volc} = Pb_{tot.} - (Pb_{subst} + Pb_{anthr})$$

$$Pb_{anthr} = Pb_{tot.} * [(^{206}Pb/^{207}Pb)_{lich} - (^{206}Pb/^{207}Pb)_{volc}]/ [(^{206}Pb/^{207}Pb)_{anthr} - (^{206}Pb/^{207}Pb)_{volc}]$$

where $Pb_{tot.}$ is the total lead content in each lichen sample; Pb_{volc} is the amount of lead derived from volcanic aerosols; Pb_{anthr} is the anthropogenic lead; and $(^{206}Pb/^{207}Pb)_i$ is the isotopic ratio measured in each lichen samples (lich), in the anthropogenic source (anthr), and in the local volcanic rocks and aerosols (volc).

To solve this system of equations, the $^{206}Pb/^{207}Pb$ ratio of the anthropogenic source is required. Pb content in lichens represents an integral of the exposure during the last 10–20 years and not a recent exposure. As previously described, the isotopic signature of anthropogenic lead has widely varied with time. Moreover as demonstrated by our aerosol samples, a wide range of isotopic composition can be observed at different Sicilian sites, even at the present time.

Thus the overall anthropogenic signature should fall in the range defined by the extreme values measured during the last 20 years (1.080–1.165), but these extreme values can only be recorded close to emission sources, while intermediate signatures should be observed in rural areas. That is why we can reasonably consider that the mean anthropogenic signature over the last 20 years was characterized by $^{206}Pb/^{207}Pb$ of about 1.135 ± 0.020. Such a range includes the value of 1.15, which was considered as representative of the average composition of Western Europe atmosphere during the 1980s (*38–40*), and it takes into account the recent addition of unradiogenic Pb in Italian gasoline.

Table 3 shows the contributions of the three potential sources: substratum, volcanic emissions, and anthropogenic in the lichens of Vulcano and Etna. They are also graphically

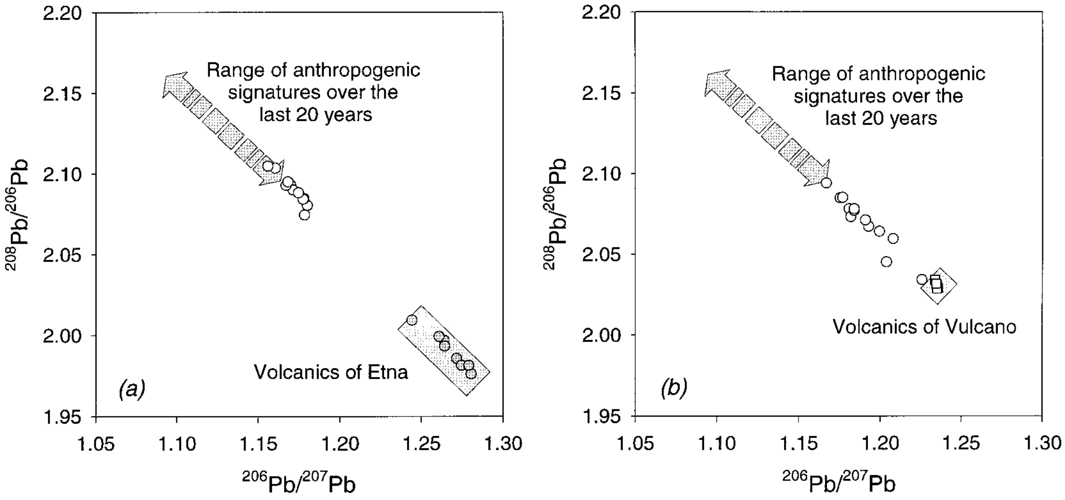

FIGURE 4. $^{208}Pb/^{206}Pb$ vs $^{206}Pb/^{207}Pb$ in lichens (○) from Mt. Etna (a) and Vulcano island (b). The compositional fields of the natural source and range of anthropogenic signatures over the last 20 years (dotted arrow) are also plotted for comparative purposes.

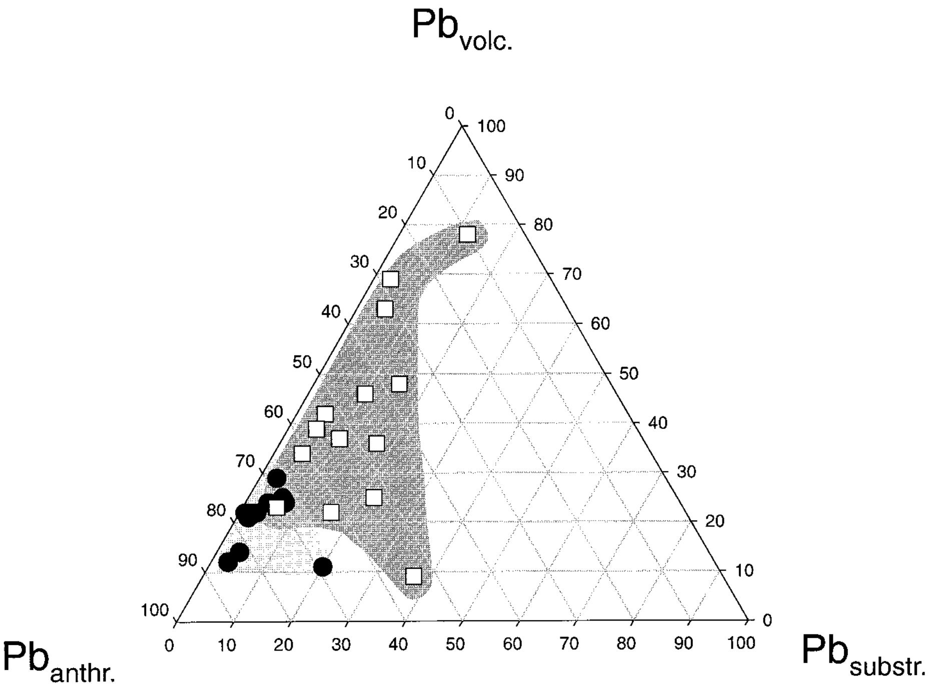

FIGURE 5. Ternary diagram representing the relative contribution of each substratum, volcanic emissions, and anthropogenic sources in lichens from Mt. Etna and Vulcano island.

expressed in the triangular plot of Figure 5. The percentages of anthropogenic lead found for lichens from Vulcano island (32−71%; av: 47%) appear lower than those from Mt. Etna (68−85%; av: 74%). This is not surprising considering the low anthropogenic activity on the island. In addition, these results reveal that volcanic activity is a significant source of lead release to the atmosphere not only during eruptive phases but also during passive (quiescent) degassing. Although Nriagu (9) has shown that, on a global scale, volcanoes account for less than 1% of the total emissions of lead (3300 t/y), our data strongly suggest that near volcanic areas the natural emissions are added significantly to anthropogenic activity, with the consequently increased risk level for lead accumulation in soil, grass, plants, and groundwaters.

Data presented in this paper, besides representing the first extensive series of measurements on the isotopic composition of lead in lichens and aerosols from Sicily, constitute a preliminary database for future surveys in air quality monitoring programs and in addressing decisions on remedial actions. On the basis of lead isotope composition, two anthropogenic sources are recognizable: gasoline, where lead is added as an antiknock compound, with $^{206}Pb/^{207}Pb$ ratios varying from 1.067 to 1.137 (av: 1.085), and industrial activities, releasing lead having a $^{206}Pb/^{207}Pb$ signature of about 1.14−1.16. This is consistent with the data observed in the neighboring European countries. Lichens appear to be a powerful tool for studying the complex mixing between anthropogenic and natural sources over long-term periods (up to 20 years). Finally, the ICP-MS technique, less precise than TIMS (Thermo Ionization Mass Spectrometry) but much more convenient, provides good reliability for extensive and relatively easy isotopic monitoring.

Acknowledgments

This research was supported by the Istituto di Geochimica dei Fluidi-CNR of Palermo and the Ministero dell'Università e della Ricerca Scientifica e Tecnologica (Funds MURST 60%) and in part by National Swiss Foundation. We wish to express many thanks to AMIA-Palermo, Comune di Catania, and Provincie Regionali di Agrigento, Siracusa, Caltanissetta, and Messina for having furnished some of the air filters. We also thank J. Dominik and M. Kanth, and the ICP-MS team B. Thomas, P.-Y. Faverger, and C. Guéguen of FOREL Institut for their technical assistance and helpful discussions.

Literature Cited

(1) Dongarrà, G.; Varrica, D. *Sci. Total Environ.* **1998**, *212*, 1.
(2) Varrica, D.; Aiuppa, A.; Dongarrà G. Submitted to *Environ. Pollut*.
(3) Schaule, B. K.; Patterson, C. C. *Earth Planet. Sci. Lett.* **1981**, *54*, 97.
(4) Hamelin, B.; Grousset, F.; Sholkovitz, E. R. *Geochim. Cosmochim. Acta* **1990**, *54*, 37.
(5) Ritson, P. I.; Esser, B. K.; Niemeyer, S.; Flegal, A. R. *Geochim. Cosmochim. Acta* **1994**, *58*, 15, 3297.
(6) Boutron, C.; Patterson, C. C. *Nature* **1986**, *323*, 222.
(7) Rosman, K. J. R.; Chisolm, W.; Boutron, C. F.; Candelone, J. P.; Hong, S. *Geochim. Cosmochim. Acta* **1994**, 58−15, 3265.
(8) Nriagu, J. O. *Nature* **1979**, *279*, 409.
(9) Nriagu, J. O. *Nature* **1989**, *338*, 47.
(10) Grousset, F. E.; Quétel, C. R.; Thomas, B.; Buat-Ménard, P.; Donard, O. F. X.; Bucher, A. *Environ. Sci. Technol.* **1994**, *28*, 1605.
(11) Kramers, J. D.; Tolstikhin, I. N. *Chem. Geol.* **1997**, *139*, 1−4, 75.
(12) Harrison, R. M.; Sturges, W. T. *Atmos. Environ.* **1983**, *17*, 311.
(13) Sturges, W. T.; Hopper, J. F.; Barrie, L. A.; Schnell, R. C. *Atmos. Environ.* **1993**, *27A-17/18*, 2865.
(14) Nageotte, S. M.; Day, J. P. *Analyst* **1998**, *123*, 59.
(15) Jaakkola, T.; Heinonen, O. J.; Keinonen, M.; Salmi, A.; Miettinen, J. K. *Int. J. Mass Spec. Ion Phys.* **1983**, *48*, 347.
(16) Carignan, J.; Gariépy, C. *Geochim. Cosmochim. Acta* **1995**, *59*, 4427.
(17) Notcutt, G.; Davies, F. B. M. *Environ. Geol. Water Sci.* **1989**, 14−3, 209.
(18) Bargagli, R.; Barghigiani, C.; Siegel, B. Z.; Siegel, S. M. *Sci. Total Environ.* **1991**, *102*, 209.
(19) Nimis, P. L.; Castello, M.; Perotti, M. In *Plants as Biomonitors. Indicators for heavy metals in the Terrestrial Environment*; Markert, B., Ed.; V.C.H.: Weinheim, 1993; p 265.
(20) Dongarrà, G.; Ottonello, D.; Sabatino, G.; Triscari, M. *Environ. Geol.* **1995**, *26*, 139.
(21) Dongarrà, G.; Triscari, M.; Sabatino, G.; Ottonello, D.; Romano, S. *Acqua Aria* **1996**, *10*, 873.
(22) Barberi, F.; Innocenti, F.; Ferrara, G.; Keller, J.; Villari L. *Earth Planet. Sci. Lett.* **1974**, *21*, 269.
(23) Chester, D. K.; Duncan, A. M.; Guest, J. E.; Kilburn, C. R. J. *Mount Etna: the anatomy of a volcano*; Chapman and Hall, London, 1985.
(24) Keller, J. *Rend. Soc. It. Mineral. Petrol.* **1980**, *36*, 369.
(25) Monna, F.; Lancelot, J. R.; Croudace, I. W.; Cundy, A. B.; Lewis, J. T. *Environ. Sci. Technol.* **1997**, *31*, 2277.
(26) Monna, F.; Loizeau, J.-L.; Thomas, B. A.; Guéguen, C.; Favarger, P.-Y. *Spectrochim. Acta, Part B* **1998**, *53*, 1317.
(27) Carter, S. R.; Civetta, L. *Earth Planet. Sci. Lett.* **1977**, *36*, 168.
(28) Ferrara, G.; Garavelli, A.; Pinarelli, L.; Vurro, F. *Bull. Volcanol* **1995**, *56*, 621.
(29) Bacon, J. R.; Jones, K. C.; McGrath, S. P.; Johnston, A. E. *Environ. Sci. Technol.* **1996**, *30*, 2511.
(30) Chow, T. J.; Snyder, C. B.; Earl, J. L. *Proc. United Nations FAO Intl. Atom. Energy Assoc. Symp. IAEA-SM* **1975**, *191/4*, 95.
(31) Elbaz-Poulichet, F.; Holliger, P.; Martin, J.-M.; Petit, D. *Sci. Total Environ.* **1986**, *54*, 61.
(32) Facchetti, S.; Geiss, F.; Gaglione, P.; Colombo, A.; Garibaldi, G.; Spallanzani, G.; Gilli, G. *CEE Status Rep. I* EUR 8352 EN, **1982**.
(33) Colombo, A.; Facchetti, S.; Gaglione, P.; Geiss, F.; Leyendecker, W.; Rodari, R.; Trincherini, P. R.; Versino, B.; Garibaldi, G. 1988. The isotopic lead experiment. Impact of petrol lead on human blood and air. *Commission of the European Communities*. Final report, EUR 12002, p 66.
(34) Hamester, M.; Stechmann, H.; Steiger, M.; Dannecker, W. *Sci. Total Environ.* **1994**, 146/147, 321.
(35) Sturges, W. T.; Harrison, R. M. *Atmos. Environ* **1986**, 20−3, 577.
(36) Dongarrà, G.; Aiuppa, A.; Varrica, D. *Plinius* **1998**, *20*, 107.
(37) Buat-Ménard, P.; Arnold, M. *Geophys. Res. Lett.* **1978**, 5−4, 245.
(38) Maring, H.; Settle, D. M.; Buat-Ménard, P.; Dulac, F.; Patterson, C. C. *Nature* **1987**, *300*, 154.
(39) Hopper, J. F.; Ross, H. B.; Sturges, W. T.; Barrie, L. A. *Tellus* **1991**, *43b*, 45.
(40) Véron, A. J.; Church, T. M. *EOS* **1993**, *74*, 78 (abstr.).

Received for review November 30, 1998. Revised manuscript received May 6, 1999. Accepted May 13, 1999.

ES9812251

Analusis, **2000**, *28*, 750-757

Noise identification and sampling frequency determination for precise Pb isotopic measurements by quadrupole-based Inductively Coupled Plasma Mass Spectrometry

F. Monna[1,2*], J.-L. Loizeau[1], B. Thomas[1], C. Guéguen[1], P.-Y. Favarger[1], R. Losno[3], J. Dominik[1]

[1]*Institut F.-A. Forel, Université de Genève, 10 route de Suisse, CH-1290 Versoix, Switzerland*
[2]*GéoSol, CST, UMR-INRA, Université de Bourgogne, 6, bd. Gabriel, F-21000 Dijon, France (Present address)*
[3]*LISA, Faculté des Sciences, 61, av. du Gal de Gaulle, F-94010 Créteil, Cedex France*

Abstract. Analytical precision of the isotope ratios measured by quadrupole-based ICP-MS is drastically controlled by the low-frequency noises which originate from nebulisation and vaporisation processes, and from sample introduction systems. The undesirable influence of these latter can be however reduced by choosing efficiently the operating parameters. In the present study, the choice of the stabilisation time necessary in peak jump mode, and the one of the number of sweeps are discussed in the light of noise power spectra obtained with various speeds of the peristaltic pump used as sample introduction system. Obviously, the settings proposed are probably efficient only on our own ICP-MS, but they can be determined without any difficulty on any other equipment, only by following the methodology detailed here. With such guidelines, experimental within-run RSD % were observed following closely those predicted by the counting statistics (~ 110 %). The isotopic measurements of natural samples (overbank sediments, airborne particulate matter, lichens and rainwater) exhibited fair accuracy and good reproducibility, making highly convenient the use of the ICP-MS, at least in an environmental purpose.

Keywords. Inductively coupled plasma mass spectrometry – lead isotope ratios – instrumental parameters – optimisation – noise – quality control.

Introduction

The precision of isotopic ratios measurements by quadrupole-based ICP-MS is known as ultimately limited by the counting statistics. Starting from the observations done by Quétel *et al.* [1] about the importance of the time management, we have previously investigated how, for a given acquisition time, the within-run relative standard deviation (RSD %) of the isotopic ratios could be reduced [2]. We proposed to divide optimally the available time in order to compensate the differences of abundance of the isotopes used in ratioing. This work gave clues for reducing the theoretical random error on the basis of the best time sharing, but did not investigate the operating parameters which must be taken into account to approach this theoretical precision limit. Many sources of noises, identified by power analysis of noise, have also an ominous influence on the precision, the detection limits, and the dynamic range. They may originate from the sample introduction system, the main power or from other parts of the instrument [3-11]. However, their amplitude can be directly reduced. For instance, the audiofrequency peaks associated with instability at the boundary of the plasma with surrounding atmosphere, may be removed by using an adapted torch arrangement, while the white noise is efficiently reduced when the spray chamber is cooled [10]. Another complementary alternative consists to optimise the acquisition parameters for minimising their influence on the precision. It was found out that rapid sweeps act as a substitute of simultaneous measurements, as that can be done with multi-collector system [9]. As a matter of fact, it can be mathematically demonstrated that all the noises occurring at period more than twice that of the sampling frequency (that means the time elapsed between the start of the measurement of the first isotope and the end the last one) are reduced by ratioing the isotopes.

In the present study, we attempt to give some guidelines to obtain a precision on isotopic ratios close to that predicted by counting statistics. Investigations were undertaken to determine the most efficient sampling frequency, (i) by reducing the stabilisation time necessary to ensure the stability of the quadrupole after each jump, and (ii) by increasing the sweeps. Noise power spectra, established with various peristaltic pump speeds, were also examined to minimise as much as possible the amplitude of low-frequency, discrete, and white noises.

---

*Correspondence and reprints.

Received July 4, 2000; revised September 8, 2000; accepted September 19, 2000.

Experimental part

Reagents

Deionised water was produced by a Milli-Q-system presenting conductivity always better than 18 MΩ.cm^{-1}. Suprapure nitric acid was supplied by Merck, Germany. NBS 981 isotopic standard Pb solution was obtained from the National Bureau of Standards (newly NIST, USA). Chemical preparation and dilutions were all achieved in a clean lab (class 100-1000).

Apparatus

The ICP-MS used was a POEMS1 (Thermo Jarrell Ash Co, USA), installed in a clean and thermostatised room. The vacuum pumps were placed outside the ICP-MS room in order to reduce the vibrations in the immediate vicinity of the instrument. The solutions were introduced in a cross-flow nebulizer *via* a 8 rollers peristaltic pump (Ismatec, especially designed for the POEMS1 instrument) with a software controlling the flow rate. The pressure of the rollers on the tube was fixed following the conventional technique, which consisted to apply just enough strength to disable the free aspiration. The plasma and the MS were lighted-up 1-2 hours before measurements to enable a good stability of the system. The torch was positioned as close as the torch box allowed (only a few millimeters). The instrument was tuned to give enough sensitivity in combination with a low background, a maximum of stability and well-shaped peaks: symmetric, and as flat as the ICPMS allows (Fig. 1, Tab. I). A dead time correction of 36.2 ns was experienced efficient on our instrument up to an ion flow of about 7×10^5 ions.s^{-1} [2].

It was previously observed that low resolution may induce a significant overlap from one peak on the next left [12]. As a result, an over-estimation of the ^{206}Pb/^{204}Pb and ^{207}Pb/^{204}Pb ratios, and a slight under-estimation of the ^{206}Pb/^{207}Pb ratios may occur. Preliminary investigations with a resolution varying from 80 to 90 showed that 86 produces fair sensitivity and acceptable overlap of 0.037 %.

Isotope measurements

The measurements of Pb/Pb ratios were done in peak jump mode (also named “peak hopping” by some constructors). This mode is more precise than plain scanning, in particular because the integration time can be adapted for compensating the isotopic abundance. 42 seconds of total acquisition time were consumed as follows: 20 s, 9 s, 9 s, and 4 s for ^{204}Pb, ^{206}Pb, ^{207}Pb and ^{208}Pb isotopes respectively. When the control of the less abundant ^{204}Pb isotope was not necessary, or impossible because of the low Pb content, the same timing than above was kept for the three remaining isotopes. Such a time distribution was found as providing the best theoretical precision [2]. Three channels per peak were measured at 0 +/- 0.008 a.m.u. Various dwell times were investigated by changing the number of sweeps.

Table I. Operating parameters. The most usual settings are given between parenthesis.

ICP conditions	Auxiliary gas	1.5 L.min^{-1}
	Nebuliser gas	0.64 L.min^{-1}
	RF power	1350 W
	Nebuliser type	Concentric Meinhard
	Spray chamber	Scott chamber
	Pump rate	Variable*: 0.54 to 1.50 mL.min^{-1}
Mass spectrometer	Lens settings	L1: –242 to –105 (~ –110 V)
		L2: –25 to 26 (~ 20 V)
		L3: –21 to 43 (~ 20 V)
		L4: –140 to –250 (~ –210 V)
		L5: –30 to 50 (~ 30 V)
		L6: –10 to 5 (~ –8 V)
		L7: –43 to -20 (~ –30 V)
		L8: –180 to –30 (~ –45 V)
		Def.: 0 to 10 (~ 0 V)
		Off.: 4 to 6 (6 V)
		Coll.: 750 to 1150 (~800 V)
	Resolution	86
	Measurement mode	Peak jumping
	Dwell time/ number of sweeps	Variable*
	Replicate	10
	Points/peak	3
	Total replicate time	22 s or 42 s*

***** see text for details

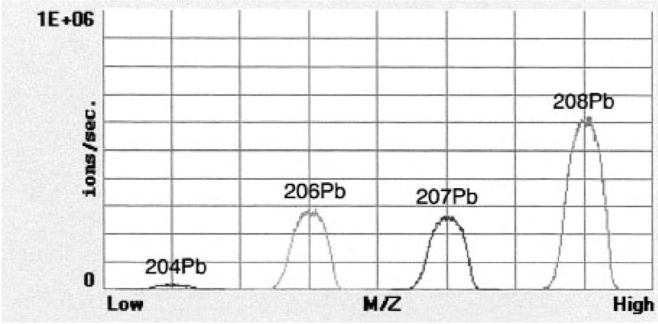

Figure 1. Shape peak requirement for ICP-MS isotopic measurements.

The expected precision (counting statistics alone) was also calculated for a comparative purpose. It was reported in term of within-run RSD % (relative standard deviation) and was determined as follows:

$$\text{r.s.d.}_{\left(I_i/I_j\right)_{\text{mes}}} = \sqrt{\text{r.s.d.}^2_{I_i} + \text{r.s.d.}^2_{I_j}} = \sqrt{\frac{1}{f_i \cdot t_i} + \frac{1}{f_j \cdot t_j}} \qquad (1)$$

where $\text{r.s.d.}_{(I_i/I_j)_{\text{mes}}}$ is the relative standard deviation of the ratio I_i/I_j, f_i and t_i are the ion flow and the total integration time of the isotope i respectively.

Noise identification

Noise power spectra (NPS) were computed following approximately the procedure described in Begley and Sharp [9]. They were obtained from the analysis of transient signals of a Pb solution producing about $\sim 2 \times 10^6$ cps at m/z = 208. Such a high ion flow cannot be used for isotopic measurements, because at that rate a reliable correction of dead time is no longer possible, but it is quite convenient for noise identification. Data collections were operated at: (i) 20 Hz (512 samples), allowing a resolution of 0.019 Hz, and (ii) at 1000 Hz (4096 samples) giving a resolution of 0.12 Hz. The resulting Nyquist frequency were of 10 Hz and 500 Hz respectively. The signals so obtained were filtered using a low pass filter of 10 Hz and 400 Hz respectively. Fast Fourier Transform (FFT) analysis were computed with the STATISTICA software package using a Hanning window. Noise amplitudes were obtained by calculating the sum of the squares of the real and imaginary components of the transformed data and of the signal average. Amplitude spectra were converted to power spectra using:

$$\text{dB} = 20 * \log\,(\text{noise amplitude/signal amplitude}) \qquad (2)$$

The whole procedure was repeated 12 times at 20 Hz, and 24 times at 1000 Hz. These individual runs were averaged to get a more reliable NPS.

Results and discussion

Stabilisation time

With the peak jump mode, a short time of latency after each jump (T_{stab}) is necessary to ensure a good stability of the quadrupole before acquisition. If four masses are monitored (as for Pb), and N_{sw} sweeps are set, the total time spent for stabilisation TT_{stab} is:

$$TT_{\text{stab}} = 4.\ T_{\text{stab}}\ .\ N_{\text{sw}} \qquad (3)$$

By default, T_{stab} is fixed at 20 ms on the POEMS1 ICP-MS, but can also be diminished up to 10 ms without any problem. This means that 40 ms are systematically spent at each sweep. The use of a high number of sweeps increases the sampling frequency and, in all likelihood, should improve the precision. However, the overall time consumed only for stabilisation grows up proportionally, whereas the one purely dedicated to acquisition remains unchanged. It results that a considerable percentage of analytical time may be wasted only for stabilisation, therefore reducing drastically the speed of analyses. For example, 40 s are lost for stabilisation when the four Pb isotopes are measured during 42 s with 1000 sweeps; that means that about 50 % of the total analytical time are definitely wasted (Fig. 2). In this case, the elapsed time between the start of the measurement of the first isotope and the end of the last one is 72 ms (42 ms + 3 × 10 ms), making a sampling frequency of ~13.9 Hz. Our purpose is thus to find a good compromise between high precision (generally produced by high sampling frequency) and fair time management, both being somehow mutually exclusive. In addition, it must be insured that a too high sweep frequency does not affect the accuracy of the Pb/Pb ratios.

Choice of a sweep frequency

An experiment has been conducted with an isotopically-known Pb solution in order to examine how the accuracy and the precision of the ^{206}Pb/^{204}Pb, ^{207}Pb/^{204}Pb, ^{208}Pb/^{204}Pb and ^{206}Pb/^{207}Pb ratios vary with the number of sweeps (*cf.* Tab. II for the ^{206}Pb/^{204}Pb ratios, and the legend for the analytical conditions).

The accuracy appears to be affected by the choice of the number of sweeps. Up to 500 sweeps, the measured ratios are close to the expected value, but they progressively shift with the increase of the sampling frequency. High sampling frequencies do not seem to be suitable as they probably result in a loss in the recording of the different isotopes more or less perceptible following the duration of their individual integration.

At 100 sweeps, the within-run RSD % is rather high: ~ 0.8 % (Tab. II), probably because the sampling frequency (2.22 Hz) is almost the same to this issuing from the rollers of the pump (2.13 Hz). As a matter of fact, the fundamental noise (F_n) due to the pump corresponds to the frequency

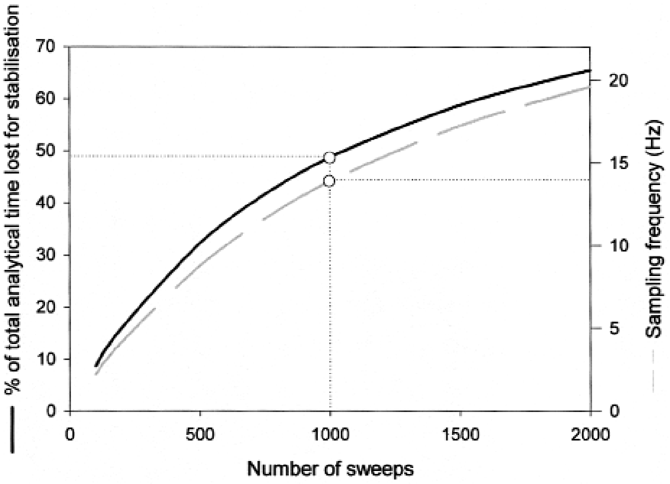

Figure 2. Percentage of total analytical time lost for stabilisation and sampling frequency *vs.* number of sweeps. The calculation was operated on a basis of 10 ms of stabilisation time, and 42 s of acquisition on the four Pb isotopes per replicate. Pump rotation speed of 16 rpm.

Table II. Accuracy expressed as deviation from the expected value (in %), and within-run precision of $^{206}Pb/^{204}Pb$ ratios varying with the number of sweeps.

Number of sweeps	*Deviation from the expected value (in %)*	*Within-run RSD %*
100	0.34	0.83
250	–0.16	0.42
500	–0.16	0.30
750	–1.07	0.29
1000	–1.70	0.30

at which each individual roller squeezes the sample introduction tube [7]. It is obtained by:

$$F_n = N.\omega\ /\ 60 \tag{4}$$

where N is the number of rollers of the pump (in our case: 8), ω is the rotation speed expressed in revolutions per minute. The experiment has been done at 16 rpm; that means a fundamental noise of 2.13 Hz. From 500 sweeps (making a sampling frequency of 8.77 Hz), the within-run RSD % decreases at about 0.3 %, and is not further improved by setting more sweeps.

To summarise, the use of 10 ms as stabilisation time and 500 sweeps for 42 s of acquisition time appeared to be a good compromise. These settings give an acceptable proportion of analytical time really dedicated to ion counting (67 %) and good accuracy.

Noise identification

Fast Fourier Transforms (FFT) of the transient signal were carried out with various rotation speed of the peristaltic pump: 11.2, 16, 24 and 32 rotations per minute; corresponding to solution uptakes of 0.54, 0.75, 1.15 and 1.50 mL.min^{-1} respectively (Fig. 3a, left). An additional experiment was also performed using free aspiration (~ 0.8 mL.min^{-1}). Noise power spectra in the 0-10 Hz range (Fig. 3a) are similar to those already reported [5,9]. They can be decomposed into three different distinct components: (i) the white noise, actually the asymptote at the higher end of the frequency axis, (ii) the discrete noises, and (iii) the flicker noise, due to little fluctuation present in low frequency domain, so-called 1/*f*. This latter frequency-dependent noise is known as mainly originating from the instabilities during nebulisation, desolvation and vaporisation processes which cause a drift [13]. Discrete noises are observed when the sample uptake was operated by the peristaltic pump. These shift through high frequency at high pump speed: 1.48, 2.11, 3.16 and 4.22 Hz for pump speed of 11.2, 16, 24 and 32 rpm respectively. Such frequencies fit almost perfectly to those expected by eq. 4. Additional discrete noises, corresponding to the harmonics, are also detected at 24 and 32 rpm, but not at 11.2 and 16 rpm. The amplitude of the noises coming from the pump increases when the pulses become more frequent in opposition to that was previously reported [4]. As expected, no discrete noise is detected when the sample is freely aspirated, but white noise (~ – 65 dB) and 1/*f* noise are greater than when sample introduction is mechanically constrained, similarly to that was already reported [7]. At that time the Ar flow alone controls the sample uptake.

In the range 0-400 Hz, discrete noises are pointed out at 50 Hz and sometimes at 100 Hz (only one spectrum is presented on Fig. 3b). These issues from the power supply ripple, and are supposed to originate from the r.f. generator and from the electronic devices. The presence of higher harmonics have been already reported [6,8,9], but they are not perceived here. Another discrete and audible “singing” noise, so-called audiofrequency peak, is often recognised between 200 and 600 Hz, depending on the plasma conditions, and is explained as the interaction of the surrounding air with the hot plasma going out of the torch [5,8,11]. Here its absence may be due to the fact that the torch is placed as close as possible to the aperture, because of a efficient torch design, or simply because it occurs at more than 400 Hz, and is not recorded.

Precision of the Pb/Pb ratios

The highest sensitivities are observed with sample introduction rate of 0.75 mL.min^{-1} (16 rpm), 0.80 mL.min^{-1} (free aspiration) and 1.15 mL.min^{-1} (24 rpm). The use of 0.54 mL.min^{-1} (11.2 rpm) produces a response about 30 % lower, whereas a decline of more than 10 % is recorded at 1.50 mL.min^{-1} (32 rpm), likely as a consequence of the cooling down of the plasma. The worst within-run RSD % of the Pb/Pb ratios is observed in this later case (Fig. 3a, right), where the signal is the most unstable as suggested by high white noise (~ – 62 dB), large amplitude of discrete noises, and the presence of strong harmonics. The sweep frequency of 8.77 Hz is also probably too close to the first harmonic (8.53 Hz). So, the use of high sample uptake is, in this case, neither beneficial to the signal stability, nor to the counting statistics because of the fall of sensitivity. Relatively high within-run RSD % are also generated by the take of sample at 11.2 rpm, in part because the counting statistics is penalised by a loss of sensitivity. Sample uptakes of 0.75 mL.min^{-1} (16 rpm) and 1.15 mL.min^{-1} (24 rpm) produce approximately the same precision: within-run RSD % at about 0.2 % for $^{206}Pb/^{204}Pb$, $^{207}Pb/^{204}Pb$ and $^{208}Pb/^{204}Pb$ ratios, and 0.1 % for $^{206}Pb/^{207}Pb$ and $^{208}Pb/^{206}Pb$ ratios. At 0.75 mL.min^{-1}, less sample is necessary to complete an analysis, the white noise is low (~ – 68 dB), and the pump noise comes down at a frequency of 2.11 Hz, making efficient the reduction of its influence by ratioing. All these clues strongly support its use. As mentioned above, high white and 1/*f* noises are observed with free aspiration. In consequence the Pb/Pb ratios suffer of a lack of precision comparatively to the use of the pump in optimal conditions.

All the above tests were carried out with Pb solutions presenting concentrations close to the acceptable upper limit for allowing accurate isotopic measurements. That permitted a

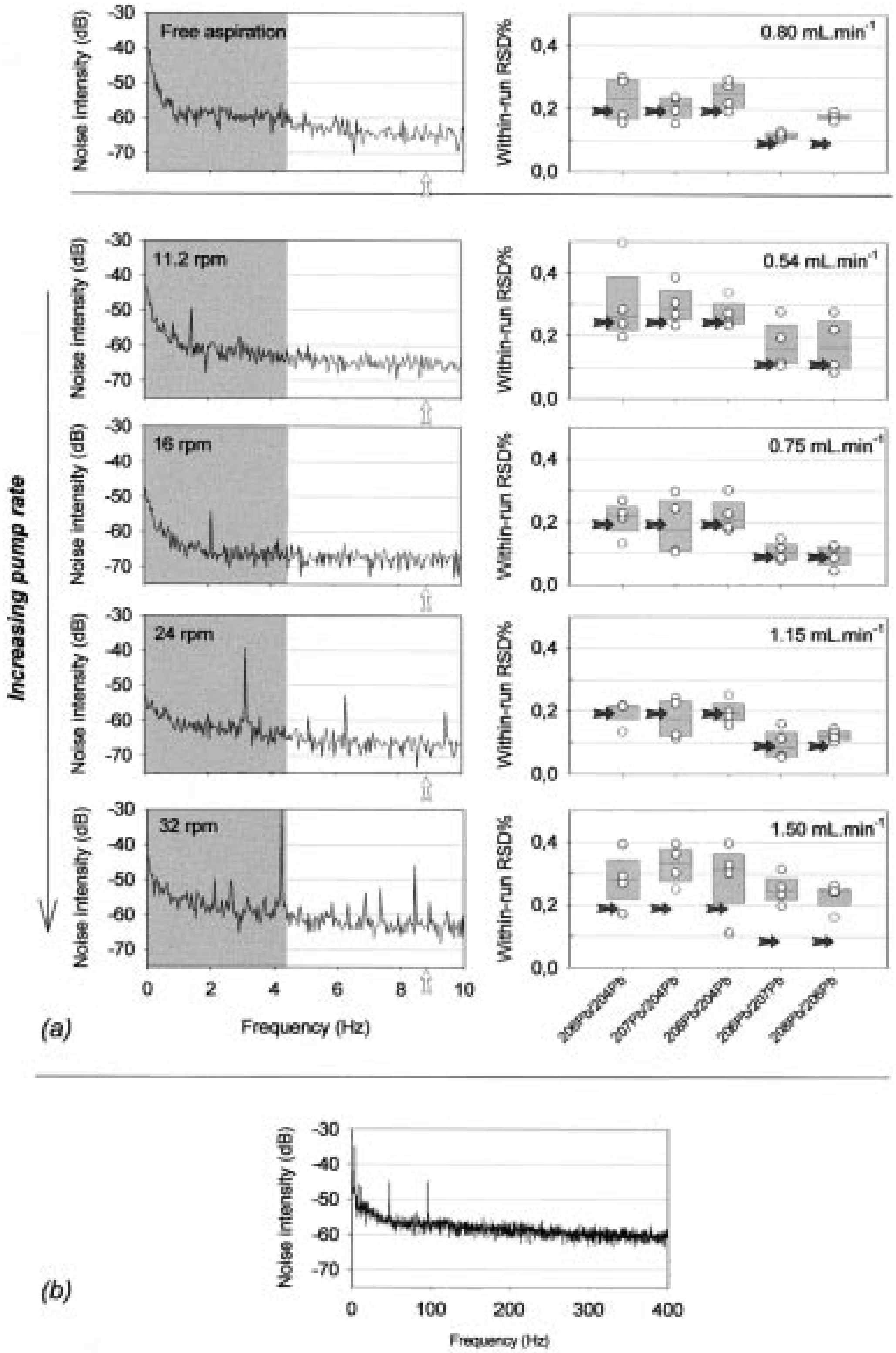

Figure 3. (a): Noise-power spectra from 0 to 10 Hz, and experimental within-run RSD % using free pumping and different pump rotation speeds (11.2, 16, 24 and 32 rpm). Left: the white arrows indicate the sampling frequency. The grey area represents the range of frequency in which the influence of noises is reduced by ratioing. Right: the open circles represent the experimental within-run RSD% of four consecutive analyses make of 10 replicates each, all done with the same settings. Median of RSD %, 25th and 75th percentiles as vertical boxes. Black arrows are the predicted RSD % by the Poisson’s law. (b): Noise-power spectra from 0 to 400 Hz.

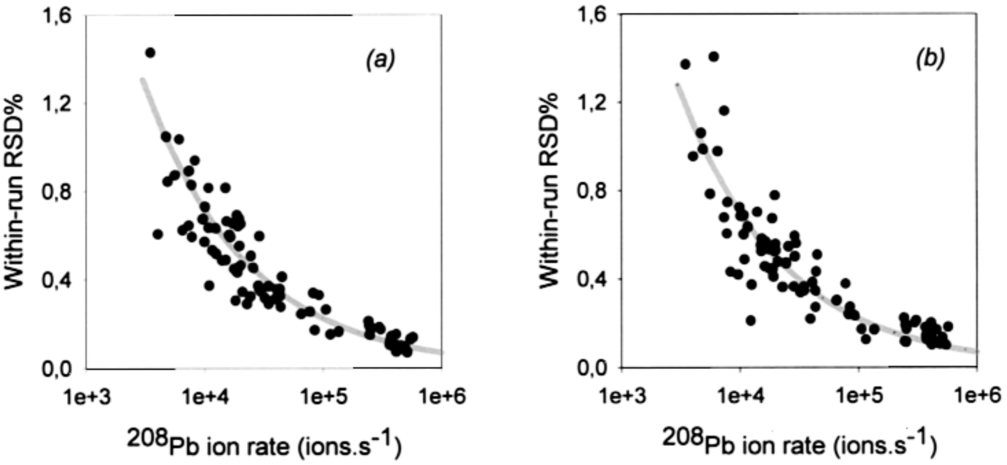

Figure 4. Experimental within-run RSD % of ^{206}Pb/^{207}Pb ratios (a), and ^{208}Pb/^{206}Pb ratios (b) of 74 rainwater solutions, and 16 Pb standards exhibiting ^{208}Pb ions flow ranging from 3 500 to 580 000 ions.s^{-1}. Operating conditions: 22 s of total analytical time divided as follows 9 s, 9 s and 4 s for ^{206}Pb, ^{207}Pb, and ^{208}Pb respectively; stabilisation time: 10 ms; 500 sweeps. The grey curves represent the predicted RSD % considering the Poisson's law, and are given for a comparative purpose.

fair counting statistics and a precise measurement of the ^{204}Pb isotope. However, in some natural objects weakly concentrated, such natural waters, it is not always possible to reach an ion rate of $\sim 7 \times 10^5$ ions.s^{-1} without a time consuming and potentially contaminant pre-concentration. In order to evaluate what degree of precision is reachable, 74 natural rainwater and 16 NBS 981 Pb solutions were directly analysed for their ^{206}Pb/^{207}Pb and ^{208}Pb/^{206}Pb ratios without any pre-concentration. They exhibited ^{208}Pb ions flow ranging from 3500 to 580000 ions.s^{-1} The operating conditions were the following: 22 s of total analytical time divided in 9 s, 9 s and 4 s for the ^{206}Pb, ^{207}Pb, and ^{208}Pb isotopes respectively. Stabilisation time, number of sweeps and pump speed were kept as optimally determined in the first part of this study: 10 ms, 500 sweeps, and 16 rpm supplying 0.75 mL.min^{-1} of sample. The figure 4a-b reports the within-run RSD % of the ^{206}Pb/^{207}Pb and ^{208}Pb/^{206}Pb ratios resulting from the experiment. They clearly show that the precision closely follows the RSD % predicted by the counting statistics whatever the Pb content (grey curve on the figures). Dropping the ^{204}Pb isotope increases the sweep frequency up to 15.63 Hz, and reduces the influence of all the noises occurring on a wide frequency window (0-7.81 Hz). The long-term instabilities of the signal have practically no more significant influence on the overall precision, which is almost totally governed by the counting statistics (average of measured RSD % are 102 % and 109 % of that predicted by Poisson's law for the ^{206}Pb/^{207}Pb and ^{208}Pb/^{206}Pb ratios, respectively).

Application to natural samples

After mass bias correction obtained by frequent measurement of NBS981 Pb standard solutions inserted in the set of unknown samples (see [2] for operational details), measurements show precision, accuracy and reproducibility as suggests the comparison with the results provided by precise thermo-ionisation mass spectrometry (TIMS) method, and numerous replicates performed on lichens, sediments and rainwater samples (Tab. III). The precision so reached is about two orders of magnitude lower than the maximum range of variations observed in the nature. Indeed, the ^{206}Pb/^{207}Pb ratios can vary from ~ 1.08 in gasoline to ~ 1.21 for geogenic Pb of Western Europe [14,15], whereas the analytical precision of the same ratio is typically 1-3.10^{-3}, at least when the Pb concentrations are sufficiently high. That makes the use of the ICP-MS quite suitable and convenient for quick environmental monitoring.

Conclusion

Whatever the type of spectrometer, it should be beneficial for the precision to reduce as much as possible the time needed for stabilisation of the quadrupole after a jump from one mass to another, in view to increase the sampling frequency. For the same reason, the number of sweeps set during an isotopic analysis should be kept as great as possible, but attention must be paid (i) to overall accuracy when the number of sweeps becomes high, and (ii) to not consume a considerable analytical time only for stabilisation. The close examination of noise power spectra established with various sample uptake rates does not only reveal the frequencies at which the noises occur, but also their amplitude, making so easier the choice of a pump speed in regard to the acquisition parameters. Some sample introduction flows appear practically more suitable than others, because they produce low white and frequency-dependent noises, and because the fundamental noise issuing from the pump itself can be more efficiently reduced by ratioing operations. Such a preliminary investigation is easy and fast to perform. It can provide information beneficial to the quality of measurements as demonstrated by the experimental within-run RSD % which closely follows that predicted by counting statistics.

Acknowledgement

We wish to express special thanks to B. Sharp and I. Begley and E. Verrecchia for their precious advises, to A. Leroy and S. Luan for their technical assistance on the ICP-MS.

Tab. III. Accuracy and reproducibility of Pb isotopic measurements on natural environmental samples (sediments, lichens, airborne particulate matters, and natural rainwater).

	$^{206}Pb/^{204}Pb$	$^{207}Pb/^{204}Pb$	$^{208}Pb/^{204}Pb$	$^{206}Pb/^{207}Pb$	$^{208}Pb/^{206}Pb$
Accuracy					
Aerosols					
Toulouse	17.87 ± 0.04	15.57 ± 0.04	37.77 ± 0.08	1.147 ± 0.002	2.113 ± 0.004
Toulouse (TIMS)[1]	17.892 ± 0.004	15.622 ± 0.004	37.90 ± 0.01	1.1453 ± 0.0001	2.1184 ± 0.0004
Le Havre	17.23 ± 0.05	15.54 ± 0.06	37.03 ± 0.16	1.109 ± 0.002	2.149 ± 0.005
Le Havre (TIMS)[1]	17.236 ± 0.004	15.536 ± 0.005	37.09 ± 0.01	1.1094 ± 0.0001	2.1517 ± 0.0003
Reproducibility					
Lichens[2]					
81EP	18.17 ± 0.05	15.56 ± 0.05	38.06 ± 0.13	1.168 ± 0.002	2.095 ± 0.006
81EP#	18.21 ± 0.05	15.60 ± 0.06	38.12 ± 0.12	1.168 ± 0.002	2.094 ± 0.004
25VUP	18.47 ± 0.03	15.71 ± 0.03	38.43 ± 0.08	1.176 ± 0.001	2.081 ± 0.004
25VUP#	18.51 ± 0.05	15.74 ± 0.04	38.60 ± 0.09	1.177 ± 0.001	2.085 ± 0.002
40VUP	18.74 ± 0.06	15.76 ± 0.05	38.73 ± 0.12	1.190 ± 0.001	2.067 ± 0.003
40VUP#	18.74 ± 0.04	15.75 ± 0.04	38.81 ± 0.09	1.191 ± 0.001	2.071 ± 0.001
Overbank sediments[3]					
SB 42/1.3	18.80 ± 0.06	15.75 ± 0.06	38.91 ± 0.14	1.194 ± 0.001	2.070 ± 0.002
SB 42/1.3#	18.66 ± 0.04	15.63 ± 0.05	38.52 ± 0.10	1.194 ± 0.002	2.065 ± 0.003
SB 43/1.1	18.44 ± 0.03	15.58 ± 0.03	38.36 ± 0.06	1.183 ± 0.002	2.079 ± 0.004
SB 43/1.1#	18.49 ± 0.06	15.62 ± 0.05	38.39 ± 0.11	1.184 ± 0.002	2.076 ± 0.002
SB 43/1.3	18.46 ± 0.05	15.53 ± 0.05	38.28 ± 0.21	1.189 ± 0.003	2.075 ± 0.006
SB 43/1.3#	18.56 ± 0.04	15.61 ± 0.05	38.49 ± 0.11	1.189 ± 0.002	2.073 ± 0.006
SB 44/1.1	18.62 ± 0.04	15.73 ± 0.04	38.75 ± 0.08	1.184 ± 0.001	2.081 ± 0.002
SB 44/1.1#	18.65 ± 0.05	15.74 ± 0.05	38.79 ± 0.08	1.185 ± 0.001	2.080 ± 0.002
Rainwaters					
RW2	-	-	-	1.146 ± 0.002	2.122 ± 0.006
RW2#	-	-	-	1.142 ± 0.005	2.133 ± 0.008
RW10	-	-	-	1.156 ± 0.002	2.109 ± 0.006
RW10#	-	-	-	1.153 ± 0.003	2.119 ± 0.003
RW17	-	-	-	1.156 ± 0.003	2.114 ± 0.005
RW17#	-	-	-	1.153 ± 0.005	2.114 ± 0.005
RW25	-	-	-	1.157 ± 0.003	2.107 ± 0.005
RW25#	-	-	-	1.160 ± 0.004	2.107 ± 0.005
RW27	-	-	-	1.154 ± 0.004	2.113 ± 0.007
RW27#	-	-	-	1.157 ± 0.004	2.117 ± 0.010
RW28	-	-	-	1.155 ± 0.005	2.110 ± 0.007
RW28#	-	-	-	1.160 ± 0.004	2.105 ± 0.007
RW28#	-	-	-	1.158 ± 0.005	2.113 ± 0.007
RW40	-	-	-	1.154 ± 0.006	2.129 ± 0.009
RW40#	-	-	-	1.151 ± 0.002	2.125 ± 0.005
RW51	-	-	-	1.155 ± 0.003	2.099 ± 0.006
RW51#	-	-	-	1.156 ± 0.007	2.110 ± 0.015
RW56	-	-	-	1.158 ± 0.004	2.107 ± 0.008
RW56#	-	-	-	1.157 ± 0.003	2.103 ± 0.009

[1]: TIMS values from [16]; [2]: lichens isotopic composition from [17]; [3]: overbank sediments from [18] ; (-): not determined. The errors are given at 95 % confidence level.

References

1. Quétel, C. R.; Thomas, B.; Donard, O.F.X.; Grousset, F. E. *Spectrochim. Acta B* **1997**, *52,* 177.
2. Monna, F.; Loizeau, J.-L.; Thomas, B.; Guéguen, C.; Favarger, P.-Y. *Spectrochim. Acta B* **1998**, *53*, 1317-1333.
3. Crain, J.S.; Houk, R.S.; Eckels D.E. *Anal. Chem*. **1989**, *61*, 606-612.
4. Goudzwaard, M. P.; de Loos-Vollebregt, M. T. C. *Spectrochim. Acta B* **1990**, *45*, 8, 887-901.
5. Furuta, N. *J. Anal. At. Spectrom*. **1991**, *6*, 199-203.
6. Easley, S. F.; Monnig, C. A.; Hieftje, G. M. *Appl. Spectroscopy*. **1991**, *45*, 8, 1368-1371.
7. Luan, S.; Pang, H.; Shum, S. C. K.; Houk, R. S. *J. Anal. Atom. Spectrom*. **1992**, *7*, 799-805.

8. Ince, A.T.; Williams, J.G.; and Gray, A. L. *J. Anal. At. Spectrom*. **1993**, *8*, 899-903.
9. Begley, I.S.; Sharp, B.L. *J. Anal. At. Spectrom*. **1994**, *9*, 171-174.
10. Pollmann, D.; Pilger, C.; Hergenröder, R.; Leis, F.; Tschöpel, P.; Brooekaert, J. A. C. *Spectrochim. Acta B* **1994**, *49*, 7, 683-690.
11. Gray, A.L.; Williams, J.G.; Ince, A.T.; Liezers, M. *J. Anal. At. Spectrom*. **1994**, *9*, 1179-1181.
12. Ketterer, M.E.; Peters, M.J.; Tisdale, P.J. *J. Anal. At. Spectrom.* **1991**, *6*, 439-443.
13. Hobbs, P.; Spillane, D. E. M.; Snook, R. D.; Thorne, A. P. *J. Anal. At. Spectrom.* **1988**, *3*, 543-546.
14. Grousset, F.E.; Quétel, C.R.; Thomas, B.; Buat-Ménard, P.; Donard, O.F.X.; Bucher, A. *Environ. Sci. Technol.* **1994**, *28*, 1605-1608.
15. Hamester, M.; Stechmann, H.; Steiger, M.; Danneker, W. *Sci. Tot. Environ.* **1994**, *146/147*, 321-323.
16. Monna, F.; Lancelot, J.; Croudace, I.; Cundy, A.B.; Lewis, T. *Environ. Sci. Technol*. **1997**, *31*, 2277-2286.
17. Monna, F.; Aiuppa A.; Varrica D.; Dongarrà G. *Environ. Sci. Technol*. **1999**, 33, 2517-2523.
18. Monna, F.; Hamer, K.; Lévêque, J.; Sauer, M. *J. Geochem. Explor*. **2000**, *68*, 201-210.

Available online at www.sciencedirect.com
SCIENCE DIRECT®

Science of the Total Environment 327 (2004) 197–214

Science of the Total Environment
An International Journal for Scientific Research into the Environment and its Relationship with Humankind

www.elsevier.com/locate/scitotenv

Environmental impact of early Basque mining and smelting recorded in a high ash minerogenic peat deposit

F. Monna[a,b,*], D. Galop[c], L. Carozza[d], M. Tual[a], A. Beyrie[e], F. Marembert[f], C. Chateau[g], J. Dominik[h], F.E. Grousset[i]

[a] *Laboratoire GéoSol, UMR INRA – Université de Bourgogne A111, CST, 6 bd Gabriel, F-21000 Dijon, France*
[b] *Archéologies, Cultures et Sociétés. Bourgogne et France Orientale du Néolithique au Moyen Age, UMR 5594 CNRS-Université de Bourgogne, Bat. Gabriel, F-21000 Dijon, France*
[c] *Laboratoire de Chrono-Ecologie, UMR 6565 CNRS, UFR des Sciences et Techniques, Université de Besançon, 16 route de Gray, F-25030 Besançon Cedex, France*
[d] *INRAP Grand-Est UMR 8555, Centre d'Anthropologie, F-21000 Dijon, France*
[e] *UTAH – UMR 5608 CNRS, Maison de la Recherche, Université Toulouse – le Mirail, F-31058 Toulouse Cedex, France*
[f] *Centre d'anthropologie, UMR 8555 CNRS, 30 allée Jules Guesde, F-31000 Toulouse, France*
[g] *Centre des Sciences de la Terre, 6 bd Gabriel, F-21000 Dijon, France*
[h] *Institut F.-A. Forel, Université de Genève, 10 route de Suisse, CH-1290 Versoix, Switzerland*
[i] *Département de Géologie et Océanographie, UMR CNRS 5805 EPOC, Université Bordeaux 1, Avenue des Facultés, F-33405 Talence, France*

Received 1 June 2003; received in revised form 28 January 2004; accepted 30 January 2004

Abstract

More than four metres of core, covering almost 5000 years of deposition, were collected in a high ash minerogenic peat deposit located in the High Aldudes valley (Basque country), an area well known for its mineral abundance, exploited from Roman Times at least. Although minerogenic peatlands are not generally considered as the best archives to reconstruct past atmospheric metal deposition history, lead isotopic geochemistry demonstrates the integrity of the Pb record at least within the three upper meters; that is to say over the last four millennia. Zn, Cd and Cu may have been widely redistributed either by biological cycling, advective groundwater movements, or diffusional processes. Anthropogenic lead input phases are clearly pinpointed by positive shifts in Pb/Sc ratios with concomitant sharp drops in ^{206}Pb/^{207}Pb ratios. They are often accompanied by significant declines in tree taxa, interpreted as increasing demand for wood to supply energy for local mining and/or metallurgical operations. Periods of mining and/or smelting activity are identified during Antiquity and Modern Times, and are also confirmed by textual and field evidence. Inputs from the Rio Tinto (Southern Spain), often invoked as a major lead contributor to the European atmosphere during Roman Times, were not detected here. This remote source was probably masked by local inputs. Other mining and/or smelting phases, only suspected by archaeologists, are here identified as early as the Bronze Age. Although the durations of these phases are possibly overestimated because of detrital inputs consequent to the release of lead from polluted soils over a long period of time after major pollutant inputs, the periods at which pollution peaks occur are in good agreement with archaeological knowledge and palaeo-botanical data. The

---

*Corresponding author. *Present address*: UMR 5594 CNRS-Université de Bourgogne CST, 6 bd Gabriel, F-21000 Dijon, France. Tel.: +33-3-80-396-360; fax: +33-3-80-396-387.

E-mail address: Fabrice.Monna@u-bourgogne.fr (F. Monna).

0048-9697/04/$ - see front matter
doi:10.1016/j.scitotenv.2004.01.010

combination of geochemical and palaeo-botanical techniques with field archaeology, therefore provides a powerful tool in studying the interaction of early human societies with their environment, as regards early mining and smelting.

Keywords: Pollution; Lead isotopes; Peat deposit; Atmospheric deposition; Mining; Smelting

1. Introduction

The oldest French settlement of copper miners and metalworkers (3rd millennium BC) has been recently discovered close to Montpellier–Southern France (Ambert et al., 2002). Such exploitation was probably initiated under the stimulus of populations living in the Alpine arc, themselves influenced by precursor cultures from the Balkans, Hungary, Poland and Germany (Chapman and Tylecote, 1983; Gale et al., 1991). Early metallurgical centres seem also to have existed, probably as far back as the Late Neolithic, in Northern Africa and Southern Spain, although definitive proof is still lacking (Rovira, 1998). This forces us to reconsider the relationships between populations living in Eastern and in South-West Europe from the Late Neolithic to the Bronze Age. The mineral-rich Basque country, with its key geographical position, may have interlinked both these cultures. However, even if remains of local extraction during antiquity are numerous, no proof of earlier mining has yet been found. Prehistoric mining was superficial, focusing on a simple hand-picking of minerals, and evidence may have been masked or destroyed by subsequent activities.

However, traces of historical mining or smelting may have been recorded in natural archives. The efficiency of such an environmental approach has been successfully demonstrated at least for lead, at continental scale as well as at local scale, in sediments (Brännvall et al., 1997; Schettler and Romer, 1998; Camarero et al., 1998; Brännvall et al., 1999; Monna et al., 2000a; Renberg et al., 2000, 2001; Ariès, 2001; Eades et al., 2002; Degryse et al., 2003), polar ice (Hong et al., 1994; Rosman et al., 1997), and peatlands (Glooschenko et al., 1986; Van Geel et al., 1989; Kempter et al., 1997; Weiss et al., 1997; Farmer et al., 1997; Kempter and Frenzel, 2000; Shotyk et al., 1998, 2001; Mighall et al., 2002; Martínez-Cortizas et al., 1997, 2002). Concerning peatlands, it is generally accepted that the most appropriate media are ombrotrophic peat bogs because their chemistry and hydrology tend to promote the immobility of metals deposited (Lee and Tallis, 1973; Jones and Hao, 1993; Shotyk, 1996a; Norton et al., 1997; Martínez-Cortizas et al., 1997; Shotyk et al., 1998; MacKenzie et al., 1998a). Evidence of post-depositional lead migrations has already been noticed, at the time scale of the last century, in minerogenic peatlands with ash content less than 10%, making historical interpretation impossible (MacKenzie et al., 1998b). However, at the millennia time scale, coherent lead records have also been reported in marshes featured by high ash content reaching up to 94% (Alfonso et al., 2001). Other studies performed in mineral-rich peatlands (Espi et al., 1997; Shotyk, 2002), indicate that even predominantly minerogenic sites may properly preserve the record of anthropogenic atmospheric Pb deposition or, at least, may provide a qualitative surrogate for historical pollution (Shotyk, 1996b, 2002). In all cases, anthropogenic inputs have to dominate over detrital contribution (Weiss et al., 1999), and mineral dissolution of the underlying sediments must not contribute measurably to the lead inventory (Shotyk, 2002). Invaluable information on the sources may be obtained by the measurement of lead isotopic compositions (Brännvall et al., 1997; Shotyk et al., 1998; MacKenzie et al., 1998b; Weiss et al., 1999; Dunlap et al., 1999; Renberg et al., 2000; Alfonso et al., 2001; Ariès, 2001; Weiss et al., 2002; Martínez-Cortizas et al., 2002; Shotyk et al. 2002a,b; Monna et al., 2004).

Regrettably ombrotrophic peat bogs are not available in the High Aldudes Valley, a Basque valley well known for its mineral abundance, so we had to investigate the possible use of geochemical signals archived in high ash minerogenic peatlands to constrain the history of local mining and smelting operations. The pollen record has been investigated too. It generally mirrors the influence of climate and anthropogenic pressure, such as cultivation, pastoral activities and forest clearance (Williams, 2000), but signs of deforestation may also be related to energy demands for metal production (Galop and Jalut, 1994; Blanchot et al., 2001), unless they result from agricultural extension. All these new data are confronted to the sparse archaeological knowledge available.

2. The site and local history

Palaeozoic Basque mountains and Permo-Triassic cover contain abundant mineral resources, so that exploration was re-launched in the late 1970s (Fig. 1). Most of the ore deposits are found in upper ordovician detrital formations composed of bulky sandstones, alternation of pelites and sandstones, and black pelites. Mined from Roman Times (Galop et al., 2001; Beyrie et al., in press), ores of Fe, Cu, Ag, Sb, and to a lesser extent of Pb and Zn, consist of sub-concordant piles or secant veins governed by fractures. In the Middle Ages, this district furnished Bayonne with silver for coinage (Gapillou, 1981). Before the French Revolution, annual production reached more than 100 tons of copper, but exploitation then collapsed because of the lack of wood consequent to intense deforestation. In 1793, Spanish troops plundered the village of Banca and destroyed Cu smelting installations. Marginal exploitation is reported throughout the 19th and 20th centuries. This area yielded more than 20 000 tons of metallic copper (it is the richest district in France) and approximately 400 tons of silver.

The district of St. Martin d'Arrossa lies directly on Palaeozoic formations. It mainly consists of pile and vein stockwork of siderite, which can be locally associated with Cu. Also, mined by Romans, it was sporadically worked for iron from the 18th century, and more substantially from the late 19th century to the World War I.

The Quinto Real peat deposit (cf. Fig. 1) is located close to the Spanish border (910 m a.s.l.), almost at the interfluve of the Baztan and Aldudes valleys. It lies on a surface of approximately 1 ha on Palaeozoic terrain. *Sphagnum*-dominated at the top, it is fed by some temporary streams originating from a small catchment area (Galop et al., 2001). The site is far from any current settlements.

3. Material and methods

3.1. Sampling

Sampling was carried out using a Russian GIK-type corer (8 cm in diameter) following the conventional two-borehole technique. The samples were wrapped in clean plastic bags in order to prevent external contamination. Sub-sampling for geochemical analysis was performed by cutting 2-cm thick sections at intervals of 4 cm, after removing with a PTFE spatula the outer parts, which could have been in contact with the corer, the tube or the plastic film. A few coarse roots, mostly present at the top, were removed using clean plastic pliers. Samples were transferred to LDPE beakers and slowly dried at 60 °C for 3 days. They were finely powdered in an automatic agate mortar pre-cleaned with diluted HCl and MilliQ water, then stored in the dark before further analyses. Sub-sampling for pollen analysis was carried out at 4 cm intervals in the first metre, and at 8 cm intervals to the bottom. These latter were kept wet until pollen preparation as described below.

3.2. Chemical composition

Lost on ignition (LOI) was performed by heating approximately 1 g of peat samples to 90 °C, and then by combustion at 450 °C for 4 h. Total organic carbon (TOC) was also measured twice on half of the samples by Nitrogen Carbon Analyser (NA 1500 W-2—Carlo Erba) at a precision of 5%. LOI and TOC were closely correlated ($\mathrm{LOI} = 1.81 \times \mathrm{TOC}$, $r^2 > 0.99$, $P < 0.01$). Refractory elements such as Sc, Th, Cr, Rb and La and REE were measured by instrument neutron activation analysis (INAA) at Actlabs (Ontario, Canada). Accuracy was checked within ±10–15% on the basis of standards routinely measured and NIST 1547, PACS-1, BCSS-1 added to the set.

For complementary determinations, approximately 500 mg of powdered samples were oxidized

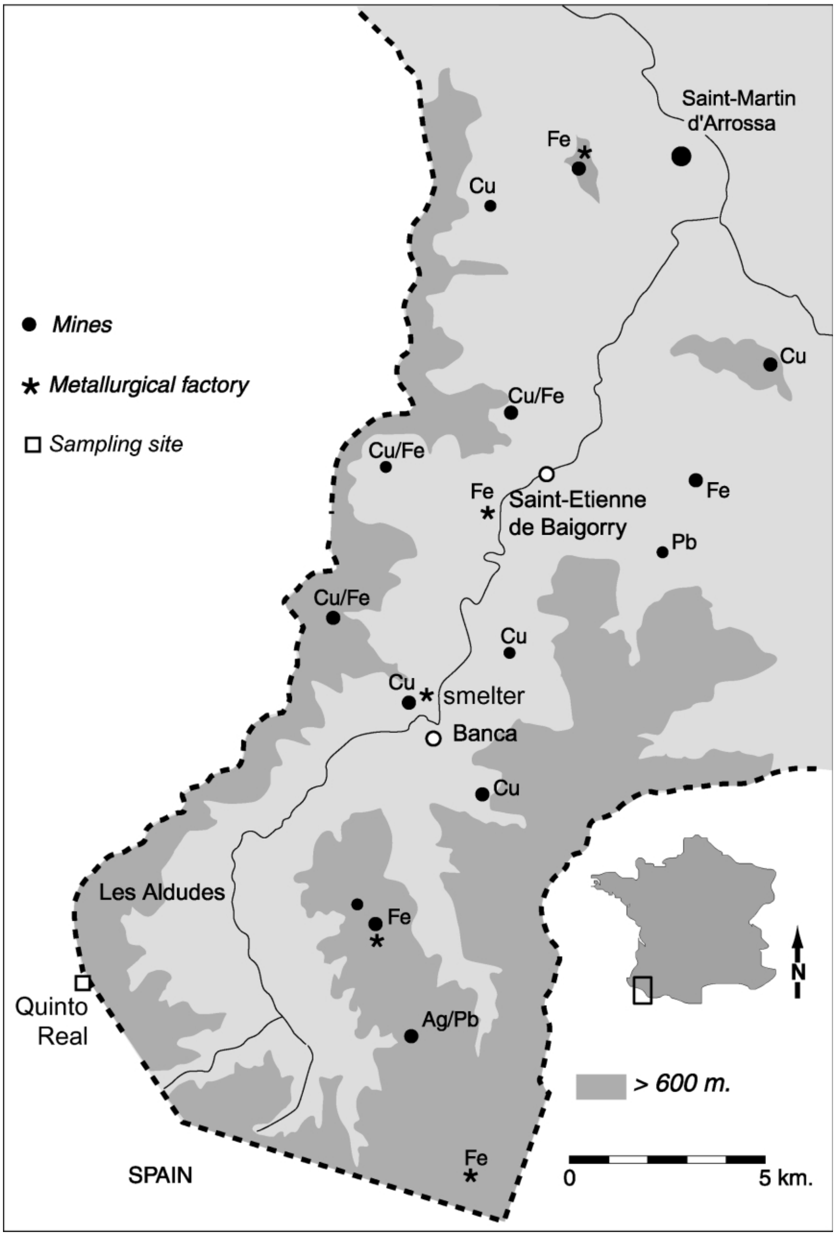

Fig. 1. Map of the Basque country. The ore guides and their nature have been reported.

with 4 ml of Suprapur H_2O_2 (Merck–Germany), reacting on hot plate at 40 °C overnight. Once dried, samples were digested with a mixture of Suprapur and concentrated HCl, HNO_3 and HF (Merck, Germany) in closed PTX vessels under Milestone-ETHOS microwave assistance (Monna et al., 2000a). One blank and one reference material standard (RMS), among NIST 1547, JSD 1 and JSD 2, were added to each set.

A one-third aliquot of solution was measured at the F.-A. Forel Institute by HP 4500 inductively coupled plasma–mass spectrometer (ICP-MS) for

Cu, Zn, Cd and Pb concentration determination using both external and internal (Re, Rh) calibrations. The whole procedure was performed in a clean room (US class 1000–10 000). Blanks were found negligible for all elements compared to the amount contained in the samples. Pb, Cd and Cu concentrations were in good agreement with the certified values of RMSs (within ± 10% for lead and copper, and at worst approximately ± 15–20% for Cd and Zn). Lead from the two-thirds aliquot was pre-concentrated on ionic resin AG1X4 (Biorad) and measured for isotopic abundance by HP 4500 ICP-MS (Monna et al., 1998, 2000b). Precisions of $^{206}Pb/^{207}Pb$ and $^{208}Pb/^{206}Pb$ ratios were approximately 0.27% and 0.31%, respectively. Seven samples were duplicated with the Perkin Elmer 6100 ICP-MS at the University of Neuchâtel. In all cases, the 95% confidence intervals overlapped. Pristine fragments of artefacts were obtained by scratching with a stainless steel tool. They were washed with a mixture of diluted Suprapur HCl and HNO_3 to remove any remains of corrosion or pollution. The fragments were dissolved and lead isotopes were measured following the procedure described above.

3.3. Radiocarbon dating

Three peat samples were dated using ^{14}C-beta counting at the Centre des Sciences de la Terre-University of Lyon (Table 1, Fig. 2), and two others by AMS at Beta Analytic Inc laboratory, Miami. All ^{14}C-dates were calibrated using Calib 4.1.3 software (Stuiver et al., 1998).

3.4. Pollen determination

Briefly, pollen preparation consists in treatments with 10% HCl, 10% KOH, HF, acetolysis and final mounting in glycerine. More than 500 terrestrial pollen grains, defined according to Reille (1992) and Moore et al. (1986) were counted in each sample. *Cyperaceae* and spores were systematically excluded from the pollen sum, as was *Alnus*; its over-representation may mask the dynamics of other taxa (Wiltshire and Edwards, 1993). Pollen spectra have been given elsewhere (Galop et al., 2001). They will be used here only for discussion.

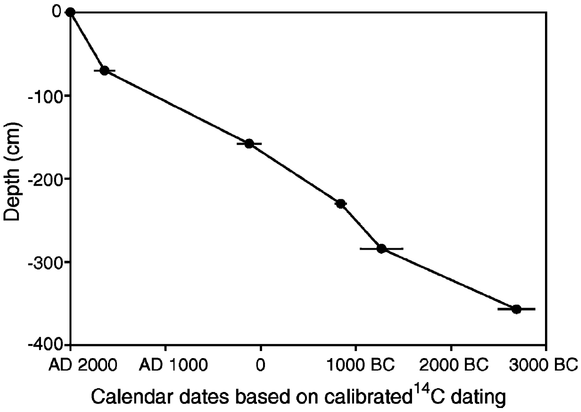

Fig. 2. Depth plotted against calibrated radiocarbon calendar dates at Quinto Real, Basque country, France.

4. Results

4.1. Organic matter and lithophilic elements

The LOI profile (Table 2, Fig. 3) exhibits wide variations, from 7% in the layer richest in sand (321-cm depth) to 85% at the top. The first 300 cm are the most organic (avg: 60%); although two sections, at 63–86 and 134–157-cm depth, are more mineral. The uppermost 300 cm can be

Table 1
Age-depth relationship for the Quinto Real core. The data are calibrated to calendar dates AD or BC

Laboratory no.	Depth (cm)	Uncalibrated date	Calibrated date, and uncertainties (2σ)
Beta-156998	69–71	290 ± 40	1486 (1640) 1664 cal AD
Ly-10587	157–159	1895 ± 50	3 (88, 100, 125) 240 cal AD
Ly-10588	229–231.5	2645 ± 45	896 (804) 787 cal BC
Ly-10589	283–285	3045 ± 70	1485 (1368, 1362, 1315) 1051 cal BC
Beta-156997	357	4120 ± 40	2876 (2662, 2646, 2625) 2501 cal BC

Table 2
Lost on ignition (LOI), Cu, Zn, Cd, Pb, Sc contents and $^{206}Pb/^{207}Pb$ and $^{208}Pb/^{206}Pb$ ratios. The errors for isotopic ratios are given at 95% confidence level. See Section 3 paragraph for errors in concentration measurements

Name	Depth (cm)	LOI%	Cu $\mu g\ g^{-1}$	Zn $\mu g\ g^{-1}$	Cd $\mu g\ g^{-1}$	Pb $\mu g\ g^{-1}$	Sc $\mu g\ g^{-1}$	$^{206}Pb/^{207}Pb$	±	$^{208}Pb/^{206}Pb$	±
R 007	−7	nd	3.9	47.5	0.34	75.1	nd	1.159	0.003	2.103	0.006
R 012	−12	nd	17.9	133.3	1.35	267.6	nd	1.160	0.003	2.100	0.006
R 016	−16	nd	5.5	102.7	1.19	765.0	0.5	1.165	0.004	2.105	0.006
R 020	−20	nd	4.4	39.8	1.03	109.2	0.8	1.163	0.009	2.105	0.006
R 028	−28	85.2	10.4	30.0	1.02	140.7	2.3	1.172	0.004	2.095	0.006
R 036	−36	59.7	10.5	16.3	0.34	19.2	6.5	1.179	0.003	2.086	0.008
R 045	−45	54.1	13.4	19.8	0.32	5.4	6.5	1.183	0.002	2.102	0.005
R 055	−55	50.9	15.3	16.7	0.20	7.9	9.7	1.194	0.003	2.088	0.006
R 063	−63	42.9	7.9	7.9	0.31	8.8	10.7	1.197	0.002	2.105	0.006
R 071	−71	37.8	8.9	14.6	0.23	14.1	13.1	1.191	0.008	2.107	0.007
R 078	−78	nd	8.1	12.6	nd	10.3	12.1	nd	nd	nd	nd
R 086	−86	41.6	12.7	16.0	0.21	19.2	13.0	1.190	0.003	2.099	0.005
R 095	−95	55.6	11.2	21.6	0.23	9.2	9.1	1.190	0.003	2.105	0.005
R 101	−101	57.0	14.3	16.2	0.11	13.8	8.9	1.183	0.001	2.101	0.008
R 113	−113	62.6	12.7	10.2	0.19	10.2	7.4	1.188	0.004	2.091	0.007
R 117	−117	59.5	13.6	16.0	nd	13.3	7.7	nd	nd	nd	nd
R 124	−124	58.1	10.8	9.6	0.20	11.5	8.1	1.190	0.002	2.100	0.005
R 134	−134	45.2	8.8	9.8	0.31	nd	10.3	1.196	0.003	2.098	0.008
R 136	−136	40.4	11.8	11.2	0.15	29.0	12.2	1.180	0.003	2.109	0.006
R 140	−140	30.7	6.9	10.0	0.29	25.0	14.2	nd	nd	nd	nd
R 148	−148	43.6	10.4	9.6	0.25	32.5	12.2	1.186	0.002	2.092	0.004
R 157	−157	45.1	12.6	11.7	0.38	nd	12.0	1.183	0.003	2.099	0.006
R 161	−161	50.6	15.8	12.9	0.37	32.5	11.2	1.183	0.003	2.101	0.008
R 169	−169	76.3	10.2	11.9	0.41	13.2	5.9	nd	nd	nd	nd
R 177	−177	51.9	12.5	16.1	0.20	15.4	11.1	1.187	0.002	2.097	0.003
R 185	−185	63.4	6.5	12.8	0.29	5.0	7.5	1.190	0.004	2.093	0.008
R 192	−192	64.0	6.9	10.2	0.25	7.1	7.2	1.200	0.005	2.090	0.012
R 201	−201	57.9	9.7	11.5	0.29	5.6	9.4	nd	nd	nd	nd
R 209	−209	73.6	11.5	14.4	0.23	9.4	5.7	1.178	0.002	2.094	0.004
R 217	−217	66.9	7.1	12.0	0.23	10.6	6.7	1.177	0.005	2.099	0.011
R 221	−221	71.6	6.5	10.2	0.19	10.6	5.0	1.176	0.002	2.095	0.004
R 224	−224	68.4	7.4	12.9	nd	10.4	6.3	nd	nd	nd	nd
R 233	−233	75.6	6.6	20.6	0.21	10.6	4.6	1.177	0.003	2.095	0.008
R 241	−241	74.5	5.9	39.4	0.30	12.8	6.3	1.172	0.004	2.099	0.008
R 247	−247	59.3	7.4	29.6	nd	15.1	7.9	nd	nd	nd	nd
R 252	−252	60.2	6.3	21.5	0.21	6.2	7.2	1.207	0.003	2.087	0.007
R 261	−261	61.9	7.9	12.5	0.24	9.7	8.9	1.190	0.002	2.100	0.010
R 269	−269	52.5	7.1	9.1	0.20	7.3	9.0	1.208	0.002	2.091	0.004
R 273	−273	51.9	6.9	10.1	0.27	6.1	11.0	nd	nd	nd	nd
R 281	−281	57.1	9.6	10.7	0.19	9.6	8.3	1.188	0.004	2.101	0.008
R 285	−285	62.5	11.2	17.9	0.25	7.0	10.4	1.191	0.002	2.094	0.004
R 294	−294	40.2	21.0	21.9	0.14	14.0	12.1	1.187	0.003	2.110	0.008
R 300	−300	24.2	12.7	29.8	0.52	2.9	18.1	1.227	0.003	2.073	0.006
R 305	−305	17.0	10.8	53.3	0.12	6.7	11.7	1.215	0.004	2.083	0.006
R 313	−313	7.6	6.3	24.6	0.34	1.3	10.4	nd	nd	nd	nd
R 321	−321	7.0	6.2	34.9	0.18	6.2	9.1	1.219	0.002	2.085	0.005
R 323	−323	6.9	5.9	45.5	0.35	5.9	12.6	1.233	0.005	2.062	0.010
R 333	−333	16.9	10.7	45.1	0.28	9.9	13.4	1.218	0.004	2.087	0.009
R 341	−341	20.2	nd	nd	nd	16.3	18.9	1.199	0.003	2.106	0.009
R 345	−345	21.6	10.9	47.1	0.11	7.4	14.7	1.206	0.002	2.100	0.005
R 350	−350	21.5	10.4	40.2	nd	9.2	16.4	nd	nd	nd	nd
R 359	−359	42.6	9.1	25.2	0.24	9.2	8.8	1.200	0.003	2.094	0.005

Table 2 *(Continued)*

Name	Depth (cm)	LOI%	Cu $\mu g\ g^{-1}$	Zn $\mu g\ g^{-1}$	Cd $\mu g\ g^{-1}$	Pb $\mu g\ g^{-1}$	Sc $\mu g\ g^{-1}$	$^{206}Pb/^{207}Pb$	±	$^{208}Pb/^{206}Pb$	±
R 366	−366	57.2	10.1	17.6	0.31	8.5	7.5	1.194	0.004	2.092	0.008
R 375	−375	57.0	7.1	12.7	0.19	8.6	7.5	1.189	0.003	2.099	0.005
R 379	−379	45.6	12.6	21.8	nd	13.0	12.3	nd	nd	nd	nd
R 386	−386	37.8	7.9	14.6	0.19	5.7	6.0	1.204	0.003	2.079	0.007
R 390	−390	39.7	5.9	21.5	0.25	4.3	7.2	1.200	0.003	2.092	0.004
R 398	−398	25.8	6.7	14.5	0.19	7.1	7.1	1.206	0.004	2.083	0.008
R 403	−403	32.4	6.1	17.8	0.23	3.3	8.8	1.221	0.004	2.069	0.007
R 414	−414	23.4	5.6	22.5	0.21	6.0	7.6	nd	nd	nd	nd

nd: Not determined.

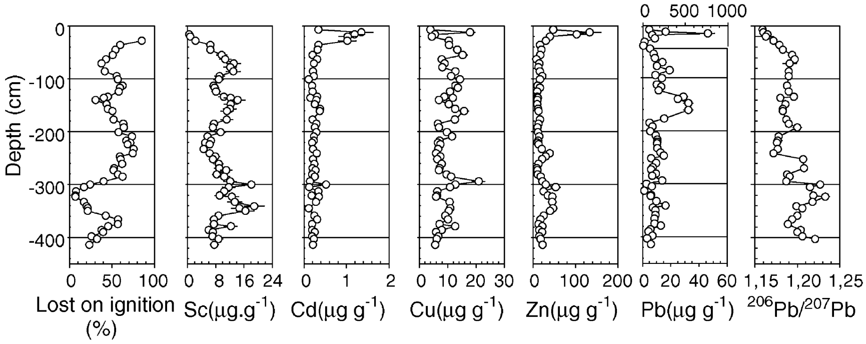

Fig. 3. Lost on ignition, scandium, cadmium, copper, zinc, lead and $^{206}Pb/^{207}Pb$ ratios plotted against depth. Note the break in the lead concentration axis. Most of errors represent less than the size of dots; otherwise the error bars represent a confidence level of 95%.

classified as peat and muck interbedded (Kivinen, 1980; Moris, 1989) or as low-ash carbonaceous sediments with interbedded high ash carbonaceous sediments and peat layers (Andrejko et al., 1983), but this latter classification rather matches the use of peat as fuel for industry (Wüst et al., 2003).

Considering the whole core, Sc content is inversely correlated to LOI ($r^2 = 0.46$, $P < 0.01$), but the correlation is improved if only the uppermost 300 cm are taken into account ($r^2 = 0.89$, $P < 0.01$) (Fig. 4). The same observation is made with other lithophilic elements (La, Th, Cr, Rb and REE not presented here), which are all strongly correlated with Sc ($r^2 > 0.85$, $P < 0.01$ for Rb and $r^2 > 0.96$ for the others).

4.2. Heavy metals

Cd, Zn and Pb concentrations increase in the topmost 40 cm and peak in approximately the

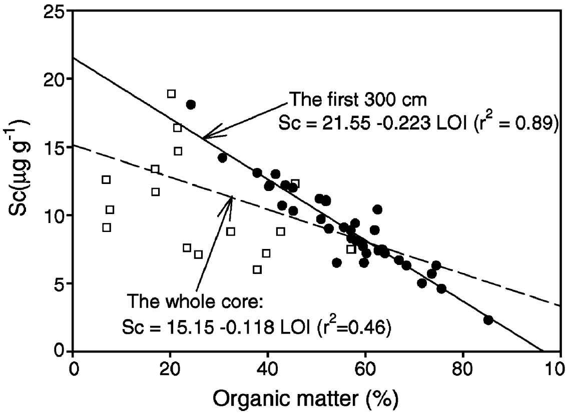

Fig. 4. Scandium content plotted against organic matter content; (●): the 300 cm topmost samples, (□): the others.

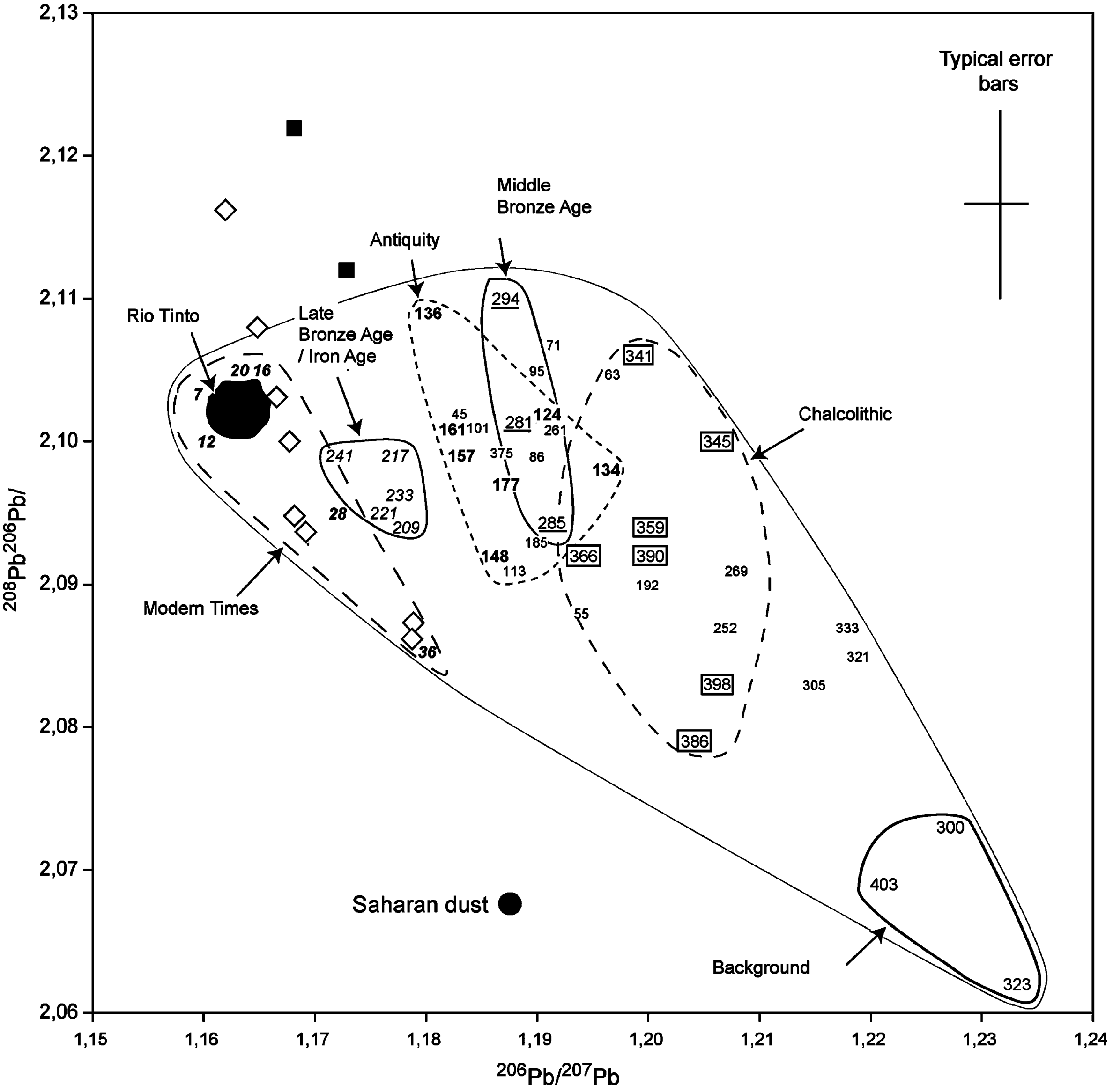

Fig. 5. ^{208}Pb/^{206}Pb vs. ^{206}Pb/^{207}Pb diagram. The peat samples are represented by their depth. Five clusters have been defined among the horizons featuring high Pb/Sc and low ^{206}Pb/^{207}Pb ratios on the basis of the cultural periods in which they appear (see text for more details). The isotopic compositions of artefacts dating from the Late Bonze Age (◇) and antiquity (■) (this study), and those of Saharan dusts (●) (Grousset et al., 1995) and Rio Tinto (Stos-Gale et al., 1995) are also plotted for further comparison.

same horizon at 1.35 μg g^{-1}, 133 μg g^{-1} and 765 μg g^{-1}, respectively, then decrease to the surface (Fig. 3). Below, the Cd profile is rather flat, whereas Zn exhibits smooth variations with two peaks at 241 and 305–350-cm depth. Pb rises more or less from the bottom to approximately 150-cm depth, except for a fall in the detrital horizon (310-cm depth), before decreasing to 5 μg g^{-1} at 45-cm depth. No clear tendencies are detected in the Cu profile. Its maximum value (21 μg g^{-1}) does not occur in the top horizons, but at 294-cm depth. Cd, Cu and Pb do not present any relationship with LOI as indicated by insignificant Spearman's coefficient values, whereas Zn shows a weak inverse correlation ($r_{sp} = -0.347$, $P < 0.01$).

4.3. Lead isotopic compositions

$^{206}Pb/^{207}Pb$ ratios vary widely from 1.233, in the most detrital layers (300–320-cm depth), to 1.159 at the top (Fig. 3). This evolution is not regular but presents five major shifts toward low $^{206}Pb/^{207}Pb$ ratios: (i) at approximately 375-cm depth; (ii) between 280 and 290-cm depth; (iii) between 209 and 241-cm depth; (iv) at 160-cm depth; and finally (v) an almost linear decline, from 63 cm to the top. Reported on a $^{208}Pb/^{206}Pb$ vs. $^{206}Pb/^{207}Pb$ diagram (Fig. 5), peat samples form a triangle rather than falling on a characteristic binary mixing line. The samples from the most detrital horizons (300, 403, 323-cm depth) define the first summit of the triangle featured by highest $^{206}Pb/^{207}Pb$ and lowest $^{208}Pb/^{206}Pb$ ratios. The second summit corresponds to samples having high $^{208}Pb/^{206}Pb$ ratios (approx. 2.105) with intermediate $^{206}Pb/^{207}Pb$ values (approx. 1.19–1.20). The last one matches the uppermost samples (7–20-cm depth) with the lowest $^{206}Pb/^{207}Pb$ ratios (<1.17) and $^{208}Pb/^{206}Pb$ ratios of approximately 2.100–2.105. Artefacts produced during the Late Bronze Age and Antiquity are also reported on the diagram for further comparison.

5. Discussion

5.1. Origin of mineral material and assessment of anthropogenic contribution

Previous studies have shown that mineral matter may affect the distribution of metals in a peat core (Shotyk, 1996a,b; Weiss et al., 1997). The extent of anthropogenic contribution by comparison to natural contribution can, however, be estimated by normalising total metal concentrations to a conservative element, which has no anthropogenic origin. Lithophilic elements such as Sc, but also Zr, Ti, Al (Martínez-Cortizas et al., 1997, 2002; Schettler and Romer, 1998; Kempter and Frenzel, 2000; Shotyk et al., 2001, 2002a,b; Shotyk, 2002; Weiss et al., 2002) or ash content (West et al., 1997; Alfonso et al., 2001) are generally used for normalisation. This procedure implicitly assumes that natural Metal/Sc ratios of natural inorganic material are constant over time. However, atmospheric inorganic matter derives from sources, which may vary according to climate and human land occupation, thus affecting the consistency of natural Metal/Sc ratios (Shotyk et al., 2002a). As a matter of fact, large variations in ratios of lithophilic elements, such as La/Sc, were reported in an ombrotrophic peat bog in the Jura Mountains, and were interpreted as being the result of changes in the nature of atmospheric mineral inputs (Shotyk et al., 2001).

In the mineral-dominated Quinto Real core, the La/Sc and Th/Sc ratios exhibit only small variations around upper continental crust (UCC) values (La/Sc = 4.61 and Th/Sc = 1.47, Wedepohl, 1995) (Fig. 6). Moreover, when normalized to the shales, REEs display typical flat patterns (not shown here), reflecting a constant crust-derived origin. Thus, local inputs have presumably always predominated, suggesting constant REE patterns and Metal/Sc ratios over time. The values of these latter could be defined as reference before any enrichment factor or anthropogenic flux calculations. They will preferably be drawn from a given location rather than from earth crust compositions, because a global average cannot account for the local variations in rock chemistry (Weiss et al., 1997). In addition, chemical fractionation of the elements by physical fractionation during dust transport has been suggested, so that using crustal proportions as reference value for normalization may be meaningless (Martínez-Cortizas et al. 2002). At Quinto Real, samples do not exhibit constant Metal/Sc values at the bottom of the core (Fig. 7). Had they been present, suggesting uncontaminated horizons, they could have been used as reference values. In Fig. 4, the deficit in scandium below 300 cm by comparison to the organic matter

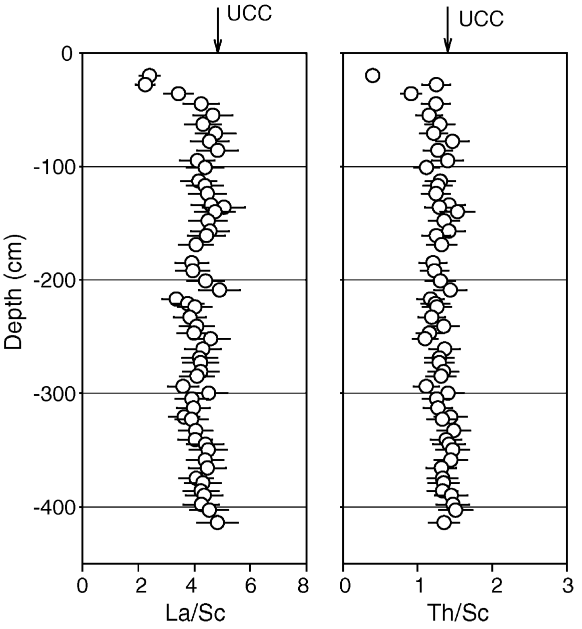

Fig. 6. Evolution of La/Sc and Th/Sc ratios with depth in the Quinto Real core. The values of the upper continental crust (UCC) (Wedepohl, 1995) are also given. The error bars represent a confidence level of 95%.

content would rather indicate the presence of an authigeneous mineral phase, possibly resulting from water circulation as minerotrophic peatlands are not hydrologically isolated from the substratum (Shotyk, 1996a,b). For these reasons, consistent values for natural Metal/Sc ratios are difficult to determine and enrichment factor or anthropogenic fluxes cannot be properly calculated. Since quantitative information is not available, our aim is now to determine if the Metal/Sc ratio profiles can at least be interpreted qualitatively. Even if our suggestion that Metal/Sc ratios of natural inorganic material are constant over time were to prove unfounded, it is still logical to suppose that any variations would not significantly affect overall Metal/Sc ratios observed in polluted peat samples.

5.2. *Evaluation of metal record integrity*

In a $^{208}\mathrm{Pb}/^{206}\mathrm{Pb}$ *vs* $^{206}\mathrm{Pb}/^{207}\mathrm{Pb}$ diagram, the natural (or background) end-member corresponds to samples possessing highest $^{206}\mathrm{Pb}/^{207}\mathrm{Pb}$ (1.22–1.23) and lowest $^{208}\mathrm{Pb}/^{206}\mathrm{Pb}$ ratios (2.06–2.07) (Fig. 5). Such values are comparable to those previously published for atmospheric inputs of crust-derived lead in Western Europe ($^{206}\mathrm{Pb}/^{207}\mathrm{Pb}$: 1.195–1.275) (Shotyk et al., 1998; Dunlap et al., 1999; Camarero et al. 1998; Alfonso et al., 2001; Martínez-Cortizas et al., 2002). The other horizons have been affected by one (or several) less radiogenic components. Five clusters can be defined

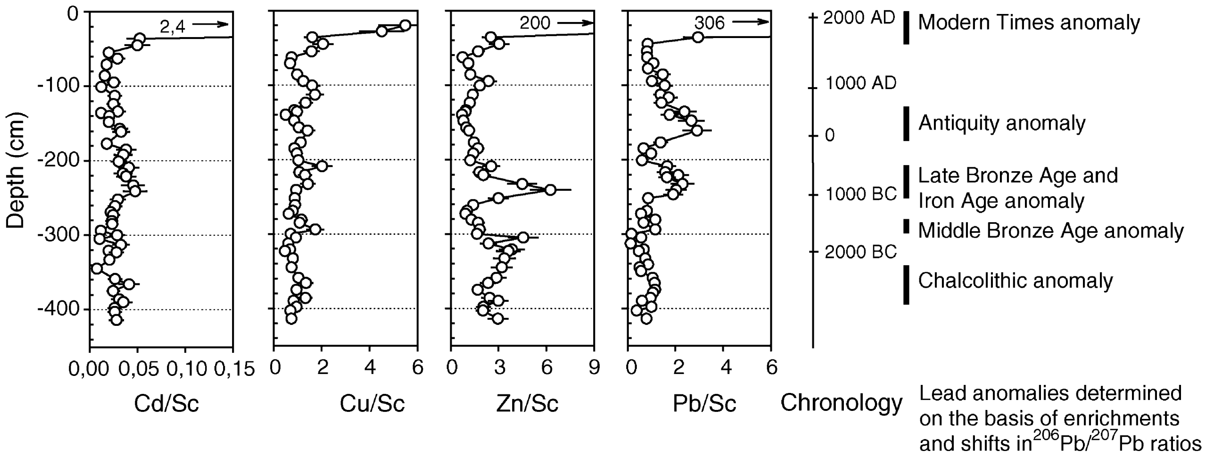

Fig. 7. Cd/Sc, Cu/Sc, Zn/Sc and Pb/Sc ratios vs. depth in the Quinto Real core. The error bars represent a confidence level of 95%.

among the horizons featuring high Pb/Sc and low $^{206}Pb/^{207}Pb$ ratios on the basis of the cultural periods in which they appear (cf. Figs. 7 and 8): Chalcolithic (samples at 341, 345, 359, 366, 386, 390, 398-cm depth), Middle Bronze Age (281, 285, 294 cm depth), Late Bronze Age–Iron Age (209, 217, 221, 233, 241-cm depth), Antiquity (124, 134, 136, 148, 157, 161, 177-cm depth) and Modern Times (7, 12, 16, 20, 28, 36-cm depth) (Fig. 5). It is clear that the lead enrichments observed in Chalcolithic horizons cannot be explained by a simple mineral dissolution of the substratum because their isotopic compositions are significantly different from those of the background. Similarly, Saharan dust inputs, very frequent in the Basque country, cannot be invoked given that the isotopic signature of this source (Grousset et al., 1995) does not fit with the data (Fig. 5). The presence of a sandy horizon at approximately 310 cm depth may have strongly facilitated the downward post-depositional translocation of lead from the Middle Bronze Age horizons. The intermediate position of the Chalcolithic group between the Middle Bronze Age horizons and the background well supports this thesis. Another possible scenario would be the real occurrence of anthropogenic inputs starting as early as the Chalcolithic. The interruption in the Pb/Sc trend observed approximately 310-cm depth in Fig. 7 would, therefore be due to the dilution of anthropogenic inputs by strong deposition of detrital inorganic matter. The study of a nearby core presenting no such variation in organic matter content could help resolve this question.

It is noteworthy that the above-mentioned clusters and the background as a whole form a triangle rather than a line (Fig. 5). The sequence in which the clusters appear, from low to high $^{206}Pb/^{207}Pb$ signatures (Modern Times, Late Bronze Age, Antiquity, Middle Bronze Age), does not correspond to any chronological order, so that it is impossible to explain their position as the result of a major migration of lead. It implies rather the result of a change in the type of mineral exploitation during these periods. Other works have already reported a very limited downward migration for Pb (Dumontet et al., 1990; Farmer et al., 1997; Vile et al., 1999), in part because almost all of the cationic species of this metal are bound to organic phase, which considerably reduces its mobility in peat (Shotyk, 1996b; Vile et al., 1999). Even in a mineral-dominated marsh in Aquitaine (with ash content up to 94%), the lead isotopic record yielded similar results to those obtained in ombrotrophic peat bogs and ice cores (Alfonso et al., 2001), and were quite consistent with the well-accepted assessment of world lead production during the last 5000 years (Settle and Patterson, 1980). Similarly, the comparison of both ombrotrophic and minerotrophic peat deposits in the Jura Mountains also demonstrated the relative immobility of lead and the possibility of using its record in minerogenic peatlands as a surrogate of past anthropogenic inputs in certain circumstances, such as the predominance of anthropogenic inputs over both detrital contribution and mineral dissolution of the substratum (Shotyk 1996a,b; Weiss et al., 1999; Shotyk, 2002). Although our core presents high ash content, the lead record at the considered time resolution appears to be well preserved, at least within the uppermost 300 cm. However, the duration of identified pollution phases may have been overestimated because of the release of lead from polluted soils over a long period of time after major atmospheric inputs.

For other metals the situation is more complex and different behaviours have been suggested depending on organic matter content, pH and fluctuations in redox potential (Shotyk, 1996b). Although copper ore deposits have been extensively mined in the valley since at least Roman Times, no clear trend in Cu/Sc ratios can be observed along the profile, except at the surface (Fig. 7). The present core does not seem suitable for the reconstruction of past atmospheric Cu inputs, unlike others previously reported (Kempter and Frenzel, 2000; Mighall et al., 2002). Like copper, Zn is an essential constituent for plants, and bioaccumulation processes may influence its distribution pattern, so that it is generally considered as a mobile metal, or at least as more susceptible to post-depositional redistribution than lead (Martínez-Cortizas et al., 1997). Here the Zn/Sc ratio profile also exhibits positive shifts in the Late Bronze Age/Iron Age and Modern Times but none is observed during Antiquity. Cadmium is not

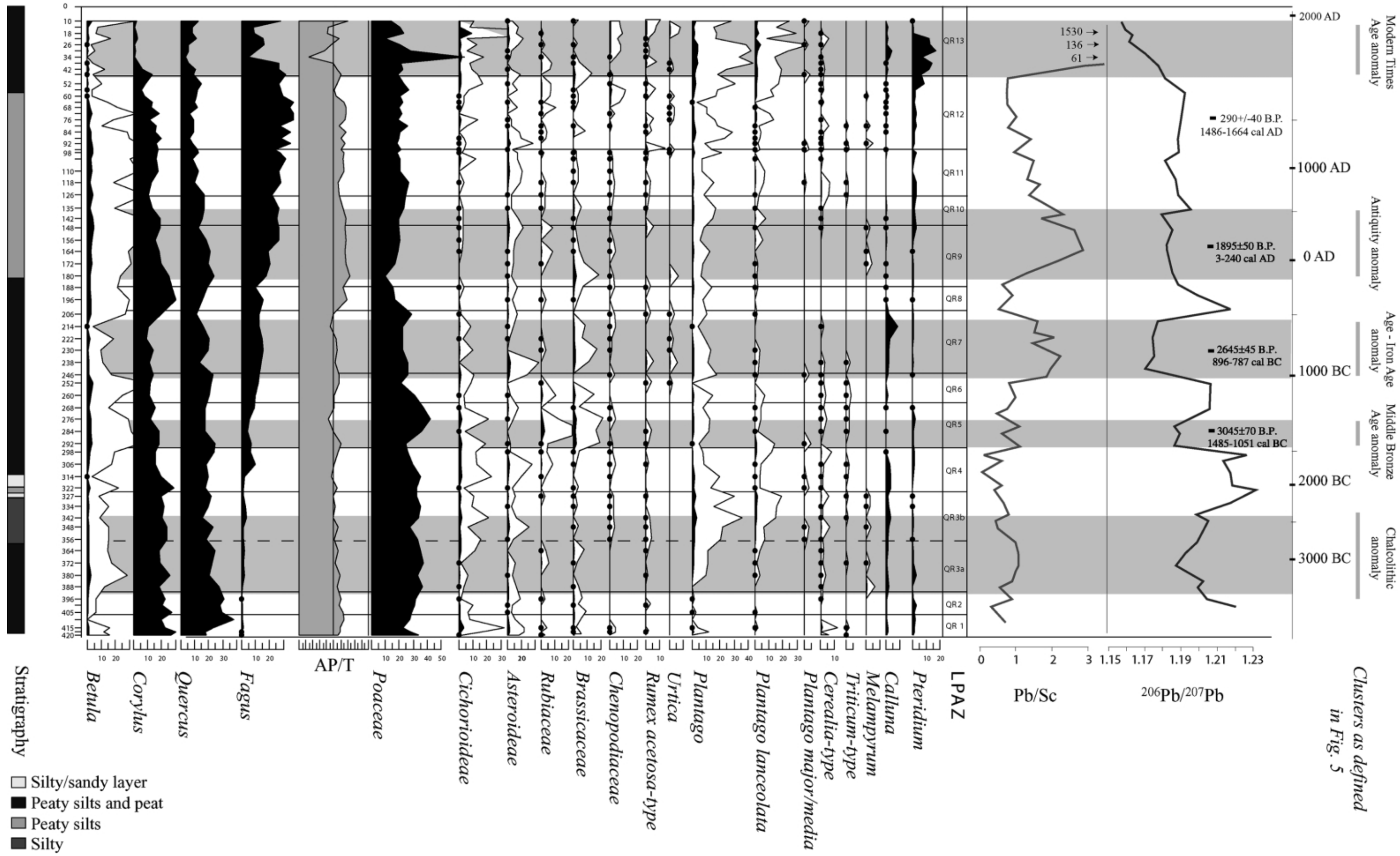

Fig. 8. Pollen record of the Quinto Real core (from Galop et al., 2001). Pb/Sc and ^{206}Pb/^{207}Pb ratios are reported to make easier historical reconstruction. The relative pollen diagram is divided into Local Pollen Assemblage Zones (LPAZ) based on relative change in land-use pollen indicators according to Behre (1981) and on relative change between trees and open-land indicators.

influenced as much as zinc and copper by plant uptake, which makes it closer to lead. Positive anomalies occur during the Late Bronze Age/Iron Age and Modern Times, as with Zn and Pb, but none is observed during Antiquity and the Middle Ages. In any case, it is hazardous to use the Zn, Cu and Cd profiles for historical purposes because these elements do not possess isotopic features comparable to lead, which would allow their degree of migration to be assessed.

5.3. Towards a historical interpretation

5.3.1. Prehistoric record

In QR 1 (cf. Fig. 8), or in other words prior to ca 3000 BC, the presence of *Cerealia*-type, *Triticum*-type and *Plantago lanceolata* in the pollen record shows significant cereal cultivation and human settlements. Later, the decline of oak (*Quercus*) combined with the extension of birch (*Betula*), a heliophilic tree, suggest a progressive deforestation which could be at the origin of the detrital layer recorded at 310-cm depth, around cal. 2000 BC.

The ^{206}Pb/^{207}Pb and Pb/Sc ratios of the Middle Bronze Age (QR5) and Late Bronze Age/Iron Age (QR 7) samples, respectively, cal. 1500–1300 BC and cal. 1000–600 BC, indicate significant anthropogenic inputs. Simultaneously, oak and hazel (*Corylus*) diminish while traces of agro-pastoral and slash-and-burn activities (*Plantago lanceolata*, *Plantago major/media*, *Melampyrum*, *Rumex*) decrease or are simply absent. Between these two phases (QR6, cal. 1300–1000 BC), Pb/Sc and ^{206}Pb/^{207}Pb ratios are more crustal, and signs of reforestation are observed. Both geochemical and pollen records are in good agreement with the sparse archaeological knowledge available. In the Middle Bronze Age, and more precisely during the 15th and 14th centuries BC, metallurgical activity increased in the Southern French Atlantic region, with high production of bronze alloys (Coffyn et al., 1995). Regional smelting and/or mining probably decreased from 1100 BC (Cantet, 1991), to start again in the Final Bronze Age, as proved by the abundant production of ornamental artefacts. The wealth of copper in the polymetallic district of Banca may, therefore have attracted early miners, although direct field evidence of Bronze Age exploitation is still lacking in the valley, apart from the discovery of a prehistoric mallet used to crush minerals (Dupré et al., 1993). Prehistoric exploitations are likely to have suffered from considerable alteration due to a humid climate on steep slopes, or more certainly to have been destroyed by later occupation. At that time lead was not exploited for itself but was emitted into the atmosphere in significant amounts subsequent to mineral extraction and smelting of other metals, so it could be a good marker for local or regional prehistoric metallurgy. Such contaminations dating as far back as the Bronze Age have been recorded in natural archives in the Jura Mountains (Weiss et al., 1997), the North-Western Iberian Peninsula (Martínez-Cortizas et al., 1997, 2002), the overbank sediments of the River Weser (Monna et al., 2000a), and in the French Morvan massif (Blanchot et al., 2001). The isotopic signatures of Late Bronze Age/Iron Age peat samples fall into line with those of contemporary bronze and copper artefacts (rings, a bracelet, pins, a sword, and other bronze fragments) recently found in the Basque country (Fig. 5), even though they may have been produced using metals locally extracted or acquired by trading. Significant changes in metalworking practices are also suggested by the change of isotopic signatures between Middle and Late Bronze Age (Fig. 5), but the strongest clue to local metalworking occurrence is given by the concomitance of anthropogenic lead enrichments and deforestations. As the latter are not consecutive to agro-pastoral extensions, they are interpreted as the result of mounting energy demands for mining and smelting, like those already reported in several parts of Pyrenees (Galop and Jalut, 1994), in the Swiss Jura Mountains for iron metallurgy (Richard and Eschenlhor, 1998), and more recently in the French Morvan massif (Blanchot et al., 2001; Monna et al., 2004).

5.3.2. Antiquity

Another major anthropogenic phase is pinpointed by Pb/Sc and ^{206}Pb/^{207}Pb from ca cal. 200 BC to approximately 200 AD (Fig. 7). At that time, oak and hazel decrease while beech seems to spread. Moderate signs of deforestation appear again without any indication of significant agricultural extension. Such an intensification of anthropogenic atmospheric inputs in Antiquity has already been reported at the continental scale, in the Pyrenean region (Ariès, 2001) as well as far beyond the Mediterranean area, as demonstrated by the studies performed in Greenland (Hong et al., 1994; Rosman et al., 1997), Sweden (Brännvall et al., 1999; Renberg et al., 2000, 2001), Northern Spain (Martínez-Cortizas et al., 2002) and the Jura Mountains (Shotyk et al., 1998). In fact, these signals are so ubiquitous in Southern and Western Europe that certain authors have suggested their use as a chronological marker in sediment deposits (Alfonso et al., 2001; Renberg et al., 2001). They are often interpreted as the result of long-range transport of contaminants originating from Spain, especially when local mining is lacking and lead isotopic compositions are compatible with those of Rio Tinto, Southern Spain, one of the major mining sites (Stos-Gale et al., 1995); *Hispania* accounting for almost 40% of the worldwide Pb production during the Roman Empire (Nriagu, 1983).

The Pb/Sc peak observed in the core corresponds well with the exploitation of iron, copper, silver and lead from the metallurgical and mining sites of the Baïgorri Valley well known in Antiquity (Machot, 1995). Apart from Roman industrial activity, numerous other small workshops were found throughout the valley of Urepel (Beyrie et al., in press). Because of the abundance of this indigenous exploitation and the incompatibility of lead isotopic signatures in peat samples with those of the Rio Tinto district (cf. Fig. 5), major influence from remote sources is not to be considered here. Any long-range input was undoubtedly masked by dominating anthropogenic local inputs. This is in good agreement with another recent study undertaken in the Lake Redó, Central Pyrenees–Spain, which clearly identified a phase of pollution, attributed to local mining operations, starting approximately 670 BC and reaching a maximum at approximately 660 AD; in other words peaking after Roman times, a period in which lead production was at a minimum in Europe (Camarero et al., 1998). Long-range transport of lead from the Rio Tinto region should appear on the flank of this peak but was not noticeable, probably because this source was also masked by dominant local emissions. The isotopic compositions of metallic tool fragments found in the Roman gallery of the Banca mine support this hypothesis since such signatures might correspond to the anthropogenic end-member which shifted isotopic ratios of peat samples towards less radiogenic signatures (cf. Fig. 5). The decline of oak can be explained by deforestation for metallurgical operations. Moreover, anthraco-analysis has established that charcoal production within the valley mainly focussed on this species (Galop et al., in press).

Human-derived lead deposition lasted for at least 400 years and did not collapse as brutally as elsewhere at the fall of the Roman Empire, possibly because the Romanisation of the Basque country had never been intense. Another explanation could also be a delay due to weathering of polluted soils by small streams, which temporarily feed the Quinto Real peatland area.

5.3.3. Medieval to modern time

After a long decline throughout the Middle Ages, Pb/Sc ratios increase markedly from the late 16th and early 17th century AD, coinciding with the decrease in $^{206}Pb/^{207}Pb$ ratios (Fig. 8). This period is abundantly mentioned in textual archives as an intense phase of metallurgical activity in the Basque country, and more particularly in the Baïgorry valley. The copper foundry of Banca started operating in 1747. Most Basque forests were dedicated to charcoal production, as demonstrated by abundant charcoal-kiln remains in present forest areas of the Aldudes valley. Yet metalworking almost totally collapsed in the middle of the 19th century. Forest taxa slump when metalworking peaked, demonstrating intense wood charcoal consumption for energy production. Recent pollution has been recorded too, but its chronology is difficult to reconstruct accurately because ^{14}C-based chronology is not detailed enough in topmost horizons. However, isotopic signatures at the surface of the core ($^{206}Pb/^{207}Pb = 1.159$) probably illustrate the impact of allochtoneous less radiogenic anti-knock compounds added until recently to leaded gasoline.

6. Conclusion

Although the origin of the earliest geochemical anomaly, recorded in Chalcolithic levels, remains unknown, two later anomalies, identifiable in Bronze Age levels, are almost certainly related to mining and smelting. The first episode, dating from the Middle Bronze Age, would probably not have been detected by the sole measurement of concentrations. Lead isotopes, however, are very sensitive to such low contaminations (Munksgaards and Parry, 1998), so that their use offers new possibilities for the recognition of precursor mining operations. The second episode occurred during the Late Bronze Age/Iron Age, at a time when metalworking was growing in magnitude throughout Western Europe. Both of these phases are accompanied by local signs of deforestation, not strictly related to agro-pastoral extensions. The strong impact of human activity during Antiquity in the nearby surroundings is clearly traced by geochemical and, to a lesser extent, pollen records. Lead emitted locally has dominated over remote sources, such as lead ore deposits intensively exploited by the Romans in Southern Spain. This latter source, often invoked as a major contributor to lead anomalies observed in European natural archives, has perhaps sometimes been overestimated because the presence of minor, but local, exploitations may have acted as point-sources. In Modern Times, human activity in the valley, in part related to mining and smelting, strongly impacted the nearby environment, as demonstrated by the drastic modification of plant cover and considerable metal pollution, with lead reaching concentrations up to 765 $\mu g\ g^{-1}$.

Combining geochemistry, palynology, and archaeological knowledge allows interpretations to be extended. If the trustworthiness of the metal record can be verified, high ash minerogenic peatlands may be successfully used to document ancient mining exploitation and metallurgy, even though the information they provide is more qualitative than quantitative. The duration of pollution phases might be overestimated because of the release of lead from polluted soils over a long period of time after mining and/or smelting operations ceased. However, in addition to the evidence furnished by lead isotopic signatures, the good agreement, in our case, between interpretations from field data and archaeological knowledge (acquired independently) confirms the reliability of the lead signal, at least over the last four millennia.

Acknowledgments

This work is part of the research program entitled ‘Palaeo-environment and dynamics of the anthropisation in the Basque Mountains (Dir. D. Galop)’ funded by the Ministry of Culture (Aquitania Archaeological Survey). We would like to thank A. Bidard, G. Bossuet, A. Lopez Saez for their assistance in the field, P. Birringer for pollen preparation, P.-Y. Favargé and D. Vignati for their precious help during ICP-MS measurements, and P. Steinmann for his very helpful comments.

References

Alfonso S, Grousset F, Massé L, Tastet J-P. A European lead isotope signal recorded from 6000 to 300 years BP in coastal marshes (SW France). Atmosph Environ 2001;35:3595–3605.

Ambert, P., Coularou, J., Cert, C., Guendon, J.-L., Bourgarit, D., Mille, B., Dainat, D., Houlès, N., Baumes, B., Le plus vieil établissement de métallurgistes de France (IIIe millénaire av. J.-C.): Péret (Hérault), C.R. Palevol, 2002;1:64–74.

Andrejko MJ, Fiene F, Cohen AD. Comparison of ashing techniques for determination of the inorganic content of peatsm. In: Jarret PM, editor. Testing of peats and organic soils. Philadelphia: American Society for Testing and Materials, 1983. p. 5–20.

Ariès S. 2001. Mise en évidence de contaminations métalliques historiques à partir de l'étude d'enregistrements sédimentaires de lacs de haute montagne, Ph.D. University Toulouse. p. 278.

Behre, K.-E., 1981, The interpretation of anthropogenic indicators in pollen diagrams. Pollen et Spores, XXIII, 2:225–245.

Beyrie A, Galop D, Monna F, Mougin V, La métallurgie du fer au Pays Basque durant l'Antiquité. Etat des connaissances dans la vallée de Baigorri. In press Aquitania.

Blanchot, C, Guillaumet, J -P, Monna, F, Petit, C, Lévêque, J, Dominik, J, Historical reconstruction of metallic pollution using a geo-ombrogenic peat bog in Eduens Gallic territory (Bibracte, France). Second European Meeting on Environmental Chemistry. 2001; pp. 12–15.

Brännvall M-L, Bindler R, Emteryd O, Nilsson M, Renberg I. Stable isotope and concentration records of atmospheric lead pollution in peat and lake sediments in Sweden. Water Air Soil Poll 1997;100:243–252.

Brännvall M-L, Bindler R, Renberg I, Emteryd O, Bartnicki J, Billström K. The medieval metal industry was the cradle of modern large-scale atmospheric lead pollution in Northern Europe. Environ Sci Technol 1999;33:4391–4395.

Camarero L, Masqué P, Devos W, Ani-Ragolta I, Catalan J, Moor HC, Pla S, Sanchez-Cabeza JA. Historical variations in lead fluxes in the Pyrenees (North-East Spain) from a dated lake sediment core. Water Air Soil Poll 1998;105:439–449.

Cantet J-P. L'âge du bronze en Gascogne gersoise, Archéologies, No. 4, Archéologies Vesuna, 1991; p. 240.

Chapman J-C, Tylecote R-F. Early copper in the Balkan. Proc Prehist Soc 1983;49:373–379.

Coffyn A, Moreau J, Bouris J-R. Les dépôts de bronze de Soulac-sur-mer. Aquitania 1995;13:7–31.

Degryse Ph, Muchez P, Six S, Waelkens M. Identification of ore extraction and metal working in ancient times: a case study of Sagalassos (SW Turkey). J Geochem Explor 2003;77:65–80.

Dumontet S, Lévesque M, Mathur SP. Limited downward migration of pollutant metals (Cu, Z, Ni, Pb) in acidic virgin peat soils near a smelter. Water Air Soil Poll 1990;49:329–342.

Dunlap CE, Steinnes E, Flegal AR. A synthesis of lead isotopes in two millenia of European air. Earth Planet Sci Lett 1999;167:81–88.

Dupré E, Parant D, Saint-Arroman C, Tobie J-L, 1993. Note sur un site minier et métallurgique antique de la commune d'Urepel (Pyrénées-Atlantiques), Cahiers du G.A.P.O., 12: pp. 91–100.

Eades LJ, Farmer JG, MacKenzie AB, Kirika A, Bailey-Watts AE. Stable lead isotopic characterization of the historical record of environmental lead contamination in dated freshwater lake sediment cores from Northern and Central Scotland. Sci Tot Environ 2002;292:55–67.

Espi E, Boutron CF, Hong S, Pourchet M, Ferrari C, Shotyk W, Charlet L. Changing concentrations of Cu, Zn, Cd, and Pb in a high altitude peat bog from Bolivia during the past three century. Water Air Soil Poll 1997;100:289–296.

Farmer JG, Mackenzie AB, Sugden CL, Edgar PJ, Eades LJ. A comparison of the historical lead pollution records in peat and freshwater lake sediments from Central Scotland. Water Air Soil Poll 1997;100:253–270.

Gale N-H, Stos-Gale Z-A, Livov P, Dimitov M, Todorov T, 1991. Recent studies of neolithic copper ores and artefacts in Bulgaria. In: Découverte du métal. Eluère, Mohen dir, Paris, (ed.). Picard, coll. ' Millénaires', pp. 49–75.

Galop D, Jalut G. Differential human impact and vegetation history in two adjacent Pyrenean valleys in the Ariège basin, Southern France, from 3000 BP to the present. Veg Hist Archaeobot 1994;3:225–244.

Galop D, Monna F, Beyrie A, Carozza L, Marembert F, Parent G, Mougin V, (in press), Métallurgie et histoire de l'environnement au cours des cinq derniers millénaires en Pays basque nord (Vallée de Baigorri, P.-A., France): premiers résultats d'une approche interdisciplinaire. Archeologia Postmedievale.

Galop D, Tual M, Monna F, Dominik J, Beyrie A. Pour une histoire des activités métallurgiques en montagne basque. Les apports d'une démarche intégrée alliant palynologie et géochimie isotopique du plomb. Sud Ouest Européen 2001;11:3–15.

Gapillou C., Vers une apporche métallogénique d'une region Presque oubliée. Les minéralisation à: Cu, Ag, Pb, Zn et les sidérites du paléozoïque et du trias du Pays Basque français entre Aïnhoa et Banca. 1981. Ph.D Thesis, University of Paris 6, 275.

Glooschenko WA, Holloway L, Arafat N. The use of mires in monitoring the atmospheric deposition of heavy metals. Aquat Bot 1986;25:179–190.

Grousset FE, Quetel CR, Thomas B, Donard OFX, Lambert CE, Guillard F, Monaco A. Anthropogenic vs. lithogenic origins of trace elements (As, Cd, Pb, Rb, Sb, Sc, Sn, Zn) in water column particles: North-Western Mediterranean Sea. Mar Chem 1995;48:291–310.

Hong S, Candelone J-P, Patterson CC, Boutron CF. Greenland ice evidence of hemispheric lead pollution two millennia ago by Greek and Roman civilizations. Science 1994;265:1841–1843.

Jones JM, Hao J. Ombrotrophic peat as a medium for historical monitoring of heavy metal pollution. Environ Geochem Health 1993;15:67–74.

Kempter H, Görres M, Frenzel B. Ti and Pb concentrations in rainwater-fed bogs in Europe as indicators of past anthropogenic activities. Water Air Soil Poll 1997;100:367–377.

Kempter H, Frenzel B. The impact of early mining and smelting on the local tropospheric aerosol detected in ombrotrophic peat bogs in the Harz, Germany. Water Air Soil Poll 2000;121:93–108.

Kivinen E. 1980. Proposal for a general classification of virgin peat, In: Grubich, D.M. Farnham, R.S., Itkoten, B. (Eds). Proceedings of the 6th International Peat Congress, Duluth, Minnesota, USA. International Peat Society, Duluth, USA, p. 47.

Lee JA, Tallis JH. Regional and historical aspects of lead pollution in Britain. Nature 1973;245:216–218.

Machot P., 1995. Mines et établissements métallurgiques da Banca, Biaritz/Saint-Etienne de Baïgorri, Editions Izpegi, p. 406.

MacKenzie AB, Logan EM, Cook GT, Pulford ID. A historical record of atmospheric depositional fluxes of contaminants in West-Central Scotland derived from an ombrotrophic peat core. Sci Tot Environ 1998a;222:157–166.

MacKenzie AB, Logan EM, Cook GT, Pulford ID. Distributions, inventories and isotopic composition of lead in ^{210}Pb-dated peat cores from contrasting biogeochemical environments: Implications for lead mobility. Sci Total Environ 1998b;223:25–35.

Martínez-Cortizas A, Pontevedra-Pombal X, Nóvoa-Muñoz JC, García-Rodeja E. Four thousand years of atmospheric Pb, Cd and Zn deposition recorded by the ombrotrophic paet bog of Penido Vello (North-Western Spain). Water Air Soil Poll 1997;100:387–403.

Martínez-Cortizas A, Garcia-Rodeja E, Pontevedra Pombal X, Nóvoa-Muñoz JC, Weiss D, Cherbulin A. Atmospheric Pb deposition in Spain during the last 4600 years recorded by two ombrotrophic peat bogs and implications for the use of peat as archive. Sci Total Environ 2002;292:33–44.

Mighall TM, Abrahams PW, Grattan JP, Hayes D, Timberlake S, Forsyth S. Geochemical evidence for atmospheric pollution derived from prehistoric copper mining at Copa Hill, Cwmystwyth, mid-Wales, UK. Sci Total Environ 2002;292: 69–80.

Monna F, Loizeau J-L, Thomas BA, Guéguen C, Favarger P-Y. Pb and Sr isotope measurements by inductively coupled plasma-mass spectrometer: efficient time management for precise improvement. Spectrochim Acta B 1998;59:1317–1333.

Monna F, Hamer K, Lévêque J, Sauer M. Pb isotopes as a reliable marker of early mining and smelting in the Northern Harz province (Lower Saxony, Germany). J Geochem Explor 2000a;68:201–210.

Monna F, Loizeau J-L, Thomas B, Guéguen C, Favarger P-Y, Losno R, Dominik J. Noise identification and sampling frequency determination for precise isotopic measurements by quadrupole-based inductively coupled plasma mass spectrometry. Analusis 2000b;28:750–757.

Monna F, Petit C, Guillaumet J-P, Jouffroy-Bapicot I, Blanchot C, Dominik J, Losno R, Richard H, Lévêque J, Château C. History and environmental impact of mining activity in Celtic aeduan territory recorded in a peat bog (Morvan, France). Environ Sci Technol 2004;38(3):657–673.

Moore PD, Evans AR, Chater M. In: Behre K-E, editor. Palynological and stratigraphic evidence for hydrological changes in mires associated with human activity, Anthropogenic indicators in pollen diagrams. Rotterdam: A.A. Balkema, 1986. p. 209–220.

Moris N. Composition of organic materials of peat soils in Peninsular Malaysia. In: Zauyah S, Wong CB, Paramanathan S, editors. Recent developments in soil genesis and classification, Kuala Lumpur, Malaysia. Kaula Lumpur, MY: Malaysian Society of Soil Science, 1989. p. 81–87.

Munksgaards NC, Parry DL. Lead isotope ratios determined by ICP-MS: Monitoring of mining-derived metal particulates in atmospheric fallout, Northern Territory, Australia. Sci Total Environ 1998;217:113–125.

Norton SA, Evans GC, Kahl JS. Comparison of Hg and Pb fluxes to hummocks and hollows of ombrotrophic big heath bog and to nearby Sergeant Mt. pond, Maine, USA. Water Air Soil Poll 1997;100:271–286.

Nriagu JO. Lead and lead poisoning in antiquity. New York: Wiley, 1983.

Reille M, 1992. Pollen et spores d'Europe et d'Afrique du Nord. Ed. Laboratoire de botanique historique et palynologie. Marseille.

Renberg I, Brännvall M-J, Bindler R, Emteryd O. Atmospheric lead pollution history during four millenia (2000 BC to 2000 AD) in Sweden. Ambio 2000;29:150–156.

Renberg I, Bindler R, Brännvall M-L. Using the historical atmospheric lead-deposition record as a chronological marker in sediment deposits in Europe. Holocene 2001;11:511–516.

Richard H, Eschenlhor L. Essai de correlation entre les données polliniques et les données archéologiques: le cas des forêts de Lajoux dans les Franches-Montagnes (Lajoux-Suisse). Rev. darchéométrie 1998;22:29–37.

Rosman KJR, Chisoholm W, Hong S, Candelone J-P, Boutron CF. Lead from Carthaginian and roman Spanish mines isotopically identified in Greenland ice dated from 600 BC to 300 AD. Environ Sci Technol 1997;31:3413–3416.

Rovira S. 1998. Origin and diffusion of metallurgy in Spain: a review at the light of radiocarbone dates. Symposium C14 Archéologie, pp. 219–224.

Schettler G, Romer RL. Anthropogenic influences on Pb/Al and lead isotopic signature in annually layered Holocene Maar lake sediments. Appl Geochem 1998;13(6):787–797.

Settle D, Patterson C. Lead in albacore: guide to lead pollutions in Americans. Science 1980;207:1167–1176.

Shotyk W. Peat bog archives of atmospheric metal deposition: geochemical evaluation of peat profiles, natural variations in metal concentrations, and metal enrichment factors. Environ Rev 1996a;4:149–183.

Shotyk W. Natural and anthropogenic enrichments of As, Cu, Pb, Sb, and Zn in ombrotrophic vs. minerotrophic peat bog profiles, Jura Mountains, Switzerland. Water Air Soil Poll 1996b;90:375–405.

Shotyk W, Weiss D, Appleby P, Cherbukin A, Frei R, Gloor M, Kramer J, Reese S, Van der Knaap W. History of atmospheric lead deposition since 12 370 ^{14}C yr BP from a peat bog, Jura Mountains, Switzerland. Science 1998;281:1635–1640.

Shotyk W, Weiss D, Kramers JD, Frei R, Cherbukin AK, Gloor M, Reese S. Geochemistry of the peat bog at Etang de la Gruère, Jura Mountains, Switzerland, and its record of atmospheric Pb and lithogenic trace metals (Sc, Ti, Y, Zr, and REE) since 12 370 ^{14}C yr BP. Geochem Cosmochim Acta 2001;65(14):2337–2360.

Shotyk W. The chronology of anthropogenic, atmospheric Pb deposition recorded by peat cores in three minerogenic peat deposits from Switzerland. Sci Total Environ 2002;292:19–31.

Shotyk W, Krachler M, Martinez-Cortizas A, Cheburkin AK, Emons H. A peat bog record of natural, pre-anthropogenic enrichments of trace elements in atmospheric aerosols since 12 370 ^{14}C yr BP, and their variation with Holocene climate change Earth. Planet Sci Lett 2002a;199:21–37.

Shotyk W, Weiss D, Heisterkamp M, Cheburkin AK, Appleby PG, Adams FC. New peat bog record of atmospheric possultion in Switzerland: Pb concentrations, enrichment factors, isotopic composition, and organolead species. Environ Sci Technol 2002b;36:3893–3900.

Stos-Gale Z, Gale NH, Houghton J, Speakman R. Lead isotope data from the isotrace laboratory, Oxford: archaeometry data base 1, ores from Western Mediterranean. Archaeometry 1995;37(2):407–415.

Stuiver M, Reimer PJ, Bard E, Beck JW, Burr GS, Hughen KA, Kromer B, McCormac FG, Plicht J, Spurk M. INTCAL98 radiocarbon age calibration 24 000-0 cal BP. Radiocarbon 1998;40:1041–1083.

Van Geel B, Bregman R, Van der Molen PC, Dupont LM, Van Driel-Murray C. Holocene raised bog deposits in the Netherlands as geochemical archives of prehistoric aerosols. Acta Bot Neerl 1989;38:467–476.

Vile MA, Wieder RK, Novàk M. Mobility of lead in *Sphagnum*-derived peat. Biogeochem. 1999;45:35–52.

Wedepohl KH. The composition of the crust. Geochim Cosmochim Acta 1995;59(7):1217–1232.

Weiss D, Shotyk W, Cherburkin AK, Gloor M, Reese S. Atmospheric lead deposition from 12 400 to ca. 2000 yrs BP in a peat bog profile, Jura Mountians, Switzerland. Water Air Soil Poll 1997;100:311–324.

Weiss D, Shotyk W, Appleby PG, Kramers JD, Cheburkin AK. Atmospheric Pb deposition since the Industrial Revolution recorded by five Swiss peat profiles: enrichment factors, fluxes, isotopic composition, and sources. Environ Sci Technol 1999;1999(33):1340–1352.

Weiss D, Shotyk W, Boyle EA, Kramers JD, Appleby PG, Cheburkin AK. Comparative study of the temporal evolution of atmospheric lead deposition in Scotland and Eastern Canada using blanket peat bogs. Sci Total Environ 2002;292:7–18.

West S, Charman DJ, Grattan JP, Cherburkin AK. Heavy metals on Holocene peats from South-West England: detecting mining impacts and atmospheric pollution. Water Air Soil Poll 1997;100:343–353.

Williams M. Dark ages and dark areas: global deforestation in the deep past. J Hist Geo 2000;26:28–46.

Wiltshire PEJ, Edwards KJ. In: Chambers FM, editor. Mesolithic, early neolithic, and later prehistoric impacts on vegetation at a riverine site in Derbyshire, England, climate change and human impact on the landscape. Chapman and Hall, 1993. p. 157–168.

Wüst RAJ, Bustin RM, Lavkulich LM. New classification systems for tropical organic-rich deposits based on studies of the Tasek Bera Basin, Malaysia. Catena 2003;751:1–31.

History and Environmental Impact of Mining Activity in Celtic Aeduan Territory Recorded in a Peat Bog (Morvan, France)

F. MONNA,*,†,‡ C. PETIT,‡
J.-P. GUILLAUMET,‡
I. JOUFFROY-BAPICOT,§ C. BLANCHOT,†
J. DOMINIK,‖ R. LOSNO,⊥ H. RICHARD,§
J. LÉVÊQUE,† AND C. CHATEAU#

Laboratoire GeoSol, UMR INRA-Université de Bourgogne, Bat. Gabriel, F-21000 Dijon, France; Archéologies, Cultures et Sociétés. Bourgogne et France Orientale du Néolithique au Moyen Age, UMR 5594 CNRS-Université de Bourgogne, Bat. Gabriel, F-21000 Dijon, France; Laboratoire de Chrono-écologie, UMR 6565 CNRS, UFR des Sciences et Techniques, Université de Besançon, 16 route de Gray, F-25030 Besançon Cedex, France; Institut F.-A. Forel, Université de Genève, 10 route de Suisse, CH-1290 Versoix, Switzerland; LISA, Universités Paris 7 and Paris 12, CNRS, Faculté des Sciences, 61 av. du Gal de Gaulle F-94010 Créteil Cedex, France; and Centre des Sciences de la Terre, Université de Bourgogne, Bat. Gabriel, F-21000 Dijon, France

The present study aims to document historical mining and smelting activities by means of geochemical and pollen analyses performed in a peat bog core collected around the Bibracte oppidum (Morvan, France), the largest settlement of the great Aeduan Celtic tribe (ca. 180 B.C. to 25 A.D.). The anthropogenic Pb profile indicates local mining operations starting from the Late Bronze Age, ca. cal. 1300 B.C. Lead inputs peaked at the height of Aeduan civilization and then decreased after the Roman conquest of Gaul, when the site was abandoned. Other phases of mining are recognized from the 11th century to modern times. They have all led to modifications in plant cover, probably related in part to forest clearances necessary to supply energy for mining and smelting. Zn, Sb, Cd, and Cu distributions may result from diffusional and biological processes or from the influence of groundwater and underlying mineral soil, precluding their interpretation for historical reconstruction. The abundance of mineral resources, in addition to the strategic location, might explain why early settlers founded the city of Bibracte at that particular place. About 20% of the anthropogenic lead record was accumulated before our era and about 50% before the 18th century, which constitutes a troublesome heritage. Any attempts to develop control strategies in accumulating environments should take into account past human activities in order to not overestimate the impact of contemporary pollution.

Introduction

When dealing with current metal pollution in accumulating environments such as soils, sediments, or peatlands, reliable information about the extent and origin of the anthropogenic impact at a regional scale is an essential prerequisite for choosing among the environmental strategies available: remediation, restriction of pollutant emissions, or isolation of the contaminated environment from the surroundings. The estimate of ‘pristine’ natural conditions therefore constitutes a preliminary step because a reference level is needed for any further comparisons with current environments. This assessment obviously presents a strong historical connotation because it is supposed to reflect a period at which mankind did not significantly affect, at least for metals, the surrounding environment. However, the introduction of history into the environmental sciences goes much further. Knowledge of local history may help to resolve the complex question of pollutant origin in soils by distinguishing recent emissions from those inherited from earlier human societies, as metals accumulate indistinctly in surface horizons. The possession of historical data also allows the use of natural analogues to determine the long-term behavior of past pollution from field studies and, hence, by extension the fate of our current emissions. This is particularly significant with lowly mobile metals such as lead, for which any migration rate determination is problematic at the human time scale in natural field conditions. Archaeologists and palaeobotanists are also interested in any fingerprint of early human activity on the environment because it may help to elucidate the organization and development of primitive societies. Although the ultimate objectives of environmentalists, palaeobotanists, and archaeologists may be different, their attempts to understand the interaction of man and environment may be mutually enriching. In this light, the present study intends to reconstruct local metalwork history at the largest settlement of the vast Aeduan territory through its impact on the environment. Described by Caesar in “*De Bello Gallico*” in 58 B.C. as one of the greatest and richest oppida of Gaul, Bibracte was located upon Mount Beuvray, one of the highest points of the granitic Morvan. This strategic site corresponds to the limit of the Saône, Loire, and Seine watersheds in central France. The Celtic city, with its thousands of inhabitants, was founded ca. 180 B.C. and spread over approximately 200 ha. It was an important trade center, including metalworking, as the presence of numerous bronze and iron workshops demonstrates (*1*). Under Roman Empire domination (ca. 25 A.D.), the population gradually left Bibracte to settle 25 km away, in the new city of *Augustodunum* (*2*), nowadays known as Autun. Evidence of settlements before Celtic occupation is rare, except for some artifacts dating from the Neolithic, Late Bronze Age, and Early Iron Age (*3*). This can partly be explained by geographical conditions: the agricultural potential of acidic soils is low, climate conditions are rugged (precipitations, 1500 mm; mean temperatures, 8.5°C), slopes are steep, and valleys are narrow (*4*). Geomorphological anomalies, such as wide trenches and gullies, have recently been found on the site and interpreted as remains of mining excavations. On this basis, archaeologists have assumed that one of the reasons which may have attracted early settlers is the abundance of

---

* Corresponding author phone: +33 (0)3 80 39 63 50; fax: +33 (0)3 80 39 63 87; e-mail: Fabrice.Monna@u-bourgogne.fr.
† Laboratoire GeoSol, Université de Bourgogne.
‡ Archéologies, Université de Bourgogne.
§ Université de Besançon.
‖ Université de Genève.
⊥ Universités Paris 7 and Paris 12.
Centre des Sciences de la Terre, Université de Bourgogne.

10.1021/es034704v CCC: $27.50

mineral resources. However, this assumption is not yet an established fact because of the lack of clear field evidence, the extent of the current forest making difficult any pedestrian or aerial geophysical prospecting. Remains of early local mining exploitation may also have been destroyed, buried, or masked either by the building of Bibracte or by any further metal extraction up to and including that of the 20th century. In such a situation of successive periods of mining activity, the reconstruction of the industrial history of the site may be envisaged through the geochemical analysis of peat bogs (cf. *The Science of the Total Environment, Special Issue,* 2002, vol. 292, 1−2), which also provides quantitative information about the environmental legacy. Elemental compositions were therefore measured in a peat core sampled around Mount Beuvray ('Port-des-Lamberts', Glux-en-Glenne, Nièvre). However, metals buried in peatlands may possibly result from a combination of multiple sources (*5*), while postdepositional migrations, already observed at decadal scale, may totally preclude any utilization for historical reconstruction (*6*, *7*). That is why lead isotopic composition, which can help to dispel such ambiguities, is nowadays often determined (*5*, *7*−*11*). Lead has the advantage of being one of the less mobile metals in such an environment. Its isotopic geochemistry is based on the atom ratio differences existing between natural and anthropogenic sources, the latter depending on U/Pb and U/Th ratios and the age of the ore deposits from which the metal derives (*12*). Mining may also have affected nearby vegetation through possible deforestation performed in response to increasing energy demands for metalworking (*13*, *14*). Geochemistry was therefore supplemented by pollen analyses.

Given this new set of data, we will examine the earliest signs of extensive mining and smelting to establish whether mineral abundance in the area acted as a magnet for the first Aeduan settlers, an important question recently raised by archaeologists. From an environmental point of view, we will try to quantify the weight and behavior of the contaminant heritage, and the impact on vegetation of past metalwork in a rural area which today presents no major industrial activity.

Setting

Mount Beuvray is located in the Morvan, northern Massif Central. It is a Hercynian massif (900 m, asl maximum at Haut Folin) mainly composed of granitic rocks, although volcano-sedimentary terrains (rhyolites and conglomerates) are also exposed (Figure 1). The whole massif is crosscut by several microgranitic and quartz veins. Three main types of mineral deposits were recognized: (i) late Hercynian stratiform barytic and fluoritic outcrops, such as those of the Argentolle district mining area (*15*); (ii) abundant polymetallic mineralization (Pb, Zn, Ag) in NNW−SSE and NNE−SSW veins, and, to a lesser extent, (iii) in conglomerates outcropping on Mount Beuvray (*16*, *17*). Although the presence of ancient mining activities has already been suggested in the Mount Beuvray region, textual and field evidence indicates exploitation of fluorine, Barite, and lead from the late 18th century, which continued until the mid-1980s.

The Port-des-Lambert peat deposit (cf. Figure 1) is situated at about 4−5 km from both Mount Beuvray and known ore deposits (Figure 1) and lies on a surface of about 3 ha. *Sphagnum*-dominated and organic-rich at the top, it is fed by some temporary streams originating from a small catchment area.

Material and Methods

Sampling. The peat column was collected in October 2000 following the conventional two-borehole technique with the help of a Russian GYK-type corer. It consists of about 2 m of organic-rich material. The core, well preserved in a plastic bag to protect against contamination and evaporation, was subsampled a few hours later in 2-cm-thick subsections using an acid precleaned PTFE spatula. The outer part was systematically discarded, as it could have been polluted by contact with any metallic parts of the corer or plastic bag. A fraction of subsamples was kept wet for pollen analysis, while the remainder was transferred to precleaned LDPE beakers and dried for 3 days at 60 °C. Once dried, the subsamples were powdered in an automatic agate mortar systematically precleaned with diluted HCl and Milli-Q water.

Geochemical Analyses. Total organic carbon (TOC) and nitrogen contents were measured by elemental analyzer (NCS 1500, Carlo Erba). The whole procedure from preparation to measurement for isotopic and elemental concentration determination by inductively coupled plasma−mass spectrometry (ICP-MS) and inductively coupled plasma−atomic emission spectrometry (ICP-AES) was performed in US class 1000−10000 clean rooms. About 200 mg of samples were first oxidized overnight using 4 mL of Suprapure H_2O_2 (Merk, Germany) and dried. Two millimeters each of Suprapure-grade HCl, HNO_3, and HF (Merk, Germany) was then added. The dissolution was achieved under microwave assistance Ethos (Milestone). One blank and one reference material standard (RMS), Peach leaves NIST 1547 or JSD 1−2, were added to each set of seven unknown samples.

Pb, Zn, Cd, and Cu contents were measured after external and internal (Re, Rh) calibrations on an HP 4500 ICP-MS. The same elements together with Sb, Al, and S were also determined on one-half of the samples by ICP-AES using a micronebulizer or conventional Scott chamber. Both methods always yielded similar results within ±10% of RMS certified values. Lead was first purified from an aliquot of the solution on AG1 × 4 ionic resin (Biorad). Isotopic ratios were then determined on quadrupole-based HP 4500 ICP-MS. Mass bias correction was operated by bracketing several NIST 981 lead standards every five samples. Further details about the complete procedure and instrumental settings can be found elsewhere (*18*, *19*). Blank corrections were never required as they appeared negligible compared to the total amount of lead in the aliquots. Precisions of $^{206}Pb/^{207}Pb$ and $^{208}Pb/^{206}Pb$ ratios were about 0.27% and 0.31%, respectively. Previous comparisons between isotopic measurements made by quadrupole-based ICP-MS and more precise thermo ionization mass spectrometry (TIMS) always demonstrated the accuracy of the ICP-MS results, within 95% confidence intervals (*19*).

Refractory elements such as Sc, Th, La, and Ce were precisely measured by instrumental neutron activation (INAA) at Actlabs (Ontario, Canada). Routinely measured standards and Peach Leaves NIST 1547 added as blind samples yielded results within about ±10−15% of certified values.

Pollen analyses were performed at a subsampling interval of 8 cm. Preparation followed a standard procedure, according to a physicochemical protocol adapted to this type of sediment to eliminate mineral and organic matrix (namely, the Frenzel method, explained elsewhere (*20*)). There were no sterile levels, and palynomorphs were well preserved. Pollens were identified with the aid of keys (*21*), photographs (*22*), and reference to a modern-type slide collection. At least 400 pollen grains, in addition to dominant taxa, were counted in each level.

Radiocarbon Dating. Four peat samples were dated using ^{14}C. They were measured by beta counting at the Centre des Sciences de la Terre−University of Lyons (Table 1, Figure 2). All dates were calibrated using Calib 4.1.3 software (*23*).

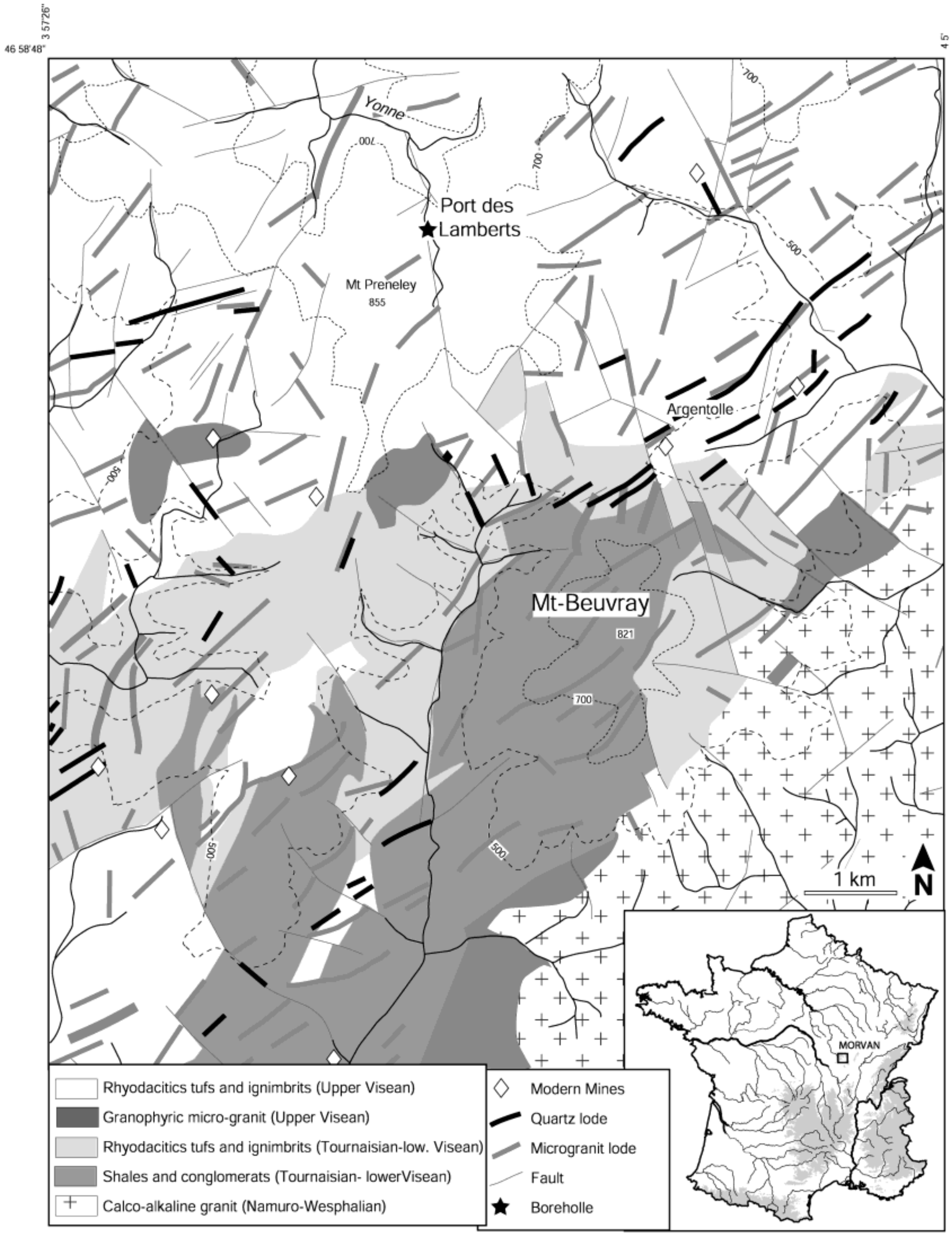

FIGURE 1. Map of the Morvan and location of sampling site; major mining exploitations and archaeological sites are also represented.

TABLE 1: Age−Depth Relationship for the 'Port-des-Lamberts' Peat Core

name	lab name	^{14}C BP	calibrated dates[a]	max. probabilities
PDL 75	LY-10942	1070 ± 50	888−1028 A.D.	984, 905, 965, 1015
PDL 97	LY-10943	1460 ± 60	441−664 A.D.	605, 617, 635, 585, 565
PDL 126	LY-10944	2480 ± 40	790−407 B.C.	−583, −643, − 661, −587, −544
PDL 163	LY-10945	3117 ± 54	1515−1225 B.C.	−1406, −1325, −1425, −1355, −1485

[a] The data are calibrated to calendar dates A.D. or B.C..

Results and Discussion

Trophic Status of the Core. Total organic carbon concentration is mostly in the range 45−50%, which indicates a high organic matter content between 80% and 95% (Figure 3). On this basis, the deposit can be classified as peat (*24*). Organic matter exhibits inverse variations to that of Sc or other lithophilic elements such as Al, Th, or rare earth elements (not shown here). C/N ratios slightly decrease from the bottom to the top, respectively, from 24 to 17. Such values,

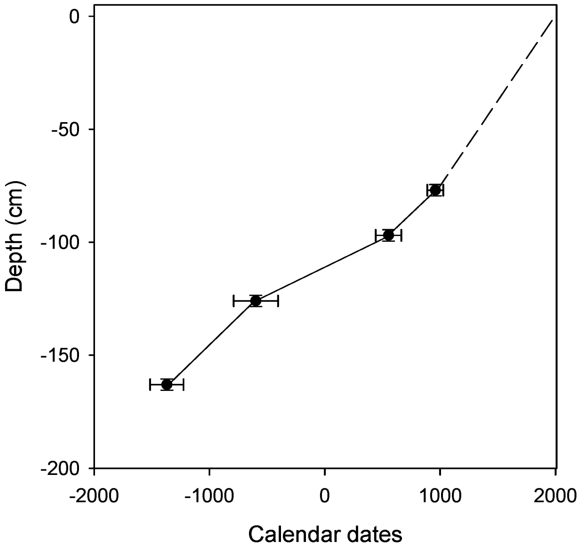

FIGURE 2. Depth vs ^{14}C-based calibrated calendar dates. The error bars are given at 95% confidence level.

together with those of organic matter, are characteristic of minerotrophic fen peat (*25*).

Chronology. ^{14}C-Derived dates are coherent with the depth at which they were determined (Table 1, Figure 2). Although no complementary dating was available within the topmost 75 cm, the extrapolation of the dated sequence acceptably fits the top of the core (dashed line on graph 2). However, the growth rate was probably slower between ca. cal. 500 B.C. and cal. 1000 A.D., as indicated by a significant change in the curve slope.

Data Preparation. Total concentration profiles are often used for a direct historical reading, but such an operation must be undertaken with care because (i) the distribution of metals in the core can be affected by variations in inorganic matter content (*8, 26*), (ii) changes in vegetation, compaction, or primary production (*6*), and (iii) in minerotrophic peatlands, the redistribution of metals after postdepositional migrations may occur (*7, 27*). Inputs from groundwater are also possible when peatlands are not hydrologically isolated from the substratum (*5, 28*). The elimination of mineral matter influence and further calculation of anthropogenic metal contents is theoretically operated by subtracting the detrital contribution from the total amount (*5*). Mineral contribution is evaluated by taking as a reference a refractory lithophilic element, such as Sc, or Zr, REE, Th, Al, Ti, which is considered to be conservative in peat profiles and has no anthropogenic origin (*26, 29*)

$$\mathrm{M_{anthr.}} = \mathrm{M_{sample}} - \mathrm{Sc_{sample}}\cdot\left(\frac{M}{\mathrm{Sc}}\right)_{\mathrm{natural}} \qquad (1)$$

with $\mathrm{M_{anthr.}}$ being the anthropogenic metal content; $\mathrm{M_{sample}}$ and $\mathrm{Sc_{sample}}$, respectively, are the total metal and scandium concentrations, and $\mathrm{(M/Sc)_{natural}}$ is the natural ratio assumed to be constant. $\mathrm{(M/Sc)_{natural}}$ values are generally assimilated to those of the continental crust or upper continental crust (UCC) or may alternatively be deduced from the bottom of the core, provided it fully reflects natural inputs.

In the present core, Pb/Sc ratios roughly decrease from the top to the bottom. An almost constant $\mathrm{(Pb/Sc)_{sample}}$ ratio

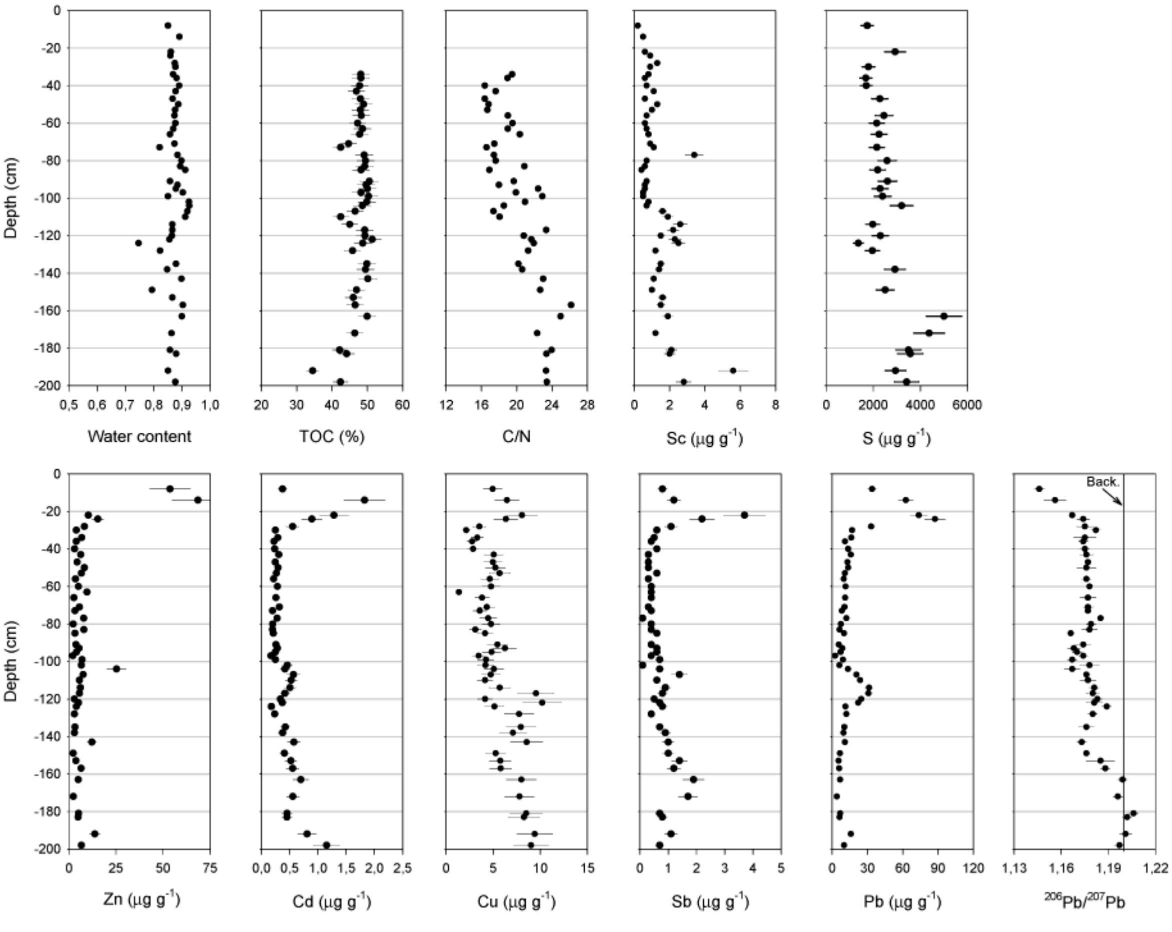

FIGURE 3. Water content, C/N and ^{206}Pb/^{207}Pb ratios, total organic carbon (TOC), and Sc, Pb, Zn, Cd, Cu, Sb, and S concentrations versus depth. The error bars correspond to a 95% confidence level.

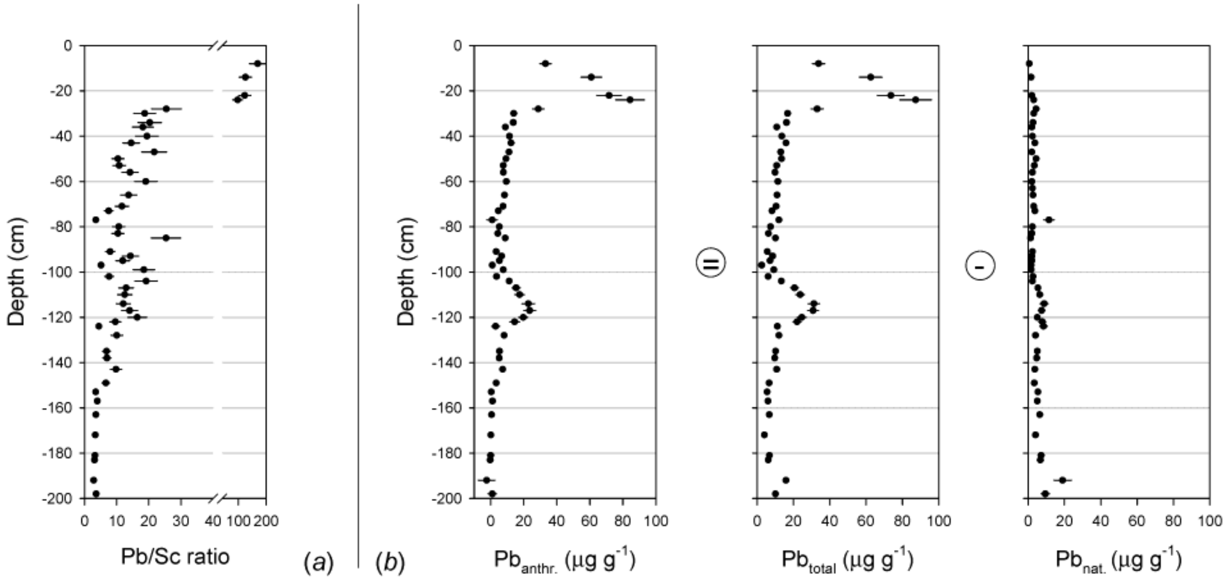

FIGURE 4. (a) Pb/Sc ratios versus depth (cm). (b) Calculation of anthropogenic lead concentration ($Pb_{anthr.}$) by subtracting natural lead ($Pb_{nat.} = Sc \times 3.3$; see text for details) from total lead concentration (Pb_{total}). The error bars correspond to a 95% confidence level.

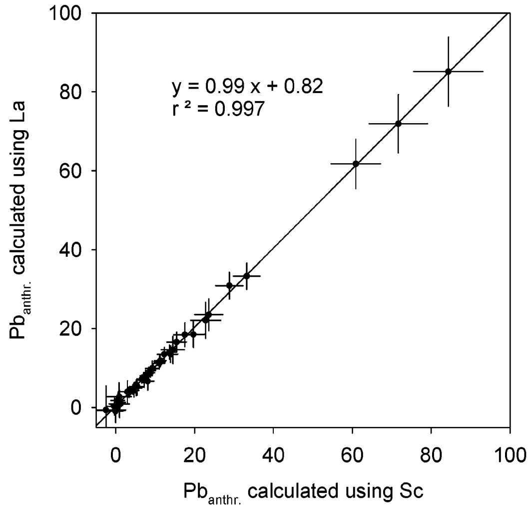

FIGURE 5. Comparison of anthropogenic lead concentrations calculated using Sc or La as reference element. See text and Figure 4 for $(Pb/Sc)_{natural}$ determination, $(Pb/La)_{natural}$ ratio taken at ~0.82 from the last 40 cm of the core (against 0.53 for the UCC value, *31*). The error bars correspond to a 95% confidence level.

value of 3.3 ± 0.7 (2σ) is found within the deepest 40 cm (Figure 4a), while $^{206}Pb/^{207}Pb$ signatures (ca. 1.20, Figure 3) are typical of preindustrial sediments in France (*10, 30*). Using the value of 3.3 ± 0.7 (2σ) for $(Pb/Sc)_{natural}$ enables the minor oscillations observed in the last 40 cm of the total lead profile to be filtered (cf. Figure 4b), because they can be attributed to a significant addition of mineral matter from underlying sediments. In fact, all the other lithophilic refractory elements measured, La, Th, Ce, Sc, and Al, are strongly intercorrelated ($r > 0.9$, $p < 0.001$), similar to what was found elsewhere (*26*), and yield similar calculations of anthropogenic lead contribution when their reference ratio is derived from the bottom of the core (i.e., the comparison calculation operated using Sc and La in Figure 5). The difference between the Pb/Sc ratio taken as reference (3.3) and that of UCC (2.4) (*31*) might be explained by a fractionation between heavy and light particles occurring during long-range atmospheric transportation (*26*) or by the preponderant influence of local background characterized by a higher Pb/Sc ratio. In any case, our calculation of anthropogenic lead will be not affected because our reference values, obtained from the core and not from a theoretical crust, already integrate such a potential fractionation. As a consequence, the positive anomaly of lead content around 120 cm depth cannot solely be explained by the amount of mineral matter (Figure 4). A dominant anthropogenic component has to be considered, also confirmed by $^{206}Pb/^{207}Pb$ signatures at this depth (~1.18) which indicate the presence of human-derived lead.

Regrettably, applying the same procedure for Zn, Cu, Sb, or Cd profiles (Figure 3) is far from straightforward, in part because these elements have no isotopic features which would allow zones without any anthropogenic contribution to be clearly identified. Zn and Cu are also essential nutriments for plants, which recycle them into the root zone. That is why their good preservation in peat bogs is generally difficult to observe, except in cases where pollution has been strong (*32, 33*). After eliminating the polluted topmost 30 cm samples Cu, Sb, and Cd profiles show an overall decreasing trend from the bottom to the top (Figure 3), which might result from the influence of groundwater and underlying mineral soil. In these horizons, Sb and Cd are significantly correlated to S ($r_{Pearson} = 0.74$, $p < 0.001$ and $r_{Pearson} = 0.63$, $p < 0.001$, respectively), suggesting that they may also have been partly redistributed in the core, to be finally associated with stable sulfur. Zn does not vary disproportionately to Sc except in the topmost horizons, where recent anthropogenic inputs have been such that they are still present. If large amounts of anthropogenic zinc were deposited in the past, they are no longer visible because of major translocation. Although, above 130 cm depth, cadmium almost matches the lead profile (cf. Figure 3) and presents variations out of proportion with those of Sc, the data suggest that none of these metals can be used as an appropriate monitor for atmospheric input reconstruction.

Isotopic Signature Contribution. Concerning lead, invaluable information about its possible postdepositional migration and hence about its utility for past industrial history reconstruction is provided by its isotopic composition. The procedure to determine graphically the isotopic signatures of anthropogenic inputs consists generally in representing the samples in a diagram of $^{206}Pb/^{207}Pb$ vs $1/[Pb]_{tot}$ (*12*). The background is considered as a constant end member, and the isotopic composition of anthropogenic lead of one

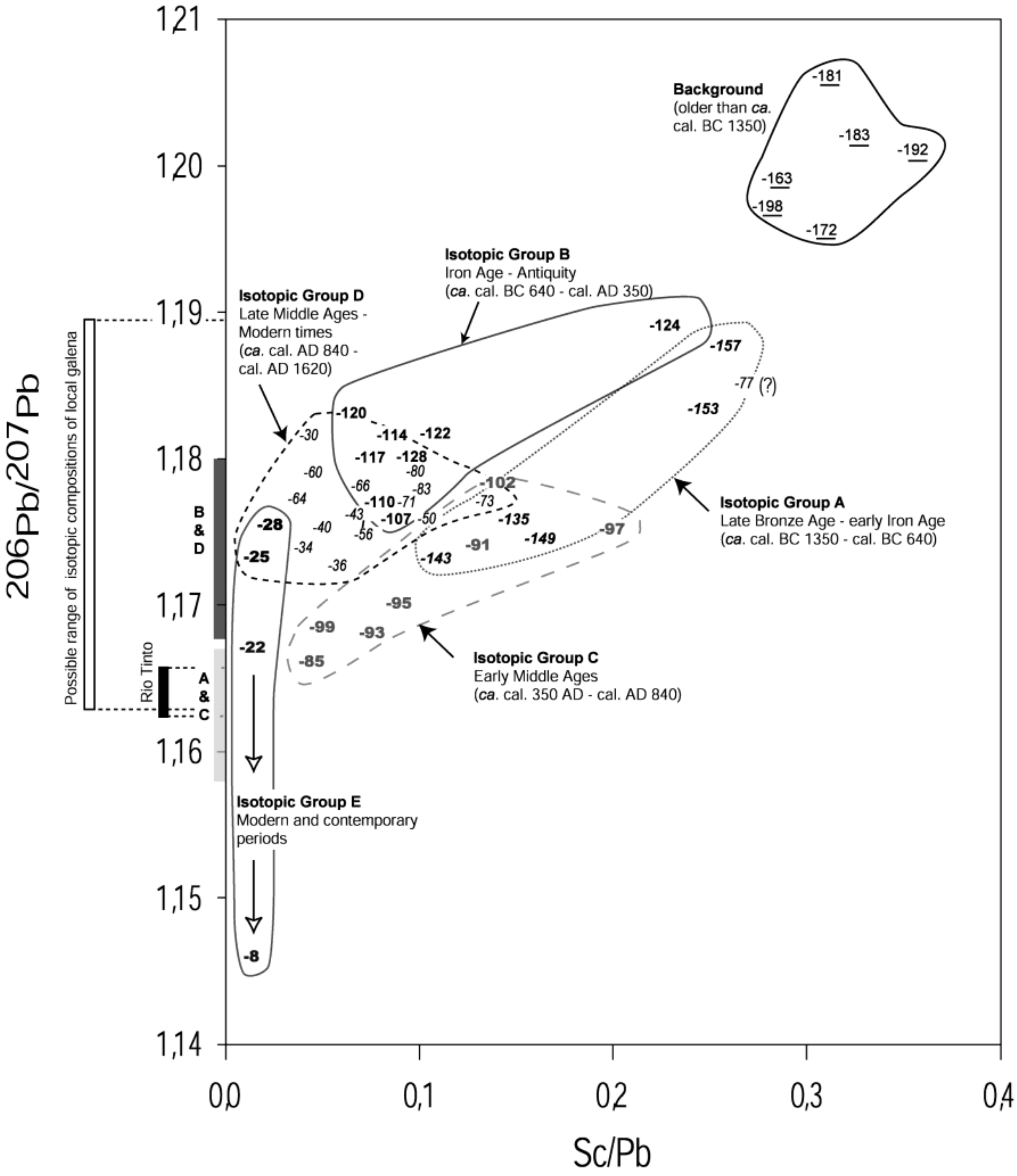

FIGURE 6. ^{206}**Pb/**^{207}**Pb versus Sc/Pb ratios. Samples are represented by their depth and grouped on the basis of their isotopic characteristics and the cultural periods to which they belong. The latter is assessed using the curve presented in Figure 2.**

contaminated sample can be read at the *Y*-axis intercept of the straight line linking the background domain and the sample. However, the use of $[\mathrm{Sc}]_{\mathrm{tot}}/[\mathrm{Pb}]_{\mathrm{tot}}$ in place of $1/[\mathrm{Pb}]_{\mathrm{tot}}$ on the *X*-axis produces a considerably more restrained background domain when natural Pb concentrations vary subsequently to changes in mineral matter contents. In such a situation, both Pb and Sc concentrations evolve proportionally, so that the $[\mathrm{Sc}]_{\mathrm{tot}}/[\mathrm{Pb}]_{\mathrm{tot}}$ ratio remains almost constant. For polluted samples, the procedure also eliminates dispersions due to variations in natural lead content on the *X*-axis, while the *Y*-axis intercept is interpreted as an end member featured by no Sc and high Pb content, in other words as the isotopic signature of the pure anthropogenic component. In our core, this representation is particularly well adapted since mineral matter content varies enough along the peat column not to be neglected (Figure 4b). The set of data does not fall on a line, which would have been an indicator of a unique anthropogenic source (or possibly multiple sources possessing the same isotopic signature), but widens close to the *Y*-axis, suggesting changes in exogenous lead sources (Figure 6). Six groups of samples can be graphically defined from their isotopic characteristics and the cultural periods to which they belong: the background end member before cal. B.C. 1750 (Group Background in Figure 6), late Bronze Age–early Iron Age, where anthropogenic lead inputs start (Isotopic Group A), Iron Age–Antiquity (Isotopic Group B), early Middle Ages (Isotopic Group C), late Middle Ages–Modern times (Isotopic Group D), and finally modern and contemporary samples (Isotopic Group E), although the age of the latter are rough estimations obtained by considering a constant accumulation rate between the 11th century and the present (see Figure 2).

The position of these groups in Figure 6 indicates that the isotopic compositions of the pollutant inputs have oscillated

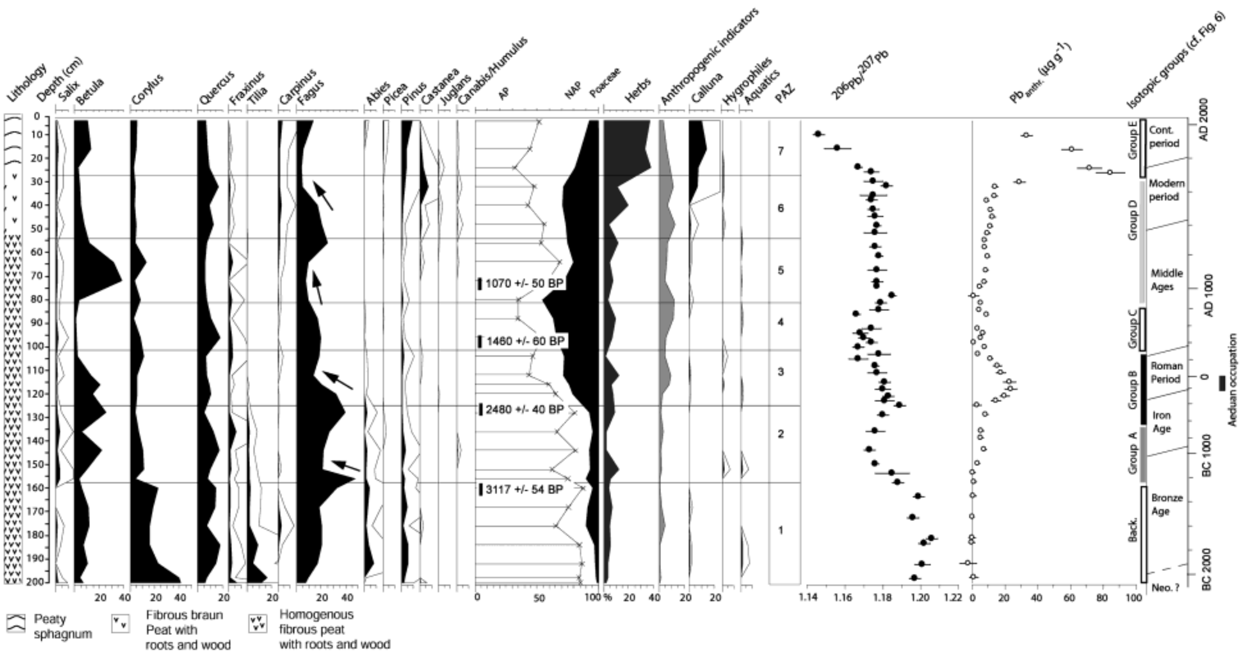

FIGURE 7. Lithology and pollen diagram organized in pollen assemblage zones (PAZ) according to major plant communities. For better legibility, dominant taxa *Alnus* and *Cyperaceae* were removed to form a simplified palynological diagram expressed as a percentage of taxa (*34*). ^{206}Pb/^{207}Pb ratios and anthropogenic lead concentrations are also represented on the depth scale accompanied by a chronological scale.

between low (^{206}Pb/^{207}Pb, 1.160−1.165 for phase A and C) and higher radiogenic signatures (^{206}Pb/^{207}Pb, 1.165−1.180 for phase B and D). The chronological order in which these phases appear is incompatible with any postdepositional migration of lead within the profile. As an example, the isotopic signature of the anthropogenic contribution corresponding to phase B cannot be explained by a translocation of lead from underlying or overlying horizons, simply because the anthropogenic lead buried during phases A and C is not radiogenic enough. The good integrity of both lead concentrations and isotope profiles is unambiguously demonstrated, at least at this time resolution; therefore, the lead record can be used for monitoring historical pollution. For comparative purposes, isotopic and anthropogenic lead concentration profiles are juxtaposed to palynological data organized in pollen assemblage zones (PAZ) according to major plant communities (Figure 7).

History Reconstruction. The Early Bronze Age is initially dominated by woodland taxa: *Corylus* (hazel), *Fagus* (beech), *Quercus* (oak), and to a lesser extent *Tilia* (lime) (Figure 7, PAZ 1). Anthropogenic indicators, such as cereal-type pollens, are already present in herbaceous taxa (*35*, *36*) and testify to early local human occupation. While the ^{206}Pb/^{207}Pb ratios of ∼1.20 in PAZ 1 merely reflect natural mineral matter (Background Isotopic Group), anthropogenic lead inputs start to be detected from PAZ 2 (ca. cal. B.C. 1300) by a significant fall in ^{206}Pb ^{207}Pb ratios and a slight rise in anthropogenic lead concentrations. The beginning of PAZ 2 in the late Bronze Age shows a drop in *Fagus, Corylus, and Quercus* taxa percentage. The low percentage of anthropogenic pollen indicators recorded in these levels seems to indicate that forest clearing was not related to any agropastoral extension. It is precisely at that time that the earliest substantial human-derived inputs are noticed by means of sizable anthropogenic lead concentrations while ^{206}Pb/^{207}Pb ratios continue to decline toward more anthropogenic values (Isotopic Group A). Such a concommitance is a hint of a close connection between metallic contamination and forest clearance. Moreover, as we shall see later, *Fagus* decline is systematically associated with anthropogenic input intensification, so that these observations in Late Bronze Age horizons, when metalworking developed in Western Europe (*37*), are not fortuitous. More locally, in Blanot, 30 km from the site, an abundant set of metallic artifacts dating from this period has been discovered (*38*). Vegetation cover may have been drastically affected by selective deforestation operated in response to an increasing demand in energy for mining and smelting, as noticed elsewhere (*13*, *14*). This suggests that this anthropogenic lead did not originate from remote areas after long-range atmospheric transport but was primarily emitted locally. Our results tend therefore to confirm that the Mount Beuvray area was, as previously suspected by some archaeologists, an early mining center. Extraction and smelting of copper, silver, or gold would have emitted into the atmosphere enough lead-enriched dust and gases to be archived in surrounding environments.

Throughout the Iron Age, the percentage of woodland taxa, dominated by *Fagus,* gradually increases (PAZ 2) while anthropogenic lead concentrations remain stable. Human pressure on the forest must have declined at that period. A turning point in this tendency is, however, observed in the Late Iron age (beginning of PAZ 3): *Fagus* taxa collapse again, anthropogenic herb indicators increase, while anthropogenic lead concentrations peak at the apogee of Aeduan civilization (first third of PAZ 3). Large forest openings probably enhanced erosion and accumulation of mineral matter in peat deposits (*39*), so that the reduction in accumulation rate (Figure 2) and the Sc anomaly (cf. Figure 3) pinpointed during the Aeduan occupation are not surprising. Intensification of lead anthropogenic inputs has been often documented between ca. B.C. 500 and A.D. 500 in multiple European environments (*8*, *10*, *39*, *40*), as far as Scandinavia (*11*, *41*) and Greenland (*42*, *43*). In the absence of dominating local sources, they are attributed, at least partly, to long-range transport of polluted airborne particulate matter coming from Southern Spain (*8*, *43*), this region accounting for up to 40% of worldwide lead production during the Roman Empire (*44*). At that time, the use of this metal was such that it was aptly called the Roman metal (*45*). Nonetheless, if there is no longer any doubt about the importance of lead of Spanish origin in high latitude regions, this source must not be overestimated in continental Europe, where local emissions may have acted as point sources even overriding the temporal pattern of large-scale pollution emission (*9*, *14*). Here, the isotopic signatures of the pollutant buried in peat (Isotopic Group B) are distinctly more radiogenic than those of Rio Tinto (1.162−1.166, *46*, *47*) (cf. Figure 6), while high anthropogenic lead concentrations come with major forest clearance, underlying their indigenous character. The Aeduans are well-known to have been fine metalworkers. Our results suggest the presence of major mining activity which, together with the numerous metallurgical workshops found out at Bibracte, could at least partly explain the tribe's wealth. Isotopic signatures of anthropogenic emissions clearly indicate variations in primary origin of lead between the Bronze Age and Antiquity (Figure 6), which might result from changes in the type of minerals exploited, although direct archaeological evidence is still lacking. Unfortunately, except for two values yielding ^{206}Pb/^{207}Pb ratios of 1.188−1.189 (*17*), there are no isotopic measurements available for local galena in the literature. However, by southward extension to the Massif Central, where much work has been done on similar Mesozoic galena, one can reasonably expect ^{206}Pb/^{207}Pb ratios comprised between 1.164 and 1.189 (*48*) (cf. Figure 6). This range, despite its size, is nevertheless compatible with the values of the anthropogenic inputs determined from the position of the different isotopic groups in Figure 6.

A decline in anthropogenic pollen indicators and lead fluxes (mid PAZ 3) marks the beginning of our era. Concurrently, the percentage of *Fagus* taxa stabilizes or even increases. After the Roman conquest of Gaul, the entire population of Bibracte was transferred 25 km away, to found the new city of *Augustodunum* (*2*). Local mining and smelting probably declined since mineral resources could have been provided by trade with the Romans and smelting transferred to *Augustodunum*, which became a metallurgical center. However significant anthropogenic lead fluxes are noticed at least until A.D. 300, which might signify persistent minor activities in the area or simply be the result of the release of lead from polluted soils over a long period of time after Aeduan mining operations ceased.

No remarkable change in geochemical is observed during the early Middle Ages (PAZ 4). For that period, archaeological knowledge is crucially lacking, so that the origin of the low anthropogenic inputs is rather uncertain. Following the fall of the Roman Empire, ancient industrial techniques were partially abandoned or even forgotten, which is probably what happened here. Around the 12th century (PAZ 5), human-derived lead concentrations rise, *Fagus* representation drops, and *Betula* (birch), a heliophilous and pioneer tree, dominates woodland cover. Such a renewal is contemporary with the great deforestation phases observed at the European scale (*49*). Almost everywhere, Roman mines were progressively reopened, while new ones were discovered (i.e., Germany, Balkans, etc.) (*33*, *50*). Anthropogenic inputs continue in PAZ 6 and even amplify drastically later (PAZ 7), although the chronology established from ^{14}C does not allow a precise dating of this phase. The peak of anthropogenic lead concentration at almost $80\,\mu g\,g^{-1}$ probably corresponds to the phase of local mining exploitation, which is well documented by textual archives during the 18th and 19th century. The fact that *Fagus* pollen almost totally disappears at that time tends to support this thesis. Such a fall may also be due to the intense exploitation of Morvan forests from the 16th to the beginning of the 20th century, which were operated to furnish Paris with firewood (*51*). The sequence seems to be dilated in the topmost centimeters, as suggested by the ^{206}Pb/^{207}Pb ratio measured at 14 cm depth (1.156), supposedly dating from 1900, which actually reflects the recent use of nonradiogenic lead for industry. Apart from these persistent doubts in the most recent samples, the new set of geochemical and pollen data presented here is in good agreement with the archaeological and historical knowledge available. The use of isotopic geochemistry combined with the Sc correction of total lead measurements enables controlled distinction and apportioning of anthropogenic versus natural materials. The isotopic signal was found, as previously (*52*), to be more sensitive than the sole measurement of concentrations when anthropogenic contribution is low. This technique makes possible here a fine recognition of early contaminations dating as far back as the Late Bronze Age. They are interpreted as the first signs of local metallurgy, which may have attracted later settlers who founded Bibracte, its indigenous character being underlined by the correspondence with the pollen record. By combining geochemical and palaeobotanical techniques with archaeological knowledge, the past seems therefore to become less opaque.

In the sequence studied, about 20% of the total anthropogenic lead was deposited before our era and probably about one-half of the pool before the 18th century. Together with the archaeological answers exposed above, the importance of the environmental impact of our ancestors' industrial activities has been demonstrated in a region which is nowadays one of the less industrialized areas of France. This heritage should be taken into account when evaluating the quality of the environment in order to not overestimate the impact of modern pollution. The reconstruction of the interactions which existed between early societies and their environment is a key factor, which may well be of assistance in the management of current and future environmental problems.

Acknowledgments

We thank Pierre Yves Favargé, Sylvie Philippe, Marie-Jeanne Milloux, and Davide Vignati for their technical assistance. We also thank four anonymous reviewers who greatly improved the manuscript by their thoughtful comments.

Literature Cited

(1) Gruel, K.; Vitali, D. *Gallia* **1999**, *55*, 1.
(2) Rebourg, A. *Gallia* **1999**, *55*, 141.
(3) Gran-Aymerich, J. In *La civilisation de Hallstatt, bilan de la rencontre de Liége*; Etudes et recherches archéologiques de l'université de Liége; 1989; E.R.A.U.L. no. 36; pp 343−355.
(4) Buchsenchutz, O.; Richard, H. In *L'environnement du Mont Beuvray;* Centre archéologique european du Mont Beuvray; Glux-en-Glenne, 1996; Collection Bibracte no. 61616; 1, p 207.
(5) Weiss, D.; Shotyk, W.; Appleby, P. G.; Kramers, J. D.; Cheburkin, A. K. *Environ. Sci. Technol.* **1999**, *33*, 1340.
(6) Urban, N. R.; Eisenreich, S. J.; Grigal, D. F.; Schurr, K. T. *Geochem. Cosmochem. Acta* **1990**, *54*, 3329.
(7) MacKenzie, A. B.; Logan, E. M.; Cook, G. T.; Pulford, I. D. *Sci. Tot. Environ.* **1998**, *223*, 25.
(8) Shotyk, W.; Weiss, D.; Appleby, P. G.; Cheburkin, A. K.; Frei, R.; Gloor, M.; Kramers, J. D.; Reese, S.; Van Der Knaap, W. O. *Science* **1998**, *281*, 1635.
(9) Camarero, L.; Masqué, P.; Devos, W.; Ani-Ragolta, I.; Catalan, J.; Moor, H. C.; Pla, S.; Sanchez-Cabeza, J. A. *Water Air Soil Pollut.* **1998**, *105*, 439.
(10) Alfonso, S.; Grousset, F.; Massé, L.; Tastet, J.-P. *Atmos. Environ.* **2001**, *35*, 3595.
(11) Renberg, I.; Bindler, R.; Brännvall, M.-J. *Holocene* **2001**, *11*, 511.
(12) Faure, G. *Principles of Isotope Geology*, 2nd ed.; Wiley: New York, 1986.
(13) Richard, H.; Eschenlhor, L. *Rev. d'archéométrie* **1998**, *22*, 29.
(14) Galop, D.; Tual. M.; Monna, F.; Dominik, J.; Beyrie, A.; Marembert, F. *Sud Ouest Eur.* **2001**, *11*, 3.
(15) Lhégu, J.; Jebrak, M.; Touray, J. C.; Ziserman, A. *Bulletin BRGM;* BRGM, Orléans, 1982; section II, no. 61616; 2, pp 165−177.
(16) Delfour, J. *BRGM report no. 61616*; 78 SGN 611, BRGM: Orléans, 1978; p 11.
(17) Marcoux, E. Ph.D. Thesis, University of Clermont-Ferrand II, 1986; p 299.
(18) Monna, F.; Loizeau, J.-L.; Thomas, B. A.; Guéguen, C.; Favarger, P.-Y. *Spectrochim. Acta B* **1998**, *59*, 1317.

(19) Monna, F.; Loizeau, J.-L.; Thomas, B.; Guéguen, C.; Favarger, P.-Y.; Losno R.; Dominik, J. *Analusis* **2000**, *28*, 750.

(20) Moore, P. D.; Webb, J. A.; Collinson, M. E. *Pollen analysis*, 2nd ed.; Blackwell: Oxford, 1991.

(21) Feagri, K.; Iversen, J.; *Textbook of Pollen Analysis*; John Wiley & Sons: New York, 1989.

(22) Reille, M. *Pollen et spores d'Europe et d'Afrique du Nord*; Laboratoire de Botanique Historique et Palynologie, URA CNRS 1152: Marseille, 1992; p 550.

(23) Stuiver, M.; Reimer, P. J.; Bard, E.; Beck, J. W.; Burr, G. S.; Hughen, K. A.; Kromer, B.; McCormac, F. G.; Plicht, J.; Spurk, M. *Radiocarbon* **1998**, *40*, 1041.

(24) Würst, R. A. J.; Bustin, R. M.; Lavkulich, L. M. *Catena* **2003**, *751*, 1.

(25) Zeitz, J. In *Geochemie und Umwelt;* Matschullat, J., Tobschall, H. J., Voight, H.-J, Eds.; Springer-Verlag: Heidelberg, 1997; 443p.

(26) Shotyk, W.; Weiss, D.; Kramers, J. D.; Frei, R.; Cheburkin, A. K.; Gloor, M.; Reese, S. *Geochim. Cosmochim. Acta.* **2001**, *65*, 2337.

(27) Jones, J.; Hao, J. *Environ. Geochem. Health* **1993**, *15*, 67.

(28) Bozkurt, S.; Lucisano, L.; Moreno, L.; Neretniekds, I. *Earth Sci. Rev.* **2001**, *53*, 95.

(29) Shotyk, W. *Environ. Rev.* **1996**, *4*, 149.

(30) Monna, F.; Lancelot, J. R.; Croudace, I. W.; Cundy, A. B.; Lewis, J. T. *Environ. Sci. Technol.* **1997**, *31*, 2277.

(31) Wedepohl, K. H. *Geochim. Cosmochim. Acta* **1995**, *59*, 1217.

(32) Mighall, T. M.; Abrahams, P. W.; Grattan, J. P.; Hayes, D.; Timberlake, S.; Forsyth, S. *Sci. Tot. Environ.* **2002**, *292*, 69.

(33) Kempter, H.; Frenzel, B. *Water Air Soil Pollut.* **2000**, *121*, 93.

(34) Janssen, C. R. *Acta Bot. Neerlandia* **1959**, *8*, 55.

(35) Behre, K.-E. *Anthropogenic indicators in pollen diagrams;* Balkema: Rotterdam, 1986.

(36) Richard, H. In *L'homme et la dégradation de l'environnement*; XVéme Rencontres Internationales d'Archéologie et d'Histoire d'Antibes; APDCA: Gap, 1995.

(37) Huth, C. Metals make the world go round. In *Metal circulation, communication and tradition of craftmanship in Late Bronze Age and Early Iron Age Europe;* Pare, C. F. E., Ed.; Oxbow Books; Oxford, 2000.

(38) Thévenot, J. P. *Revue archéologique de l'Est et du Centre-Est;* Dijon, 1991; 11th supplément.

(39) Van Geel, B.; Bregman, R.; van der Molen, P. C.; Dupont, L. M.; Van driel-Murray, C. *Acta Bot. Neerl. 38*, 467.

(40) Martínez-Cortizas, A.; García-Rodeja, E.; Pontevedra-Pombal, X.; Nóvoa Muñoz, J. C.; Weiss, D.; Cheburkin, A. *Sci. Tot. Environ.* **2002**, *292*, 33.

(41) Renberg, I.; Wik-Persson, M.; Emteryd, O. *Nature* **1994**, *368*, 323.

(42) Hong, S.; Candelone, J.-P.; Patterson, C. C.; Boutron, C. F. *Science* **1994**, *23*, 1841.

(43) Rosman, K. J. R.; Chisoholm, W.; Hong, S.; Candelone, J.-P.; Boutron, C. F. *Environ. Sci. Technol.* **1997**, *31*, 3413.

(44) Nriagu, J. O. *Lead and lead poisoning in Antiquity*; Wiley: New York, 1983.

(45) Nriagu, J. O. *Environment* **1990**, *32*, 7.

(46) Stos-Gale, Z.; Gale, N. H.; Houghton, J.; Speakman, R. *Archaeometry* **1995**, *37*, 407.

(47) Pomiès, C.; Cocherie, A.; Guerrot, C.; Marcoux, E.; Lancelot, J. *Chem. Geol.* **1998**, *144*, 137.

(48) Brévart, O.; Dupré, B.; Allègre, C. J. *Econ. Geol.* **1982**, *77*, 429.

(49) Berglund, B. E.; Birks, H. J. B.; Ralska-Jasiewiczowa, M.; Wright, H. E. *Palaeoecological events during the last 15 000 years. Regional syntheses of palaeoecological studies of lakes and mires in Europe*; John Wiley & Sons: New York, 1996.

(50) Brännvall, M.-L.; Bindler, R.; Renberg, I.; Emteryd, O.; Bartnicki, J.; Billström, K. *Environ. Sci. Technol.* **1999**, *33*, 4391.

(51) Vigreux, M. *Courrier du Parc naturel régional du Morvan* **1994**, *25*, 9.

(52) Munksgaards, N. C.; Parry, D. L. *Sci. Tot. Environ.* **1998**, *217*, 113.

Received for review July 3, 2003. Revised manuscript received November 3, 2003. Accepted November 6, 2003.

ES034704V

Environ. Sci. Technol. **2004**, *38,* 1513−1521

Modeling Lead Input and Output in Soils Using Lead Isotopic Geochemistry

R. M. SEMLALI,† J.-B. DESSOGNE,‡
F. MONNA,*,§ J. BOLTE,‖ S. AZIMI,⊥
N. NAVARRO,# L. DENAIX,○ M. LOUBET,▽
C. CHATEAU,◆ AND F. VAN OORT†

INRA, Unité de Science du Sol, RD10, F-78026 Versailles Cedex, France, GéoSol, UMR INRA-Université de Bourgogne, Centre des Sciences de la Terre, Université de Bourgogne, Bat Gabriel, F-21000, Dijon, France, UMR 5594 CNRS-Université de Bourgogne, Laboratoire Archéologie, Cultures et Sociétés, Université de Bourgogne, Bat Gabriel, F-21000, Dijon, France, ACSIOM, Départment de Mathématiques, CNRS-FRE 2311, cc. 051, Université de Montpellier II, Place Eugène Bataillon, F-34095 Montpellier Cedex 5, France, CEREVE, Université Paris XII, 61 Avenue Général de Gaulle, F-94010 Créteil Cedex, France, Biogéosciences, UMR 5561 CNRS-Université de Bourgogne, Centre des Sciences de la Terre, Université de Bourgogne, Bat Gabriel, F-21000, Dijon, France, INRA, Unité d'Agronomie, Centre de Recherche de Bordeaux-Aquitaine, BP 81, F-33883 Villenave d'Ornon Cedex, France, UMR 5563, Université Paul Sabatier, Laboratoire de Géochimie, 38, Rue des 36 Ponts, F-31400 Toulouse, France, and Centre des Sciences de la Terre, Université de Bourgogne, Bat Gabriel, F-21000, Dijon, France

The aim of this study is to model downward migration of lead from the plow layer of an experimental site located in Versailles (about 15 km southwest of Paris, France). Since 1928, samples have been collected annually from the topsoil of three control plots maintained in bare fallow. Thirty samples from 10 different years were analyzed for their lead and scandium contents and lead isotopic compositions. The fluxes are simple because of the well-controlled experimental conditions in Versailles: only one output flux, described as a first-order differential function of the anthropogenic lead pool, was taken into account; the inputs were exclusively ascribed to atmospheric deposition. The combination of concentration and isotopic data allows the rate of migration from the plowed topsoil to the underlying horizon and, to a lesser extent, the atmospheric fluxes to be assessed. Both results are in good agreement with the sparse data available. Indeed, the post-depositional migration of lead appears negligible at the human time scale: less than 0.1% of the potentially mobile lead pool migrates downward, out of the first 25 cm of the soil, each year. Assuming future lead inputs equal to 0, at least 700 yr would be required to halve the amount of accumulated lead pollution. Such a low migration rate is compatible with the persistence of a major anthropogenic lead pool deposited before 1928. Knowledge of pollution history seems therefore to be of primary importance.

Introduction

Among heavy metals, lead is probably the most widely emitted by anthropogenic activities throughout the history of mankind. Significant atmospheric Pb pollution started in Europe from Antiquity (*1, 2*), but the major peak of pollution occurred only recently during the 1970s due to extensive use of lead-based antiknock agents in petrol (*3, 4*). Since Pb is recognized as toxic for most animals and plants (*5, 6*), environmental policies in most industrialized countries over the last two decades have resulted in a significant decrease of Pb contents in the atmosphere (*3, 7*). However, high Pb contents are still frequently reported worldwide in accumulating environments such as soils (*8, 9*), peat bogs (*10, 11*), and sediments (*12, 13*). They are generally ascribed to the persistence of past contaminations originating from automotive traffic; coal ash, ore-mining, and smelting activities; agricultural inputs; waste incineration; or pollution of unknown origin. Lead is predominantly concentrated in the surface horizon and generally considered as being much less mobile than Zn, Cd, or Cu (*14*). Nevertheless, limited downward migration has frequently been demonstrated not only in contaminated soils (*8, 15−17*) but also in soils affected only by diffuse atmospheric deposition (*18*). Environmental risk related to metal mobility after soil contamination has often been studied via chemical partitioning, this latter subordinating bioavailability and long-term migration. As a result, several models of metal speciation have been developed and compared to field data or laboratory experiments (*19*). They yielded important information, but sequential extractions are often criticized for poorly constraining the dissolved chemical phases (*20*). Moreover, such methods do not allow any quantification of migration rate in natural conditions, although they indicate a certain migratory ability. Another approach for assessing the release rate of metals from soils consists of lixiviation experiments operated in batch columns (*21*) or long-term studies using lysimeters in the field (*15, 16*). Other scientists prefer the study of metal distribution in natural soil profiles or batch columns (*22*) in order to evaluate metal incorporation. Retention can then be determined by using a speciation scheme, by examining the shape of the profile in the soil, or by a combination of both. However, the approach focusing on vertical distribution in soils to estimate downward migration processes is better adapted to elements for which the input function is well-constrained. One of the most widely studied in this context is probably ^{137}Cs, which was deposited in European soils in known quantities after the Chernobyl accident. In undisturbed conditions, the concentration profiles approximately follow an exponential decline with depth, which can be described by various time-dependent diffusion models (*23, 24*), allowing the rate of change of vertical distribution to be calculated (*25, 26*). In the case of lead, the situation is greatly complicated, as mentioned above, by the long history of its emission into the atmosphere. Most of the time, its fluxes are not precisely known over time, and it is hazardous to calculate any mass balance or migration rate (*8*) except when assumptions are made as to the history and nature of lead inputs (*27*). Some authors have also

---

* Corresponding author e-mail: Fabrice.Monna@u-bourgogne.fr; phone: +33 (0)3 80 39 63 55; fax: +33 (0)3 80 39 63 87.

† INRA, Unité de Science du Sol.

‡ GéoSol, UMR INRA-Université de Bourgogne.

§ UMR 5594 CNRS-Université de Bourgogne.

‖ Université de Montpellier II.

⊥ Université Paris XII.

Biogéosciences, UMR 5561 CNRS-Université de Bourgogne.

○ Centre de Recherche de Bordeaux-Aquitaine.

▽ Université Paul Sabatier.

◆ Centre des Sciences de la Terre, Université de Bourgogne.

10.1021/es0341384 CCC: $27.50

TABLE 1. Pb and Sc Concentrations and Pb Isotopic Compositions of Samples Collected in Three Control Parcels (T1−T3) in 10 Different Years and Parent Material

yr of collection[a]	control parcel	Pb (μg g^{-1})	Pb$_{\text{Mean}}$ (μg g^{-1})	±	Sc (μg g^{-1})	Sc$_{\text{Mean}}$ (μg g^{-1})	±	^{206}Pb/^{207}Pb	^{206}Pb/^{207}Pb$_{\text{Mean}}$	±
1929	T1	48.5	49.1	3.9	5.7	5.6	0.5	1.1833	1.183	0.001
	T2	47.8			5.4			1.1833		
	T3	50.9			5.8			1.1826		
1934	T1	49.6	51.3	3.8	6.0	5.9	0.3	1.1828	1.183	0.001
	T2	52.6			5.7			1.1827		
	T3	51.6			5.9			1.1835		
1939	T1	54.2	55.3	2.3	5.8	5.7	0.4	1.1824	1.182	0.002
	T2	55.7			5.5			1.1814		
	T3	55.9			5.8			1.1829		
1945	T1	55.6	54.3	6.3	5.8	5.8	0.5	1.1807	1.182	0.003
	T2	51.4			5.6			1.1830		
	T3	56.0			6.0			1.1825		
1954	T1	62.3	61.5	1.7	6.0	5.9	0.9	1.1810	1.182	0.003
	T2	61.1			5.5			1.1824		
	T3	61.1			6.2			1.1832		
1963	T1	61.5	60.6	8.9	5.9	5.9	0.1	1.1816	1.181	0.003
	T2	56.6			5.9			1.1803		
	T3	63.6			5.9			1.1823		
1972	T1	69.4	68.1	3.2	5.9	5.9	0.4	1.1805	1.182	0.003
	T2	67.9			5.7			1.1815		
	T3	66.8			6.0			1.1825		
1981	T1	63.5	60.7	11.6	6.0	5.9	0.2	1.1803	1.181	0.002
	T2	55.3			5.8			1.1812		
	T3	63.3			5.9			1.1817		
1991	T1	69.4	69.0	1.2	5.9	5.7	0.4	1.1787	1.180	0.003
	T2	68.5			5.6			1.1796		
	T3	69.2			5.6			1.1808		
2000	T1	74.1	71.3	14.7	5.9	5.7	0.5	1.1783	1.179	0.002
	T2	75.2			5.5			1.1796		
	T3	64.5			5.7			1.1799		
parent material		15.8			5.6			1.2035		

[a] For each year, the concentration and isotopic average of the three parcels is given as well as the 95%.confidence interval.

proposed interesting combinations of these approaches with the use of lead isotopic geochemistry. Fundamentals of this method applied to soils are based on the isotopic difference existing between anthropogenic lead and endogenous lead derived from rocks and soils and are extensively described elsewhere (*18, 27−34*). Lead isotopic geochemistry is generally more powerful than concentration measurement to identify any minor anthropogenic component.

In the present study, we examine the fate of Pb concentrations and isotopic compositions in soils sampled annually from an experimental field managed by the French National Research Institute of Agronomy (INRA) since 1928. This experimental site, originally created for the study of long-term effects of various fertilizing agents on the quality of bare soils (*35*), provides an invaluable and unique (at least for France) set of available samples with a 70-yr topsoil library. To study the behavior of lead in soil from these samples, we took as a basis a previously published model (*36, 37*), which was developed to estimate critical loads of trace metals in soils. However, as it originally applied to a whole soil submitted to constant lead inputs, it was adapted to fit the present experimental conditions. Hence, we attempted to assess downward Pb migration and, to a lesser extent, atmospheric lead fluxes.

Setting

The site, known as "42 plots", is located in a peri-urban area next to the gardens of the Chateau of Versailles, about 15 km from Paris. The soil is an aquic Hapludalf (luvisols), developed in eolian loess deposits, typical of the Paris basin. Ten reference plots did not receive any fertilizing amendments but were maintained in bare fallow, except episodically for potato cultivation during World War II. The others were annually amended with basic slugs, ammonium phosphate, superphosphate, Moroccan rock-phosphate, farmyard manure, and calcium carbonate (*38*). All were plowed twice a year, at a mean depth of 0.25 ± 0.05 m.

Experimental Section

Sampling. From 1929 onward, about 1 kg representing the mixed and plowed 0−0.25-m A horizon was collected annually from each reference plot. The soil samples were dried, crushed, and stored in hermetically closed glass bottles. Because of the exceptional importance of the "42 plots" device for long-term studies, no dig was operated in underlying soils, which means that no such samples were available in the soil library. However, in an adjacent field (200 m away), at more than 0.80 m depth, we collected a sample supposed to be representative of the undisturbed C horizon and, hence, of pristine parent material.

Analysis. Ten years were selected among the 70-yr archive: 1929, 1934, 1939, 1945, 1954, 1963, 1972, 1981, 1991, and 2000. For each year, three samples from three different reference plots were analyzed for their Pb and Sc contents and Pb isotopic compositions (Table 1). Chemical preparation followed the procedure AFNOR NF X31-151 (*39*), which consists of ashing 250 mg of powdered samples at 450 °C for 3 h and total acid dissolution by Merck Suprapur and concentrated HF, $HClO_4$, and HNO_3. Pb concentrations were analyzed by inductively coupled plasma-mass spectrometer (ICP-MS) (relative standard deviation, rsd, <5%), while Sc contents were determined by inductively coupled plasma-atomic emission spectrometry (ICP-AES) (rsd < 2%). For isotopic measurements, lead contained in an aliquot of the above-mentioned solution was purified twice using AG1X8 (Bio-Rad) anion-exchange resin (*18, 40*). Pb solution was dried down with 10 μL of 0.05 M H_3PO_4 and then loaded on a degassed Re single filament. The whole procedure was performed in a clean room. Lead isotopic compositions were measured on a Finnigan MAT 261 thermoionization-mass spectrometer (TIMS). Results were corrected for mass fractionation by systematic NIST 981 measurements, yielding a value of about 0.14% per atomic mass unit. Blanks were systematically checked and were always found negligible in relation to the amount of material analyzed.

We used scandium as a conservative element because (i) it is not of any significant anthropogenic origin and (ii) it is hosted by the most refractory minerals (*41*). Endogenous lead contribution in soil samples ($\mathrm{Pb_{end}}$) was estimated following the conventional equation:

$$\mathrm{Pb_{end}} = \mathrm{Sc_{bulk}}\left(\frac{\mathrm{Pb}}{\mathrm{Sc}}\right)_{\text{parent material}} \tag{1}$$

where $\mathrm{Sc_{bulk}}$ represents Sc sample concentration and $(\mathrm{Pb/Sc})_{\text{parent material}}$ is the ratio of parent material (*18*, *41*, *42*). Given that the majority of exogenous lead derives from human activity, anthropogenic lead ($\mathrm{Pb_{anthr}}$) was then obtained by subtracting endogenous contribution ($\mathrm{Pb_{end}}$) from measured total Pb concentration ($\mathrm{Pb_{bulk}}$):

$$\mathrm{Pb_{anth\mathit{r}}} = \mathrm{Pb_{bulk}} - \mathrm{Pb_{end}} \tag{2}$$

Model. A first natural approach to treat these results would have consisted in considering only one input function, which would have corresponded to atmospheric deposition, and no lead migration from topsoil; this element being viewed as lowly mobile. From the available 70-yr collection of topsoils, it would be tempting to reconstruct the history of atmospheric lead fluxes and hence the evolution of isotopic compositions of anthropogenic deposition over time. However, such a reconstruction yields either uncertain or simply aberrant values for both fluxes and isotopic signatures (see Supporting Information for more details). Anthropogenic lead deposited between two successive samples is very low in comparison with the pool already accumulated so that the propagation of error is huge. In addition to which, there is relatively high dispersion of field data from the three control parcels. The present soil library cannot be treated in such a way, unlike sedimentary or peat archives which are time-resolved. Nonetheless, a previous model elaborated by Pačes to assess critical loads of trace metals in soils can be adapted to fulfill the purpose in view (*36*, *37*). In this model, soils were seen as black boxes receiving metal fluxes from atmosphere (F_{atm}), agriculture (F_{agr}), and bedrock weathering (F_{wea}), whereas outputs were considered to be biological uptakes (F_{up}) and runoff (F_{run}). With P, the bioavailable pool, a mass balance equation was formulated by

$$\mathrm{d}P/\mathrm{d}t = F_{\mathrm{atm}} + F_{\mathrm{agr}} + F_{\mathrm{wea}} - F_{\mathrm{up}} - F_{\mathrm{run}} \tag{3}$$

Annual input ($F = F_{\mathrm{atm}} + F_{\mathrm{agr}} + F_{\mathrm{wea}}$) was assumed constant in time, whereas outputs were supposed to be proportional (k, positive factor) to the biologically available pool P at time t, $P(t)$:

$$\frac{\mathrm{d}P}{\mathrm{d}t}(t) = F - k{\cdot}P(t) \tag{4}$$

In the Pačes model, k was a constant (expressed as $\mathrm{yr^{-1}}$), which corresponds to a coefficient of annual lead loss from the whole soil (*36*, *37*). By integrating from an initial pool P_0 at t_0, this became

$$P(t) = \frac{F}{k} - \frac{F - k{\cdot}P_0}{k}\mathrm{e}^{-k(t-t_0)} \tag{5}$$

Pačes determined the bioavailable pool using chemical extraction applied to soils. The k factor and local fluxes used to run the model came from the literature. Future evolution of concentrations was calculated first. The moment at which critical concentrations (established by ecotoxicological studies) were reached enabled critical time to be forecast.

In the present study, due to the information from the Versailles site, we are able to check the validity of this first-order differential model by confronting field values with those predicted by modeling. Adding lead isotopic geochemistry may also produce a better understanding of how lead entered the soil system and how it has migrated through underlying horizons. Interestingly, experimental conditions at the Versailles device allow simplification with respect to the original model, which means that a new degree of complexity can be introduced: the variability of input fluxes. The modifications performed to match our experimental conditions are listed below:

(i) The black box now corresponds to the plowed mixed 0−0.25-m layer instead of the whole soil of the Pačes model.

(ii) The fluxes related to agriculture are simplified because no amendments were operated ($F_{\mathrm{agr}} = 0$) and because there was no harvest ($F_{\mathrm{up}} = 0$).

(iii) Bedrock weathering does not measurably occur during the considered time scale ($F_{\mathrm{wea}} = 0$). This assumption will be discussed later.

(iv) Lateral runoff can reasonably be ignored because plot slope is negligible ($F_{\mathrm{run}} = 0$). Consequently, only one unique output flux is taken into account. It corresponds to downward transfer by lixiviation from the 0−0.25-m layer to the underlying horizons (F_{out}).

(v) It is well-known that past atmospheric lead deposition varied widely during the last century (ref *4* and references therein). Therefore, we do not consider atmospheric lead fluxes (F_{in}) as constant over the period of collection.

(vi) If the above assumptions are verified, in particular the insignificant release of lead by minerals over a 70-yr time scale, the only potentially mobile pool must originate from anthropogenic atmospheric deposition (P_{anthr}). Hence, no further consideration will be given to the biologically available lead pool of the Pačes model, which is here replaced by the anthropogenic pool for computation.

To take into account the fluctuation of input fluxes over time, a natural approach would consist in generalizing the Pačes model directly:

$$\frac{\mathrm{d}P_{\mathrm{anthr}}}{\mathrm{d}t}(t) = F_{\mathrm{in}}(t) - F_{\mathrm{out}}(t) \tag{6}$$

$$F_{\mathrm{out}}(t) = k{\cdot}P_{\mathrm{anthr}}(t) \tag{7}$$

$$\frac{\mathrm{d}P_{\mathrm{anthr}}}{\mathrm{d}t}(t) + k{\cdot}P_{\mathrm{anthr}}(t) = F_{\mathrm{in}}(t),\ t \in [1929, 2000] \tag{8}$$

with k now corresponding to the annual lead losses from the 0−0.25-m horizon (expressed as $\mathrm{yr^{-1}}$). As we shall see later, introducing isotopic parameters will decisively improve the efficiency of the model. One of the major drawbacks of the aforementioned equation is that it ignores isotopic variations of the anthropogenic component through time, although it is well-known that such isotopic signatures varied widely during the last century depending on the primary origin of the metal (the fundamentals of these variations are explained elsewhere) (*7*, *43*−*45*). As a consequence, each annual input must be examined individually regarding its pool and isotopic composition (Figure 1).

Modeling Total Lead Concentrations. For each year i, let $P^{i}_{\mathrm{anthr}}(t)$ denote the anthropogenic lead pool deposited at year i per surface unit, observed at time t (Figure 1). If F^{i}_{in} is the anthropogenic flux of year i, the Pačes model states that

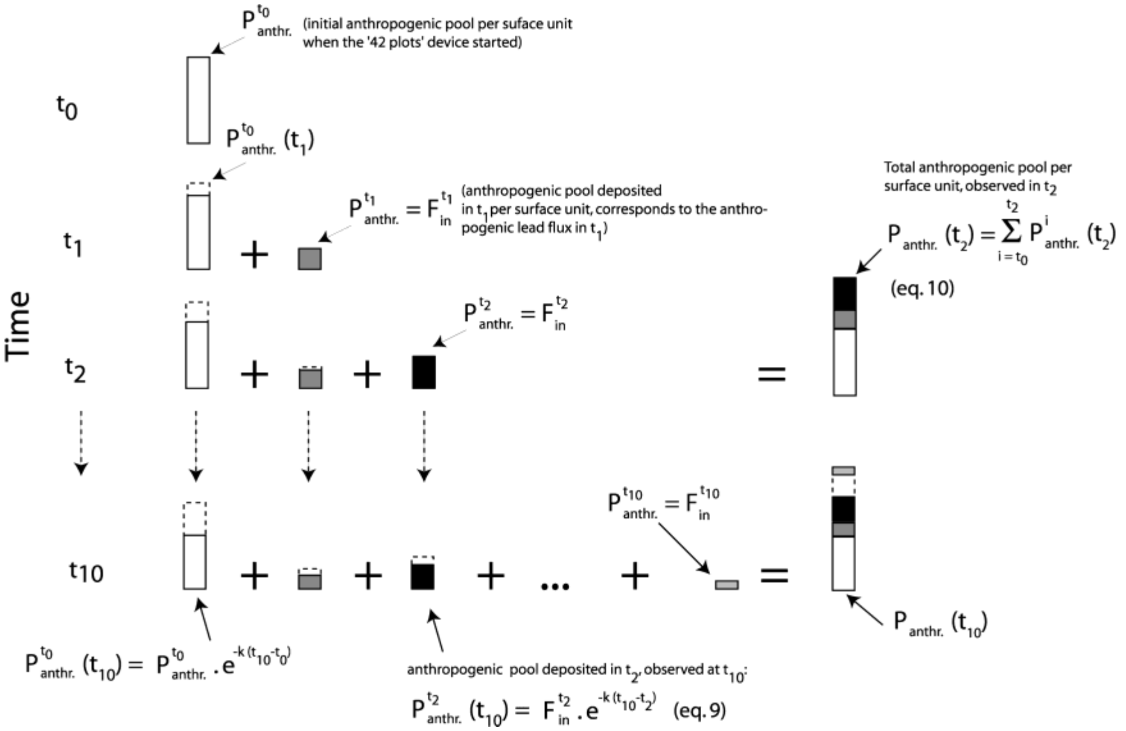

FIGURE 1. Scheme of the model. Each anthropogenic pool is represented by a gray tone, which symbolizes its own isotopic signature.

P^i_{anthr} evolves according to the following differential equation:

$$\frac{\mathrm{d}P^i_{\text{anthr}}(t)}{\mathrm{d}t} + k{\cdot}P^i_{\text{anthr}}(t) = 0, \text{ for all } t \geq i$$

$$P^i_{\text{anthr}}(i) = F^i_{\text{in}}$$

$$P^i_{\text{anthr}}(t) = 0 \text{ if } t < i$$

A straightforward integration gives this:

$$P^i_{\text{anthr}}(t) = F^i_{\text{in}}\mathrm{e}^{-k(t-i)}, \text{ for all } t \geq i \qquad (9)$$

At year t, the total pool, $P_{\text{anthr}}(t)$, is the sum of all remaining annual contributions:

$$P_{\text{anthr}}(t) = \sum_{i=t_0}^{t} P^i_{\text{anthr}}(t) \qquad (10)$$

where t_0 is the first sampling year (1929 in our case); $P^{t_0}_{\text{anthr}}$ being the initial anthropogenic lead pool.

Instead of expressing this equation in terms of pool, it can be reformulated in terms of concentration of potentially mobile lead, $\text{Pb}_{\text{anthr}}(t)$:

$$\text{Pb}_{\text{anthr}}(t) = \frac{P_{\text{anthr}}(t)}{h{\cdot}d_{\text{A}}} \qquad (11)$$

with h as thickness of plowed horizon and d_{A} as bulk density. Finally, the total lead concentration observed at year t becomes

$$\text{Pb}_{\text{bulk}}(t) = \text{Pb}_{\text{anthr}}(t) + \text{Pb}_{\text{end}} \qquad (12)$$

Modeling Lead Isotopic Compositions. Considering a conventional mixing model (*46*), the $^{206}\text{Pb}/^{207}\text{Pb}$ ratio of the sample theoretically becomes

$$\left(\frac{^{206}\text{Pb}}{^{207}\text{Pb}}\right)_{\text{bulk}}(t) \approx \frac{1}{\text{Pb}_{\text{bulk}}(t)}\left[\text{Pb}_{\text{end}}\left(\frac{^{206}\text{Pb}}{^{207}\text{Pb}}\right)_{\text{end}} + \sum_{i=t_0}^{t}\left(\text{Pb}^i_{\text{anthr}}(t)\left(\frac{^{206}\text{Pb}}{^{207}\text{Pb}}\right)^i_{\text{anthr}}\right)\right] \qquad (13)$$

where $(^{206}\text{Pb}/^{207}\text{Pb})_{\text{bulk}}(t)$, $(^{206}\text{Pb}/^{207}\text{Pb})^i_{\text{anthr}}$, and $(^{206}\text{Pb}/^{207}\text{Pb})_{\text{end}}$ are the isotopic compositions of bulk soil collected in year t, anthropogenic lead deposition in year i, and endogenous lead, respectively. To sum up, the present model basically aims to calculate theoretical $\text{Pb}_{\text{bulk}}(t)$ and $(^{206}\text{Pb}/^{207}\text{Pb})_{\text{bulk}}(t)$ and to compare them to that measured in the field in order to assess the value of the k factor.

Results and Discussion

Sample Integrity. Little information is available about sampling and handling procedures in the past because different workers were involved in this long-term experiment. It is noteworthy that there was no environmental objective when monitoring started. Consequently, despite precautions taken by successive technicians and researchers, potential contamination may have occurred throughout the entire process from sampling to storage. Table 1 and Figure 2a,b report mean lead concentrations and lead isotopic composition of the three reference plots. Lead contents increase from about 49 to 71 μg g^{-1} from 1929 to 2000; whereas $^{206}\text{Pb}/^{207}\text{Pb}$ ratios decrease slightly from 1.183 to 1.179. Such an isotopic shift is much lower than that observed between parent material ($^{206}\text{Pb}/^{207}\text{Pb} = 1.2035$) and the first sample of the set (1929: $^{206}\text{Pb}/^{207}\text{Pb} = 1.183$). Similarly, there is a larger difference in terms of concentrations between parent material and the 1929 sample than over the last 70 yr. The results are coherent and the absence of any sudden shift or disruption strongly favors sample integrity (cf. Figure 2).

Potentially Mobile Lead Pool. As indicated by Figure 2c, scandium concentrations do not significantly vary in time (Table 1). The mean scandium concentration of the 30 samples composing the set is 5.7 ± 0.1 μg g^{-1}, which is the

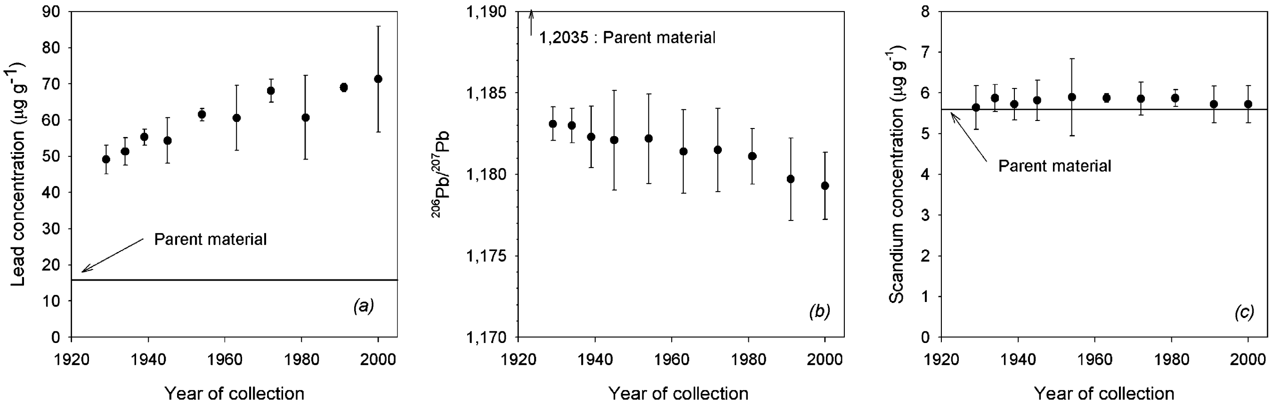

FIGURE 2. Lead concentrations (a), ^{206}Pb/^{207}Pb ratios (b), and scandium contents (c) vs year of collection. The values correspond to the mean of the three control parcels, and the error bar is the confidence interval at a level of 95%.

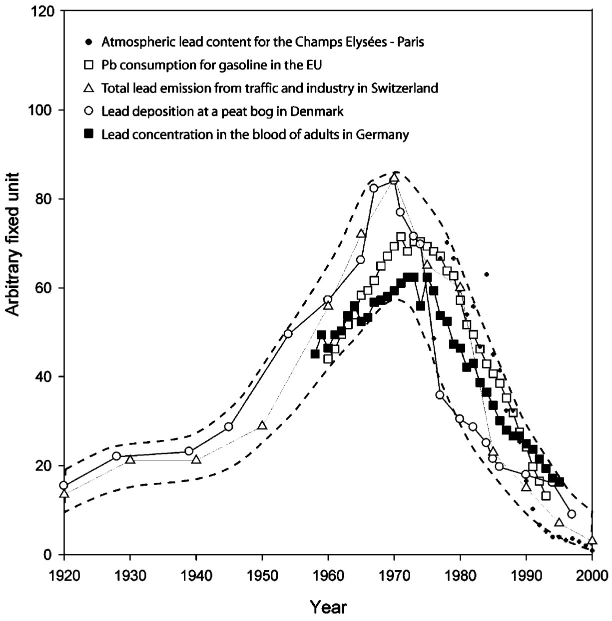

FIGURE 3. Composite curve and uncertainties (see text for construction and references) used as a surrogate of lead input fluxes at the INRA site from 1920 to 2000, within a factor *a*. The *y*-axis unit was arbitrarily fixed.

same as that of parent material (5.6 μg g^{-1}), suggesting the absence of significant selective weathering of minerals at least at the considered time scale. Even if some natural lead also enters the soil system by dust deposition, atmospheric lead input is widely dominated by anthropogenic (*47*, *48*) sources as demonstrated by the high enrichment factors reported even in remote areas (*2*). Thus, the potentially mobile lead pool almost exclusively derives from anthropogenic inputs and can be attributed to atmospheric input. This is in good agreement with other works that have demonstrated that petrol lead in roadside soils is associated with the most labile fractions of the soil, whereas natural lead is mainly hosted in the most stable minerals (*27*, *29*, *30*).

Atmospheric Fluxes. Unfortunately, no continuous values of atmospheric fluxes since 1929 (F_{in}^{i}) are available around Paris, although such a database would be required to run the model (cf. eq 9, Figure 1). Nonetheless, from knowledge of pollution history, it is possible to propose a curve ($t \rightarrow f(t)$) describing the shape of the evolution of anthropogenic atmospheric lead fluxes in the Paris region. Hence, the specific fluxes for Versailles can be estimated by multiplying this curve by an *a* factor:

$$F_{\text{in}}^{i} = a\cdot f(i) \qquad (14)$$

From the 1960s to the late 1980s, anthropogenic emissions were probably dominated by gasoline-derived lead, as there were no heavy industrial point sources close to the INRA site. There is a strong correlation between Pb consumption for gasoline in the EU (white squares in Figure 3) and atmospheric lead content in Paris during the period for which both statistics exist: the linear correlation of data from 1972 to 1993 is featured by $R^2 = 0.9312$ for the Champs Elysées (black circles in Figure 3) and $R^2 = 0.9381$ for Avenue Victor Basch (not shown here) (Paris Police Central Laboratory, personal communication). These trends are comparable to others previously published, such as lead concentrations in the blood of adults in Germany (black squares) (*4*), total lead emission from traffic and industry in Switzerland (white triangles) (*49*), and lead deposition rate at a peat bog in Denmark (white circles) (*50*); the latter two allowing the extension to the 1920s to be performed. At this period, lead from industrial activities and coal combustion, used as heat sources, were the major contributors. Figure 3 was thus drawn by combining all these data. Although rough, the evolution domain of anthropogenic lead fluxes so determined is certainly more realistic than assuming constant lead fluxes over time. The error estimate, shown by dashed curves in Figure 3, will be integrated into further calculations in order to evaluate the uncertainties of the modeled results.

Mean annual precipitations within each sampling interval were also checked because rainfall intensity plays an important role in the deposition and behavior of metals in soils (*28*). The variations within each sampling interval do not exceed ± 14%, so that it is not necessary to take the rainfall parameter into account.

Isotopic Compositions of Anthropogenic Lead Deposition. The evolution of anthropogenic lead isotopic ratios is only partially known in France, unlike the U.K. where studies have been performed on herbage samples and sphagnum mosses collected since the mid-19th century (*51*, *52*). Here, we have attempted to overcome this by compiling and combining previously published isotopic data obtained from both urban and rural areas. In 1966, ^{206}Pb/^{207}Pb ratio of French gasoline, the dominant source of lead in the environment at that time, was about 1.162−1.163 (*53*) (cf. Figure 4). Later, in the 1980s, the lead added as antiknock compound was much less radiogenic because of the increasing use of metal from old and remote ore deposits, such as those of Australia, so that airborne particulate matter collected in Paris and Montpellier gave low ^{206}Pb/^{207}Pb ratios of 1.09−1.11 (*43*−*45*). During the 1990s, there was a turning point in the ^{206}Pb/^{207}Pb ratios measured in the atmosphere of major French urban centers, which tended to increase, even close to highways (*44*, *45*, *54*, *55*). The gasoline end-member was still dominant, but due to the progressive use of unleaded gasoline

TABLE 2. Summary of Known Data, Initial Values, and Unknowns Used to Run the Model

parameter	name	value(s)
	Known (Measured or Calculated)	
plowed depth	h	0.25 ± 0.05 m, known
bulk density	d_a	1.25 Mg m^{-3}, determined in field
endogenous Pb concn	$\mathrm{Pb_{end}}$	15.8 μg g^{-1}, measured[a]
bulk Pb concn in year t	$\mathrm{Pb_{bulk}}(t)$	measured (cf. Table 1)
shape of temporal evolution of anthropogenic inputs	$f(i)$	function rebuilt for present study in arbitrary fixed unit (cf. Figure 3)
isotopic composition of endogenous Pb	$\left(\frac{^{206}\mathrm{Pb}}{^{207}\mathrm{Pb}}\right)_{\mathrm{end}}$	1.2035, measured (corresponds to C horizon of an adjacent field)
anthropogenic Pb isotopic composition deposited in year i	$\left(\frac{^{206}\mathrm{Pb}}{^{207}\mathrm{Pb}}\right)^{i}_{\mathrm{anthr}}$	function rebuilt for the present study (cf. Figure 4)
isotopic composition of bulk soils in year t	$\left(\frac{^{206}\mathrm{Pb}}{^{207}\mathrm{Pb}}\right)_{\mathrm{bulk}}(t)$	measured (cf. Table 1)
	Initial Values	
initial anthropogenic Pb concentration	$\mathrm{Pb}^{1929}_{\mathrm{anthr}}$	35 ± 2 μg g^{-1}, calculated (using eq 2; data from Table 1)
initial anthropogenic Pb isotopic composition	$\left(\frac{^{206}\mathrm{Pb}}{^{207}\mathrm{Pb}}\right)^{1929}_{\mathrm{anthr}}$	1.175 ± 0.002, calculated (using eq 13; data from Table 1)
	Unknown	
coeff applied to $f(i)$ to obtain annual fluxes	a	sought value (cf. eq 14)
coeff of annual loss from 0−25-cm plow horizon	k	sought value (cf. eq 9)

[a] Corresponds to C horizon of an adjacent field; supposed constant through time, as Sc concentrations in soils do not vary in time.

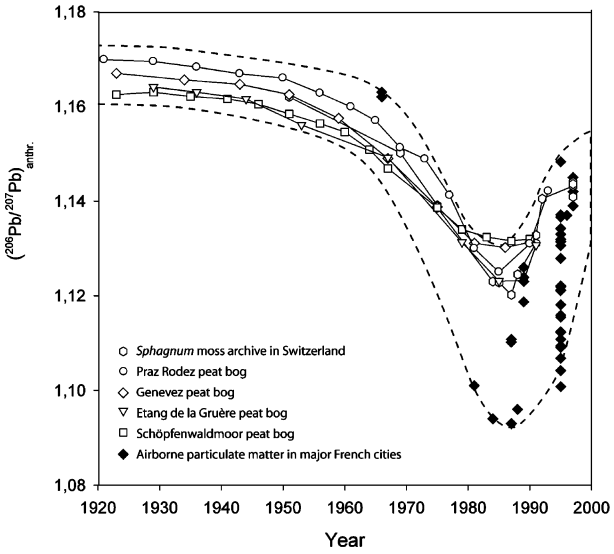

FIGURE 4. $^{206}\mathrm{Pb}/^{207}\mathrm{Pb}$ ratios and uncertainties of anthropogenic deposition from 1920 to 2000 (cf. text for details of construction and references).

after more strict environmental policies, lead derived from other more radiogenic sources (natural and industrial) started to rise in relative terms (*44*). Although sparse and limited to the mid-1960s, this whole set of isotopic compositions gives an insight into the evolution of lead isotopic compositions in areas highly affected by automotive traffic. On the other hand, the $^{206}\mathrm{Pb}/^{207}\mathrm{Pb}$ ratios of lead recorded in Swiss peat bogs (*56*) and *Sphagnum* moss archives (*57*) constantly decreased from the 20s ($^{206}\mathrm{Pb}/^{207}\mathrm{Pb} \sim 1.160-1.170$) to the 1960s ($^{206}\mathrm{Pb}/^{207}\mathrm{Pb} \sim 1.155-1.165$) because of the progressive replacement of coal by oil after the 20s (Figure 4). Later during the 1960s−1980s, the incorporation of nonradiogenic Australian lead in gasoline also led to a pronounced decline of $^{206}\mathrm{Pb}/^{207}\mathrm{Pb}$ ratios, while a return to more radiogenic values was detected following the introduction on the market of unleaded gasoline in 1985 (*56*, *57*). At sites that correspond to rural areas, the proportion of gasoline-derived lead has never reached that observed in major French cites, so that lead isotopic compositions have always been significantly more radiogenic. The Versailles site is located in a peri-urban area. We can therefore reasonably assume that the $^{206}\mathrm{Pb}/^{207}\mathrm{Pb}$ ratios of anthropogenic lead accumulated in these soils were comprised between those measured in rural and urban areas. The uncertainty of $^{206}\mathrm{Pb}/^{207}\mathrm{Pb}$ signatures, as represented in Figure 4 between the dashed curves, will be taken into account when running the model.

Model Testing Procedure. The model was computed using Matlab 5.02 software with data summarized in Table 2, carefully transformed in order to make the units compatible. For each pair (a; k), with $a \in [0; 2]$ and $k \in [0; 10^{-1}]$, theoretical lead concentrations and lead isotopic compositions were calculated through time. However, the input data [(i) the composite curve used as a surrogate of lead input fluxes (Figure 3), (ii) the evolution of $^{206}\mathrm{Pb}/^{207}\mathrm{Pb}$ ratios of anthropogenic deposition over time (Figure 4), (iii) the depth of the plowed horizon, (iv) initial anthropogenic lead concentrations, and (v) initial isotopic compositions (cf Table 2)] present significant uncertainties. The model was therefore computed 1000 times using random sampling within the estimate range of each parameter. The first two are supposed to be uniformly distributed and the others normally distributed. Hence 1000 theoretical output curves of lead concentrations and lead isotopic compositions were obtained for each pair (a; k). Mean curves and associated envelopes, corresponding to a confidence level of 95%, were also calculated. The error appears to be mainly propagated by the depth of the plowed horizon and by the values of the initial parameters: $\mathrm{Pb}^{1929}_{\mathrm{anthr}}$ and $(^{206}\mathrm{Pb}/^{207}\mathrm{Pb})^{1929}_{\mathrm{anthr}}$. This is probably due to the fact that (i) more than half the anthropogenic lead present nowadays in the topsoil was deposited before the start of the experiment in 1928 and (ii) the depth h of plowing acts strongly on the lead pool considered in the model. These theoretical flux and isotopic curves were then compared to those observed in the field in order to define a domain of compatible (a; k) values. The quality of the adjustment was evaluated by calculating fit errors for concentrations ($\mathrm{FE_{conc}}$) and isotopic compositions ($\mathrm{FE_{ic}}$) as follows:

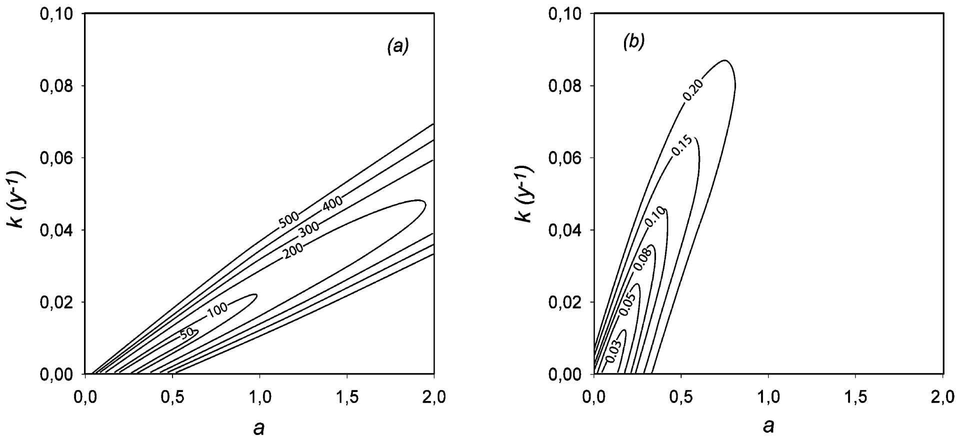

FIGURE 5. Fit errors for lead concentrations (a) and lead isotopic compositions (b) reported on diagrams *k* versus *a* using a gray-scale code. The lower the value, the better the concordance between modeled and field data.

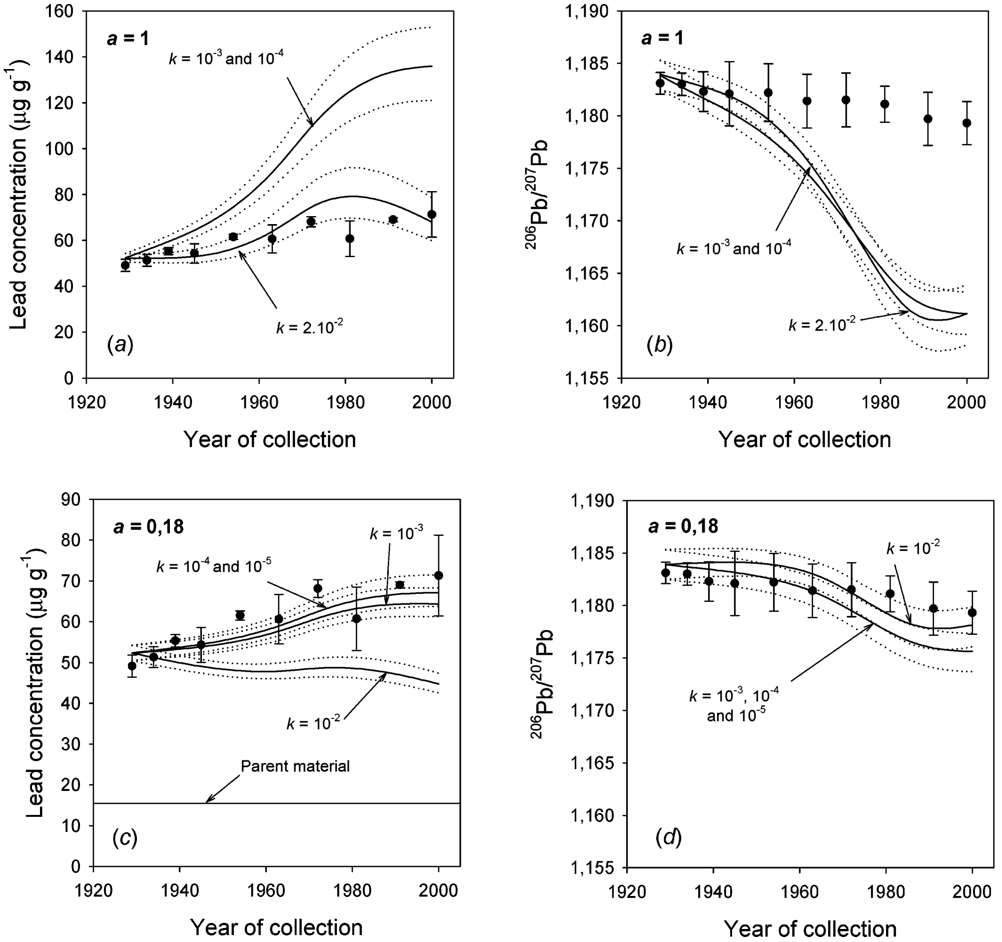

FIGURE 6. Simulation of evolution of lead concentrations and lead isotopic compositions vs time (solid line). For *a* = 1 and *k* varying: 2 × 10^{-2}, 10^{-3}, and 10^{-4} (panels a and b, respectively); and for *a* = 0.18 and *k* varying: 10^{-2}, 10^{-3}, 10^{-4}, and 10^{-5} (panels c and d, respectively). The envelopes (dotted lines) represent the propagation of input parameter errors and correspond to a confidence level of 95%. For purposes of comparison, the field data are reported as bold circles with error bars corresponding to a confidence level of 95%.

$$\mathrm{FE}_{\mathrm{conc}} = \sum_{i=0}^{9} w_i[\mathrm{Pb}_{\mathrm{model}}(t_i) - \mathrm{Pb}_{\mathrm{measured}}(t_i)]^2 \qquad (15)$$

$$\mathrm{FE}_{\mathrm{ic}} = \sum_{i=0}^{9} z_i\left[\left(\frac{^{206}\mathrm{Pb}}{^{207}\mathrm{Pb}}\right)_{\mathrm{model}}(t_i) - \left(\frac{^{206}\mathrm{Pb}}{^{207}\mathrm{Pb}}\right)_{\mathrm{measured}}(t_i)\right]^2 \qquad (16)$$

where t_0, ..., t_9 correspond to times at which samples have been collected. Results from the three different reference plots were sometimes scattered (cf. Table 1) and produce uncertainties in the concentration and isotopic composition averages. As mentioned above, errors are also associated with the modeled curves, so that weights inversely proportional to the square root of the sum of the variances of both field and modeled data were used in eqs 15 and 16: w_i and z_i, respectively. Fit errors are plotted in Figure 5a,b allowing the best pair values within $a \in [0; 2]$ and $k \in [0; 10^{-1}]$ to be distinguished, despite the introduction and propagation of uncertainties in the parameters feeding the model. Figure 5a shows a linear-shaped domain, indicating a good correspondence between simulation and field data. If a increases, k has to increase simultaneously; in other words, high inputs have to be compensated by high losses. However, the use of lead isotopic compositions allows the range of possible pairs (a; k) to be restrained (Figure 5b).

Computing for $a = 1$. This example is presented in Figure 6a,b, where $a = 1$ and k varies between 10^{-4} and 2×10^{-2}. There is a k value around 2×10^{-2} for which the model matches measured concentrations well (Figure 6a), but no k will produce predicted isotopic compositions comparable with those measured, in particular for the 1950−2000 period (Figure 6b). If fluxes had been that high, isotopic compositions would have been much less radiogenic than those measured because of the wide use of nonradiogenic lead as antiknock compounds from the 1980s (Figure 4). As a result, $a = 1$ is not realistic.

Computing for $a = 0.18$. There is a range of [a; k] values in which the simulation produces approximately the expected concentration and isotopic results: $a \in [0.15; 0.2]$ for $k < 10^{-3}$. Figure 6c,d presents the computation with $a = 0.18$ where k varies from 10^{-5} to 10^{-2}. A minor divergence is still observed for lead isotopic compositions from the 1980s. A slight underestimation of $^{206}Pb/^{207}Pb$ ratios of the anthropogenic end-member may have occurred. In that case, the relative contribution of gasoline may have been overestimated in comparison to an industrial component, generally found to be more radiogenic (*32*, *58*).

Implications for Atmospheric Fluxes and Behavior of Lead in Soil. It is important to recall that the main purpose of this study was not to reconstruct lead atmospheric flux history. However, our flux values are in relatively good agreement with the rare data available in the literature. For 1991, we calculate an atmospheric lead flux of 2.9 ± 1.4 $\mu g\ cm^{-2}\ yr^{-1}$ (data for $a = 0.18$), which is compatible with the value of 3.6 $\mu g\ cm^{-2}\ yr^{-1}$ measured around Paris the same year (*59*). Likewise, the model produces a flux of 1.9 ± 1.2 $\mu g\ cm^{-2}\ yr^{-1}$ for 1994 (data for $a = 0.18$), comparable to 2.31 $\mu g\ cm^{-2}\ yr^{-1}$ measured at Rueil-Malmaison, about 10 km from Versailles (*60*). Finally, atmospheric lead deposition flux, determined directly at the INRA site in 2002, was 0.22 $\mu g\ cm^{-2}\ yr^{-1}$ (S. Azimi, unpublished data), while the model yields 0.45 ± 0.44 $\mu g\ cm^{-2}\ yr^{-1}$ for 2000.

Although the value of the k factor is valid only for the Versailles site, such Hapludalf soils (luvisols) are frequent throughout Western Europe. These soils were continuously disturbed and homogenized in the 0−0.25-m horizon because they were plowed twice a year. Moreover, as they were maintained in bare fallow for more than 70 yr, the plowed layers today show remarkably low quantities of organic compounds (approximately 6 $\mu g\ g^{-1}$) (*61*); organic matter being generally supposed to favor lead retention in topsoil. All these conditions should have promoted the mobility of lead, in part because of greater leaching from a more exposed surface area in turned soil, so that the post-depositional migration rates calculated here are probably overestimated in comparison with natural unaltered soil systems. Even if the model does not enable the k factor to be calculated more precisely, a value of $k < 10^{-3}$ corresponds to very low mobility: in other words, more than 99.9% of the potentially mobile lead pool remains in the topsoil each year Similar values for lead have been reported using independent approaches for other soils: $k = 3.6 \times 10^{-4}$ (*37*). Hence, the evolution of the lead stock can easily be simulated with a decay equation for future lead inputs assumed equal to 0: more than 700 yr would be required to halve the anthropogenic pool. It might also be interesting to apply the present model to the data obtained from the experimental farm of Rothamsted (U.K.), where a similar experimental device, but under pasture land, has been conducted since 1860 and where lead concentration and isotopic signatures are available (*51*). This model could also be adapted to the study of ^{137}Cs migration for which flux history is well-constrained, with a worldwide peak of deposition in 1963/1964 because of nuclear weapon tests in the atmosphere and the Chernobyl accident in 1986.

Our field results demonstrate that the major part of the anthropogenic lead pool was integrated into the soil before 1928, which is long before the pollution peak of the mid-1970s. This historical accumulation of lead also strongly underlines its limited downward migration. The question of pollution history seems therefore to be of primary importance. Many recent studies focusing on sedimentary records, ice cores, or peat bogs have pointed out early metallurgical activities that strongly impacted the global environment (*1*, *2*). In all likelihood, a significant fraction of exogenous lead detected nowadays in soils was integrated before the 20th century and probably well before the Industrial Revolution, as demonstrated in certain sites (*9*).

Acknowledgments

This work was funded by the French Environmental Agency ADEME. We thank Sébastien Ariès and the Laboratoire Central de la Préfecture de Police de Paris for invaluable assistance and Tom Pačes, Amélie Quiquérez, and four anonymous reviewers for their precious comments.

Supporting Information Available

Another approach to the reconstruction of the history of lead fluxes and isotopic compositions of the anthropogenic end-member through time, assuming $k = 0$. This material is available free of charge via the Internet at http://pubs.acs.org.

Literature Cited

(1) Rosman, K. J. R.; Chisoholm, W.; Hong, S.; Candelone, J.-P.; Boutron, C. F. *Environ. Sci. Technol.* **1997**, *31*, 3413.
(2) Shotyk, W.; Weiss, D.; Appleby, P. G.; Cheburkin, A. K.; Frei, R.; Gloor, M.; Reese, S.; Van der Knaap, W. O. *Science* **1998**, *281*, 1635.
(3) Flament, P.; Bertho, M.-L.; Deboult, K.; Puskaric, E. *Sci. Total Environ.* **1996**, *192*, 193.
(4) Von Storch, H.; Hagner, C.; Costa-Cabral, M.; Feser, F.; Pacyna, J.; Pacyna, E.; Kolb, S. *EOS, Trans. Am. Geophys. Union* **2002**, *83*, 399.
(5) Seregin, I. V.; Ivanov, V. B. *Russ. J. Plant Physiol.* **2001**, *48*, 523.
(6) Adriano, D. C. In *Trace elements in terrestrial environments, Biogeochemistry, bioavailability and risk of metals*, 2nd ed.; Springer-Verlag: Berlin, 2001.
(7) Grousset, F. E.; Quétel, C. R.; Thomas, B.; Buat-Ménard, P.; Donard, O. X.; Buchet, A. *Environ. Sci. Technol.* **1994**, *28*, 1605.
(8) Sterckeman, T.; Douay, F.; Proix, N.; Fourrier, H. *Environ. Pollut.* **2000**, *107*, 377.
(9) Pyatt, F. B.; Gilmore, G.; Grattan, J. P.; Hunt, C. O.; McLaren, S. *J. Archaeol. Sci.* **2000**, *27*, 771.
(10) Sonke, J. E.; Hoogewerff, J. A.; van der Laan, S. R.; Vangronsveld, J. *Sci. Total Environ.* **2002**, *20*, 101.
(11) Martínez Cortizas, A.; García-Rodeja, E.; Pontevedra Pombal, X.; Nóvoa Muñoz, J. C.; Weiss, D.; Cherburkin, A. *Sci. Total Environ.* **2002**, *20*, 33.
(12) Monna, F.; Dominik, J.; Loizeau, J.-L.; Pardos, M.; Arpagaus, P. *Environ. Sci. Technol.* **1999**, *33*, 2850.
(13) Farmer, J. G.; Eades, L. J.; MacKenzie, A. B.; Kirika, A.; Bailey-Watts, T. E. *Environ. Sci. Technol.* **1996**, *30*, 3080.
(14) Camobreco, V. J.; Richards, B. K.; Steenhuis, T. S.; Peverly, J. H.; McBride, M. B. *Soil Sci.* **1996**, *161*, 740.
(15) Denaix, L.; Semlali, R. M.; Douay, F. *Environ. Pollut.* **2001**, *113*, 29.
(16) Citeau, L.; Lamy, I.; van Oort, F.; Elsass, F. *Colloids Surf. A* **2003**, *217*, 11−19.
(17) Jensen, D. L.; Ledin, A.; Christensen, T. H. *Water Res.* **1999**, *33*, 2642.
(18) Semlali, R. M.; van Oort, F.; Denaix, L.; Loubet, M. *Environ. Sci. Technol.* **2001**, *35*, 4180.
(19) Cancès, B.; Ponthieu, M.; Castec-Rouelle, M.; Aubry, E.; Benedetti, M. F. *Geoderma* **2003**, *113*, 341.

(20) Bermond, A. *Environ. Technol.* **1992**, *13*, 1175.
(21) Hodson, M. E. *Geochim. Cosmochim. Acta* **2002**, *66*, 819.
(22) Plassard, F.; Winiarski, T.; Petit-Ramel, M. *Contam. Hydrol.* **2000**, *42*, 99.
(23) He, Q.; Walling, D. E. *Appl. Radiat. Isot.* **1997**, *48*, 677.
(24) Toso, J. P.; Velasco, R. H. *J. Environ. Radioact.* **2001**, *53*, 133.
(25) Isaksson, M.; Erlandsson, B. *J. Environ. Radioact.* **1998**, *41*, 163.
(26) Velasco, R. H.; Toso, J. P.; Belli, M.; Sansone, U. *J. Environ. Radioact.* **1997**, *37*, 73.
(27) Erel, Y.; Véron, A.; Halicz, L. *Geochim. Cosmochim. Acta* **1997**, *61*, 4495.
(28) Teutsch, N.; Erel, Y.; Halicz, L.; Chadwick, O. A. *Geochim. Cosmochim. Acta* **1999**, *63*, 3499.
(29) Teutsch, N.; Erel, Y.; Halicz, L.; Banin, A. *Geochim. Cosmochim. Acta* **2001**, *65*, 2853.
(30) Emmanuel, S.; Erel, Y. *Geochim. Cosmochim. Acta.* **2002**, *14*, 2517.
(31) Walraven, N.; van Os, B. J. H.; Klaver, G. Th.; Baker, J. H.; Vriend, S. P. *J. Geochem. Explor.* **1997**, *59*, 47.
(32) Hansmann, W.; Köppel, V. *Chem. Geol.* **2000**, *171*, 123.
(33) Harlavan, Y.; Erel, Y.; Blum, J. D. *Geochim. Cosmochim. Acta* **1998**, *62*, 33.
(34) Wong, S. C.; Li, X. D.; Zhang, G.; Qi, S. H.; Min, Y. S. *Environ. Pollut.* **2002**, *119*, 33.
(35) Burgevin, H.; Hénin, S. *Ann. Agron.* **1939**, *9*, 771.
(36) Pačes, T. *Water, Air, Soil Pollut.* **1998**, *105*, 451.
(37) Pačes, T. In *Geochemistry of the Earth's Surface*; Armannson, Ed.; Balkerna: Rotterdam, The Netherlands, 1999; p 143.
(38) Juste, J.; Tauzin, J. *C. R. Acad. Agric. Fr.* **1986**, *72*, 734.
(39) AFNOR. *Qualité des sols. Recueil de normes françaises*; AFNOR: Paris, France, 1996.
(40) Manhès, G. Ph.D. Thesis, University of Paris 6, 1982.
(41) Shotyk, W. *Environ. Rev.* **1996**, *4*, 149.
(42) Shotyk, W.; Blaser, P.; Grünig, A.; Cheburkin, A. K. *Sci. Total Environ.* **2000**, *249*, 281.
(43) Elbaz-Poulichet, F.; Holliger, P.; Huang, W.; Martin, J.-M. *Nature* **1984**, *308*, 409.
(44) Monna, F.; Lancelot, J. R.; Croudace, I. W.; Cundy, A. B.; Lewis, J. T. *Environ. Sci. Technol.* **1997**, *31*, 2277.
(45) Véron, A.; Flament, P.; Bertho, M. L.; Alleman, L.; Flegal, R.; Hamelin, B. *Atmos. Environ.* **1999**, *33*, 3377.
(46) Faure, G. *Principles of Isotope Geology*, 2nd ed.; Wiley: New York, 1986.
(47) Nriagu, J. O.; Pacyna, J. M. *Nature* **1988**, *333*, 134.
(48) Nriagu, J. O. *Nature* **1989**, *338*, 47.
(49) BUWAL. *Vom Menschen verursashte Luftshaldstoffe-Emissionen in der Schwiez von 1900 bis 2010*; Bundesamt für Umwelt, Wald und Landschaft: Bern, Switzerland, 1995.
(50) Goodsite, M. E.; Rom, W.; Heinemeier, J.; Lange, T.; Ooi, S.; Appleby, P. G.; Shotyk, W.; van der Knap, O.; Lohse, C.; Hansen, T. S. *Radiocarbon* **2001**, *43*, 495.
(51) Bacon, J. R.; Jones, K. C.; McGrath, S. P.; Johnston, A. E. *Environ. Sci. Technol.* **1996**, *30*, 2511.
(52) Farmer, J. G.; Eades, L. J.; Atkins, H.; Chamberlain, D. F. *Environ. Sci. Technol.* **2002**. *36*, 152.
(53) Chow, T. J.; Earl, J. L. *Nature* **1973**, *176*, 510.
(54) Roy, S. Ph.D. Thesis, University of Paris 7, 1996.
(55) Deboudt, K.; Flament, P.; Weis, D.; Mennessier, J.-P.; Maquinghen, P. *Sci. Total Environ.* **1999**, *237*, 57.
(56) Weiss, D.; Shotyk, W.; Appleby, P. G.; Kramers, J. D.; Cheburkin, A. K. *Environ. Sci. Technol.* **1999**, *33*, 1340.
(57) Weiss, D.; Shotyk, W.; Kramers, J. D.; Gloor, M. *Atmos. Environ.* **1999**, *33*, 3751.
(58) Chiaradia, M.; Cupelin, F. *Atmos. Environ.* **2000**, *34*, 959.
(59) Granier L. Ph.D. Thesis, University of Paris 6, 1991.
(60) Garnaud S. Ph.D. Thesis, Ecole Nationale des Ponts et Chaussées, Paris, 1999.
(61) Pernes-Debuyser, A.; Tessier, D. *Etude Gestion Sols* **2002**, *9*, 177.

Received for review February 17, 2003. Revised manuscript received November 25, 2003. Accepted December 3, 2003.

ES0341384

Available online at www.sciencedirect.com
ScienceDirect
Atmospheric Environment 40 (2006) 6554–6566
ATMOSPHERIC ENVIRONMENT
www.elsevier.com/locate/atmosenv

Origin of atmospheric lead in Johannesburg, South Africa

F. Monna[a,*], M. Poujol[b,g], R. Losno[c], J. Dominik[d], H. Annegarn[e], H. Coetzee[f]

[a]Archéologie, Culture et Sociétés, Centre des Sciences de la Terre, UMR 5594 CNRS—Université de Bourgogne, Bat. Gabriel, F-21000 Dijon, France
[b]Economic Geology Research Institute, Private Bag 3, University of the Witwatersrand, WITS 2050, South Africa
[c]LISA, Faculté des Sciences, Universités Paris 7 Paris 12, CNRS, 61 av. du Gal de Gaulle F-94010 Créteil Cedex, France
[d]Institut F.-A. Forel, Université de Genève, 10 route de Suisse, CH-1290, Versoix, Switzerland
[e]University of Johannesburg, PO Box 524, Auckland Park 2006, South Africa
[f]Environmental Geoscience Unit, Council for Geoscience, Pretoria 0001, South Africa
[g]Laboratoire de Geochimie isotopique et de Géochronologie, UMR 6118- Géosciences Rennes, Université de Rennes 1, Avenue du Général Leclerc, 35 042 Rennes Cedex, France

Received 28 February 2006; received in revised form 19 May 2006; accepted 25 May 2006

Abstract

The origin of lead in the atmosphere of Johannesburg, South Africa was investigated on the basis of elemental and lead isotopic analyses of coals, mine dumps, gasoline, and about 30 epiphytic lichen samples. Lead predominantly comes from automotive exhausts in urban and suburban areas, as leaded antiknock additives were still in use in South Africa at the time of the study. Although dust emissions from the numerous mine-tailing dumps were expected to contribute significantly to the heavy metal budget, the southern townships that are surrounded by the dumps (such as Soweto and other historically Black residential areas) do not appear to be more than partially influenced by them, and this influence seems to be geographically limited. Domestic coal burning, suspected to account for the total lead content in the air, is also recognised, but only acts as a minor source of lead, even in townships.

Keywords: Lichen; Lead isotope; Pollution; Mine dump; Mixing model

---

1. Introduction

The city of Johannesburg was founded in 1886 after the discovery of the rich gold deposits of the Witwatersrand Basin. With 3.2 million inhabitants, it is the largest city in southern Africa and the second largest on the African continent. Most of the mining activity stopped in the immediate vicinity of the city more than a decade ago, and around 200 mine-tailing dumps, some as high as 50 m, are still exposed in the metropolis along an east–west axis (Fig. 1a). Some of the older mine dumps, however, have been reprocessed due to considerable improvements in extractive metallurgy of gold.

Although lead-free fuel was available on the market, leaded gasoline still held an 80% market share at the time of this study (leaded fuel was taken off the South African market in January 2006). Automotive exhaust gases were thus an important contributor for lead contamination in Johannesburg

---

*Corresponding author. Tel.: +33 (0)380 396 360; fax: +33 (0)380 396 387.
E-mail address: Fabrice.Monna@u-bourgogne.fr (F. Monna).

1352-2310/$ - see front matter © 2006 Elsevier Ltd. All rights reserved.
doi:10.1016/j.atmosenv.2006.05.064

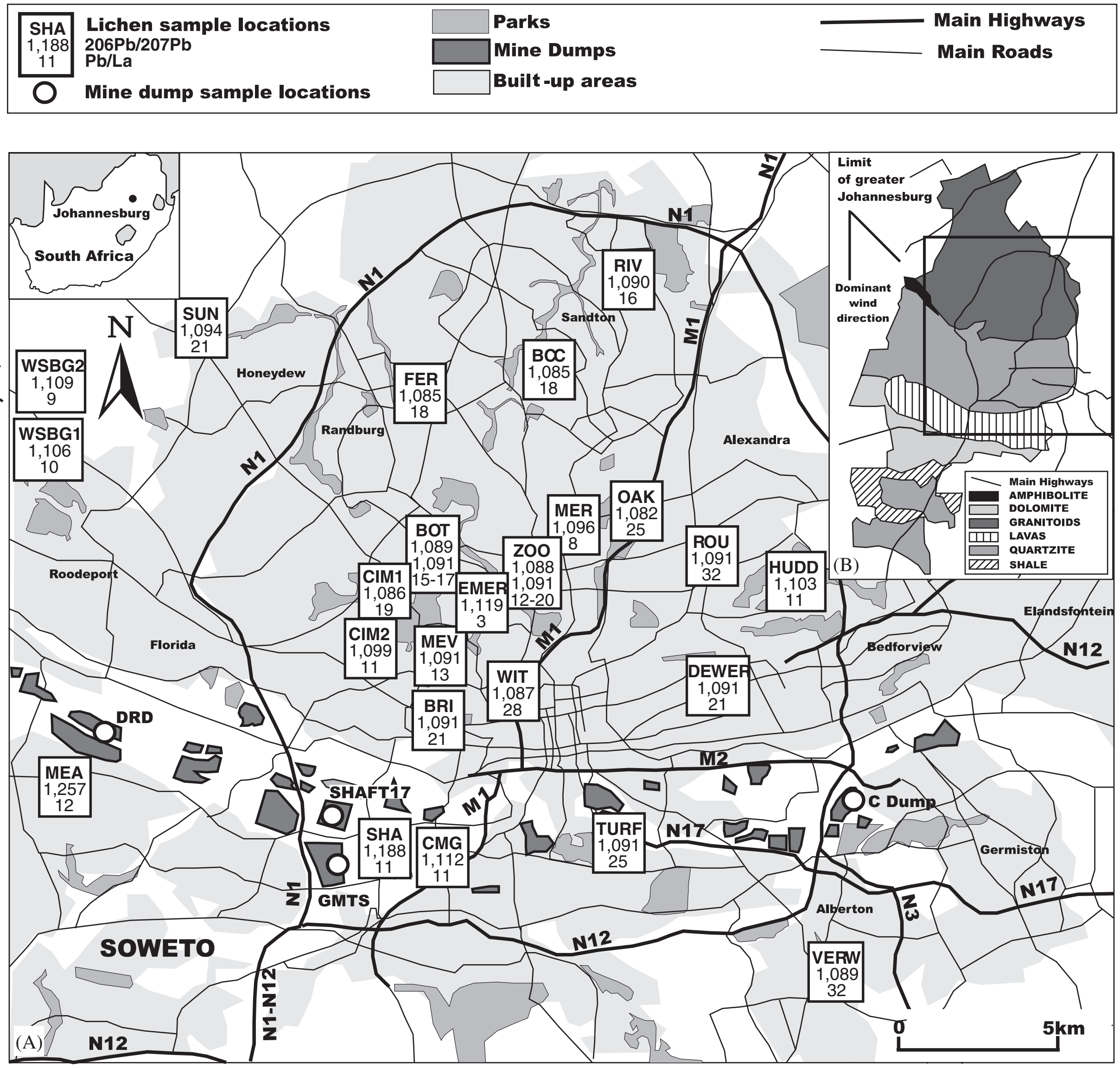

Fig. 1. (a) Map of Johannesburg and sampling sites, (b) simplified lithological map.

(Formenti et al., 1998), but many other sources may be involved, such as widespread domestic coal burning, dust from unpaved roads in poor townships, and surface mining operations. This means that in historically Black residential suburbs adjacent to mining areas, heavy metals associated with dust emissions from dumps and mining extraction are additional sources of pollution, which combine with contamination emitted by other human activities. This may enhance the breathable pollution risk level for populations living in the vicinity of mining operations. To date, exposure of historically disadvantaged communities to wind-blown mine tailings is the subject of intensive public debate.

Although it is of great importance to know the different origins of heavy metals when considering long-term strategies and environmental policies for reducing emissions, apportioning the various sources is not a trivial task. Heavy metal contents in the atmosphere are generally highly variable, depending on meteorological conditions, industrial and diurnal cycles, and density of the automotive traffic (Bergametti et al., 1989; Remoudaki et al., 1991; Monna et al., 1997; Flament et al., 2002; Chen et al., 2005). While deciphering the sources on the sole basis of heavy metal concentrations may sometimes produce ambiguous conclusions, lead isotopic abundances are particularly informative in these types of analyses as anthropogenic emissions and natural lead are usually characterised by different isotopic signatures (see the Clair C. Patterson Special Issue, Geochim. Cosmochim. Acta, 1994; Munksgaard and Parry, 1998). Furthermore, this approach often offers the opportunity to discriminate specific emissions among anthropogenic groups, e.g., alkyl lead additives, various industrial emissions, domestic wood and coal burning (i.e., Chiaradia et al., 1997; Åberg et al., 1999; Véron et al., 1999; Chiaradia and Cupelin, 2000; Kurkjian et al., 2002; Widory et al., 2004; Chen et al., 2005). Instead of collecting and measuring a large and costly set of airborne particles, some authors have chosen to apply the isotopic techniques on biological receptors such as trees, even though the meaning of the information drawn is currently subject to debate (Marcantonio et al., 1998; Tommasini et al., 2000; Bellis et al., 2002a, b; Bindler et al., 2004). Another approach consists in using moss (Kunert et al., 1999; Haack et al., 2004) and lichens (Jaakkola et al., 1983; Carignan and Gariépy, 1995; Monna et al., 1999; Getty et al., 1999; Doucet and Carignan, 2001; Carignan et al., 2002; Simonetti et al., 2003; Watmough and Hutchinson, 2004; Spiro et al., 2004; Cloquet et al., 2006), because they are supposed to represent integrated signals of atmospheric pollution. Lichens are slow-growing organisms which, over their lifespan, are expected to accumulate and retain high levels of mineral elements present in the atmosphere, but not from the host tree limb or rocks from which they are suspended (Getty et al., 1999; Loppi and Pirintsos, 2003). Their metabolism with respect to metals is not yet perfectly understood. While most of the authors state that lichens tend to average the atmospheric signal over a period of a few years (Carignan et al., 2002), some suggest quick compositional changes in relation to atmospheric pollution magnitude (Spiro et al., 2004). In any case, as their age is unknown, they cannot be used for temporal studies (Carignan and Gariépy, 1995). In the present work, we attempt to discriminate the different sources of lead in the atmosphere of Johannesburg by means of geochemical and isotopic analyses of epiphytic lichens sampled both within and around the city. To the best of our knowledge, the present set of data constitutes the first database of this type ever gathered in South Africa.

2. The site

Located at about 1700 m above sea level, the city of Johannesburg covers 1645 km^2 of mostly residential and wooded areas (Fig. 1a). The city's traffic network represents more than 9000 km of mostly (90%) tarred roads, with the M1 highway between Johannesburg and Pretoria being the busiest in the Southern hemisphere. The climate of Johannesburg is mild with north–northwest dominant winds, especially in winter. Although four seasons exist, spring and autumn are very short. Average seasonal rainfall ranges from 19 mm during the 3 months of winter to up to 563 mm during the 5 months of summer, leading to an annual precipitation of about 750 mm. Johannesburg lies on the Archaean Kaapvaal craton, which is comprised of a large variety of rocks representing different ages (3.34–2.7 billion years). To simplify a rather complex local geology, rock types of the sampling area include, from north to south, granitoids and amphibolites, quartzites, lavas and dolomite (Fig. 1b).

3. Materials and methods

3.1. Sampling and sample preparation

A total of 31 thalli of epiphytic lichens (all belonging to the Parmeliaceae family, and mostly *Parmelia sulcata*) have been collected in and around Johannesburg during two sampling campaigns undertaken in May 2001 and April 2003 (Fig. 1a). The sampling site network could not however be properly distributed because of the extreme scarcity or even absence of lichens in many areas of the city, and more particularly in Black-dominated residential suburbs. Lichens growing on trees were collected between 1 and 3 m above ground level by means of pre-cleaned plastic knives. Lichens were sometimes moistened with Milli-Q water to facilitate their removal from the trunks. They were immediately transferred into a clean plastic bag and stored in the laboratory after any remaining pieces of bark were removed from the lichens by hand. Lichens were then rinsed with Milli-Q water in an ultrasonic bath for 1 min to eliminate dust and any remaining leaf debris (Getty et al., 1999). They were then dried at 80 °C over a period of 2 days and crushed manually in a pre-cleaned agate mortar to obtain a fine and homogeneous powder.

A few millilitres of leaded-gasoline from each of the major petrol companies present in South Africa (Total, Caltex, Zenex, Engen, Shell and BP) were also collected by directly pumping the petrol into separate glass vials for each sample. In addition, several samples of sand (1 kg each) were taken from different mine-tailing dumps (DUMPC, SHAFT 17, DRD, GMTS), which lie south of the M2 motorway (Fig. 1a). Two coal samples, sold to the people of Soweto for domestic use, were also collected.

3.2. Chemical procedure

As, Br, Cr, Fe, Sb, Sc, Th and La were measured using instrumental neutron activation analysis (INAA) by Actlabs (Ontario, Canada). Measurements of standards (WMG1 and peach leaves NIST 1547) did not differ from certified values by more than ±10% for Sc, Th and La and about ±15% for the other elements. For Pb, Zn, Cu and Cd concentration and Pb isotopic composition determinations, between 70 and 100 mg of powdered lichen were transferred to a beaker with 2 mL each of concentrated HNO_3, HF and HCl of suprapure grade (Merck, Germany). The dissolution was achieved under microwave assistance (Ethos, Milestone, 9 positions) at the F.-A. Forel Institute, University of Geneva. A blank and a peach leaves reference material (NIST 1547) were processed systematically for each of the seven-lichen batches. All the following procedures were carried out in a clean room (US class 100–1000). One-third of the solution was evaporated, retaken with concentrated HNO_3, diluted with MilliQ water, and introduced in an HP 4500 inductively coupled plasma-mass spectrometer (ICP-MS). Elemental concentrations were measured using both internal (Re, Rh) and external calibrations. Results of six NIST 1547 measurements were within ±15% of the certified values. Measurements of 19 MilliQ washing solutions of lichens indicated that approximately 10% of Zn, Cd and Cu, and less than 3% of other elements were lost during the washing procedure. Lead in the other aliquot solution was pre-concentrated using ionic resin AG1 × 4 (Biorad) and isotopic ratios were determined using the quadrupole-based HP 4500 belonging to the F.-A. Forel Institute or, for some samples, a PQ2+ ICP-MS from the University of Montpellier II, France. Mass bias was monitored and corrected by bracketing a NIST 981 isotopic lead standard every five measurements. Further details about the complete procedure and instrumental settings can be found elsewhere (Monna et al., 1998, 2000). Blank corrections were never required, as the contamination by the chemical procedure appeared negligible compared to the total amount of lead in the treated samples. Some samples were duplicated, demonstrating the reproducibility of the analytical method within errors.

Mine dump samples were treated using the same procedure as the lichens. Approximately 100 mg of powdered and ashed coal was digested in aqua regia in covered Savillex beakers for 24 h on a hot plate. One millilitre of $HClO_4$ was then added to the evaporated solution to complete the digestion (Giusti, 1988). Lead was extracted following the procedure described above and measured for its isotopes on a MAT 262 thermal ionisation-mass spectrometry (TIMS) at the Memorial University of Newfoundland, Canada following the technique described in Pillet et al. (2005). One millilitre of the six leaded petrol samples was evaporated to dryness in Savilex beakers. The residues were dissolved using 1 mL of concentrated HNO_3 overnight on a hot plate. The solutions were then diluted with MilliQ water and lead isotopic compositions were measured using the HP 4500 ICP-MS as described earlier.

4. Results

4.1. Trace element contents

Elemental concentrations and isotopic compositions of mine dumps, coals and lichens are reported in Table 1. Mine dumps and coals are characterised by rather homogeneous compositions for lithophilic elements such as Th, Sc, La or Fe and, to a lesser extent, for chalcophylic elements (Pb, Zn, Cu, etc.). There is no significant difference in isotopic signatures or elemental concentrations, using Mann–Whitney *U*-tests, between the lichens collected in 2001 and those collected in 2003 from sites with equivalent exposition to car traffic. The largest variations in lichens are observed for Pb (7–388 $\mu g\,g^{-1}$) and Sb (0.1–9.7 $\mu g\,g^{-1}$), and also for Th (0.2–6.8 $\mu g\,g^{-1}$). The other elements, and particularly La, are less variable, within approximately one order of magnitude or less. Because this study is the first of its kind in South Africa, it was necessary to characterise the isotopic compositions

Table 1
Lead isotopic compositions and trace element contents (expressed in $\mu g\,g^{-1}$, except iron content in percent)

Name	Description	$^{206}Pb/^{207}Pb$	±	$^{208}Pb/^{207}Pb$	±	Pb	Cu	Zn	Cd	As	Br	Cr	Fe (%)	Sb	Sc	Th	La
Coal																	
COAL2		1.2050	0.0001	2.4691	0.0001	11	9.1	<0.2	<0.01	3.5	1.5	29	0.35	0.6	5.4	6.8	24
COAL1		1.2159	0.0002	2.4853	0.0002	17	7.8	<0.2	<0.01	1.7	1.2	28	1.2	0.6	4.9	5.0	33
Dumps																	
DRD	Mine dump	2.232	0.011	2.105	0.005	8.8	2.2	8	<0.01	7.5	<0.5	142	0.71	0.8	3.4	3.0	18
DUMPC (a)	Mine dump	2.182	0.007	1.977	0.002	21	8.7	20	<0.01	15	<0.5	144	1.5	0.9	4.1	4	20
DUMPC (b)	Mine dump	2.607	0.013	1.864	0.005	24	32	62	<0.01	77	<0.5	160	2.3	1.2	5.4	3.9	23
DUMPC (c)	Mine dump	2.735	0.016	1.817	0.005	19	33	55	<0.01	33	<0.5	139	1.6	1	4.5	3	21
GMTS1	Mine dump	2.813	0.016	1.807	0.002	14	24	33	0.05	94	0.9	185	2.9	1.7	5.3	4.4	23
GMTS2	Mine dump	2.615	0.009	1.861	0.004	8.7	14	18	0.03	62	<0.5	146	1.8	1.1	4.3	4.2	19
SHAFT17	Mine dump	2.878	0.005	1.707	0.001	23	25	64	<0.01	77	<0.5	228	2.6	1.7	6.2	4.2	31
SHAFT17bis	*Mine dump*	*2.882*	*0.006*	1.712	*0.002*	—	—	—	—	—	—	—	—	—	—	—	—
Lichens																	
BCC1	Open space urban	1.084	0.005	2.353	0.014	61	23	65	0.32	2.5	12	134	0.35	1.6	1.1	0.9	3.6
BCC2	Open space urban	1.086	0.007	2.351	0.030	63	24	53	0.55	4.6	15	91	0.27	1.5	0.8	1.3	3.4
BOT1	Open space urban	1.091	0.004	2.351	0.010	71	16	73	0.24	6.8	23	130	0.50	1.9	1.3	1.9	4.6
BOT2	Open space urban	1.089	0.003	2.344	0.008	98	32	83	0.28	5.9	15	277	0.68	2.9	2.3	2.3	6.4
BOT3	Open space urban	1.093	0.004	2.344	0.013	179	41	93	0.32	9.0	19	339	1.1	4.8	2.8	4.2	10
BRI*	Low traffic urban	1.091	0.003	2.358	0.006	186	39	227	0.25	13	46	205	1.3	5.8	3.2	3	8.9
CIM1*	Open space urban	1.086	0.003	2.351	0.005	49	16	86	0.09	3.4	17	42	0.27	1.1	0.8	0.5	2.6
CIM2*	Open space urban	1.099	0.003	2.359	0.005	90	37	121	0.29	7.7	20	175	1.2	2.2	3.9	2.3	8.5
CMG	Open space dumps	1.112	0.005	2.348	0.011	53	21	101	0.29	9.7	15	83	0.50	1.9	1.3	1.8	4.8
DEL	Open space urban	1.091	0.003	2.357	0.009	70	24	71	0.25	6.8	17	163	0.54	2.0	1.7	1.1	5.0
DEWER	Open space urban	1.091	0.006	2.365	0.013	90	21	67	0.34	6.9	21	121	0.51	2.5	1.6	1.5	4.3
EMER	Low traffic urban	1.119	0.005	2.370	0.013	41	55	70	0.14	5.3	12	90	1.6	1.6	5.6	2.8	13
FER*	Low traffic urban	1.085	0.002	2.356	0.006	217	57	162	0.25	8.2	35	482	1.3	4.7	4	4	12
HUDD	Open space suburb	1.103	0.003	2.370	0.008	47	21	82	0.23	3.8	14	147	0.54	2.2	1.7	1.1	4.2
MEA*	Open space dump	1.257	0.003	2.305	0.005	141	93	145	0.15	14	42	120	3.2	1.8	5.8	6.2	12
MER*	Low traffic urban	1.096	0.003	2.364	0.006	66	26	103	0.22	3.4	23	59	0.4	1.6	1.7	1.5	8
MEV	Low traffic urban	1.091	0.001	2.358	0.003	143	53	133	0.19	9.2	36	389	1.3	4.3	3.7	2.8	11
OAK*	Med. traffic urban	1.082	0.001	2.351	0.005	157	41	124	0.18	6.1	30	179	0.81	6.9	2.2	1.8	6.4
OAK bis	*Med. traffic urban*	*1.084*	*0.003*	2.358	*0.007*	—	—	—	—	—	—	—	—	—	—	—	—
PILA	Pilannesburg Park	1.147	0.002	2.403	0.012	6.9	15	37	0.08	2.6	5.1	256	0.38	<0.1	0.9	1.7	8.3
RIV*	High traffic urban	1.090	0.003	2.358	0.004	159	41	173	0.47	7.3	28	154	0.79	4.2	2.5	2.6	9.9
ROU*	Low traffic urban	1.091	0.003	2.364	0.006	302	81	172	0.55	10	44	158	0.93	4.6	2.4	4.7	9.4
SHA*	Open space dump	1.188	0.002	2.337	0.005	132	57	136	0.59	12	42	130	2.5	2.3	5	6.8	13
SUN*	Open space suburb	1.094	0.001	2.353	0.007	70	22	118	0.34	9.6	14	65	0.26	2.1	0.9	0.2	3.4
TURF	Open space suburb	1.091	0.007	2.360	0.013	123	27	82	0.40	6.1	15	88	0.60	1.8	1.6	0.8	4.9
VERW	Open space suburb	1.089	0.004	2.373	0.009	217	36	274	1.39	8.1	29	177	0.96	6.8	2.6	2.1	6.9
WIT*	High traffic urban	1.087	0.002	2.356	0.006	388	66	169	0.22	15	40	486	1.9	9.7	5	4.5	14
WSBG1*	Open space rural	1.106	0.001	2.358	0.003	56	34	88	0.08	5.3	18	210	0.67	1.2	2	1.6	5.7
*WSBG1 bis**	*Open space rural*	*1.107*	*0.003*	2.361	*0.004*	—	—	—	—	—	—	—	—	—	—	—	—
WSBG2*	Open space rural	1.105	0.002	2.362	0.003	51	24	68	0.11	6	14	234	0.67	1	1.9	1.2	5.5
ZOO1*	Open space urban	1.088	0.003	2.356	0.007	54	15	86	0.10	2.8	16	74	0.31	1.1	1	0.7	2.7
ZOO2*	Open space urban	1.092	0.002	2.356	0.003	51	18	90	0.05	6.2	24	54	0.82	3.2	1.8	2.7	4.0
*ZOO2 bis**	*Open space urban*	*1.092*	*0.001*	2.358	*0.006*	—	—	—	—	—	—	—	—	—	—	—	—
ZOO3*	Open space urban	1.094	0.003	2.364	0.006	101	45	113	0.20	9.5	17	158	0.79	2.6	2.3	3.7	7.8

The errors for isotopic measurements are given at a 95% confidence level; see the text for uncertainties regarding elemental concentrations. '*bis*' = duplicated material. *: lichen collected in May 2001; the other samples were collected in April 2003.

of the potential lead sources around Johannesburg (Tables 1 and 2). The isotopic compositions of leaded gasoline produced by Caltex, Zenex, Engen, Shell and BP are rather homogeneous with $^{206}Pb/^{207}Pb$ values ranging from 1.057 to 1.072, and $^{208}Pb/^{207}Pb$ varying from 2.330 to 2.344 (Table 2, Figs. 2a,b and 3a,b). Gasoline from Total Company is just outside this group with higher $^{206}Pb/^{207}Pb$ and $^{208}Pb/^{207}Pb$ ratios of 1.096 and 2.366, respectively. Raw coal samples collected in two different coal yards from the township of Soweto yield consistent $^{206}Pb/^{207}Pb$ and $^{208}Pb/^{207}Pb$ ratios of about 1.21 and 2.48, respectively. Since fractionation of lead isotopes is not expected during coal burning (Ault et al., 1970), the isotopic signatures of resulting fly ashes are supposed to be the same as in raw material. Samples collected from the four mine dumps are characterised by much higher $^{206}Pb/^{207}Pb$ ratios ranging from 2.182 to 2.882, due to the high uranium content of Witwatersrand goldfields (Cole, 1998; Poujol et al., 1999), and by exceptionally low $^{208}Pb/^{207}Pb$ ratios, ca. 1.707–2.105 (Table 1). A systematic analysis of the local substrate was not performed because of its complex geological diversity (Poujol and Anhaeusser, 2001). However, a few data are available in the literature (Barton et al., 1999). They concern Archaean granodiorites and tonalites constituting the Johannesburg Dome (reported as granitoids in Fig. 1b) and exhibit highly variable isotopic signatures which, in some cases, are close to those measured in mine dumps (Figs. 2a,b and 3a,b). Most of the lichens collected in or around Johannesburg display a homogeneous isotopic field slightly more radiogenic than present-day leaded gasoline (higher $^{206}Pb/^{207}Pb$ and $^{208}Pb/^{207}Pb$ ratios), constrained by $^{206}Pb/^{207}Pb$ ratios within 1.082–1.103, and $^{208}Pb/^{207}Pb$ ratios within 2.344–2.373. Nonetheless, some samples (MEA, SHA, PILA, EMER and CMG, and to a lesser extent both WSBG1 and WSBG2) plot outside this group due to their higher $^{206}Pb/^{207}Pb$ ratios.

Table 2
Lead isotopic compositions of petrol from the major petrol companies

Petrol company	$^{206}Pb/^{207}Pb$	±	$^{208}Pb/^{207}Pb$	±
Total	1.096	0.004	2.366	0.006
Caltex	1.072	0.004	2.344	0.008
Zenex	1.057	0.002	2.330	0.006
Engen	1.060	0.002	2.331	0.005
Shell	1.066	0.003	2.340	0.005
BP	1.063	0.002	2.337	0.005

5. Discussion

5.1. Preparation and treatment of concentration data

Elemental concentrations measured in lichens exhibit non-normal and positively skewed distributions, even after logarithmic transformation. The possible relationships between elements must therefore be examined using non-parametric statistics. In a Spearman's correlation coefficient matrix, almost all of the elements appear to be significantly correlated to one another (Table 3), with the highest

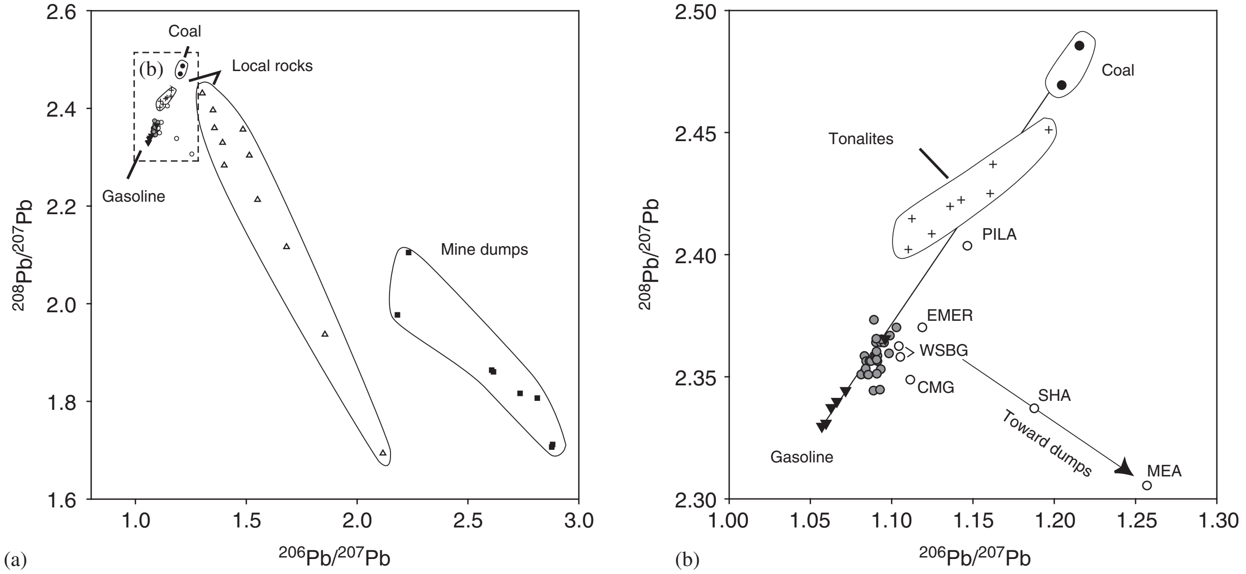

Fig. 2. (a, b) $^{208}Pb/^{207}Pb$ vs. $^{206}Pb/^{207}Pb$ in leaded gasoline (▼), raw coal (●), mine dumps (■), lichens collected either in urban open space or in traffic areas (●), lichens collected close to the dumps or outside the city (○). Lead isotopic compositions of selected rocks from the Johannesburg Dome are reported for comparative purposes: granites and granodiorites (△), tonalites (+); data from Barton et al. (1999).

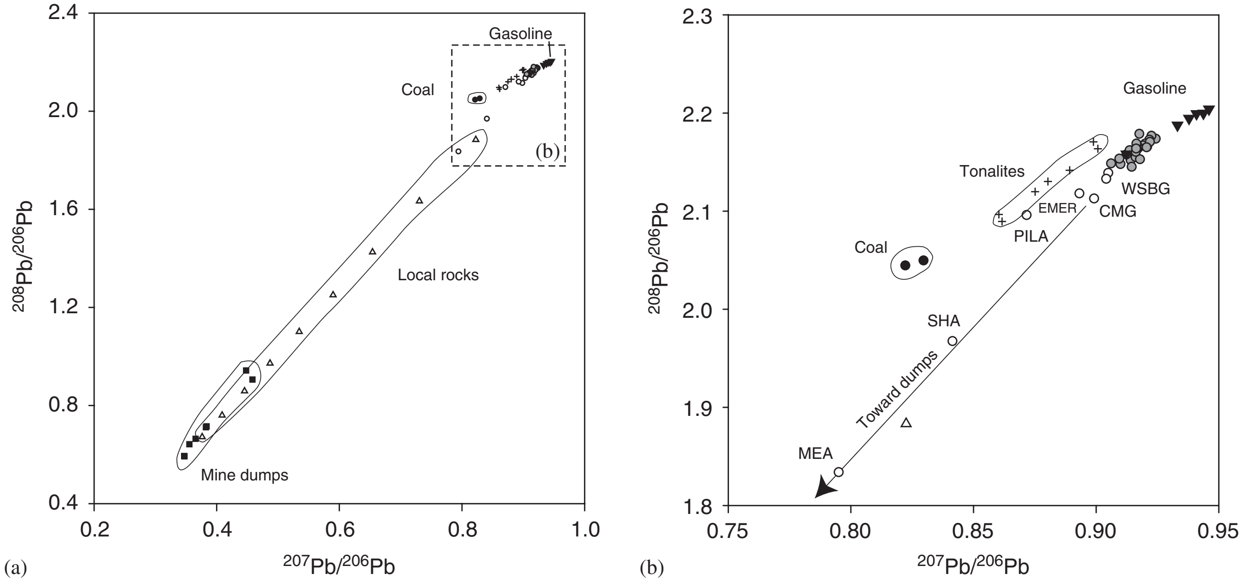

Fig. 3. (a, b) $^{208}Pb/^{206}Pb$ vs. $^{207}Pb/^{206}Pb$ in leaded gasoline (▼), raw coal (●), mine dumps (■), lichens collected either in urban open space or in traffic areas (●), lichens collected close to the dumps or outside the city (○). Lead isotopic compositions of selected rocks from the Johannesburg Dome are reported for comparative purposes: granites and granodiorites (△), tonalites (+); data from Barton et al., (1999).

Table 3
Spearman's correlation coefficient matrix between raw elemental concentrations

	Pb	Cu	Zn	Cd	As	Br	Sb	Cr	Fe	Sc	Th
Cu	0.73**										
Zn	0.77**	0.65**									
Cd	0.51**	0.24	0.25								
As	0.72**	0.63**	0.73**	0.36*							
Br	0.76**	0.61**	0.80**	0.15	0.67**						
Sb	0.81**	0.55**	0.70**	0.38*	0.65**	0.66**					
Cr	0.48**	0.45*	0.24	−0.01	0.26	0.24	0.47**				
Fe	0.60**	0.84**	0.61**	0.04	0.64**	0.65**	0.60**	0.49**			
Sc	0.60**	0.87**	0.64**	0.08	0.61**	0.60**	0.58**	0.49**	0.97**		
Th	0.62**	0.79**	0.61**	0.10	0.69**	0.69**	0.60**	0.44*	0.87**	0.84**	
La	0.57**	0.84**	0.55**	0.06	0.55**	0.54**	0.45*	0.55**	0.86**	0.88**	0.84**

**$p<0.01$; *$p<0.05$.

correlation coefficients observed between the terrigeneous elements: Fe, Sc, Th and La ($0.84<r_{sp}<0.97$; $p<0.01$). A second group, comprising Pb, Zn, As, Br and Sb, is also highly inter-correlated ($0.65<r_{sp}<0.81$; $p<0.01$). All of these elements present lower but significant relationships with those of the crustal group. Although Cr and Cu are correlated to most of the other elements, they tend to be more closely correlated to those belonging to the terrigeneous group. Finally Cd does not show a clear relationship with the other elements, except with Pb ($r_{sp}=0.51$; $p<0.01$) and, in a lesser extent, with Sb and As.

Such correlations are common and are generally induced by factors that are not directly linked to the local atmospheric depositional fluxes but rather to accumulation efficiency and the life span of lichens. Indeed, as the sampled lichens are not necessarily of the same age, the older may have accumulated more trace elements than the younger ones. Lichens might have also been exposed to varying amounts of particle fall-out and their specific morphologies may have affected their trapping capacities (Carignan et al., 2002). Variable combinations of these factors can lead to large differences in chemical compositions inducing correlations between all elements.

A common geochemical approach may consist in normalising elemental concentrations to those of an element that has no anthropogenic origin such as Sc, Ti, Al or La (Dongarrà et al., 1995; Carignan and Gariépy, 1995; Doucet and Carignan, 2001). If we consider that all the elements are continuously and similarly accumulated in lichens during their lifetime, the resulting ratio should be proportional to the enrichment with respect to the crust-derived contribution. Hence, a new matrix of Spearman's correlation coefficients was computed after normalising elemental concentrations to La contents (Table 4). It must, however, be kept in mind that parametric correlations of ratios formed of pairs which have parts in common are often spurious because induced high correlations are expected, more particularly when the coefficient of variation of the common denominator is greater than those of the variables used at the numerator places (Rollinson, 1993). In our case, the coefficient of variations of Pb, Cd, Zn, Sb, As and Br are higher than that of La. Moreover, non-parametric Spearman's correlation coefficients should be less affected by the above-mentioned problems than Pearson's correlation coefficients when outlier samples are present. In Table 4, all ratios including potentially anthropogenic elements (Pb/La, Zn/La, Cd/La, Sb/La, As/La and Br/La) still appear to be significantly intercorrelated, but they are no longer correlated with those calculated from elements belonging to the terrigenous group (Th/La, Fe/La and Sc/La), which pleads in favour of the statistical relevance of the normalisation procedure. The differences observed between the two matrices (Tables 3 and 4) tend therefore to prove that most of the variations related to the age, growing rate, exposition and morphology of the lichens have been efficiently removed using the La normalisation. These correlations do not necessarily mean that Pb, Zn, Cd, Sb, As and Br come from a common anthropogenic source, but simply that anthropogenic activities have introduced these elements into the atmosphere in larger magnitude than natural emissions. It is worth noticing that normalisation produces almost normal new distributions. A principal component analysis (PCA) computed on the standardized new set of variables is reported in Fig. 4, which depicts the projection of samples on the factor-plane F2 vs. F1 with both axes representing more than 60% of the total variance. There is no clear pattern, except that samples MEA and SHA, collected near the mine dumps, plot in the upper part of the diagram, while the PILA sample, collected in the Pilanesberg National Park some 250 km to the west of the city plots in the opposite direction. The other samples do not define any clear clusters, which might indicate a pollution gradient within the city or possibly a particular pollution point source.

5.2. *Mixing model on the basis of lead isotopes*

Lead isotopic compositions reflect the relative contributions and isotopic signatures of the different sources involved, so that the isotopic approach is generally more robust in identifying the origin of lead than models built from bulk concentrations alone. There is no urban incinerator, smelter, lead ore exploitation, or heavy industry using lead around Johannesburg. The clustering of most of the lichens observed in Figs. 2 and 3, and more particularly those collected either in urban open spaces or in traffic areas, therefore indicates that leaded gasoline is an important lead contributor. Similar isotopic compositions have already been measured in airborne particulate matter sampled during the late 90s in Cape Town and Pretoria

Table 4
Spearman's correlation coefficient matrix between elemental concentrations normalised to lanthanum contents

	Pb/La	Zn/La	Cu/La	Cd/La	Sb/La	As/La	Br/La	Th/La	Sc/La
Zn/La	0.54**								
Cu/La	0.50**	0.42*							
Cd/La	0.50**	0.54**	0.33						
Sb/La	0.74**	0.61**	0.30	0.42*					
As/La	0.39*	0.53**	0.28	0.40*	0.37*				
Br/La	0.49**	0.69**	0.44*	0.34	0.51**	0.62**			
Th/La	0.10	−0.07	0.10	−0.02	0.22	0.28	0.19		
Sc/La	−0.09	−0.03	0.09	−0.24	0.06	0.04	0.16	0.21	
Fe/La	0.04	−0.04	0.03	−0.27	0.12	0.13	0.22	0.30	0.89**

**$p < 0.01$; *$p < 0.05$.

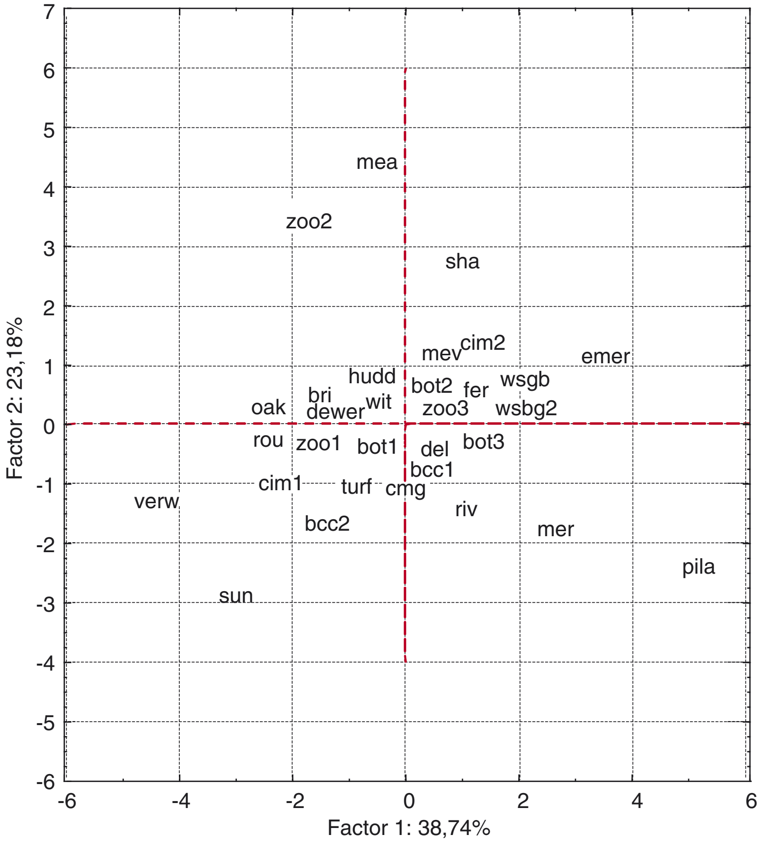

Fig. 4. Principal component analysis, projection of the lichens (see Table 1 for lichen abbreviations) on the factor plane.

($^{206}Pb/^{207}Pb \sim 1.067$–$1.090$), and were also interpreted as the result of a dominant contribution of alkyl lead from gasoline (Bollhöfer and Rosman, 2000). In Johannesburg, however, none of the lichens exactly matches the average isotopic composition of gasoline. This implies that minor inputs from another source (or from several other sources) are involved. In both Figs. 2 and 3, most of the lichens collected either in urban open spaces or in traffic areas fall close to a straight line limited by the gasoline field and by the coal end-members. Similar results are reported by Coetzee et al. (2004) for lead isotope ratios determined on blood samples from children living in Johannesburg. However, tonalites reported by Barton et al. (1999) also appear in co-linear position between gasoline and coals, but they cannot represent alone the average geological background contribution. Because of its homogeneous isotopic composition, lead emitted by domestic coal burning is therefore a better candidate, as a small but significant participant in the total lead budget of lichens. Isotope ratios then suggest that, in samples collected either in urban open spaces or in traffic areas, between 80% and 90% of the lead comes from automotive traffic, the remainder coming probably from coal burning. Among the other samples (open circles in Figs. 2 and 3), both WSBG1 and WSBG2 lichens developed in the Walter Sisulu National Botanical Garden, about 20 km outside the city. Their isotopic compositions do not match those of the lichens collected inside the city, suggesting a slightly lower contribution from gasoline. Further away from the gasoline field in Figs. 2 and 3 is the PILA sample collected in the Pilanesberg National Park, about 250 km away from the city. A gradient of lead pollution linked to automotive traffic is therefore observed from inside to outside the city.

Lichens sampled near Johannesburg's townships in the immediate vicinity of dumps (MEA, SHA and CMG) do not fit this overall scenario. Unlike the other lichens, they all plot, as shown in Figs. 2 and 3, in the direction of mine dumps. Particles from the tailing dumps are likely to be resuspended by winds and incorporated in the lichens growing nearby but, due to their low lead content they do not contribute more than 15% of the total lead (calculated upon the basis of isotopic mixings), with the remaining lead content being mainly related to automotive traffic (cf. Figs. 2 and 3). It is interesting to note that the lichens sampled just at few kilometres away from the goldfields, even in open spaces or low traffic areas, do not show any impact from mine dumps (i.e., see DEWER, CIM1 and CIM2 in Fig. 1). Long-distance transport of any significance is doubtful because of the large size of particles from dumps, so that this source is progressively and rapidly obliterated by diffuse lead emissions from cars.

5.3. Combining lead isotope and La/Pb ratios

In a classic mixing model combining concentrations and isotopic compositions, the 1/Pb ratio

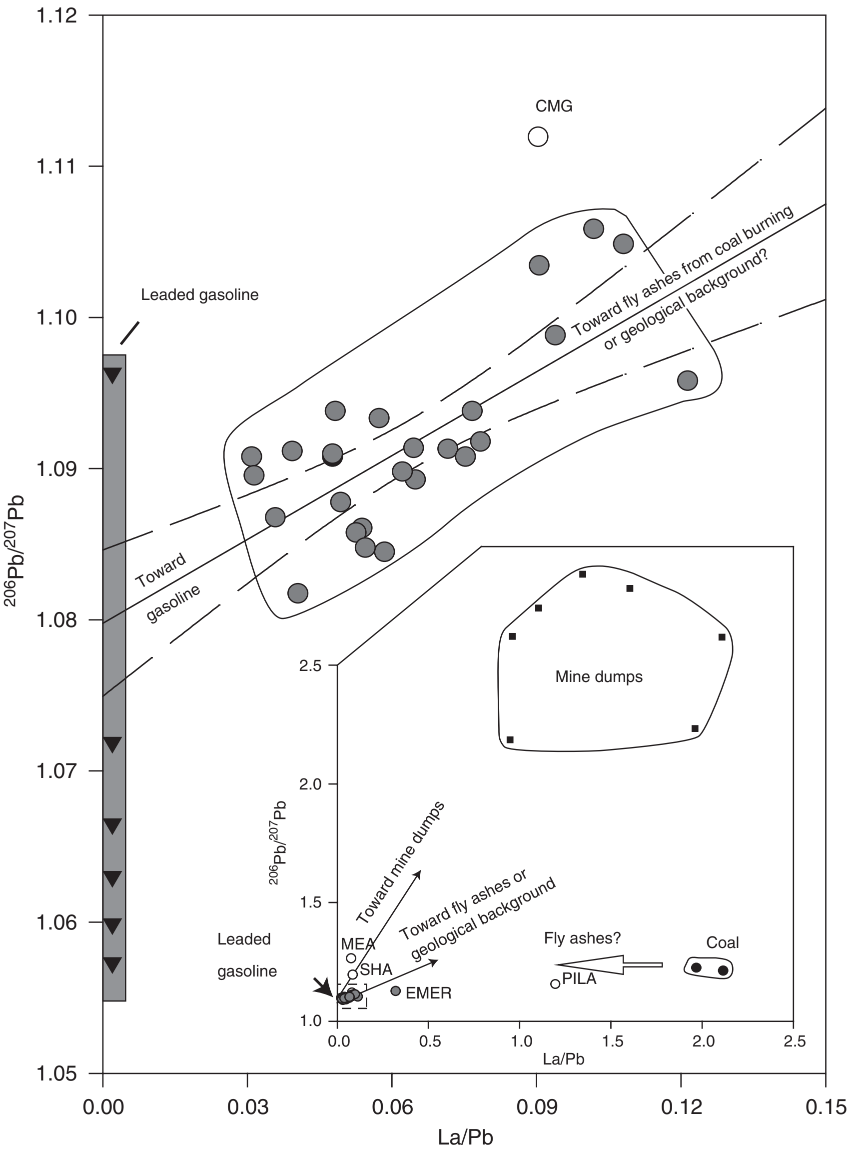

Fig. 5. $^{206}Pb/^{207}Pb$ vs. La/Pb in leaded gasoline (▼), raw coal (●), mine dumps (■), lichens collected either in urban open space or in traffic areas (●), and those collected close to the dumps or outside the city (○). The possible fly ash position from coal burning is given by an arrow, see text for details. The linear regression is calculated only from lichens collected either in urban open spaces or in traffic areas, $r = 0.73$, $p < 0.01$, and the long dash curves correspond to the 95% confidence intervals of the linear regression.

represents the *X*-axis and one of the Pb/Pb ratios the *Y*-axis: see e.g. Faure (1986) for fundamentals and Cloquet et al. (2006) for specific use in lichens. However, this procedure may not be the most advisable solution here because lead content in lichens is expected to vary, not only as a function of atmospheric pollution magnitude, but also because of the age, growing rate, exposition, morphologies or trapping capacities of the different lichens. Consequently, the La/Pb ratio was preferred to the 1/Pb ratio (Fig. 5) as was recently the case with Sc/Pb for the study of a long-term pollution record in a peat bog (Monna et al., 2004), and with Al/Pb for the identification of the impact of a Cu smelter in Russia using lichen transplants (Spiro et al., 2004). As a matter of fact, the La/Pb ratio somehow reflects the way in which anthropogenic lead exceeds the natural contribution, independently from the above-mentioned factors that are expected to influence Pb concentrations. Although La/Pb ratios of raw coal materials are fairly homogeneous between 0.3 and 0.5, lithophilic elements are known to be far less volatile than chalcophylic metals (Tolvanen, 2004), so that fly ashes are likely to present lower La/Pb ratios than original coal materials (shown in Fig. 5 by an arrow). The present-day leaded gasoline field is plotted directly on the *Y*-axis because of the negligible amounts of La compared to Pb in automotive exhaust emissions, while the mine dumps have La/Pb ratios between 1 and 2. Lichens collected either in urban open spaces or in traffic areas present very low La/Pb ratios which undoubtedly indicate high anthropogenic lead contamination. They also plot close to the gasoline field, confirming again the preponderance of lead from automotive exhausts in the Johannesburg's atmosphere. These same samples define a significant linear pattern ($r = 0.73$, $p < 0.01$, see Fig. 5) interpreted as the result of a binary mixing between gasoline and one other minor source that likely results from coal burning. Again, samples collected close to mine dumps, CMG, SHA and MEA, are found outside the group formed by the other lichens, and plot in the direction of mine dumps. The ^{206}Pb/^{207}Pb vs. La/Pb graphical representation produces a coherent picture of the complex multi-component mixings observed in the Johannesburg's atmosphere, suggesting that the fractionation between lanthanum and lead during their absorption and retention in the lichens is not significant. In this type of study where lichens are used as bioaccumulators, La normalisation is therefore particularly efficient and complementary to the examination of lead isotope ratios to apportion the different sources involved.

6. Conclusion

Isotopic compositions of potential pollution sources in Johannesburg are extremely contrasted with ^{206}Pb/^{207}Pb ratios from 1.06 to about 2.9, and ^{208}Pb/^{206}Pb between 0.6 and 2.20. Such a wide range is very rarely encountered because uranium-rich sources like mine dumps are infrequently involved in the surface cycle of lead. This specificity considerably extends the discrimination power of the isotopic method, especially when isotopic information is combined with elemental concentrations expressed as La/Pb ratios. The La normalisation is necessary because absolute concentrations are perturbed by other factors than atmospheric pollution. Lead associated with dust transported by winds from the numerous mine dumps is recorded in small amounts within the immediate vicinity of the dumps, but quickly becomes insignificant just a few kilometres away. Lead emitted by domestic coal burning in historically Black residential areas never contributes more than 20% of the total lead budget. Everywhere in the city, all of these sources are obliterated by leaded antiknock compounds added to the gasoline, which constituted the major lead emitter for the Johannesburg's atmosphere at the time of the study. Consequently, the promotion of unleaded petrol in South Africa will drastically decrease lead concentrations in the atmosphere.

Acknowledgements

This work has been funded in part by a CNRS/NRF agreement (13281 CNRS/NRF 2002). We greatly thank Olivier Bruguier and Pierre Yves Favargé for their technical assistance in measuring lichens, Sylvain Salavy for his help during sampling, Jean Carignan and Carmela Chateau for their precious experience and discussions. We also wish to express special thanks to two anonymous reviewers who greatly improved the manuscript by their thoughtful comments.

References

Åberg, G., Pacyna, J.M., Stray, H., Skjelkvåle, .B.L., 1999. The origin of atmospheric lead in Oslo, Norway, studied with the use of isotopic ratios. Atmospheric Environment 33, 3335–3344.

Ault, W.A., Senechal, R.G., Erlebach, W.E., 1970. Isotopic compositions as a natural tracer of lead in the environment. Environmental Science and Technology 4, 305–313.

Barton, J.M., Barton, E.S., Kroener, A., 1999. Age and isotopic evidence for the origin of the Archaean granitoid intrusives of the Johannesburg Dome, South Africa. Journal of African Earth Sciences 28, 693–702.

Bellis, D.J., McLeaod, C.W., Satake, K., 2002a. Pb and ^{206}Pb/^{207}Pb isotopic analysis of a tree bark pocket near Sheffield, UK recording historical change in airborne pollution during the 20th century. Science of the Total Environment 289, 169–176.

Bellis, D.J., Sakate, K., Noda, M., Nishimura, N., McLeaod, C.W., 2002b. Evaluation of the historical records of lead pollution in the annual growth rings and bark pockets of a 250-year-old *Quercus crsipula* in Nikko, Japan. Science of the Total Environment 295, 91–100.

Bergametti, G., Dutot, A.L., Buat-Ménard, P., Losno, R., Remoudaki, E., 1989. Seasonal variability of the elemental composition of atmospheric aerosol particles over the Northwestern Mediterranean. Tellus 41B, 351–353.

Bindler, R., Renberg, I., Klaminder, J., Emteryd, O., 2004. Tree rings as Pb pollution archives? A comparison of ^{206}Pb/^{207}Pb isotope ratios in pine and other environmental media. Science of the Total Environment 319, 173–183.

Bollhöfer, A., Rosman, K.J.R., 2000. Isotopic source signatures for atmospheric lead: the Southern Hemisphere. Geochimica et Cosmochimica Acta 64 (19), 3251–3262.

Carignan, J., Gariépy, C., 1995. Isotopic composition of epiphytic lichens as a tracer of the sources of atmospheric lead emission in southern Québec, Canada. Geochimica et Cosmochimica Acta 59 (21), 4427–4433.

Carignan, J., Simonetti, A., Gariépy, C., 2002. Dispersal of atmospheric lead in northeastern North America as recorded by epiphytic lichens. Atmospheric Environment 36, 3759–3766.

Chen, J.M., Tan, M.G., Li, Y., Zhang, Y., Lu, W., Tong, Y., Zhang, G., Li, Y., 2005. A lead isotope record of Shanghai atmospheric lead emissions in total suspended particles during the phasing out of leaded gasoline. Atmospheric Environment 39, 1245–1253.

Chiaradia, M., Cupelin, F., 2000. Behaviour of airborne lead and temporal variations of its source effects in Geneva (Switzerland): comparison of anthropogenic versus natural processes. Atmospheric Environment 34, 959–971.

Chiaradia, M., Gulson, B.L., James, M., Jamerson, C.W., Johnson, D., 1997. Identification of secondary lead sources in the air of an urban environment. Atmospheric Environment 31, 3511–3521.

Cloquet, C., Carignan, J., Libourel, G., 2006. Atmospheric pollutant dispersion around an urban area using trace metal concentrations and Pb isotopic compositions in epiphytic lichens. Atmospheric Environment 40, 574–587.

Coetzee, H., Monna, F., Manton, W.I., Poujol, M., Rademeyer, M., Losno, R., Annegarn, H., 2004. Lead isotopes in the Gauteng environment. Geoscience Africa, Johannesburg 11-16 July 2004.

Cole, D.I., 1998. Uranium. In: Wilson, M.G.C., Anhausser, C.R. (Eds.), The Mineral Resources of South Africa Handbook, vol. 16. Council for Geoscience, pp. 642–652.

Dongarrà, G., Ottonello, D., Sabatino, G., Triscari, M., 1995. Use of lichens in detecting environmental risk and in geochemical prospecting. Environmental Geology 26, 139–146.

Doucet, F.J., Carignan, J., 2001. Atmospheric Pb isotopic composition and trace metal concentration as revealed by epiphytic lichens: an investigation related to two altitudinal sections in Eastern France. Atmospheric Environment 35, 3681–3690.

Faure, G., 1986. Principles of isotope geology, second ed. Wiley, New York, 589pp.

Flament, P., Bertho, M.-L., Deboudt, K., Véron, A., Puskaric, E., 2002. European isotopic signatures for lead in atmospheric aerosols: a source apportionment based upon ^{206}Pb/^{207}Pb ratios. Science of the Total Environment 296, 35–57.

Formenti, P., Annegarn, H.J., Picket, S.J., 1998. Time resolved aerosol monitoring in the urban centre of Soweto. Nuclear Instrumentation & Methods in Physics Research Section B-Beam Interactions with Materials and Atoms 136–138, 948–954.

Getty, S.R., Gutzler, D.S., Asmeron, Y., Shearer, C.K., Free, S.J., 1999. Chemical signals of epiphytic lichens in southwestern North America, natural versus man-made sources for airborne particulates. Atmospheric Environment 33, 5095–5104.

Giusti, L., 1988. U–Pb isotopic data for sulfides of the Varkenskraal granite (Western Transvaal, South Africa) and their bearing on the age and origin of uranium mineralization in the Witwatersrand basin. Chemical Geology 72, 311–328.

Haack, U., Kienholz, B., Reimann, C., Schneider, J., Stumpfl, E.F., 2004. Isotopic composition of lead in moss and soil of the European Arctic. Geochimica et Cosmochimica Acta 68, 2613–2622.

Jaakkola, T., Heinonen, O.J., Keinonen, M., Salmi, A., Miettinen, J.K., 1983. Use of ^{206}Pb/^{204}Pb isotope ratio in lichen, air filter, incinerator ash and gasoline samples as pollution source indicator. International Journal of Mass Spectrometry and Ion Physics 48, 347–350.

Kunert, M., Friese, K., Weckert, V., Markert, B., 1999. Lead isotope systematics in *Polytrichum formosum*: an example from biomonitoring field study with mosses. Environmental Science and Technology 33, 3502–3505.

Kurkjian, R., Dunlap, C., Flegal, A.R., 2002. Lead isotope tracking of atmospheric response to post-industrial conditions in Yerevan Armenia. Atmospheric Environment 36, 1421–1429.

Loppi, S., Pirintsos, S.A., 2003. Epiphytic lichens as sentinels for heavy metal pollution at forest ecosystems (central Italy). Environmental Pollution 121, 327–332.

Marcantonio, F., Flowers, G., Thien, L., Ellgaard, E., 1998. Lead isotopes in tree rings: chronology of pollution in Bayou Trepagnier, Louisiana. Environmental Science and Technology 32, 2371–2376.

Monna, F., Lancelot, J., Croudace, I.W., Cundy, A.B., Lewis, J.T., 1997. Pb isotopic composition of airborne particulate material from France and the Southern United Kingdom: implications for Pb pollution sources in urban areas. Environmental Science and Technology 31, 2277–2286.

Monna, F., Loizeau, J.-L., Thomas, B.A., Guéguen, C., Favarger, P.-Y., 1998. Pb and Sr isotope measurements by inductively coupled plasma-mass spectrometer: efficient time management for precision improvement. Spectrochimica Acta B 59/09, 1317–1333.

Monna, F., Aiuppa, A., Varrica, D., Dongarrà, G., 1999. Pb isotopic compositions in lichens and aerosols from Eastern Sicily: insights on the regional impact of volcanoes on the environment. Environmental Science and Technology 33, 2517–2523.

Monna, F., Loizeau, J.-L., Thomas, B., Guéguen, C., Favarger, P.-Y., Losno, R., Dominik, J., 2000. Noise identification and sampling frequency determination for precise isotopic measurements by quadrupole-based inductively coupled plasma mass spectrometry. Analusis 28, 750–757.

Monna, F., Petit, C., Guillaumet, J.-P., Jouffroy-Bapicot, I., Blanchot, C., Dominik, J., Losno, R., Richard, H., Lévêque, J., Chateau, C., 2004. History and environmental impact of mining activity in Celtic Aeduan territory recorded in a peat-bog (Morvan—France). Environmental Science and Technology 38, 657–673.

Munksgaard, N.C., Parry, D.L., 1998. Lead isotope determined by ICP-MS: monitoring of mining-derived metal particulates in atmospheric fallout, Northern Territory, Australia. Science of the Total Environment 217, 118–125.

Pillet, S., Hernandez, J., Sylvester, P.J., Poujol, M., 2005. The metasomatic alternative for Ocean Island basalt chemical heterogeneity. Earth and Planetary Science Letters 236 (1–2), 148–166.

Poujol, M., Anhaeusser, C.R., 2001. The Johannesburg Dome, South Africa: new single zircon U–Pb isotopic evidence for early Archaean granite-greenstone development within the Central Kaapvaal Craton. Precambrian Research 108, 139–157.

Poujol, M., Robb, L.J., Respaut, J.P., 1999. U–Pb and Pb–Pb isotopic studies relating to the origin of gold mineralization in the Evander Goldfield, Witwatersrand Basin, South Africa. Precambrian Research 95, 67–185.

Remoudaki, E., Bergametti, G., Losno, R., 1991. On the dynamic of the atmospheric input of copper and manganese into the Western Mediterranean Sea. Atmospheric Environment 25A, 733–744.

Rollinson, H.R., 1993. Using Geochemical Data: Evaluation, Presentation, Interpretation. Longman Publishing Group, 352pp.

Simonetti, A., Gariépy, C., Carignan, J., 2003. Tracing sources of atmospheric pollution in Western Canada using the Pb isotopic composition and heavy metal abundances of epiphytic lichens. Atmospheric Environment 37, 2853–2865.

Spiro, S., Weiss, D.J., Purvis, O.W., Mikhailova, I., Williamson, B.J., Coles, B.J., Udachin, V., 2004. Lead isotopes in lichens transplants around a Cu smelter in Russia determined by MC-ICP-MS reaveal transient records of multiple sources. Environmental Science and Technology 38, 6522–6528.

Tolvanen, M., 2004. Mass balance determination for trace elements at coal-, peat- and bark fired power plants. In: ESPOO 2004. VTT publications no. 524, 139pp.

Tommasini, S., Davies, G.R., Elliot, T., 2000. Lead isotope composition of tree rings as bio-geochemical tracers of heavy metal pollution: a reconnaissance study from Firenze, Italy. Applied Geochemistry 15, 891–900.

Véron, A., Flament, P., Bertho, M.-L., Alleman, L., Flegal, R., Hamelin, B., 1999. Isotopic evidence of pollutant lead sources in Northwestern France. Atmospheric Environment 33, 3377–3388.

Watmough, S.A., Hutchinson, T.C., 2004. The quantification and distribution of pollution Pb at a woodland in rural south central Ontario, Canada. Environmental Pollution 128, 419–428.

Widory, D., Roy, S., Le Moullec, Y., Goupil, G., Cocherie, A., Guerrot, C., 2004. The origin of atmospheric particles in Paris: a view through carbon and lead isotopes. Atmospheric Environment 38, 953–961.

Available online at www.sciencedirect.com
ScienceDirect
Environmental Pollution 152 (2008) 693–701
ENVIRONMENTAL POLLUTION
www.elsevier.com/locate/envpol

Kinetic extractions to assess mobilization of Zn, Pb, Cu, and Cd in a metal-contaminated soil: EDTA *vs.* citrate

Jérôme Labanowski [a], Fabrice Monna [b], Alain Bermond [c], Philippe Cambier [a], Christelle Fernandez [a], Isabelle Lamy [a], Folkert van Oort [a,*]

[a] *INRA, UR 251 Unité PESSAC, RD 10, F-78026 Versailles Cedex, France*
[b] *ARTeHIS, UMR 5594 CNRS, Univ. de Bourgogne Centre des Sciences de la Terre, Bat. Gabriel, F-21000 Dijon, France*
[c] *AgroParis Tech., Laboratoire de Chimie Analytique, 16 rue C. Bernard, 75231 Paris Cedex 05, France*

Received 22 June 2007; accepted 26 June 2007

Kinetically defined metal fractions mimic mobility aspects of heavy metals.

Abstract

Kinetic EDTA and citrate extractions were used to mimic metal mobilization in a soil contaminated by metallurgical fallout. Modeling of metal removal rates *vs.* time distinguished two metal pools: readily labile (Q_{M1}) and less labile (Q_{M2}). In citrate extractions, total extractability ($Q_{M1} + Q_{M2}$) of Zn and Cd was proportionally higher than for Pb and Cu. Proportions of Pb and Cu extracted with EDTA were three times higher than when using citrate. We observed similar Q_{M1}/Q_{M2} ratios for Zn and Cu regardless of the extractant, suggesting comparable binding energies to soil constituents. However, for Pb and Cd, more heterogeneous binding energies were hypothesized to explain different kinetic extraction behaviors. Proportions of citrate-labile metals were found consistent with their short-term, *in-situ* mobility assessed in the studied soil, i.e., metal amount released in the soil solution or extracted by cultivated plants. Kinetic EDTA extractions were hypothesized to be more predictive for long-term metal migration with depth.

Keywords: Kinetic extraction modeling; Heavy metals; EDTA; Citrate; Metal mobility; Soils

1. Introduction

Fate of heavy metals in soils is of great environmental concern. They represent major risks regarding contamination of natural waters after release by metal-bearing soil constituents and migration *via* the soil solution downward to the water table (van Oort et al., 2006). Studying soil solution collected *in situ* from different horizons in metal polluted soils, Denaix et al. (2001) and Citeau et al. (2003) reported the presence of metals either as predominantly mobile, water-soluble forms (Zn, Cd) or as colloidal forms (Pb, Cu). Incorporation of metal pollutants in soils generally leads to changes in chemical speciation. Liberated metal ions are variously trapped by a wide range of reactive soil constituents, i.e. organic matter, iron and manganese oxides and hydroxides, phyllosilicates, phosphates, carbonates. A fraction of these metals can thereafter be (re)mobilized, either in dissolved or colloidal form before migrating downward. Mobilization is defined here as the potential capacity of metals to be transferred from the solid phase into the soil solution. It depends on the various links between metals and reactive sites of solid phase surfaces.

Numerous operational chemical extraction methods, including one-step extractions (Chaignon et al., 2003; Feng et al., 2005) and sequential extraction procedures (McGrath, 1996; Gleyzes et al., 2002; Krishnamurti et al., 2002), have been developed to estimate the extractable metal pools in relation to the metal-bearing soil phases. Although informative, such extraction procedures generally suffer from lacking

---

[*] Corresponding author.
E-mail address: vanoort@versailles.inra.fr (F. van Oort).

0269-7491/$ - see front matter © 2007 Elsevier Ltd. All rights reserved.
doi:10.1016/j.envpol.2007.06.054

selectivity with respect to the targeted chemical forms of metals. Alternatively, several authors have hypothesized that kinetic metal extraction data might better reflect dynamics of metals in soils (Gutzman and Langford, 1993; Bermond et al., 1998; Lo and Yang, 1999; Bermond et al., 2005) and in sediments (Fangueiro et al., 2002, 2005; Gismera et al., 2004). For a given chemical agent, the kinetic extraction approach generates two kinds of data: (i) the proportion of metals extracted with respect to the total metal content of the soil sample; and (ii) the kinetic behavior of metals. It has been suggested that such kinetic extractions can be modeled by two first-order reactions, so-called TFOR model, which empirically define two different pools. Although chemical extractants used for experiments do not perfectly mimic natural conditions, the first pool of readily extracted metals, called ''labile'' by Fangueiro et al. (2005), and the second pool of more slowly extracted metals, called ''less labile'', might be reasonably attributed to potentially ''mobile'' and/or ''bioavailable'' metal pools (Bermond et al., 2005). In this view, Degryse et al. (2006) showed that the proportion of labile metals was well-correlated with metal uptake in plants. Particularly for sandy textured soils, the distinction of two types of extractability with time is hypothesized to provide a good expression of the diversity of metal-soil constituent interactions, i.e., to various chemical bond stabilities. In soils with strong aggregation phenomena (i.e., clay soils), disaggregation phenomena due to chemical agents or physical stirring may, however, influence the extraction of discrete kinetic pools.

Naidu and Harter (1998) stated that metals extracted by a mixture of organic acids are well-correlated with the mobile metal fraction in the soil solution. Organic acids are likely to be more representative of a mobile metal fraction that is available for biota. Low molecular weight organic acids, naturally exuded by plant roots or produced by microbial activity (Fox and Comerford, 1990), have been hypothesized to influence nutrient mobilization (van Hees et al., 2002) or translocation of metals in soil profiles (van Hees and Lundström, 2000; Li et al., 2006). Ethylene diamine tetraacetic acid (EDTA) is a well-known strong chelating agent and has been widely used in agronomy for estimating the total extractable metal pool (Alvarez et al., 2006; Manouchehri et al., 2006). EDTA was reported to remove metals organically bound, occluded in oxides, and associated with secondary clay minerals (Payà-Pérez et al., 1993). In contrast, citrate has been reported to be one of the dominant organic acids in the soil solution (van Hees et al., 2002). Among the low-molecular-weight organic acids used to simulate metal mobilization, citrate presents a moderate metal complexation strength compared to EDTA, according to thermodynamic data from Sillen and Martell (1964) and Lindsay (1979) shown in Table 1.

The present study aimed at estimating the labile fractions of different trace metals (Zn, Pb, Cu, and Cd) by applying kinetic EDTA and citrate extractions on samples from a moderately metal-contaminated agricultural soil (Labanowski et al., 2007). Comparison of EDTA and citrate extractions was used to quantify metal mobilization and to assess relationships between the energy of metal binding and the strength of the used chemical extractant. By expressing the data in terms of metal removal rates *vs.* time, we first checked the pertinence of fitting kinetic extractions with a TFOR model. Parameters provided by this modeling were then used to compare the different kinetic metal pools with results on metal mobility obtained from field studies (Citeau et al., 2003) and pot experiments (Mench et al., 2007) conducted on the same soil.

Table 1
Formation constants (log K_f) for metal-EDTA and metal-citrate complexes at 0.1 M ionic strength

	Zn	Pb	Cd	Cu
$Me[EDTA]^{2-}$	16.3	18.2	16.5	18.8
$Me[citrate]^{-}$	4.9	4.0	3.8	5.9
$Me_2[citrate]_2^{2-}$	–	–	–	13.2
$Me[citrate]_2^{4-}$	6.5	6.1	5.4	8.1

The log K_f values presented in this table are derived from those of Sillen and Martell (1964) and Lindsay (1979). They are recalculated to the same ionic strength.

2. Materials and methods

2.1. Site conditions and soil sampling

The site selected for this study was an agricultural field located about 750 m from a former metallurgical complex in northern France (Elsass et al., 2002; Labanowski et al., 2007). From 1901 to the late 1960s, the activity of a Zn smelter produced major atmospheric fallout (Thiry and van Oort, 1999), affecting agricultural land over an area of 3500 ha. The study site was a corn field representative of the most metal-contaminated agriculture areas, with reported total metal contents of 384–489 mg Zn kg^{-1}, 89–124 mg Pb kg^{-1}, 16.6–18.9 mg Cu kg^{-1}, and 3.5–3.8 mg Cd kg^{-1} (Chartier, 1998; Elsass et al., 2002; van Oort et al., 2002). For understanding overall soil development, behavior, and metal distribution patterns, a large soil pit was dug and carefully sampled according to characteristic soil horizons as well as systematic sampling at 10-cm depth increments. For the present study, focusing on the plow layer, representative bulk samples of several kilograms between 0 and 28 cm were air-dried, sieved to <2 mm and homogenized before analyses.

2.2. Soil analyses

Characteristic physico-chemical parameters of the plow layer (particle size distribution, pH, $CaCO_3$ content, CEC using cobaltihexamine) were determined by INRA's national soil analysis laboratory using standard methods (AFNOR, Agence Française de Normalisation, 1996). Total carbon content (Total C) was measured using NC 2500 C/H/N analyzer (NC Instruments). Total metal concentrations in the sample were determined by atomic absorption spectrophotometry (AAS), either flame or furnace (Varian SpectrAA 220) after HF/HNO_3 (1:3, v:v) acid digestion under microwave heating (CEM MarsX) according to the digestion applications manual (CEM, 1998). HF (40%) and HNO_3 (68%) were of analytical grade. Total metal concentrations were also measured on samples from subsurface horizons. Quality control included triplicate analyses, blanks and a standard reference soil (CRM 7001, CMI, Prague, Czech Republic). Measured concentrations of elements from the reference material always were <5% from certified values. Metal concentrations in blanks were below the detection limit.

2.3. Extraction kinetics

Extraction kinetics by EDTA or citrate were used on soil samples to study: (i) the maximal potential metal extraction capacity after 24 h; and (ii) the

Table 2
Selected physico-chemical parameters of the studied soil (plow layer)

Particle size distribution (g kg^{-1})					pH	CEC (cmol kg^{-1})	Total Org. C (g kg^{-1})	$CaCO_3$ (g kg^{-1})	Total metals (mg kg^{-1})			
Clay	Fine silt	Coarse silt	Fine sand	Coarse sand					Zn	Pb	Cu	Cd
98	76	291	449	86	6.6	6.7	14.8	2.5	411	100	16.7	3.6

extraction rates of metals released as a function of time (between 0 and 24 h). For this, 1 g of soil was shaken with 10 ml of extracting solution for different periods (5, 15, and 30 min; 1, 2, 5, 11, 17, and 24 h) and then immediately filtered on a 0.45-μm cellulose membrane. For extractions >1 h, suspensions were centrifuged 5 min at 16,786 g before filtration. All EDTA and citrate extractions were made in three replicates and yielded 54 samples. Preliminary studies (not shown here) were conducted to optimize the experimental conditions. Finally, a 0.05 M Na_2H_2-EDTA and a 0.1 M $(NH_4)_2H$-citrate solution were found optimal for assessing the maximum extractability of the metals. Since many of the reactions with the extracting agents were pH dependent, all extracting solutions used in this work had a pH adjusted to 6.6 (soil pH) by adding adapted amounts of NaOH. Fangueiro et al. (2002) showed that a pH of about 6 guaranteed minimal variations of pH during extraction and hence, prevented competitive extraction by H^+. Metal contents were determined as described above.

3. Results and discussion

3.1. Soil physico-chemical characteristics

The plow layer of the studied soil showed a slightly acidic pH and very low calcium carbonate content (Table 2). Other parameters, i.e., total carbon content (14.8 g kg^{-1}) and CEC (6.7 cmol kg^{-1}), were found to be typical for such sandy cultivated soils. Total metal concentrations reached 411 mg Zn kg^{-1}, 100 mg Pb kg^{-1}, and 3.6 mg Cd kg^{-1}. These values were much higher than those of the local geochemical background of the soils, estimated at 35, 16 and 0.2 mg kg^{-1} for Zn, Pb, and Cd, respectively (Fernandez et al., 2007). The content of Cu (16.7 mg kg^{-1}) did not point to a marked industrial pollution. However long-term effects of fertilization and application of herbicides and fungicides may have contributed to the addition of anthropogenic Cu to the soil surface.

Distribution of total Zn, Pb, Cu, and Cd concentrations between the Ap and the C horizon (Fig. 1) clearly showed their dominant accumulation in the plow layer. Below the Ap horizon, the concentrations of Zn and Cd decreased progressively indicating their migration until about 80-cm to depth, whereas Pb and Cu concentrations varied little. Such metal distribution patterns with depth are in agreement with comparable studies on other cultivated soils in the same area (Fernandez et al., 2007).

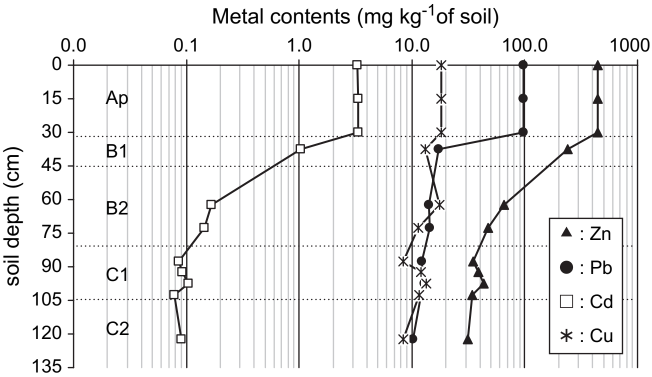

Fig. 1. Metal distribution patterns with depth in the studied soil profile (van Oort, unpublished data).

3.2. Proportion of metal extracted after 24 h

Examination of metal extraction evolutions with time showed that equilibrium was almost reached after 24 h (Fig. 2), except for Pb and to a lesser extent for Zn and Cd, when extracted with EDTA, which still showed some minor metal release at the end of the experiment. The percentages of extracted Zn, Pb, Cu, and Cd by EDTA were always higher than those extracted by citrate, although divergences were more marked for Pb and Cu than for Zn and Cd. These latter two elements can be considered as easily extractable metals, since both strong and moderately-strong chemical extracting agents were able to mobilize them in similar proportions, i.e., 45–55% for Zn and about 70–80% for Cd (Fig. 2). These results corroborate general statements that classify these two metals among the most mobile in soils, occurring frequently in appreciable amounts in the soil solution (Gray et al., 2003; Citeau et al., 2003). For Pb and Cu, however, the extracted amounts differed, depending on the strength of the used extractant (Fig. 2). With EDTA, about 90% of Pb was removed from the soil. Such a value is in agreement with other works which frequently report lead extractions >60% with EDTA (Lestan et al., 2005). Yet Pb is widely considered to be a low-mobility or immobile metal in soils. This apparent contradiction clearly highlights the discrepancy between metal-"mobilization" studied in laboratory conditions and metal-"mobility" observed in field conditions. Solubilization of a metal with a chemical extractant therefore does not imply its mobility in the soil, but means that the metal is potentially mobile under certain physicochemical conditions.

3.3. Kinetic aspects

In order to check the pertinence of the application of any first order model to kinetic extractions, the experimental results were expressed firstly in terms of metal removal rates per time unit. The amount of metal M extracted per weight unit of soil between t_i and t_{i-1}, M (mg kg^{-1}), can be defined as:

$$\mathrm{M}_{(t_{i-1}<t<t_i)} = \frac{[C_\mathrm{M}(t_i) - C_\mathrm{M}(t_{i-1})]V}{\mathrm{m}}, \qquad (1)$$

where $C_\mathrm{M}(t)$, V and m represent the metal concentration at time t, the volume of extractant solution and the sample

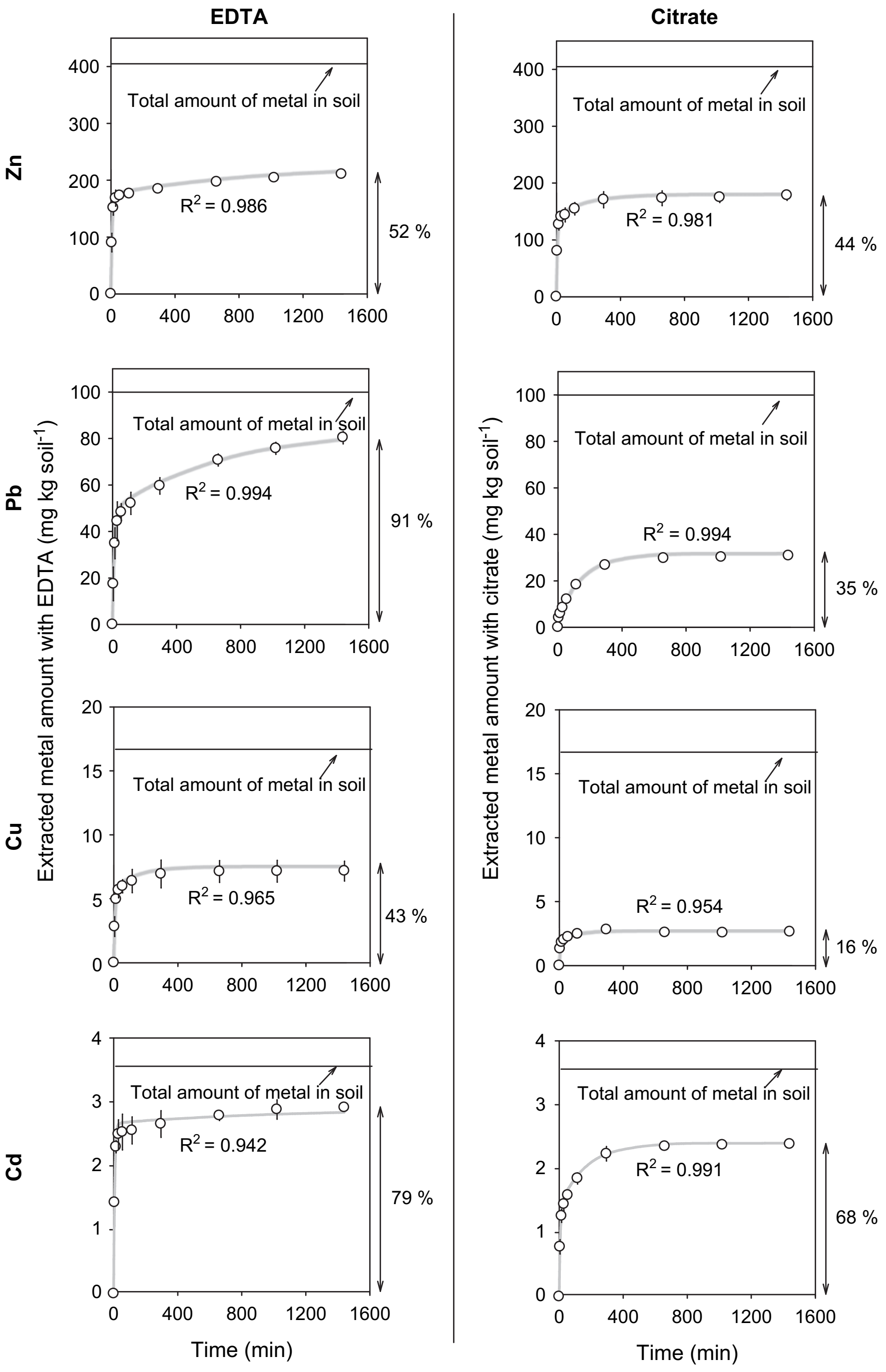

Fig. 2. Evolution of cumulative extracted amounts of Zn, Pb, Cu, and Cd metal *vs.* time with EDTA and citrate. Open circles: average of the results obtained from three replicates; error bars represent the 95% confidence level ($\bar{x} \pm s.t_{(\nu = 2;\ \alpha = 0.05,\ \text{bilateral})}/\sqrt{3}$). Thick grey line: modeled values (see text for details).

mass, respectively. Then, the average removal rate per time unit, $A_{\mathrm{M}}(t)$, between t_i and t_{i-1}, for a given metal can be written as:

$$A_{\mathrm{M}(t_{i-1}<t<t_i)} = \frac{\mathrm{M}_{(t_{i-1}<t<t_i)}}{t_i - t_{i-1}}, \qquad (2)$$

Practically, the values $A_{\mathrm{M}}(t)$ were computed for each lag time of the three independent replicates. The mean values and the 95% confidence intervals were calculated and plotted in a semi-log diagram (Fig. 3), which was another way for representing the data originally reported in Fig. 2. It appeared that the evolution of $A_{\mathrm{M}}(t)$ generally occurs as two distinct linear segments with different, non-null slopes and different intercepts on the *Y*-axis. Such clear differences of behaviour through time allow the variable $A_{\mathrm{M}}(t)$ to be modelled by the sum of two distinct pools occurring simultaneously, each of them following an exponential decreasing function:

$$A_{\mathrm{M}}(t) = A_{\mathrm{M1}}(0)\mathrm{e}^{-\lambda_{\mathrm{M1}}t} + A_{\mathrm{M2}}(0)\mathrm{e}^{-\lambda_{\mathrm{M2}}t}, \qquad (3)$$

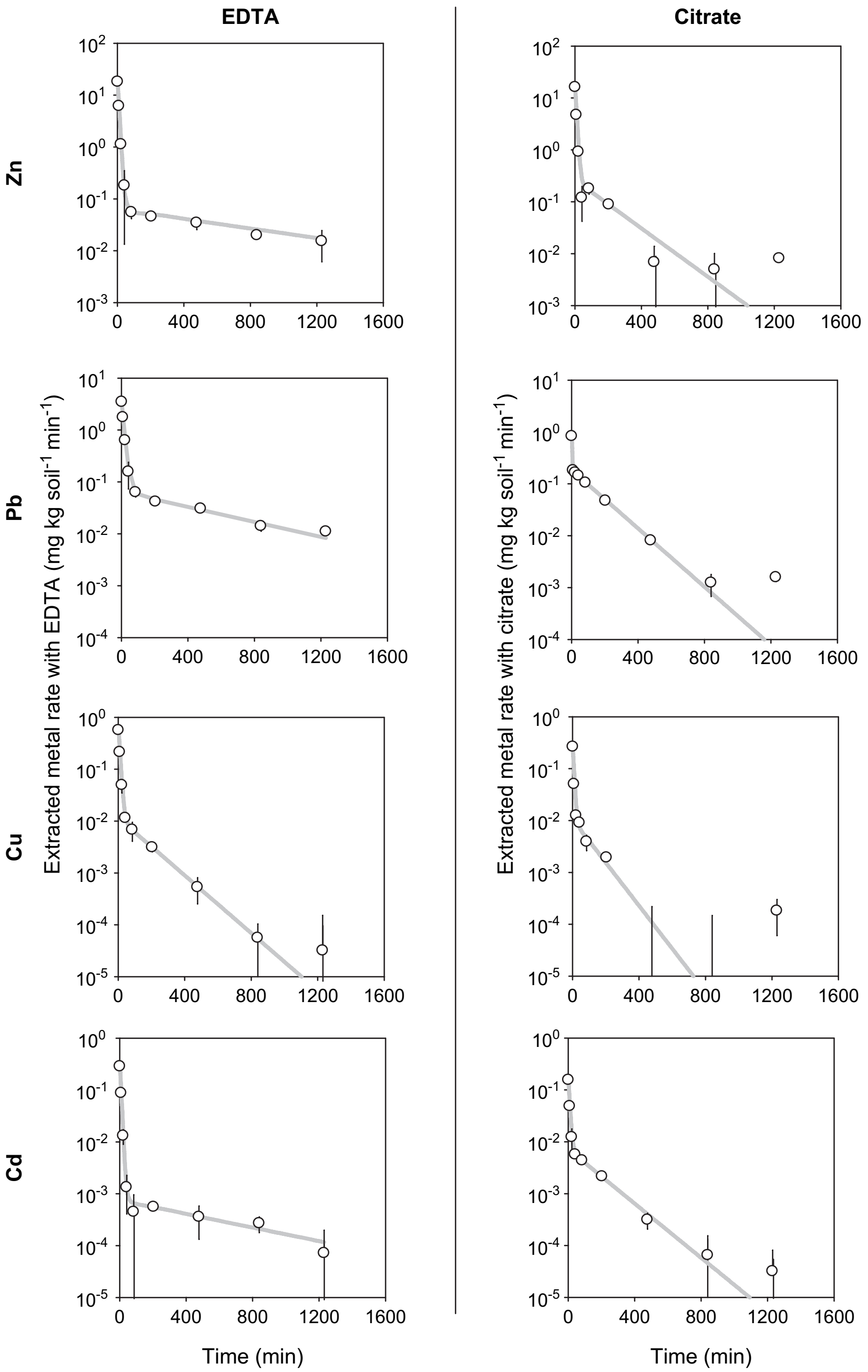

Fig. 3. Evolution of Zn, Pb, Cu, and Cd removal rate *vs.* time after with EDTA and citrate. Open circles: average of the results obtained from three replicates; error bars represent the 95% confidence level ($\bar{x} \pm s.t_{(\nu = 2;\ \alpha = 0.05,\ \text{bilateral})}/\sqrt{3}$). Thick grey line: modeled values (see text for details).

where $A_{M1}(0)$ and $A_{M2}(0)$ are the initial removal rates (at $t = 0$) of the metal M of the two pools and λ_{M1} and λ_{M2} are their apparent rate constants.

The extracted metal amounts gradually increased up to the end of the experiments with EDTA (Fig. 2) but quickly level off with citrate. Hence, it would have been tempting to model these latter using a single first order equation. As it can be seen in Fig. 3, and more particularly for extractions involving citrate, the representation using extraction rates *vs.* time reveals more clearly the presence of two metal pools than using cumulative amounts of extracted metals (Fig. 2). The metal removal rates appeared to be high at the start of the extraction, dominated by the parameter $A_{M1}(0)$ characteristic of the first pool, but the contribution of this first pool decreased quickly to become insignificant (exponential decrease governed by λ_{M1}) (Fig. 3). Then, after a while, the contribution of the second pool became preponderant, with a clear slower extraction rate which still decreased with time (following λ_{M2}).

At time t, the total amount of metal extracted corresponds to the equation:

$$Q_M(t) = \int_0^t A_M(t)\,dt \tag{4}$$

and, after integration:

$$Q_M(t) = \frac{A_{M1}(0)}{\lambda_{M1}}(1 - e^{-\lambda_{M1}t}) + \frac{A_{M2}(0)}{\lambda_{M2}}(1 - e^{-\lambda_{M2}t}) \tag{5}$$

Let us denote Q_{M1} by $A_{M1}(0)/\lambda_{M1}$ and Q_{M2} by $A_{M2}(0)/\lambda_{M2}$. Then Eq. (5) can be written as:

$$Q_M(t) = Q_{M1}(1 - e^{-\lambda_{M1}t}) + Q_{M2}(1 - e^{-\lambda_{M2}t}) \tag{6}$$

Application of Eq. (6) to metal-extraction kinetics distinguishes two pools of metal, previously defined by Fangueiro et al. (2005) as Q_{M1} corresponding to the readily extractable metal fraction, called labile, associated with the apparent rate constant λ_{M1}, and Q_{M2} corresponding to the less readily extractable metal fraction, called less labile, associated with the apparent rate constant λ_{M2}. In addition, the total non-extractable metal fraction, Q_{M3}, must also be considered. It corresponds to the difference between the total amount of metal in soil (Q_{tot}) and the above mentioned pools:

$$Q_{M3} = Q_{Tot} - Q_{M1} - Q_{M2} \tag{7}$$

Calculations of kinetic parameters diverge to some extend from those proposed by Bermond et al. (1998) and Fangueiro et al. (2005); both authors computing the parameters from the cumulative amount of metal extracted through time (Eq. (6)). In the present study, the parameters $A_{M1}(0)$, λ_{M1}, and $A_{M2}(0)$, λ_{M2}, were computed separately from both linear segments (Fig. 3). Each value was first weighted by using the inverse of its relative standard deviation, calculated on the basis of the three replicates. The parameters $A_M(0)$ and λ_M were drawn from the Y-axis intercepts and the slopes, respectively by linear fitting to Eq. (3). From their standard deviations provided by Statistica 6.0 for Windows, a 95% confidence interval was calculated (given that two degrees of freedom were lost by each linear fitting). Then, the parameters Q_M were obtained by dividing $A_M(0)$ and λ_M. Their 95% confidence intervals were calculated by combining individual errors (Tables 3 and 4).

The metal amounts extracted by citrate after about 400–800 min were very low so that the subtraction $C(t_i) - C(t_{i-1})$ performed in Eq. (1) became inaccurate (Fig. 2). Therefore, the results for $t = 1440$ min were discarded for modelling citrate data. Besides, Pb extracted with citrate seemed to fit a single exponential decrease, even though the first extract was notably enriched by comparison to the general trend (Fig. 3). Consequently, this Pb case was treated as an instantaneous extraction pulse followed by a single exponential decrease. Finally, the total amounts of metal extracted with time have been simulated using Eq. (5) and compared to experimental observations (Figs. 2 and 3) (we obtained 5 degrees of freedom for EDTA extractions because two times two degrees of freedom are lost by linear fittings, and 4 for citrate extractions because the last extract was discarded). R-square values were calculated on this basis. They provided an indication of how well the model fitted the data. All R^2 were closed to unity, indicating that almost all of the variability has been accounted for with the variables specified in the model (Tables 3 and 4).

Comparison between results of the two kinetic extraction methods indicated that both the labile and less labile metal pools were generally greater for EDTA than for citrate (Tables 3 and 4). Only Cd does not fit this scenario since the less-labile fraction represented about 30% of the total Cd with citrate *vs.* about 10% with EDTA. A second general trend is that the labile metal fraction was generally greater than the less labile fraction for both extractants ($Q_{M1}/Q_{M2} > 1$), except for Pb (Tables 3 and 4). The Q_{M1}/Q_{M2} ratios of Zn and Cu were fairly similar for EDTA and citrate extractions, in spite of significantly different total amounts of metals extracted after 24 h. This suggests that the extracted fractions of Zn and Cu were bound to soil constituents with fairly homogeneous binding strengths for each metal.

On the contrary, mobilization of Cd and Pb was markedly related to the extraction strength (i.e., the intensity of complexation measured by the log K_F values, Table 1), notably in terms of proportion of labile and less labile pools. For Pb, the relative prevalence of the less-labile pool with citrate extractions (clearly highlighted by Fig. 3) suggests a slow and

Table 3

Initial extraction rates, $A_{Mi}(0)$, kinetic parameters, λ_{Mi}, and amounts, Q_{Mi}, of metal extracted with EDTA per kg of soil for the two pools defined by the TFOR kinetic model

	$A_{M1}(0)$ (mg kg^{-1} min^{-1})	λ_{M1} (min^{-1})	Q_{M1} (mg kg^{-1}) (% of total)	$A_{M2}(0)$ (mg kg^{-1} min^{-1})	λ_{M2} (min^{-1}, $\times 10^{-3}$)	Q_{M2} (mg kg^{-1}) (% of total)	R^2	Q_{M1}/Q_{M2}	Q_3 (mg kg^{-1}) (% of total)
Zn	21.5–25.5	0.128–0.138	160–192 ∼45%	0.058–0.068	0.9–1.2	51–67 ∼15%	0.986	∼3	∼175 ∼40%
Pb	3.7–4.1	0.076–0.082	46–52 ∼50%	0.055–0.075	1.4–1.9	30–47 ∼41%	0.994	∼1.3	∼10 ∼10%
Cu	0.72–0.79	0.118–0.126	5.7–6.5 ∼35%	0.011–0.012	6.3–6.5	1.7–1.9 ∼10%	0.964	∼3.5	∼10 ∼55%
Cd	0.417–0.423	0.155–0.157	2.6–2.7 ∼75%	$5.4\ 10^{-4}$–10^{-3}	0.8–2.1	0.2–0.8 ∼10%	0.941	∼7.5	∼0.5 ∼15%

Values correspond to confidence interval at a level of 95% (see text for details). Q_3 has been evaluated by subtracting Q_{M1} and Q_{M2} from the total metal amount per kg of soil.

Table 4
Initial extraction rates, $A_{Mi}(0)$, kinetic parameters, λ_{Mi}, and amounts, Q_{Mi}, of metal extracted with citrate per kg of soil for the two pools defined by the TFOR kinetic model

	$A_{M1}(0)$ (mg kg^{-1} min^{-1})	λ_{M1} (min^{-1})	Q_{M1} (mg kg^{-1}) (% of total)	$A_{M2}(0)$ (mg kg^{-1} min^{-1})	λ_{M2} (min^{-1}, $\times 10^{-3}$)	Q_{M2} (mg kg^{-1}) (% of total)	R^2	Q_{M1}/Q_{M2}	Q_3 (mg kg^{-1}) (% of total)
Zn	18–22	0.127–0.142	133–169 ~35%	0.16–0.42	3.6–7.0	22–77 ~10%	0.981	~3.5	~200 ~55%
Pb	Almost instantaneous		3.8–4.8 ~5%	0.18–0.19	6.4–6.6	28–29 ~30%	0.994	~0.2	~65 ~65%
Cu	0.28–0.42	0.138–0.167	1.7–2.7 ~15%	$0.8\ 10^{-2}$–$1.2\ 10^{-2}$	7.4–11	0.6–1.4 ~5%	0.954	~3	~13 ~80%
Cd	0.19–0.22	0.134–0.151	1.3–1.6 ~40%	$5.9\ 10^{-3}$–$8.6\ 10^{-3}$	5.4–6.7	0.9–1.4 ~30%	0.991	~1.4	~1 ~30%

Values correspond to confidence interval at a level of 95%. Q_3 has been evaluated by subtracting Q_{M1} and Q_{M2} from the total metal amount per kg of soil. See text for details about the case of Pb.

low mobilization under moderate extraction-strength conditions, consistent with generally low Pb mobility observed in soils. For Cd, a part of the fraction easily removed by EDTA becomes less labile with citrate (Tables 3 and 4): the configuration Q_{M1}: 75%, Q_{M2}: 10% with EDTA turns into Q_{M1}: 40%, Q_{M2}: 30%, maybe because, with citrate, more time is necessary to break links between Cd and soil constituents. Yet, at the end of the experiment, both EDTA and citrate have removed comparable amounts of Cd: 85% and 70%, respectively.

In terms of kinetics, the labile pools of Zn, Cu, and Cd are extracted approximately at the same high apparent rate constant: $\lambda_{M1} \sim 0.11$–$0.17\ min^{-1}$ whatever the extractants used and the total extracted metal amounts. This means that approximately 10–20% of the remaining labile pool are removed per minute (Tables 3 and 4). Labile Pb seems to be less rapidly removed by EDTA ($\lambda_{M1} \sim 0.07$–$0.08\ min^{-1}$). The calculation with citrate was not done for the reasons mentioned above. The λ_{M2} constants characterizing the less labile pool are much lower than the λ_{M1} constants. The λ_{M2} values of Zn, Pb, and Cd obtained with EDTA are comparable: $0.8 \times 10^{-3} - 2.1 \times 10^{-3}\ min^{-1}$ while a similar homogeneity is observed for these metals, with citrate $\lambda_{M2} = 3.6 \times 10^{-3} - 11 \times 10^{-3}\ min^{-1}$. For both extractants, the λ_{M2} values of Cu are higher than those of other metals, suggesting that this Cu pool is associated with soil phases with low binding energy.

3.4. Operational use of kinetic extraction data in soil metal mobility studies

As already mentioned above, the two metal pools defined by the TFOR model have been attributed to mobile or bioavailable metal fractions (Bermond et al., 2005; Degryse et al., 2006). Significance of kinetic chemical extractions for providing detailed insight on metal speciation is still questionable yet, because different metal mobilization kinetics are observed following the reagent used. Studies connecting results from the kinetic approach with real-world investigations on metal mobility are cruelly lacking. In the present case, data issued by both approaches are interestingly available since complementary data on metal mobility and bioavailability were obtained for the soil of our study by experimental field work, and by laboratory pot experiments. Citeau and co-workers collected periodically over three years gravitational soil water by lysimeters placed at the bottom of the Ap horizon, and assumed to explore a soil volume of about 7 L (Citeau et al., 2001, 2003; Citeau, 2004). Results are reported in Table 5. Exposure of different cultivars to metal polluted soil was also studied (Chartier, 1998; Mench et al., 2007). Green salad, carrot and rye grass were cultivated in 3 replicates using 10-kg pots filled with plow layer samples sieved to <5 mm. These cultivars were harvested at the usual growth stage (about 30 days). They were carefully washed with distilled water, dried at 60 °C, ground and analyzed for total metal contents (Mench et al., 2007) (Table 5). Metals display approximately the same behavior in both experiments. Percentages of Zn and Cd extracted monthly from the Ap horizon by soil solutions or plants are remarkably close. They vary only within one order of magnitude or less and are about 10–20 and 100–200 times higher than those of Cu and Pb, respectively (Table 5). Interestingly, the same pattern is observed for the percentages of readily citrate-labile pools: Zn ~ Cd > Cu > Pb (Table 4). Hence,

Table 5
Experimental data on metal mobility determined in the soil solution and by plant uptake

	Zn	Pb	Cd	Cu
– Average % of total metal extracted from the soil by the soil solution over 1 month*	0.25	0.0005	0.17	0.01
– Average % of total metal extracted from the soil by plant over 1 month**				
Green salad	0.71	0.002	1.54	0.09
Rye grass	1.39	0.008	1.05	0.42
Carrot	0.26	0.001	0.25	0.05

*Mean values compiled from lysimeter data of metal amounts in, and volumes of gravitational water ($n = 31$) leaching out of the Ap horizon (from Citeau, 2004); **mean values compiled from pot experiment data on metal-uptake by three cultivars with replicates ($n = 3$) (from Chartier, 1998; Mench et al., 2007). Metal extraction was expressed as a percentage of total metal content in the bulk sample.

labile metals extracted by citrate might be representative of short-term metal dynamics (solid-liquid transfer, plant-availability). In contrast, there is less resemblance of behavior between the readily labile pools using EDTA and real-world experiments, in particular for lead. This can be ascribed to the high extraction strength of EDTA (Table 1) which appears out of proportion with respect to natural soil conditions. As a consequence, EDTA rather provides an upper limit of metal mobility and can be a valuable parameter to predict long-term transfer in soils.

4. Conclusion

The representation of EDTA and citrate kinetic extractions in terms of removal rate confirmed the existence of two kinetic metal pools, a labile and a less-labile pool, which can be modeled by two first order reactions. Zn and Cu showed similar kinetic behaviors (in terms of Q_{M1}/Q_{M2} ratios) regardless of the extraction strength, contrarily to Cd and Pb which were markedly related to the used extractant. These results suggest that Zn and Cu have a more homogeneous binding strengths (with one or more soil constituents) compared to Cd and Pb.

Q_{M1}-citrate values were considered to be a good indicator for short-term metal mobility as they mimic metal mobilization in field and experimental conditions and are consistent with the frequently observed mobility scheme: Zn ~ Cd > Cu > Pb. EDTA extracted greater amounts of metals from the soil compared to citrate. It may therefore provide an indication for the maximum potential metal extractability, helpful for the prediction of long-term risks.

Acknowledgements

J. L. thanks the French National research Program ToxNuc-E and INRA for a 16-month post-doc fellowship. C.F. received a grant from the French ministry of Research and Technology (MRT). The authors gratefully acknowledge Sébastien Breuil for help in soil sampling and chemical extractions. We would like to address our special acknowledgements to the reviewer for his pertinent comments and suggestions, greatly improving the manuscript.

References

AFNOR, 1996. Qualité des Sols. Recueil de Normes Françaises, Paris.

Alvarez, J.M., Lopez-Valdivia, L.M., Novillo, J., Obrador, A., Rico, M.I., 2006. Comparison of EDTA and sequential extraction tests for phytoavailability prediction of manganese and zinc in agricultural alkaline soils. Geoderma 132, 450–463.

Bermond, A., Yousfi, I., Ghestem, J.-P., 1998. Kinetic approach to the chemical speciation of trace metals in soils. Analyst 123, 785–789.

Bermond, A., Varrault, G., Sappin-Didier, V., Mench, M., 2005. A kinetic approach to predict soil trace metal bioavailability: preliminary results. Plant and Soil 275, 21–29.

CEM, 1998. Microwave Sample Preparation Note 5OS-14. CEM Microwave Digestion Applications Manual.

Chaignon, V., Sanchez-Neira, I., Herrmann, P., Jaillard, B., Hinsinger, P., 2003. Copper bioavailability and extractability as related to chemical properties of contaminated soils from a vine-growing area. Environmental Pollution 123, 229–238.

Chartier, S., 1998. Composition en éléments traces (Zn, Pb, Cd et Cu) des parties consommables de végétaux cultivés dans des terres de la zone agricole connexe de la friche industrielle de Mortagne-du-Nord – Thun-St-Amand. Master report, INRA-Agronomie, Bordeaux, France.

Citeau, L., 2004. Etude des colloïdes naturels présents dans les eaux gravitaires de sols contaminés: relation entre nature des colloïdes et réactivité vis-à-vis des métaux (Zn, Cd, Pb, Cu). Doctoral thesis, INA Paris-Grignon, France, 251 p.

Citeau, L., Lamy, I., van Oort, F., Elsass, F., 2001. Nature des sols et nature des colloïdes circulant dans les eaux gravitaires: une étude *in situ*. Comptes Rendus de l'Académie des Sciences 332, 657–663.

Citeau, L., Lamy, I., van Oort, F., Elsass, F., 2003. Colloidal facilitated transfer of metals in soils under different land use. Colloids and Surfaces A 217, 11–19.

Degryse, F., Smolders, E., Merckx, R., 2006. Labile Cd complexes increase Cd availability to plants. Environmental Science & Technology 40, 830–836.

Denaix, L., Semlali, R.M., Douay, F., 2001. Dissolved and colloidal transport of Cd, Pb, and Zn in a silt loam soil affected by atmospheric industrial deposition. Environmental Pollution 113, 29–38.

Elsass, F., van Oort, F., Le Mot, Y., Jaunet, A.M., 2002. Spéciation de métaux traces dans les sols contaminés à l'aide de la microscopie électronique analytique: cas des sols agricoles à proximité d'une friche industrielle (Mortagne-du-Nord). In: Baize, D., Tercé, M. (Eds.), Les éléments traces métalliques dans les sols. Approches fonctionnelles et spatiales. INRA Editions, Paris, France, pp. 331–352.

Fangueiro, D., Bermond, A., Santos, E., Carapuça, H., Duarte, A., 2002. Heavy metal mobility assessment in sediments based on a kinetic approach of the EDTA extraction: search for optimal experimental conditions. Analytica Chimica Acta 459, 245–256.

Fangueiro, D., Bermond, A., Santos, E., Carapuça, H., Duarte, A., 2005. Kinetic approach to heavy metal mobilization assessment in sediments: choose of kinetic equations and models to achieve maximum information. Talanta 66, 844–857.

Feng, M.-H., Shan, X.-Q., Zhang, S.-Z., Wen, B., 2005. A comparison of the rhizosphere-based method with DTPA, EDTA, $CaCl_2$, and $NaNO_3$ extraction methods for prediction of bioavailability of metals in soil to barley. Environmental Pollution 137, 231–240.

Fernandez, C., Labanowski, J., Cambier, P., Jongmans, A.G., van Oort, F., 2007. Fate of airborne metal pollution in soils as related to agricultural management: Zn & Pb distributions in soil profiles. European Journal of Soil Science 58, 547–559.

Fox, T.R., Comerford, N.B., 1990. Low-molecular-weight organic acids in selected forest soils of the south-eastern USA. Soil Science Society of America Journal 54, 1139–1144.

Gismera, M.J., Lacal, J., da Silva, P., García, R., Sevilla, M.T., Procopio, J.R., 2004. Study of metal fractionation in river sediments. A comparison between kinetic and sequential extraction procedures. Environmental Pollution 127, 175–182.

Gleyzes, C., Tellier, S., Astruc, A., 2002. Fractionation studies of trace elements in contaminated soils and sediments: a review of sequential extraction procedures. Trends in Analytical Chemistry 21, 451–467.

Gray, C.W., Mc Laren, R.G., Roberts, A.H.C., 2003. Cadmium leaching from some New Zealand pasture soils. European Journal of Soil Science 54, 159–166.

Gutzman, D.W., Langford, C.H., 1993. Kinetic study of the speciation of copper(II) bound to a hydrous ferric oxide. Environmental Science & Technology 27, 1388–1393.

Krishnamurti, G.S., Smith, L.H., Naidu, R., 2002. Method for assessing plant-available cadmium in soils. Australian Journal of Soil Research 38, 823–836.

Labanowski, J., Sebastia, J., Foy, E., Jongmans, A.G., Lamy, I., van Oort, F., 2007. Fate of metal-associated POM in a soil under arable land use contaminated by metallurgical fallout in northern France. Environmental Pollution 149, 59–69.

Lestan, D., Hanc, A., Finzgar, N., 2005. Influence of ozonation on extractability of Pb and Zn from contaminated soils. Chemosphere 61, 1012–1019.

Li, J., Xu, R., Tiwari, D., Ji, G., 2006. Mechanism of aluminium release from variable charge soils induced by low-molecular-weight organic acids: kinetic study. Geochimica et Cosmochimica Acta 70, 2755–2764.

Lindsay, W.L., 1979. Chemical Equilibria in Soils. Wiley and Sons, New York.

Lo, I.M.C., Yang, X.Y., 1999. EDTA extraction of heavy metals from different soil fractions and synthetic soils. Water, Air, and Soil Pollution 109, 219–236.

Manouchehri, N., Besancon, S., Bermond, A., 2006. Major and trace metal extraction from soil by EDTA. Equilibrium and kinetic study. Analytica Chimica Acta 559, 105–112.

McGrath, D., 1996. Application of single and sequential extraction procedures to polluted and unpolluted soils. Science of the Total Environment 178, 37–44.

Mench, M., Chartier, S., Girardi, S., Solda, P., van Oort, F., Baize, D., 2007. Exposition de végétaux aux éléments traces, évaluation et gestion des risques pour la sûreté des aliments d'origine végétale. Exemple de la zone agricole de Mortagne-du-Nord. In: Cambier, Ph., Schvartz, C., van Oort, F. (Eds.), Devenir et Effets des Contaminations Métalliques dans les Agrosystèmes et Ecosystèmes Terrestres Péri-industriels. Editions Quae, Versailles, France (in press).

Naidu, R., Harter, R.D., 1998. Effects of different organic ligands on cadmium sorption and extractability from soils. Soil Science Society of America Journal 62, 644–650.

Payà-Pérez, A., Sala, J., Mousty, F., 1993. Comparison of ICP-AES and ICP-MS for the analysis of trace elements in soil extracts. International Journal of Environmental Analytical Chemistry 51, 223–230.

Sillen, L.G., Martell, A.E., 1964. Stability of Metal-ligand Complexes. In: Sp. Publ., 17. The Chemical Society, London.

Thiry, M., van Oort, F., 1999. Les phases minérales majeures et mineures d'une friche industrielle de métallurgie des métaux non ferreux: états d'altération, évolution géochimique et devenir des métaux polluants du site de Mortagne-du Nord. In: Les cahiers du club CRIN- Club CRIN "Environnement" et Ministère de l'Environnement. ECRIN Edition, Paris, France, pp. 108–135.

van Hees, P.A.W., Lundström, A.S., 2000. Equilibrium model of aluminum and iron complexation with different organic acids in soil solution. Geoderma 94, 201–221.

van Hees, P.A.W., Jones, D.L., Godbold, D.L., 2002. Biodegradation of low molecular weight organic acids in coniferous forest podzolic soils. Soil Biology and Biochemistry 34, 1261–1272.

van Oort, F., Gaultier, J.P., Hardy, R., Bourennane, H., 2002. Distributions spatiales des métaux et stratégies d'échantillonnage dans les sols du périmètre agricole d'une friche industrielle. In: Baize, D., Tercé, M. (Eds.), Les éléments traces métalliques dans les sols. Approches fonctionnelles et spatiales. INRA Editions, Paris, France, pp. 281–297.

van Oort, F., Jongmans, A.G., Citeau, L., Lamy, I., Chevallier, P., 2006. Microscale Zn and Pb distribution patterns in subsurface soil horizons: an indication for metal transport dynamics. European Journal of Soil Science 57, 154–166.

Available online at www.sciencedirect.com

ScienceDirect

Atmospheric Environment 42 (2008) 999–1011

ATMOSPHERIC ENVIRONMENT

www.elsevier.com/locate/atmosenv

Geochemical records of limestone façades exposed to urban atmospheric contamination as monitoring tools?

F. Monna[a,*], A. Puertas[a], F. Lévêque[b], R. Losno[c], G. Fronteau[d], B. Marin[d], J. Dominik[e], C. Petit[a], B. Forel[a], C. Chateau[f]

[a]*Centre des Sciences de la Terre, ARTéHIS, UMR 5594 CNRS-Culture, Université de Bourgogne, Bat., Gabriel, F-21000 Dijon, France*
[b]*Centre Littoral de Géophysique, Université de La Rochelle, Pôle Sciences et Technologie, Avenue Michel Crépeau, F-17042 La Rochelle, Cedex 01, France*
[c]*LISA, Universités Paris 7 et Paris 12, CNRS, Faculté des Sciences, 61 av. du Gal de Gaulle, F-94010 Créteil Cedex, France*
[d]*Groupe d'Etudes sur les Géomatériaux et les Environnements Naturels et Anthropiques, EA 3795, Université de Reims Champagne-Ardenne, F-51100 Reims, France*
[e]*Institut F.-A. Forel, Université de Genève, 10 route de Suisse, CH-1290, Versoix, Switzerland*
[f]*Centre des Sciences de la Terre, Université de Bourgogne, Bat, Gabriel, F-21000 Dijon, France*

Received 2 July 2007; received in revised form 5 October 2007; accepted 8 October 2007

Abstract

Magnetic susceptibility, surface rock soiling, elemental composition and lead isotope ratios were measured in surface stone samples collected at different heights of a late 19th century building in Dijon, France. We targeted four limestone façades that differ in orientation and proximity to car traffic. It seems that zinc, copper, sulphur and cadmium are present as diffuse pollutants in urban atmosphere, at least at the scale of the building studied. In contrast, lead and arsenic exhibit point sources: automotive traffic and past coal-burning fly-ash emissions; both coherent with lead isotopic composition measurements. Parameter variations primarily result from exposition to rain washing or micro-scale runoff, and from the closeness, magnitude and origin of anthropogenic sources. Both anthropogenic particles and natural dust tend to be similarly affected by deposition/soiling and rain washing, which act dynamically as competitive processes. Examination of archival photographs suggests that soiling predominated in the past, when the air was rich in black dust, whereas equilibrium or even weathering may occur nowadays due to recent improvements or at least changes in air quality. Using the chemical composition of building façades to provide insights into the magnitude and dispersion of urban atmospheric pollutants may not always be straightforward because of uncertainties related to the period of accumulation.

Keywords: Pollution; Heavy metals; Magnetic susceptibility; Soiling; Lead isotopes

---

1. Introduction

Monitoring heavy metal pollution levels in the urban atmosphere is of environmental concern because it allows strategies to be developed to identify, and then reduce, the impact of emitting

---

*Corresponding author. Tel.: +33 3 80 396 360; fax: +33 3 80 396 387.
E-mail address: Fabrice.Monna@u-bourgogne.fr (F. Monna).

1352-2310/$ - see front matter © 2007 Elsevier Ltd. All rights reserved.
doi:10.1016/j.atmosenv.2007.10.021

sources. Surveys or prospecting studies are often performed by determining airborne particulate matter composition. Such an approach is very convenient but remains costly. Frequent sampling is needed to provide representative information because heavy metal contents in the atmosphere are highly variable and depend on meteorological conditions and diurnal cycles of anthropogenic activity (Flament et al., 2002; Bollhöffer and Rosman, 2002; Haack et al., 2002). Alternatives based on the analysis of biological receptors, such as lichens, pine needles or mosses have been developed in urban areas (e.g. Åberg et al., 1999; Alaimo et al., 2000; Tommasini et al., 2000; Cloquet et al., 2006; Monna et al., 2006) but they are strictly limited by the natural occurrence of the species studied. A more natural approach to investigate urban air pollution would consist in focussing directly on the buildings themselves. Air pollution is known to have a deleterious effect on walls since sulphur dioxide induces the transformation of calcite ($CaCO_3$) into gypsum ($CaSO_4 \cdot 2H_2O$) (i.e. Rodriguez-Navarro and Sebastian, 1996; Simão et al., 2006). Gypsum is soluble and tends to crystallise preferentially in areas sheltered from rain (Lefèvre and Ausset, 2002). It incorporates natural dust, soot carbonaceous particles resulting from combustion, and other anthropogenic particles of various origins, which give the deposit its characteristic blackness: the so-called black crust (Galletti et al., 1997; Ausset et al., 1999). The presence of gypsum increases the surface roughness of stones and facilitates the mechanical deposition of particles. Sulfation processes may also be favoured by fly ash.

Our working hypothesis is that stone surfaces of building façades may have retained over time some of the pollution to which they have been subjected, and hence may provide information about the magnitude, dispersion and origin of current and former heavy metal pollution in urban areas. Magnetic and isotopic parameters should help to validate this assumption. High temperature fossil-fuel combustion produces magnetic spherules of micronic size associated to heavy metals (Hunt et al., 1984; Hoffman et al., 1999; readers will also find reviews of this topic in Petrovsky and Ellwood, 1999). Magnetic material presents the advantage of being rapidly and accurately measurable, even at low thresholds, thus providing an inexpensive proxy to chart pollution. Various approaches to dust characterisation are described in many recent studies (Lecoanet et al., 2001, 2003; Matzka and Maher, 1999; Petrovský et al., 2000; Lehndorff et al., 2006; Jordanova et al., 2003; Moreno et al., 2003; Urbat et al., 2004; Sagnotti et al., 2006). Lead isotope ratios are known to be useful tools to determine the origin of lead in various environments if the potential sources are properly characterised by distinct isotopic signatures. More information about fundamentals can easily be found in an abundant literature (e.g. Elbaz-Poulichet et al., 1984; Walraven et al., 1997; Weiss et al., 1999; Hansmann and Köppel, 2000; Takeda et al., 2000).

For this study, geochemical and geophysical (magnetic susceptibility) parameters were measured on samples collected from four front walls of a late 19th century building in Dijon (agglomeration approx. 240 000 inhabitants) selected to present contrasting exposition to rain washing and to car traffic. The persistence of geochemical information on building façades is discussed, allowing an evaluation of the extent to which façades can be used to monitor urban atmospheric contamination.

2. The site

Carnot College, in the heart of Dijon, was built in 1893 with calcareous materials from open Burgundy quarries (Bathonian/Calovian oolitic and oobioclastic limestones). Four building façades were selected for the present study because of their geographical orientation and their exposition to urban atmospheric pollution (Fig. 1). The first façade, built entirely of calcareous stone, corresponds to the ‘Main entrance’ of the College. It faces northeast and is directly exposed to one of the busiest streets in Dijon: 22 000 cars per day on average (Car traffic regulation office, pers. comm., 2005). Two sets of traffic lights are situated opposite the entrance. The other three façades are located within a 50 m perimeter radius in a courtyard, inside the school (Fig. 1). They are close to two streets with traffic averaging approximately 5700 and 9600 cars per day (Car traffic regulation office, pers. comm., 2005). These façades are mostly composed of cement rendering, apart from doorway and window frames made of calcareous stones. The darkest façade, namely ‘Workshop’, faces northeast, while the other two, namely ‘Cafeteria/clean’ and ‘Cafeteria/dirty’, belong to the same building and face northwest. The college buildings have not been altered in any way since their construction, except for ‘Cafeteria/clean’ that was cleaned in 2002 with high-pressure washers. The heating system of the

Fig. 1. Map of Carnot College, Dijon. The blue spots represent the targeted façades: 'Main entrance', 'Workshop', 'Cafeteria/clean' and 'Cafeteria/dirty', on which in-situ and laboratory magnetic susceptibility and geochemical analyses (yellow boxes), or only magnetic analyses (blue boxes) have been performed. Sample codes are shown to the right of the façade close-up. The main wind direction when it rains in Dijon (>5 mm) is also indicated. In Dijon, the mean annual temperature and the relative humidity are about 10.7 °C and 71%, respectively. All calculations have been performed on the basis of the 1971–2000 record. (Meteo France, pers. comm., 2007).

college, first coal- and then oil-fired, was installed in the same building as 'Workshop' and smoke exited via the roof.

To sum up, targeted façades may be (i) similarly oriented but differently exposed to car traffic: 'Main entrance' vs. 'Workshop', (ii) similarly exposed to pollution but differently oriented: 'Workshop' vs. 'Cafeteria/dirty', and (iii) similarly exposed and oriented but with different exposure time: 'Cafeteria/clean' vs. 'Cafeteria/dirty'.

3. Material and methods

3.1. Sampling

Surface stone samples were collected from calcareous blocks using an aerial work platform. Fine powders were obtained by scratching manually a $20 \times 10\,\mathrm{cm}^2$ stone surface with a pre-cleaned (using diluted HCl and MilliQ water) stainless steel spatula. This operation was carried out as homogeneously as possible by targeting only the external surface of the calcareous blocks. Cement rendering, stonework jointures and any repairs were systematically avoided, as these materials could affect the overall magnetic properties (Bidegain et al., 1999; Gołuchowska, 2001). Powders were kept in pre-cleaned hermetic high-density polyethylene tubes until further analysis. Pristine limestone was also collected by drilling the blocks to a depth of 5 cm. Powder extracted from the first 0.5 cm was discarded in order to prevent contamination from surface soiling. The drills (5 mm diameter) were changed for each sample.

3.2. Geochemical analysis

About 100 mg of powder was totally digested in PTFE beakers using a mixture of HNO_3, HCl and HF of Suprapure® grade (Merck, Germany).

The beakers were disposed on a hot plate (110 °C) and HCl was first added to the powder to dissolve the calcium carbonate. After effervescence stopped (after 2–3 min), HF and HNO_3 were added, beakers were covered and left on the plate for 12 h. The solutions were evaporated to dryness, retaken with HNO_3, diluted with Milli-Q^{TM} (Millipore) water. Measurements of elemental concentrations were performed by inductively coupled plasma—atomic emission spectrometer (ICP-AES) (Perkin-Elmer Optima 3000, axial view), equipped with an ultrasonic nebulizer (CETAC). Five blanks and four international standard reference materials (SRMs: PACS1, BCSS1, JSD1 and JSD2) were measured together with samples. Blanks were systematically low in comparison to samples, so that blank correction was never required. The SRM measurements were in good agreement with certified values, approximately ±10–15%. Solutions were also measured for their lead isotopic abundances, i.e. $^{206}Pb/^{207}Pb$ and $^{208}Pb/^{206}Pb$ ratios, with a quadrupole (Q)-ICP-MS HP 4500 installed at the F.-A Forel Institute, University of Geneva. More details about measurements, mass bias corrections, operation settings and NBS-981 bracketing can be found elsewhere (Monna et al., 1998, 2000). Precisions are typically of 2–4 and of 3–7 to the third decimal place for the $^{206}Pb/^{207}Pb$ and $^{208}Pb/^{206}Pb$ ratios, respectively (at 95% confidence level).

3.3. Magnetic analysis

Before sampling, magnetic susceptibility was measured directly on the four façades using a KT9 Kappameter (Exploranium) hand-held field magnetic susceptibility metre, with a detection limit of 10^{-5} SI. Each determination corresponds to the average of 15 individual measurements obtained by shifting the apparatus over the surface of the wall within the operational area ($20 \times 10\,cm^2$), so that uncertainty is limited to about 10^{-6} SI, when samples present values sufficiently above the detection limit. Magnetic susceptibility of the powders collected by scratching was also measured at the laboratory using a low-field KLY4S Kappabridge (AGICO). Each determination corresponds to 6–12 measurements in order to reach a precision better than 0.2×10^{-6} SI. Both empty and powder-filled plastic boxes were measured in this way and weighted for blank correction. Results were finally normalised to powder weight.

3.4. Evaluation of façade soiling

Stone blackness was evaluated on the basis of several digital photographs taken before sampling. In order to correct sky reflections or differences in natural light conditions properly, a Kodak grey chart was placed at different heights on the buildings. Colour pictures were first digitally converted to an 8 bit grey scale using Adobe Photoshop CS for Windows. Then both Kodak test chart and operational areas of targeted stones were grey averaged and expressed as percentage of black. The grey values of stones were finally normalised to those of the adjacent Kodak test chart, so that they all became comparable. Precision was evaluated to about ±5%.

4. Results

Magnetic susceptibility, soiling (as blackness) and elemental compositions are reported in Table 1. To check if at least one front wall tends to yield larger values than at least one of the others, a Kruskal–Wallis test, used as a non-parametric alternative to the one-way ANOVA, was applied to each variable (Table 2). When the Kruskal–Wallis test appeared to be significant ($\alpha < 0.05$), all pairwise comparisons between groups were then made using the Conover–Inman method (Conover, 1999) implemented in the StatsDirect software. The Conover–Inman procedure corresponds to a Fisher's least significant difference method performed on ranks. The probability of each presumed "non-difference" between groups was reported when the computed α was below 0.05. When separations of groups were significant, the tendency from the highest to the lowest value was also summarised in Table 2 to make the reading clearer.

Elemental composition and magnetic susceptibility results for 'Main entrance' and 'Workshop' do not exhibit any significant difference, except for Pb and As. The highest concentrations of lead are found in the 'Main entrance' samples while for arsenic the 'Workshop' values are the highest. Both façades present higher values than 'Cafeteria/clean' and 'Cafeteria/dirty', except for Zn that is characterised by lower concentrations for the 'Cafeteria/dirty' group alone. Apart from Zn, 'Cafeteria' samples cannot be statistically distinguished. Lead isotopic compositions of surface stone samples vary within a relatively narrow range: $^{206}Pb/^{207}Pb$: 1.14–1.16, $^{208}Pb/^{206}Pb$: 2.10–2.13 (Table 1). However, surface samples from 'Main entrance' and 'Cafeteria/dirty'

Table 1
In situ and laboratory magnetic susceptibility, soiling, elemental and isotopic analyses

	In-situ κ SI ($\times 10^{-5}$)	Lab.χ $m^3 kg^{-1}$ ($\times 10^{-7}$)	Soiling (%)	Sc ($\mu g\, g^{-1}$)	Pb ($\mu g\, g^{-1}$)	Cu ($\mu g\, g^{-1}$)	Zn ($\mu g\, g^{-1}$)	Cd ($\mu g\, g^{-1}$)	S (%)	As ($\mu g\, g^{-1}$)	$^{206}Pb/^{207}Pb$	±	$^{208}Pb/^{206}Pb$	±
Detection limit	0.2	0.02	–	0.05	2	1	1	0.02	0.01	5	–	–	–	–
Main entrance (ME)														
A01	3.7	4.82	69	0.67	174	20	113	0.18	7.0	48	1.140	0.003	2.126	0.005
A03	3.9	2.90	63	0.74	155	12	100	0.26	7.0	62	1.141	0.003	2.121	0.005
A05	4.1	3.48	54	0.62	183	14	70	0.15	8.9	94	1.146	0.003	2.116	0.007
A07	4.5	5.14	54	0.77	239	11	58	0.27	8.1	91	1.143	0.003	2.117	0.004
A09	5.8	10.6	73	1.27	348	35	105	0.30	9.4	118	1.148	0.004	2.118	0.007
A11	5.6	8.43	72	1.08	270	24	103	0.26	9.1	117	1.148	0.002	2.118	0.004
A13	5.6	7.51	72	1.04	270	23	94	0.34	8.9	131	1.145	0.002	2.120	0.006
A15	5.7	7.74	68	1.10	309	31	99	0.29	8.9	116	1.140	0.003	2.127	0.005
A17	4.9	5.42	56	0.82	254	20	79	0.33	8.2	117	1.141	0.003	2.125	0.007
A19	4.5	4.85	50	0.78	199	18	73	0.32	7.8	84	1.144	0.002	2.122	0.006
A21	5.3	7.26	48	0.90	254	18	67	0.38	8.5	112	1.150	0.004	2.116	0.007
Average (Std. dev.)	4.9 (0.8)	6.2 (2.3)	62 (10)	0.9 (0.2)	240 (60)	21 (7)	87 (18)	0.28 (0.07)	8.3 (0.8)	100 (26)	1.144 (0.004)		2.121 (0.004)	
Workshop (W)														
B02	5.7	10.9	38	1.33	151	34	117	0.28	9.7	39	1.158	0.002	2.105	0.006
B04	5.4	8.54	77	1.21	164	23	95	0.88	9.9	439	1.151	0.002	2.117	0.004
B07	7.2	10.0	71	1.12	164	25	128	0.62	9.8	314	1.151	0.003	2.114	0.003
B09	3.4	5.56	67	0.68	65	7.9	93	0.32	6.4	172	1.153	0.003	2.115	0.004
B11	4.6	3.93	53	0.68	66	8.0	96	0.53	6.3	205	1.149	0.002	2.115	0.006
Average (Std. dev.)	5.3 (1.4)	7.8 (3.0)	61 (16)	1.0 (0.3)	122 (52)	20 (11)	106 (16)	0.53 (0.24)	8.4 (1.9)	233 (151)	1.152 (0.003)		2.113 (0.005)	
Cafeteria/clean (CC)														
C02	2.3	0.52	48	0.43	11	4.3	77	0.15	0.5	6.3	1.155	0.003	2.108	0.007
C05	2.9	0.36	43	0.41	10	3.2	193	0.02	0.4	6.5	1.150	0.003	2.110	0.007
C09	2.8	0.27	41	0.28	5.2	2.0	130	0.03	0.3	<	1.150	0.005	2.101	0.005
Average (Std. dev.)	2.7 (0.3)	0.38 (0.13)	44 (4)	0.37 (0.08)	8.7 (3.1)	3.2 (1.2)	133 (58)	0.06 (0.07)	0.4 (0.1)	<5.9 (0.8)	1.152 (0.003)		2.106 (0.005)	
Cafeteria/dirty (CD)														
D00	2.9	0.59	55	0.54	41	4.2	75	0.16	0.8	40	1.143	0.002	2.118	0.004
D02	2.5	0.26	54	0.30	17	2.3	31	0.10	0.3	8.9	1.142	0.003	2.119	0.008
D07	3.3	0.33	49	0.27	16	1.8	34	0.03	0.2	<	1.142	0.004	2.118	0.006
D09	2.8	0.21	43	0.28	12	2.7	26	0.05	0.2	7.4	1.141	0.003	2.123	0.007
Average (Std. dev.)	2.9 (0.3)	0.35 (0.17)	50 (6)	0.35 (0.13)	22 (13)	2.8 (1.0)	42 (23)	0.09 (0.06)	0.4 (0.3)	<15 (16)	1.142 (0.001)		2.120 (0.002)	
Pristine limestone A	–	0.11	–	<	<	3.8	37	<	0.2	<	1.201	0.004	2.045	0.010
Pristine limestone B	–	0.09	–	0.21	<	3.0	14	<	0.3	<	–	–	–	–

Errors are given at a 95% confidence level for lead isotopes. For the other parameters, see text. '<': below detection limit; '–': not determined. Detection limits were reported on the basis of concentration in the solid.

To facilitate comparison between façades, and although data are treated using nonparametric statistics, averages and standard deviations are also reported for each façade.

Table 2
p-Value of the Kruskal–Wallis test

	KW test	Conover–Inman test	Summary
In situ κ	$p = 0.003$	ME–CC ($p < 0.001$); ME–CD ($p < 0.001$); W–CC ($p < 0.001$); W–CD ($p < 0.001$)	ME–W > CC–CD
Lab. χ	$p = 0.002$	ME–CC ($p = 0.002$); ME–CD ($p < 0.001$); W–CC ($p < 0.001$); W–CD ($p < 0.001$)	ME–W > CC–CD
Black. (%)	$p = 0.053$	–	–
Sc	$p = 0.002$	ME–CC ($p = 0.002$); ME–CD ($p < 0.001$); W–CC ($p < 0.001$); W–CD ($p < 0.001$)	ME–W > CC–CD
Pb	$p = 0.0003$	ME–W ($p < 0.001$); ME–CC ($p < 0.001$); ME–CD ($p < 0.001$); W–CC ($p < 0.001$); W–CD ($p = 0.02$)	ME > W > CC–CD
Cu	$p = 0.003$	ME–CC ($p = 0.001$); ME–CD ($p = 0.001$); W–CC ($p = 0.004$); W–CD ($p < 0.001$)	ME–W > CC–CD
Zn	$p = 0.02$	ME–CD ($p = 0.02$); W–CD ($p = 0.003$); CC–CD ($p = 0.002$)	ME–W–CC > CD
Cd	$p = 0.01$	ME–CC ($p < 0.001$); ME–CD ($p = 0.001$); W–CC ($p < 0.001$); W–CD ($p < 0.001$)	ME–W > CC–CD
S	$p = 0.002$	ME–CC ($p = 0.002$); ME–CD ($p < 0.001$); W–CC ($p = 0.002$); W–CD ($p < 0.001$)	ME–W > CC–CD
As	$p = 0.002$	ME–W ($p = 0.048$); ME–CC ($p < 0.001$); ME–CD ($p = 0.001$); W–CC ($p < 0.001$); W–CD ($p < 0.001$)	W > ME > CC–CD
^{206}Pb/^{207}Pb	$p = 0.002$	ME–W ($p < 0.001$); ME–CC ($p = 0.002$); W–CD ($p < 0.001$); CC–CD ($p = 0.001$)	W–CC > ME–CD

If KW-test yielded a p-value lower than 0.05, all pairwise comparisons were made and the probability of each presumed ‘‘non-difference’’ was indicated. When the separation of groups was significant, the tendency from the highest to the lowest value was also summarized: ME for ‘Main entrance’, W for ‘Workshop’, CC for ‘Cafeteria/clean’, CD for ‘Cafeteria/dirty’.

appear to be significantly less radiogenic than those originating from ‘Workshop’ and ‘Cafeteria/clean’ façades (Table 2). Pristine calcareous fragments are markedly different, with ^{206}Pb/^{207}Pb ratios of 1.201 and ^{208}Pb/^{206}Pb ratios of 2.045 (Table 1), typical of lead naturally present in unpolluted rocks and soils in Western Europe (Shotyk et al., 1998; Semlali et al., 2004).

In a Spearman correlation coefficient matrix (Table 3), in-situ and laboratory magnetic susceptibility, façade blackness, and Al, Sc, Ti, V, Cr, Fe, Co and Ni (these latter elements are not reported in Table 1 except for Sc) appear to be significantly correlated to one another. Figs. 2a and b display soiling vs. in-situ magnetic susceptibility and Fe vs. Sc relationships respectively. The lowest elemental concentrations are generally found in pristine calcareous materials or in ‘Cafeteria’ samples (Table 1). No clear vertical gradient is observed within each façade.

Table 3
Spearman correlation coefficient matrix between in-situ κ, lab. χ, soiling and elemental concentrations of Al, Sc, Ti, V, Cr, Fe, Co and Ni

	In situ κ	Lab. χ	Soiling	Al	Sc	Ti	V	Cr	Fe	Co
Lab. χ	0.92									
Soiling	0.54	0.56								
Al	0.79	0.86	0.45							
Sc	0.93	0.97	0.55	0.87						
Ti	0.88	0.90	0.55	0.94	0.90					
V	0.89	0.92	0.58	0.91	0.93	0.94				
Cr	0.89	0.94	0.62	0.90	0.93	0.95	0.97			
Fe	0.90	0.92	0.58	0.91	0.93	0.95	0.97	0.95		
Co	0.83	0.86	0.42	0.83	0.88	0.79	0.83	0.77	0.84	
Ni	0.82	0.86	0.56	0.87	0.84	0.92	0.95	0.95	0.94	0.77

All correlations appear to be significant ($\alpha < 0.05$).

5. Discussion

5.1. *Sampling significance checked using magnetic susceptibility*

Incorporating a variable amount of preserved pristine limestone when scratching soiling from surface stones may lead to variable dilution by deeper and thus cleaner material. As a result, some parameters measured in collected powders may vary together, and hence be intercorrelated, simply because of the dilution effect of this clean material. Scratching homogeneity must therefore be tested prior to any further interpretation of geochemical and magnetic results. As field and laboratory

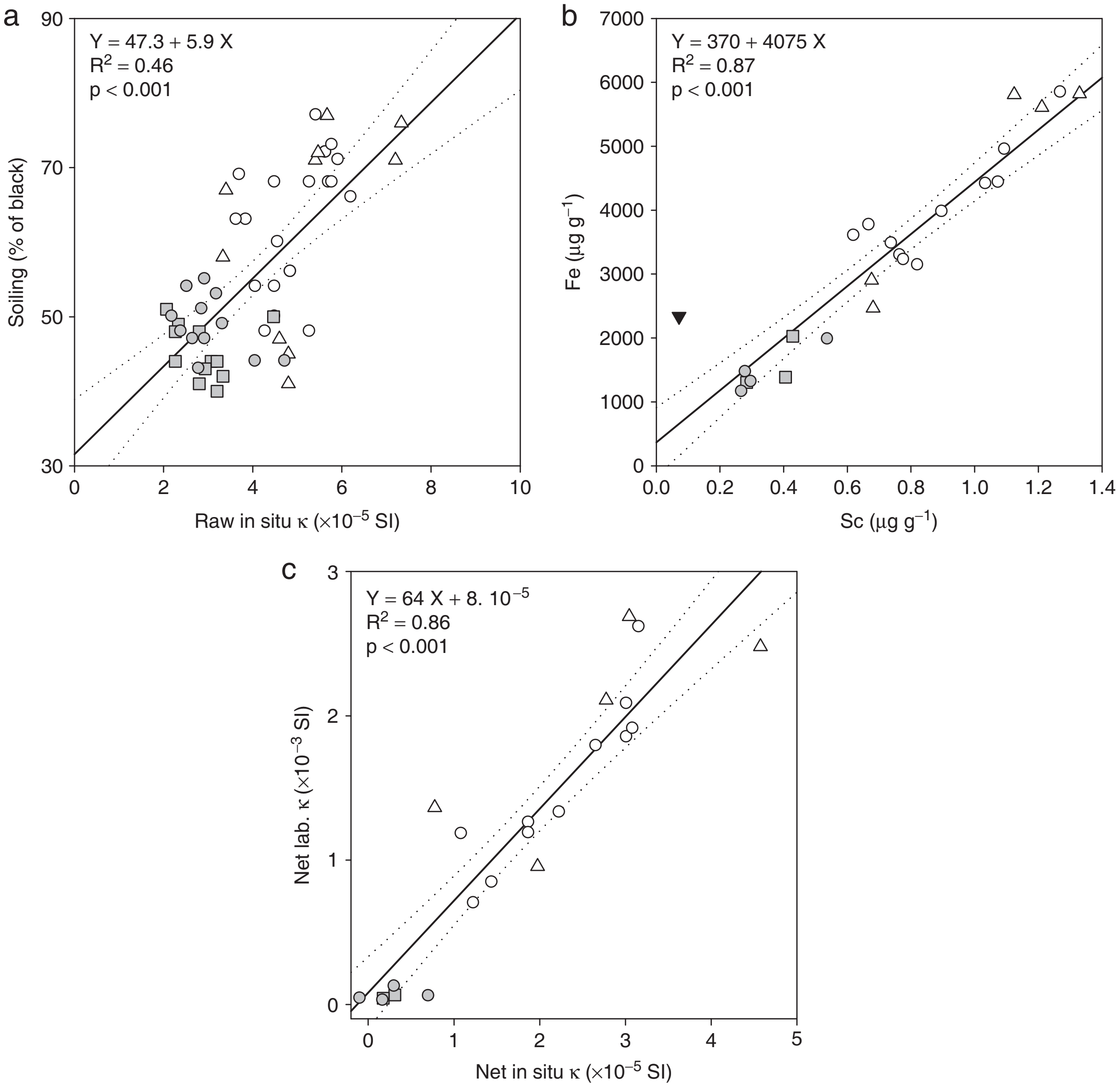

Fig. 2. (a) Soiling vs. Raw in-situ magnetic susceptibility; (b) Sc vs. Fe and (c) net laboratory magnetic susceptibility vs. net in-situ magnetic susceptibility, both corrected by the magnetic susceptibility contribution of pristine limestone (see text for details). Open circles, open triangles, closed boxes and closed circles correspond to 'Main entrance', 'Workshop', 'Cafeteria/clean' and 'Cafeteria/dirty', respectively. Closed triangle represents pristine limestone. Linear regressions and confidence intervals at 95% confidence level have been computed without taking pristine material into account.

determinations of magnetic susceptibility are normalised by volume and mass respectively, comparisons cannot be straightforward. Field and laboratory values were therefore expressed in the same SI unit and corrected for the contribution from pristine limestone. The new values, called net in-situ and net laboratory magnetic susceptibility, are computed assuming a limestone density value of 2.58 and an average magnetic susceptibility of $10^{-8}\,\mathrm{m}^3\,\mathrm{kg}^{-1}$; the value measured in drilled samples (Table 1). The strong correlation passing almost through the origin observed between net in-situ and laboratory magnetic susceptibility measurements demonstrate the efficiency of our collection procedure (Fig. 2c). Net laboratory magnetic susceptibility of powders appears to be, on average, almost 65 times higher than net in-situ measurements. The portable KT9 magnetic susceptibility metre takes into account not only surface soiling but also a considerable amount of weakly magnetic pristine material to a depth of some centimetres (KT5 estimation in Lecoanet et al., 1999), while KLY4 measurement is carried out on powders which represent a concentrate of magnetic particles.

5.2. Geochemical record of surface stones

The normalisation of Al, Ti, V, Cr, Fe, Co, and Ni contents to Sc produces an overall resemblance with the ratios assumed to characterize the upper continental crust (UCC, Fig. 3). This group of elements very probably originates from the calcareous rock itself, or from natural dust particles captured by the buildings, or both. An endogenous origin is privileged for the 'Cafeteria/dirty' and 'Cafeteria/clean' samples since they have approximately the same concentrations as pristine limestone (Table 1). As 'Main entrance' and 'Workshop' samples are generally enriched in lithogenic elements (see Sc, Table 1), an incorporation of exogenous, lithogenic-rich dust is more likely.

All these elements present higher concentrations in 'Main entrance' and 'Workshop' than in 'Cafeteria' samples. At this point, it is worth recalling that 'Workshop' and 'Main entrance' façades are oriented northeast and are therefore protected from most of the rainy events which, in Dijon, come predominantly from the west or south-west (Fig. 1). The 'Cafeteria' façades are oriented northwest and thus more frequently exposed to rainfall. Inter-façade variability could therefore be primarily due to orientation: natural dust particles deposited on all walls would settle preferably and durably on those sheltered from rain. Noticeable variations also occur at the scale of the façade itself (see all parameters in Table 1). Such intra-façade variability results from well-known micro-scale runoff variations that give façades a patchy appearance. Selective rain washing and variable water runoff within façades are therefore expected to be responsible for the high Spearman correlation coefficients observed between lithogenic elements, but also between this group of elements and magnetic susceptibility or surface soiling (Table 3). However, among all these variables, soiling is the one with the lowest correlation coefficients, which suggests that this parameter is the least related to the above-mentioned processes.

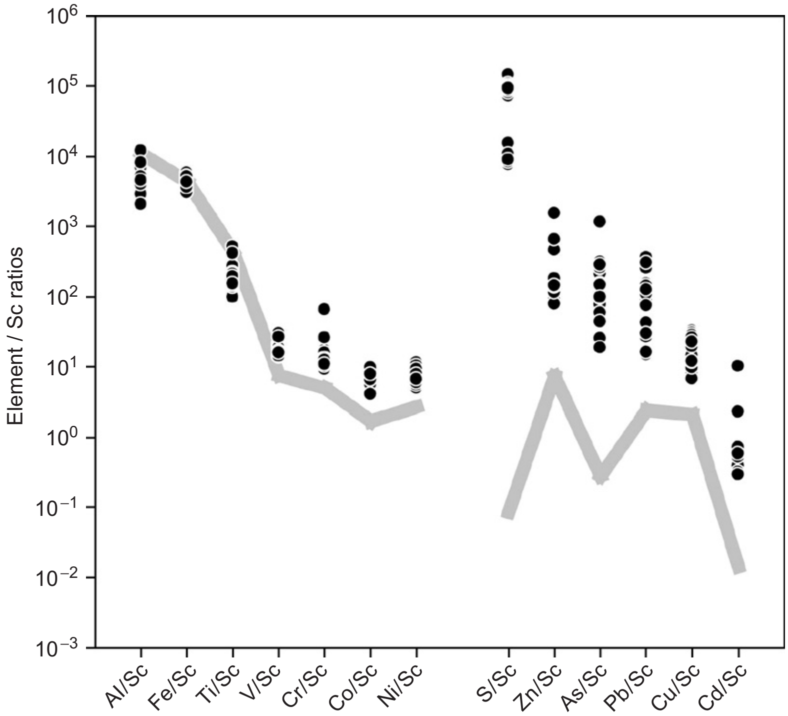

Fig. 3. Elements/Sc ratios in surface stone samples: closed circles. The grey line corresponds to the average values supposed to characterise the upper continental crust (Wedepohl, 1995).

The Pb, Cu, Zn, Cd, S and As contents were also normalised to Sc and compared to UCC values (Fig. 3) and differences of several orders of magnitude were observed. Although the generalised use in environmental studies of UCC values has been severely and justifiably criticised because they constitute a rough approximation which does not take into account the local variability of natural sources (Reinmann and de Carita, 2000, 2005), the differences are so high in this study that the origin of these elements is undoubtedly anthropogenic. The Cu, Cd and S contents display similar patterns to those of the lithophilic elements: 'Workshop'—'Main Entrance' >'Cafeteria' (Table 2). Surprisingly, the 'Cafeteria/clean' samples present high Zn contents, which might perhaps result from cleaning operations in 2002. If these samples are removed from the analysis, the behaviour of Zn becomes comparable to that of Cu, Cd and S, suggesting that particles bearing these elements are retained on the walls similarly to natural particles with respect to rain washing. That would imply diffuse pollution, at least at the scale of the college. The situation for Pb and As rather suggests the additional influence of point sources. As leaded gasoline was the major lead contributor to the urban atmosphere over a large part of the 20th century, it is not surprising to find significantly higher Pb contents in 'Main entrance' samples, in the vicinity of heavy traffic. On the other hand, smoke from the college heating system was, in the past, evacuated from the roof of the 'Workshop' building. The elevated As levels in the 'Workshop' samples might thus be due to the influence of coal and oil combustion products, since fly ash is known to be enriched in arsenic, just as lead is. Lead isotopes could allow this scenario to be explored. Isotopic composition of leaded gasoline is known to have varied from about 1.16 in the late 1960s (Chow and Earl, 1972) to about 1.08–1.10 from the 1980s until the time when lead was definitely phased out from gasoline in France, on 1st January 2000, (Elbaz-Poulichet et al., 1984; Monna et al., 1997; Véron et al., 1999). Nowadays, lead emitted by car exhausts is at the trace level and originates from crude oil. Coal burning is believed to have been an important source before it was replaced by oil combustion for domestic heating. ^{206}Pb/^{207}Pb ratios between 1.16 and 1.18 were measured in coal samples (Walraven et al., 1997) and these values are in good agreement with pollution recorded prior to the 50 s in archival soil, herbage, or sphagnum moss samples, in France, the UK and Switzerland (Bacon et al., 1996; Weiss et al., 1999; Semlali et al., 2004). Dijon has never been a major industrial centre. However, it is interesting to recall that ^{206}Pb/^{207}Pb ratios around 1.14–1.16 have often been reported for industrial emissions in France, and more generally in Western Europe, during the 1990s (Monna et al., 1997; Hansmann and Köppel, 2000).

It is clear that the ^{206}Pb/^{207}Pb ratios measured in surface stone samples (1.14–1.16) are incompatible with those of pristine limestone (~1.205), so that several anthropogenic sources must be involved (Table 1; Fig. 4). However, it is not feasible to apportion them accurately as too little information is available about the past evolution of isotopic composition of sources and the integration time of pollutants on to façades. Nonetheless, in the ^{208}Pb/^{206}Pb vs. ^{206}Pb/^{207}Pb diagram, the position of samples from 'Main entrance' tends to be closer to the gasoline domain than those from the 'Workshop' façade that seem to be proportionally more influenced by coal combustion. The 'Main entrance' and 'Cafeteria/dirty' samples present similar isotopic signatures, probably because the latter have also been submitted to direct automotive exhaust fumes from a smaller but adjacent street. The ^{206}Pb/^{207}Pb ratios of the 'Cafeteria/clean' are higher than those of the 'Cafeteria/dirty' façade. Such a finding is quite coherent with many other works dealing with lead isotopes in Western Europe. All these studies indicate that since the reduction and phasing out of lead from gasoline, isotopic signatures of airborne particulate materials tend to become more radiogenic because the relative importance of other sources increases (Grousset et al., 1994; Monna et al., 1997; Bollhöffer and Rosman, 2001; Widory et al., 2004). In any case, the significant isotopic discrepancies observed between the four façades confirm the varying influence of two or more local sources at the scale of the college.

No vertical gradient in lead concentrations or in isotopic compositions is observed at the façade scale, suggesting an intense atmospheric swirl at least as high as the building. In such an urban environment, people living on the second floor would be no less submitted to car pollution than those living on the ground floor. For this reason, even if horizontal variability at the façade scale has not been formally checked, it is logical to suppose that it is low in comparison with inter-façade variability discussed above. Etymezian et al. (1998)

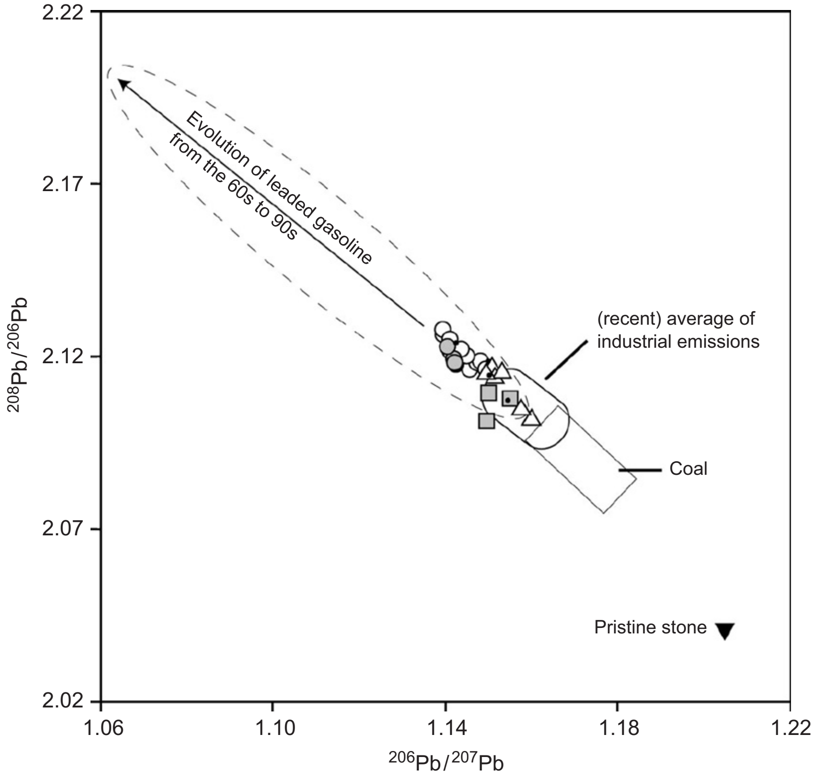

Fig. 4. $^{206}Pb/^{207}Pb$ vs. $^{208}Pb/^{206}Pb$ diagram. Open circles, open triangles, closed boxes and closed circles correspond to 'Main entrance', 'Workshop', 'Cafeteria/clean' and 'Cafeteria/dirty' respectively. Closed triangle represents pristine limestone. Potential lead sources are reported for comparative purposes, see text for details.

already noticed at the Cathedral of Learning in Pittsburgh, a much taller building, that airborne concentrations of sulphate and carbon particles were invariant with height. As in our case, soiling patterns were also ascribed to the competitive dynamic processes of pollutant deposition and rain washing. Photographs of the Cathedral from the 1930s showed a much greater amount of soiling than pictures taken recently, as air pollution levels, such as SO_2 and fly-ash concentrations, were higher in the past. Similar observations can be made by comparing old postcards of the college with recent photographs (Fig. 5). The 'Main entrance' façade experienced heavy soiling in its early years as demonstrated by the rapid soiling between 1908 and the late 1930s. Between the late 1930s and nowadays, soiling of limestone did not notably progress, and may even have regressed. As reported by Etymezian et al. (1998) in other circumstances, the rate of removal of soiling material by rain was probably equal or greater than the rate of soiling by pollutant deposition and chemical precipitation.

6. Conclusions

Our results demonstrate that lithogenic and anthropogenic elements have been deposited, and retained by the surface of the façades to some extent. Comparing in-situ and lab magnetic susceptibility is a reliable parameter to check the efficiency of the collection procedure. Cadmium, copper, sulphur and zinc are present as diffuse pollutants in the urban atmosphere, at least at the scale of the college, while lead and arsenic exhibit point sources: traffic, and coal and oil combustion. Building façades therefore conserve traces of atmospheric memory, but these may fade through exposure to rain washing or micro-scale runoff; both anthropogenic and natural particles being subject to dynamic competition between deposition/precipitation and cleaning by rain as suggested by archival photographs. Despite these difficulties, building façades can be profitably used as monitoring tools provided that certain constraints are observed: (i) exposure to rain should be minimal; (ii) buildings should be of similar age; (iii) the geochemical

Fig. 5. Archival photographs of Carnot College, main entrance. Dates for postcards are estimated on the basis of the stamp or postage date.

background of construction material should be as low as possible.

Acknowledgements

We express our gratitude to the city council of Dijon, which generously provided the aerial work platform and to the very kind employees of the city council for their precious assistance in sampling. We also appreciate the help provide by staff at the car traffic regulation office and at Carnot College. M. Mathon and D. Thévenin (Météo France) are also thanked for providing pictures and meteorological data, respectively. We are grateful to C. Durlet for thought-provoking discussions and two anonymous reviewers who improved the manuscript by their judicious comments.

References

Åberg, G., Pacyna, J.M., Stray, H., Skjelkvåle, .B.L., 1999. The origin of atmospheric lead in Oslo, Norway, studied with the use of isotopic ratios. Atmospheric Environment 33, 3335–3344.

Alaimo, M.G., Dongarrà, G., Melati, M.R., Monna, F., Varrica, D., 2000. Recognition of environmental trace metal contamination using pine needles as bioindicators. The urban area of Palermo (Italy). Environmental Geology 39, 914–924.

Ausset, P., Del Monte, M., Lefèvre, R.A., 1999. Embryonic sulphated black crusts on carbonate rocks in atmospheric simulation chamber and in the field: role of carbonaceous fly ash. Atmospheric Environment 33, 1525–1534.

Bacon, J.R., Jones, K.C., McGrath, S.P., Johnston, A.E., 1996. Isotopic character of lead deposited from the atmosphere at a grassland site in the United Kingdom since 1860. Environmental Science and Technology 30, 2511–2518.

Bidegain, J.C., Sinito, A.M., Rodriguez, M.E., 1999. Remanent magnetization in Portland-cement-based materials. Studia Geophysica et Geodaetica 43, 289–302.

Bollhöffer, A., Rosman, K.J.R., 2001. Lead isotopic ratios in European atmospheric aerosols. Physics and Chemistry of Earth, Part B 26, 835–838.

Bollhöffer, A., Rosman, K.J.R., 2002. The temporal stability in lead isotopic signatures at selected sites in the Southern and Northern hemispheres. Geochimica et Cosmochimica Acta 66, 1375–1386.

Chow, T.J., Earl, J.L., 1972. Lead isotopes in North American coals. Science 176, 510–511.

Cloquet, C., Carignan, J., Libourel, G., 2006. Atmospheric pollutant dispersion around an urban area using trace metal concentrations and Pb isotopic compositions in epiphytic lichens. Atmospheric Environment 40, 574–587.

Conover, W.J., 1999. Practical Non-parametric Statistics, third ed. Wiley, New York, 584pp.

Elbaz-Poulichet, F., Holliger, P., Huang, W.W., Martin, J.M., 1984. Lead cycling in estuaries, illustrated by the Gironde estuary, France. Nature 308, 409–414.

Etymezian, V., Davidson, C.I., Finger, S., Striegel, M.F., Barabas, N., Chow, J.C., 1998. Vertical gradients of pollutant concentrations and deposition fluxes on a tall limestone building. Journal of American Institute for Conservation 37, 187–210.

Flament, P., Bertho, M.-L., Deboudt, K., Véron, A., Puskaric, E., 2002. European isotopic signatures for lead in atmospheric aerosols: a source apportionment based upon ^{206}Pb/^{207}Pb ratios. The Science of the Total Environment 296, 35–57.

Galletti, G., Bochini, P., Cam, D., Chiavari, G., Mazzeo, R., 1997. Chemical characterization of the black crust present on the stone central portal of St. Denis abbey. Fresenius Journal of Analytical Chemistry 357, 1211–1214.

Gołuchowska, B.J., 2001. Some factors affecting an increase in magnetic susceptibility of cement dusts. Journal of Applied Geophysics 48, 103–112.

Grousset, F.E., Quetel, C.R., Thomas, B., Buat-Menart, P., Donard, O.F.X., Bucher, A., 1994. Transient Pb isotopic signatures in the Western-European atmosphere. Environmental Science and Technology 28, 1605–1608.

Haack, U., Gutsche, F.H., Plessow, K., Heinrichs, H., 2002. On the isotopic composition of Pb in cloud waters in Central Germany. A source discrimination study. Water, Air and Soil Pollution 139, 261–288.

Hansmann, W., Köppel, V., 2000. Lead-isotope as tracers of pollutants in soils. Chemical Geology 171, 123–144.

Hoffman, V., Knap, M., Appel, E., 1999. Magnetic susceptibility mapping of roadside pollution. Journal of Geochemical Exploration 66, 313–326.

Hunt, A., Jones, J., Oldfield, F., 1984. Magnetic measurements and heavy metals in atmospheric particulates of anthropogenic origin. The Science of the Total Environment 33, 129–139.

Jordanova, N., Jordanova, D., Veneva, L., Yorova, K., Petrovsky, E., 2003. Magnetic response of soils and vegetation to heavy metal pollution—a case study. Environmental Science and Technology 37, 4417–4424.

Lecoanet, H., Lévêque, F., Segura, S., 1999. Magnetic susceptibility in environmental applications: comparison of field probes. Physics of the Earth and Planetary Interiors 115, 191–204.

Lecoanet, H., Lévêque, F., Ambrosi, J.-P., 2001. Magnetic properties of salt-marsh soils contaminated by iron industry emissions (southeast France). Journal of Applied Geophysics 48, 67–81.

Lecoanet, H., Lévêque, F., Ambrosi, J.-P., 2003. Combination of magnetic parameters: an efficient way to discriminate soil-contamination sources (south France). Environmental Pollution 122, 229–234.

Lefèvre, R.A., Ausset, P., 2002. Atmospheric Pollution and Building Materials: Stone and Glass. Natural Stone, Weathering Phenomena, Conservation Strategies and Case studies. Special Publications, vol. 205. Geological Society, London, pp. 329–345.

Lehndorff, E., Urbat, M., Schwark, L., 2006. Accumulation histories of magnetic particles on pine needles as function of air quality. Atmospheric Environment 40, 7082–7096.

Matzka, J., Maher, B.A., 1999. Magnetic biomonitoring of roadside tree leaves: identification of spatial and temporal variations in vehicle-derived particles. Atmospheric Environment 33, 4565–4569.

Monna, F., Lancelot, J., Croudace, I.W., Cundy, A.B., Lewis, J.T., 1997. Pb isotopic composition of airborne particulate material from France and the Southern United Kingdom: implications for Pb pollution sources in urban areas. Environmental Science and Technology 31, 2277–2286.

Monna, F., Loizeau, J.-L., Thomas, B.A., Guéguen, C., Favarger, P.-Y., 1998. Pb and Sr isotope measurements by inductively coupled plasma-mass spectrometer: efficient time management for precise improvement. Spectrochimica Acta B 59/09, 1317–1333.

Monna, F., Loizeau, J.-L., Thomas, B., Guéguen, C., Favarger, P.-Y., Losno, R., Dominik, J., 2000. Noise identification and sampling frequency determination for precise isotopic measurements by quadrupole-based inductively coupled plasma mass spectrometry. Analusis 28, 750–757.

Monna, F., Poujol, M., Losno, R., Dominik, J., Annegarn, H., Coetzee, H., 2006. Origin of atmospheric lead in Johannesburg, South Africa. Atmospheric Environment 40, 6554–6566.

Moreno, E., Sagnotti, L., Winkler, A., Dinarès-Turell, J., Cascella, A., 2003. Biomonitoring of traffic air pollution in Rome using magnetic properties of tree leaves. Atmospheric Environment 37, 2967–2977.

Petrovsky, E., Ellwood, B.B., 1999. Magnetic monitoring of air-, land-, and water-pollution. In: Maher, B.A., Thompson, R. (Eds.), Quaternary Climates, Environments and Magnetism. Cambridge University Press, Cambridge, pp. 279–322 (Chapter 8).

Petrovský, E., Kapička, A., Jordanova, N., Knap, M., Hoffmann, V., 2000. Low-field magnetic susceptibility: a proxy method of estimating increased pollution of different environmental systems. Environmental Geology 39, 312–318.

Reinmann, C., de Carita, P., 2000. Intrinsic flaws of element enrichment factors (EFs) in environmental geochemistry. Environmental Science and Technology 34, 5084–5091.

Reinmann, C., de Carita, P., 2005. Distinguishing between natural and anthropogenic sources for elements in the environment: regional geochemical surveys versus enrichment factors. Science of the Total Environment 337, 91–107.

Rodriguez-Navarro, C., Sebastian, E., 1996. Role of particulate matter from vehicle exhaust on porous building stones (limestone) sulfation. The Science of the Total Environment 187, 79–91.

Sagnotti, L., Macri, P., Egli, R., Mondino, M., 2006. Magnetic properties of atmospheric particulate matter from automatic air sampler stations in Latium (Italy): toward a definition of magnetic fingerprints for natural and anthropogenic PM10 sources. Journal of Geophysical Research 111, B12S22.

Semlali, R.M., Dessogne, J.-B., Monna, F., Bolte, J., Azimi, S., Navarro, N., Denaix, L., Loubet, M., Chateau, C., van Oort, F., 2004. Modeling lead input and output in soils using lead isotopic geochemistry. Environmental Science and Technology 38, 1513–1521.

Shotyk, W., Weiss, D., Appleby, P., Cherbukin, A., Frei, R., Gloor, M., Kramer, J., Reese, S., Van der Knaap, W., 1998. History of atmospheric lead deposition since 12,370 ^{14}C yr BP from a peat bog, Jura Mountains, Switzerland. Science 281, 1635–1640.

Simão, J., Ruiz-Agudo, E., Rodriguez-Navarro, C., 2006. Effects of particulate matter from gasoline and diesel vehicle exhaust emissions on silicate stones sulfation. Atmospheric Environment 40, 6905–6917.

Takeda, K., Marumoto, K., Minamikawa, T., Sakugawa, H., Fujiwara, K., 2000. Three-year determination of trace metals and the lead isotope ratio in rain and snow depositions collected in Higashi-Hiroshima, Japan. Atmospheric Environment 34, 4525–4535.

Tommasini, S., Davis, G.R., Elliott, T., 2000. Lead isotope composition of tree rings as bio-geochemical tracers of heavy metal pollution: a reconnaissance study from Firenze, Italy. Applied Geochemistry 15, 891–900.

Urbat, M., Lehndorff, E., Schwark, L., 2004. Biomonitoring of air quality in Cologne conurbation using pine needles as a passive sampler–part I: magnetic properties. Atmospheric Environment 38, 3781–3792.

Véron, A., Flament, P., Bertho, M.-L., Alleman, L., Flegal, R., Hamelin, B., 1999. Isotopic evidence of pollutant lead sources in Northwestern France. Atmospheric Environment 33, 3377–3388.

Walraven, N., van Os, B.J.H., Klaver, G.Th., Baker, J.H., Vriend, S.P., 1997. Trace element concentrations and stable lead isotopes in soils as tracers of lead pollution in Graft-De Rijb in Netherlands. Journal of Geochemical Exploration 59, 47–58.

Wedepohl, K.H., 1995. The composition of the crust. Geochimica et Cosmochimica Acta 59, 1217–1232.

Weiss, D., Shotyk, W., Kramers, J.D., Gloor, M., 1999. Sphagnum mosses as archives of recent and past atmospheric lead deposition in Switzerland. Atmospheric Environment 33, 3751–3763.

Widory, D., Roy, S., Le Moullec, Y., Goupil, G., Cocherie, A., Guerrot, C., 2004. The origin of atmospheric particles in Paris: a view through carbon and lead isotopes. Atmospheric Environment 38, 953–1061.